

Design with Regard to Explosion

Response of a structural system and equivalent 2DOF model

Master's Thesis in the Master's Programme Structural Engineering and Building Technology

SIMON ELIASSON

ADAM SCIEGAJ

Department of Civil and Environmental Engineering

Division of Structural Engineering

Concrete Structures

CHALMERS UNIVERSITY OF TECHNOLOGY

Gothenburg, Sweden 2015

Master's Thesis 2015:86

MASTER'S THESIS 2015:86

Design with Regard to Explosion

Response of a structural system and equivalent 2DOF model

*Master's Thesis in the Master's Programme Structural Engineering and Building
Technology*

SIMON ELIASSON
ADAM SCIEGAJ

Department of Civil and Environmental Engineering
*Division of Structural Engineering
Concrete Structures*

CHALMERS UNIVERSITY OF TECHNOLOGY

Gothenburg, Sweden 2015

Design with Regard to Explosion
Response of a structural system and equivalent 2DOF model

*Master's Thesis in the Master's Programme Structural Engineering and Building
Technology*

SIMON ELIASSON
ADAM SCIEGAJ

© SIMON ELIASSON , ADAM SCIEGAJ, 2015

Examensarbete 2015:86/ Institutionen för bygg- och miljöteknik,
Chalmers tekniska högskola 2015

Department of Civil and Environmental Engineering
Division of Structural Engineering
Concrete Structures
Chalmers University of Technology
SE-412 96 Gothenburg
Sweden
Telephone: +46 (0)31-772 1000

Cover:
Transformation into equivalent 2DOF system. Frequency spectrum of shear force oscillation.

Chalmers Reproservice
Gothenburg, Sweden 2015

Design with Regard to Explosion
Response of a structural system and equivalent 2DOF model
*Master's Thesis in the Master's Programme Structural Engineering and Building
Technology*

SIMON ELIASSON

ADAM SCIEGAJ

Department of Civil and Environmental Engineering

Division of Structural Engineering

Concrete Structures

Chalmers University of Technology

ABSTRACT

Structural elements subjected to explosion loads are often transformed to simplified Single Degree of Freedom (SDOF) mass-spring system in order to facilitate and expedite their design. This simplification has showed good results for single vibrating elements, i.e. beams or slabs on stiff supports. However, if a structural system consisting of a beam supported on two beams is considered, a 2DOF mass spring system is needed to capture the response of the structure.

Models were created in the commercial FE software ADINA, and several parametric studies were carried out for structures with various stiffness and mass ratios. First, a beam on spring supports was studied as an intermediate step between a simple beam and a structural system. Then, the beam-on-beam structural systems were modelled and the equivalent 2DOF system was created and verified so that its response was agreeing with the one obtained from Finite Element Method. Modification of ordinary SDOF systems was carried out, resulting in the systems being capable of describing the behaviour of each part of the structural system approximately.

It was discovered, that the response of the structure with an intermediate stiffness ratio (between 3 and 8) is too complex to be described by a SDOF simplification, and there an equivalent 2DOF system must be used. Outside of this range, both 2DOF and modified SDOF systems give reasonable and acceptable results. After a detailed study, it was found that treating the element as a part of a structure can result in its displacements being reduced up to 40-50 %, i.e. it may be very conservative to assume a single vibrating element in such a case.

Keywords: explosion, impulse load, reinforced concrete, SDOF, 2DOF, elastic, finite element analysis, dynamic

Dimensionering för explosionslaster

Respons hos sammansatta strukturer och ekvivalent 2DOF system

Examensarbete inom masterprogrammet Structural Engineering and Building Technology

SIMON ELIASSON

ADAM SCIEGAJ

Institutionen för bygg- och miljöteknik

Avdelningen för konstruktionsteknik

Betongbyggnad

Chalmers tekniska högskola

SAMMANFATTNING

Bärande element som utsätts för explosionslaster förenklas ofta till ett system bestående av en massa och en fjäder (SDOF), detta görs för att underlätta och snabba på konstruktionsarbetet. Denna förenkling har visat sig ge gott resultat i att beskriva beteendet hos enskilda element som kommer i svängning, t.ex. balkar och plattor som vilar på styva upplag. För en konstruktion där en balk vilar på två andra balkar blir beteendet mer komplext. För att modellera ett sådant arrangemang behövs det minst två massor och två fjädrar i ett tvåfrihetsgradssystem (2DOF).

I det kommersiella Finit Element programmet ADINA byggdes flera modeller upp. Dessa användes i parameterstudier där förhållandet mellan balkarnas massor och styvhet varierades. Först undersöktes en fritt upplagd balk som vilar på fjädrar och jämfördes med SDOF, detta var tänkt som ett första mellansteg. Därefter görs en FE-modell av en balk som vilar på två andra balkar. Ett 2DOF system skapas med målet att kunna beskriva en liknande respons som FE-modellen. Slutligen görs ett försök att ytterligare förbättra det ursprungliga SDOF systemet så att det skall kunna användas för att beskriva ett element som en del av en struktur.

Studien visar att responsen hos system, med styvhetskvoter i ett intervall av 3 till 8, är mycket mer komplex än vad ett SDOF system kan beskriva. I detta intervall fungerar 2DOF mycket bättre för att beskriva responsen. I övriga fall ger båda systemen ett tillräckligt bra resultat, men SDOF är då lättare att använda. I studien visas också att om element betraktas som en del av en struktur, kan den förväntade förskjutningen i vissa fall reduceras med uppåt 40-50 %. Med andra ord, att endast se på elementet som om det vilade på fasta stöd, kan vara väldigt konservativt.

Nyckelord: explosion, impulslast, armerad betong, enfrihetsgradssystem, tvåfrihetsgradssystem, elastisk, finit element analys, dynamisk

CONTENTS

Abstract	i
Sammanfattning	ii
Contents	iii
Preface	vii
Nomenclature	ix
1 Introduction	1
1.1 Background	1
1.2 Aim	1
1.3 Limitations	2
1.4 Method	2
1.5 Outline of the report	3
2 Theory	4
2.1 Explosion	4
2.1.1 Explosion - what is it?	4
2.1.2 Shock wave	4
2.1.3 Wave phenomena	5
2.1.4 Load on surface from explosion	6
2.2 Structural models	9
2.2.1 General notes	9
2.2.2 Linear elastic	9
2.2.3 Ideally plastic	10
2.2.4 Elastoplastic	10
2.2.5 Concrete	11
2.2.6 Reinforcing steel	11
2.3 Structural response of beams under load	12
2.3.1 Response of reinforced concrete cross section under load	12
2.3.2 Theory of plastic hinges	14
2.3.3 Plastic rotation capacity	16
2.4 Work and energy	18
2.4.1 Fundamental parameters	18
2.4.2 Characteristic impulse	20
2.4.3 External work	23
2.4.4 Internal work	24
2.5 Transformation into equivalent SDOF/2DOF system	27
2.5.1 Introduction	27
2.5.2 Single Degree of Freedom system	28
2.5.3 Two Degrees of Freedom system	28
2.5.4 Transformation factors	30
2.6 Equivalent static load	34
2.6.1 General notes	34
CHALMERS, Civil and Environmental Engineering, Master's Thesis 2015:86	iii

2.6.2	Elastic model	34
2.6.3	Plastic model	34
2.6.4	Elastoplastic model	35
2.7	Summary of SDOF system loaded with characteristic impulse	35
3	Parametric study - beam on spring supports	36
3.1	Introduction	36
3.2	Outline of the study	36
3.2.1	Parametric beams, springs and load case	36
3.2.2	Modelling in ADINA	38
3.3	Modified transformation factors	39
3.3.1	General notes	39
3.3.2	Beam subjected to uniformly distributed load	40
3.3.3	Beam subjected to point load	42
3.3.4	Discussion	43
3.4	Modified SDOF system	44
3.4.1	Description of the system	44
3.4.2	Hand calculations	45
3.5	Discussion and conclusions	46
3.5.1	Results of the parametric study	46
3.5.2	Preliminary conclusions	49
4	Transformation into 2DOF system	50
4.1	Introduction	50
4.2	Outline of the study	50
4.2.1	Parametric beams and the load case	50
4.2.2	Modelling in ADINA	53
4.3	Response of 2DOF model - transformation factors	55
4.3.1	Differential equation system	55
4.3.2	Results and conclusions	55
4.4	Calibration of the 2DOF model - frequency	59
4.4.1	General notes	59
4.4.2	Frequency domain and eigenmodes	59
4.4.3	Mass adjustment factors	63
4.4.4	Response of the 2DOF model calibrated with mass adjustment factors	67
4.5	Calibration of the 2DOF model - amplitude	71
4.5.1	General notes	71
4.5.2	Optimisation procedure and constraints	71
4.5.3	Optimisation factors	74
4.6	Response of the optimised 2DOF model	76
4.6.1	General notes	76
4.6.2	Deformation	76
4.6.3	Amplitude error	78
4.6.4	Bending moment	81
4.6.5	Shear force	84
4.7	Influence of beam length and load case	86
4.7.1	Different lengths	86
4.7.2	Different load cases	90

4.8	Response of a structural system - calculation example	94
4.8.1	Introduction	94
4.8.2	Stiffness and mass ratios	94
4.8.3	Creation of the optimised 2DOF model	95
4.8.4	Deformation	96
4.8.5	Hand calculations according to SDOF model	98
4.9	Discussion and conclusions	100
4.9.1	Two degrees of freedom model	100
4.9.2	Comparison with SDOF models	101
5	Enhanced SDOF systems	103
5.1	Introduction	103
5.2	Lower beam	104
5.2.1	Simply supported beam	104
5.2.2	Simply supported beam with a point mass	105
5.3	Upper beam	107
5.3.1	Simply supported beam	107
5.3.2	Beam on spring supports	109
5.3.3	Optimised SDOF model for the upper beam	110
5.4	Discussion and conclusions	112
5.4.1	Alternative approach to the upper beam	112
5.4.2	Lower beam with point mass and the optimised SDOF system for the upper beam	113
6	Discussion	115
6.1	General discussion	115
6.2	Limitations of the 2DOF system	115
6.3	Summary of results	117
6.3.1	Response of a structural system	117
6.3.2	Influence of the surrounding structure	118
6.4	Examples of application	120
7	Conclusions	122
7.1	Response of a structural system	122
7.2	Influence of the surrounding structure	122
7.3	Improvements and further research	123
	References	124
	Appendix A Central Difference Method	125
A.1	General Notes	125
A.2	Method	125
A.3	Stability and accuracy	127
	Appendix B Results - beam on spring supports	128
	Appendix C Octave code for solving 2DOF system	133
	Appendix D The optimization factors	136

Appendix E Results - response of a structural system	150
E.1 Spectrum of analysis	150
E.2 Eigenmodes	150
E.3 Response of the upper and lower beam	152
Appendix F Optimisation of the upper beam's model	156
F.1 Optimisation of the upper beam's model	156
F.1.1 General notes	156
F.1.2 Adjusted mass and stiffness	156
F.1.3 Empirical model fitting	158
Appendix G Stiffness transformation factor	161
G.1 General notes	161
G.2 First eigenmode	161
G.3 Second eigenmode	163
G.4 Final remarks	165

PREFACE

This Master's thesis studies the response of a beam-on-beams structural system subjected to impulse loading. It has been carried out in cooperation with the Division of Structural Engineering at Chalmers University of Technology and Reinertsen Sverige AB. The study was conducted at Reinertsen's office in Gothenburg from January to June 2015.

First of all, we would like to thank Mattias Carlsson, Reinertsen Sverige AB, who was supervising this project, for his continuous help, commitment, insight, feedback and help with the finite element software. Further, we would like to express our gratitude towards the examiner of this thesis - Morgan Johansson, Ph.D., Reinertsten Sverige AB and Chalmers University of Technology, who contributed to this study with his advice, feedback, and who was always available for guidance.

We would also like to thank Reinertsen Sverige AB for giving us the chance to take part in this project, providing necessary literature, stationary and a place to work.

Last but not least, we would like to kindly thank our colleagues at the Reinertsen office for their meaningful feedback and most of all for their company during this period.

Gothenburg, June 2015

Simon Eliasson and Adam Sciegaj

NOMENCLATURE

Roman upper case letters

A	Area
A_s	Area of reinforcement
A'_s	Area of upper reinforcement
A_+	Area of the cross section part under tension
A_-	Area of the cross section part under compression
C	Damping matrix
E	Young's modulus
E_c	Young's modulus of concrete
E_k	Kinetic energy
E_s	Young's modulus of steel
EI	Rigidity of the cross section
F	External force
F	Force vector
F_c	Force in the damper
F_e	equivalent force
F_k	Force in the spring
F_k	Characteristic load
F_s	Force in fictitious spring
I	Impulse
I	Moment of inertia
I_k	Characteristic impulse
I_I	Moment of inertia of the cross section in state I
I_{II}	Moment of Inertia of the cross section in state II
K	Stiffness matrix
L	Length
L_0	Distance between plastic hinge and adjacent zero moment section
L_1	Length of the upper beam
L_2	Length of the lower beam
M	Bending moment
M	Mass matrix
M_{cr}	Cracking moment
M_y	Yielding moment
M_L	Bending moment in the lower beam
M_{Rd}	Ultimate bending moment
M_U	Bending moment in the upper beam
P	Pressure
P_0	Atmospheric pressure
P^+	Blast overpressure
P^-	Underpressure coming from the shock wave
Q	Equivalent static load
R	Internal resistance force
R_m	Plastic resistance force
T	Period of vibration
T^+	Duration of the positive phase of the shock wave
T^-	Duration of the negative phase of the shock wave

V	Shear force
W	Energy output from the explosion
W_e	External work
W_{el}	Elastic section modulus
W_i	Internal work
W_{pl}	Plastic section modulus
Z	Scaled distance

Roman lower case letters

a	Acceleration
b	Width of the cross section
c	Damping coefficient
c	Wave propagation velocity
c_e	Equivalent damping
d	Effective depth of the cross section
f	Frequency
f_{cd}	Design value of the concrete compressive strength
f_i	i -th eigenfrequency
f_{su}	Ultimate tensile stress of steel
f_{sy}	Yield strength of reinforcing steel
h	Height of the cross section
i	Impulse intensity
i^+	Positive phase impulse intensity
i^-	Negative phase impulse intensity
k	Stiffness
k_a	Adjusted stiffness
k_e	Equivalent stiffness
k_r	Stiffness ratio
k_λ	Plastic rotation capacity multiplication factor allowing for shear slenderness
k_1	Stiffness of the upper beam
k_2	Stiffness of the lower beam
m	Mass
m_a	Adjusted mass
m_{ai}	Adjusted mass
m_e	Equivalent mass
m_{point}	Point mass
m_r	Mass ratio
m_1	Mass of the upper beam
m_2	Mass of the lower beam
m'	Mass per length
p	Momentum
q	Uniformly distributed load
r	Distance from the source of the explosion
$1/r$	Curvature
$(1/r)_u$	Ultimate curvature
$(1/r)_y$	Curvature at yielding
t	Time

t_a	Time of arrival
t_{Δ}^+	Fictitious duration of the idealised shock wave
u	Deformation
\mathbf{u}	Deformation vector
$u(x)$	Deformation shape
u_{el}	Deformation in a linear elastic material
u_{ep}	Total deformation in an elastoplastic material
$u_{ep,el}$	Elastic part of the total deformation in an elastoplastic material
$u_{ep,pl}$	Plastic part of the total deformation in an elastoplastic material
$u_{max,SDOF}$	Maximum deformation of a SDOF system
$u_{max,ADINA}$	Maximum deformation obtained from ADINA
u_{pl}	Deformation in an ideally plastic material
u_{rd}	Ultimate plastic deformation
u_s	Displacement of the system point
u_L	Deformation of the lower beam obtained from 2DOF system
u_{LA}	Deformation of the lower beam obtained from a ADINA
u_U	Deformation of the upper beam obtained from a 2DOF system
u_{UA}	Deformation of the upper beam obtained from ADINA
$u_{U,max,ADINA}$	Maximum deformation of the upper beam in ADINA
$u_{U,max,SDOF}$	Maximum deformation of the upper beam in a SDOF system
u_1	Displacement of the first system point in a 2DOF system
u_2	Displacement of the second system point in a 2DOF system
u_{1A}	Displacement of the first system point in ADINA
u_{2A}	Displacement of the second system point in ADINA
\dot{u}	Velocity
$\dot{\mathbf{u}}$	Velocity vector
\ddot{u}	Acceleration
$\ddot{\mathbf{u}}$	Acceleration vector
v	Velocity
w	Mass of the explosive
x	Coordinate
x	Height of the compression zone in the concrete cross section
z	Coordinate from neutral axis of the cross section
z	Distance between centroids of the compressed and tensioned part of the cross section
z_s	Distance between the neutral axis and the centre of gravity of the bottom reinforcement
z_+	Distance from the centroid of the tensioned part of the cross section to its elastic neutral axis
z_-	Distance from the centroid of the compressed part of the cross section to its elastic neutral axis

Greek upper case letters

Δk	Stiffness increment
Δm	Mass increment
Δt	Time increment

Greek lower case letters

α	Slope
α_s	Ratio between the Young's modulus of steel and concrete
α_R	Stress block factor for the average stress
β	Intercept
β_R	Stress block factor for the location of the stress resultant
γ_k	Stiffness adjustment factor
γ_{k_1}	Optimisation factor for the stiffness of the first body
γ_{k_2}	Optimisation factor for the stiffness of the second body
γ_m	Mass adjustment factor
γ_{m_1}	Optimisation factor for the mass of the first body
γ_{m_2}	Optimisation factor for the mass of the second body
γ_{mF_i}	Mass adjustment factor
γ_{F_1}	Optimisation factor for the force acting on the first body
γ_{F_2}	Optimisation factor for the force acting on the second body
γ_I	Correction factor for the characteristic impulse
ε	Strain
ε_s	Strain at the level of bottom reinforcement
ε'_s	Strain at the level of upper reinforcement
ε_{sh}	Steel strain at the end of plastic plateau
ε_{su}	Steel strain at rupture
ε_{sy}	Steel strain at the beginning of plastic plateau
$\varepsilon_{s,fsu}$	Steel strain at the ultimate tensile stress
ε_u	Ultimate steel strain
η	Accuracy
η	Relative deformation
θ_{pl}	Total plastic rotation
θ_{Rd}	rotation capacity of a plastic hinge
κ_k	Stiffness transformation factor
κ_m	Mass transformation factor
κ_{mF}	Quotient of the mass and force transformation factors
$\kappa_{m,mod}$	Modified mass transformation factor
κ_F	Force transformation factor
$\kappa_{F,mod}$	Modified force transformation factor
λ	Eigenvalue
ν	Poisson's ratio
ρ	Density
σ	Stress
σ_c	Stress in concrete
σ_{cc}	Compressive strength of concrete
σ_{ct}	Tensile strength of concrete
σ_s	Stress in steel
σ_y	Yield stress
ϕ_i	i-th eigenvector
ω	Angular frequency
ω_b	Angular frequency of the beam
ω_i	i-th angular eigenfrequency
ω_{SDOF}	Angular frequency of the SDOF system

1 Introduction

1.1 Background

In today's world the need for building and structures to withstand loading from such extreme sources as explosions has become more and more apparent, be it controlled detonations as at construction sites or outcomes of terrorist activity. Examples of this could be experienced in Scandinavia lately, namely in Stockholm in 2010 and in Oslo in 2011. Design against explosion is also a necessity in for example the processing industry, road tunnels and military installations.

Response of a structure subjected to impulse loading can differ greatly from its response to static load. This has made the design with regard to explosion a subject of interest, as today's comprehension in this field is still limited. Although Finite Element Modelling is nowadays possible, such modelling is time consuming and requires skill to interpret the results correctly. Therefore simplified models are of interest in order to provide engineers with easier and quicker tools when faced with explosion related design tasks. Such models have in recent years been studied at Reinertsen, in particular transforming a reinforced concrete beam or slab into a Single Degree of Freedom mass-spring system (SDOF). The SDOF simplification has been shown to describe the elastic behaviour of simple vibrating structures such as beams or slabs quite well, see Klorek and Sandberg (2013). Such system is easier and quicker to solve for displacements, which can later be transformed into internal forces. However, as far as structural systems such as slabs resting on beams, or a beam supported on beams are concerned, their response according to simplified models is not entirely conforming to the Finite Element Analysis behaviour. Therefore, there is a need for improvement of the model, preferably by considering another degree of freedom, thus creating 2DOF simplified system.

This master's thesis continues investigating the behaviour of reinforced concrete structures and structural systems consisting of several members subjected to impulse loading, as it has been done before in six Master's Theses written by Nyström (2006), Ek and Mattsson (2009), Augustsson and Härenstam (2010), Andersson and Karlsson (2012), Carlsson and Kristensson (2012) and Klorek and Sandberg (2013).

1.2 Aim

The purpose of this thesis project was to further complement the simplified analysis approach for structures subjected to explosion loads, especially structures composed of several members.

Response of a structural system is a resultant of dynamic and structural properties of its individual components, and the 2DOF simplified model is believed to describe the behaviour in a better way. Thus, one of the objectives was to develop the equivalent 2DOF mass-spring system, so that the response of a beam-on-beams structure can be described by it with good accuracy. The behaviour of individual constitutive elements of the structural system in relation to the overall structure's behaviour is of particular interest, hence an investigation of the influence of surrounding structure on its member's response was needed. Furthermore, an additional aim of this master's thesis was to optimise the ordinary SDOF models, so that they are capable of describing the movement

of the constitutive elements of the structural system in an approximate way and within a limited range.

In order to further supplement the aims of this thesis project, a survey on how much can be gained if the element is treated as a part of a structure rather than a single member was desired.

1.3 Limitations

Pressure wave caused by an explosion load consists of both a positive and a negative pressure phase. The latter although much longer, is of considerably lower magnitude. It is common to disregard the negative phase when looking at structures with significantly slower dynamic response than the duration of the positive phase (Johansson and Laine 2012a). This was the case for this survey and so the negative phase was omitted.

2DOF (as well as SDOF) models are just a simplification of a continuous structure, which has infinitely many degrees of freedom. Moreover, the response obtained from Finite Element Method is considered to represent the real behaviour of the structure.

Material response of concrete is non-linear, yet it was simplified to elastic and elasto-plastic constitutive model. The discrepancy between reality and the models is assumed to be small and its influence on the response to be acceptably small.

In order to simplify the study, only simply supported beams or structural systems consisting of such beams were investigated. Moreover, only linear elastic material response is studied.

It is known, that material might obtain considerably greater strength when exposed to high strain rates. Impulse loading is such a case. However, this phenomenon of high strain rate behaviour was neglected.

No effect of time-dependent deformation such as creep and shrinkage was taken into account, which simplified things, having in mind that the material can be exposed to impulse loading at any time of its service life. Temperature effects were disregarded as well, considering that the thermal inertia of reinforced concrete is great enough to withstand temperature difference acting in very short time.

Lastly, only the initial response of structures subjected to explosion was studied. Influence of ground shock waves, impact loading from fragments of bombs or collapsed secondary structures was disregarded.

1.4 Method

In order to attain deeper knowledge of the subject, a literature study was conducted first. Studied materials include previous Master's Theses as well as books and articles written on the subject, and the results of this study is embodied in the first part of the report.

To correctly understand the behaviour of 2DOF system, SDOF systems with different material models were thoroughly studied first. Response of a simply supported beam transformed into such system was solved both with simplified hand calculations as well as with numerical solution based on Central Difference Method in GNU Octave (2014) and Finite Element solution in the commercial finite element analysis software ADINA

(2014). This part of the study is not included in the report, since it was already performed in the old Master's Theses, e.g. in Carlsson and Kristensson (2012), and therefore it was deemed unnecessary to repeat it.

In the next part of the report, as an intermediate step between a single member and a structural system, a beam on spring supports was studied. The procedure of solution was adequately modified to take into account the flexibility of the supports. FE models of such beams were created in ADINA. The structures were then transformed into equivalent SDOF systems and were examined both numerically and with respect to hand calculations.

As a subsequent portion of the thesis project, the finite element models of the structural systems were created, the behaviour of which is considered to represent reality. An equivalent 2DOF mass-spring system was constructed to simulate the response of the structures, and was studied numerically through comparison with the results of FE analyses. Optimisation of the 2DOF system was carried out, so that the simplified model reflected the behaviour of the structure observed in FE analyses. Moreover, a concise study is conducted, stating how much can be gained in terms of smaller deformation, if the element is treated as a part of a structure rather than a separate entity.

For the last part of the report, an ordinary SDOF system was altered in order to be able to simulate the deformation of the constitutive elements of the structural system, and an approximate range of application was searched for.

1.5 Outline of the report

Chapter 2 is a theory chapter based on the literature study performed. It covers basic explosion theory, material models, structural response of beams under load as well as basic dynamics and the concept of transformation into an equivalent mass-spring system.

Chapter 3 includes a parametric study of a beam supported on springs, since it is an intermediate step between the member's response and the response of a structural system. The procedure of transformation for a structure with varying beam-to-support stiffness ratio is developed.

Chapter 4 comprises the step-by-step development of an optimised 2DOF system capable of capturing the response of a structural system consisting of beam supported on two beams. The model is verified and its response compared to the FE solution, in terms of deformation, bending moment and shear force. An example of solution of an arbitrary beam-on-beams structural system is also included.

Chapter 5 includes comparison and development of modified SDOF systems, so that the response of individual members can be approximated with quicker and easier hand calculations. It studies several simplified models and shows the range of their application.

The results are presented and discussed along with tentative conclusions in every chapter. The last discussion and conclusions chapters summarise the whole project and pertain to all of the studies. Appendices present certain theory aspects, such as the Central Difference Method, as well as provide supplementary results and tabulated values.

2 Theory

2.1 Explosion

2.1.1 Explosion - what is it?

An explosion is a rapid release of energy with incidental instantaneous increase of volume, and as a result a pressure (and also heat) wave is generated. Two types of chemical explosions can be distinguished - detonations and deflagrations (Johansson and Laine 2012a). The former requires a supersonic passage of combustion front through the medium. The latter happens when the ambient medium ignition is a result of temperature rise which accompanies the adjacent material combustion. Such ignition advances at subsonic velocities. The shock wave front is usually spherical (or half-spherical if the explosion takes place on the ground). Duration of such process is normally in the range of milliseconds.

Normally, the released energy (in Joules) can be used to describe explosions. However, according to Johansson and Laine (2012a), a more common way is to express the explosion's strength as the mass of TNT required.

The distance between the source of explosion and the body subjected to the load coming from it has substantial influence on the amount of energy that reaches the body. The larger the distance, the less energy reaches the structure. The configuration of the detonation itself (i.e. point source, line source etc.) also has a big effect on the resultant incoming energy. Since the pressure wave spreads spherically, the energy is reduced cubically with distance from the source.

2.1.2 Shock wave

An explosion results in a shock wave. Such wave can have a quite complex form, but is often simplified to an idealised shock wave. A front reaches the object at the time of arrival t_a , when there is an instantaneous raise in pressure. The wave has a positive and negative pressure phase, which can be seen in Figure 2.1.

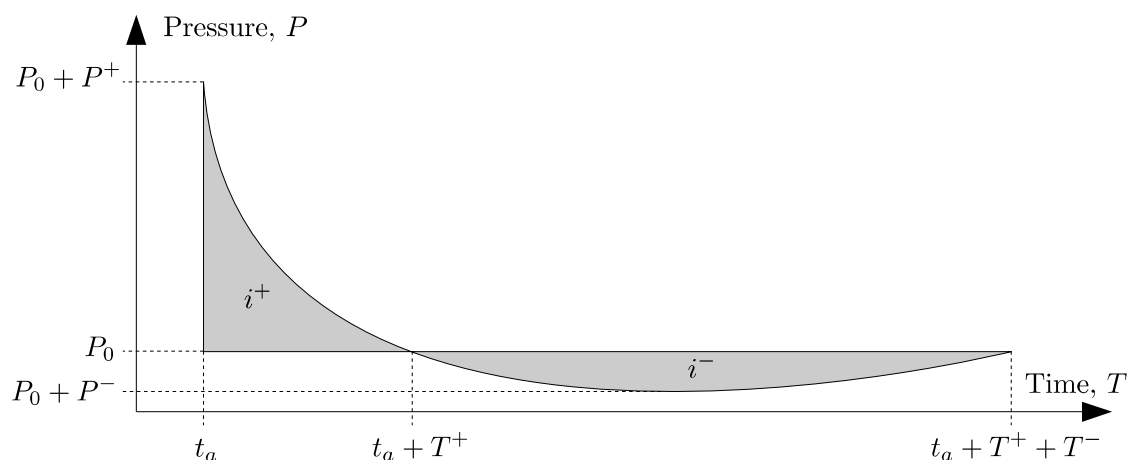


Figure 2.1: *Idealised shock wave.*

The area under the pressure-time graph is equal to the impulse intensity. The pressure of the positive phase is much larger in magnitude, but its duration is quite short compared to the negative phase. On the other hand, the negative pressure phase is of low magnitude. Because of that, the impulse load in both phases are almost equal to each other.

2.1.3 Wave phenomena

The surrounding of the source of explosion can cause various effects on the shock wave itself. Most importantly, it can and will be subjected to different wave phenomena, such as reflection or diffraction. Those can play an important role on the resulting load.

The pressure wave can reach a structure at different angles, which have influence on the pressure magnitude, but the most important fact is whether the wave is reflected by the structure or not. If the surface is perpendicular to the direction of wave propagation, then maximum reflection will take place. If the surface is parallel to the direction of propagation of the wave front, it can be considered that the wave is unreflected by the building, see Figure 2.2. The pressure of reflected wave is at least 2 up to 20 times greater than unreflected wave, which is a tremendous effect.

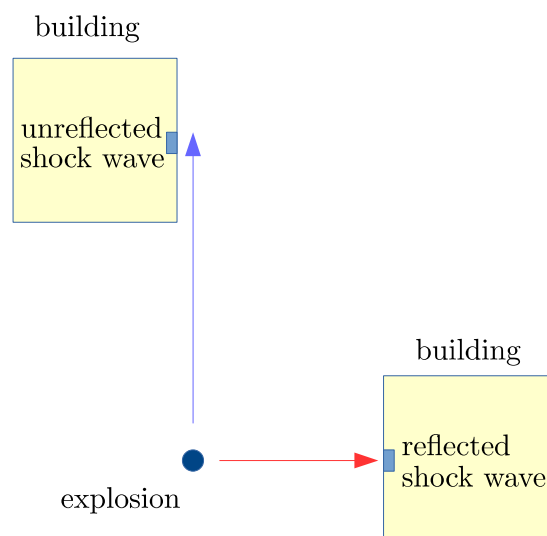


Figure 2.2: Reflection phenomenon in shock waves.

The other phenomenon of interest is diffraction. In this case diffraction can be described as change of the direction of wave propagation caused by irregularities and obstacles along its way. This means that even sides unexposed to the explosion can experience pressure load coming from an explosion. These wave phenomena are schematically illustrated in Figure 2.3.

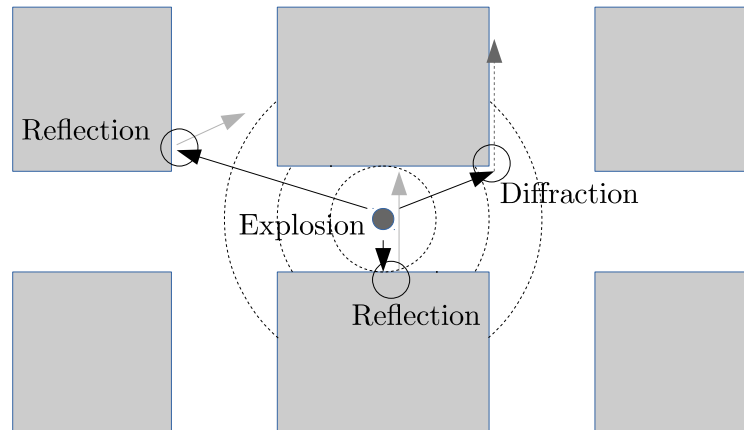


Figure 2.3: Reflection and diffraction phenomena.

2.1.4 Load on surface from explosion

Since the idealised shock wave has a complicated shape when it comes to describing the load (see Figure 2.1), a simplification is often made. The negative pressure phase is disregarded, and the positive pressure phase is converted into an equivalent triangular pressure load. In order to follow the process, the most important quantities and parameters must be introduced first.

- Amount of energy - W

Generally specified as the equivalent amount of TNT (in kg). When using other explosive than TNT, the energy output can be calculated as

$$W = w \cdot \text{equivalent weight factor} \quad (2.1)$$

where w is the mass of the explosive. Values for different types of explosive can be seen in Table 2.1.

- Scaled distance - Z

Scaled distance is a parameter that allows comparison between different charges detonated at different distances. For a detonation occurring with free expansion in every direction, a spherical wave front is created. In this case, the scaled distance can be expressed as

$$Z = \frac{r}{W^{1/3}} \quad (2.2)$$

where r is the distance from the source of explosion and W is the energy amount defined in Equation (2.1).

- Blast overpressure - P^+

This is the value of maximum overpressure that is carried by the wave front. For known scaled distance Z the value can be obtained e.g. from Figure 2.4.

Table 2.1: *Equivalent weight of various types of explosives. TNT as reference. From ConWep (1992).*

Explosive	Equivalent weight	
	Pressure	Impulse
ANFO	0.82	0.82
Composite A-3	1.09	1.07
Composite B	1.11	0.98
Composite C-4	1.37	1.19
H-6	1.38	1.15
HBX-1	1.17	1.16
Pentolite	1.42	1.00
RDX	1.42	1.00
TNT	1.00	1.00
Tritonal	1.07	0.96

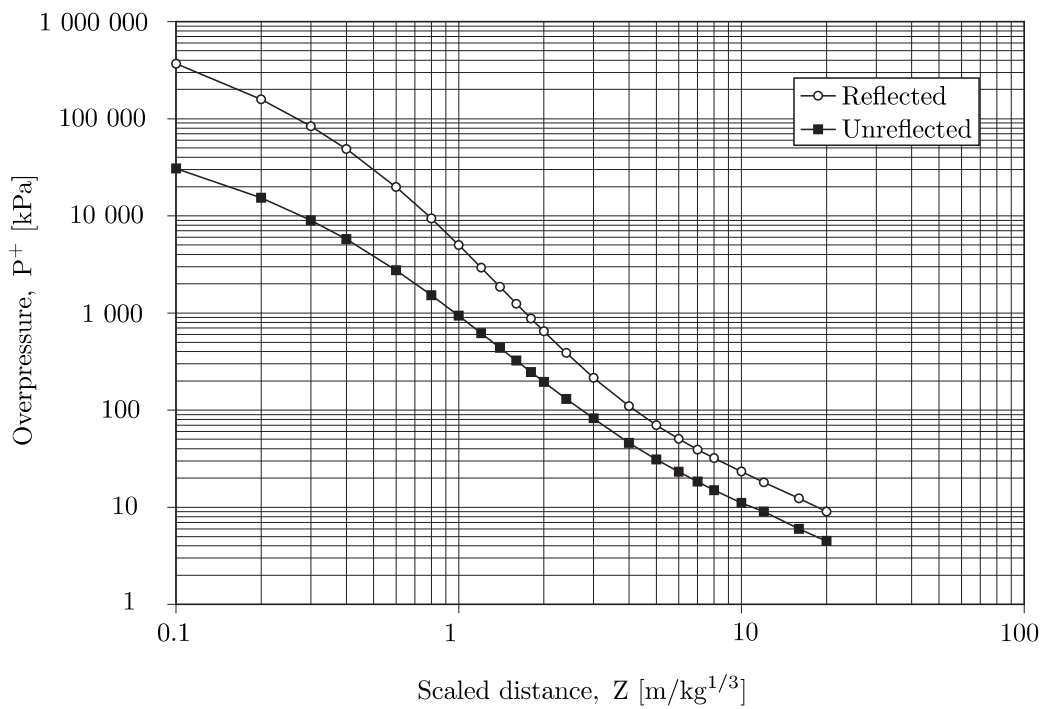


Figure 2.4: *Reflected and unreflected overpressure as a function of scaled distance Z. From Johansson et al. (2014).*

- Positive phase impulse intensity - i^+

The impulse intensity can be described as

$$i^+ = \int_{t_a}^{t_a+T^+} (P(t) - P_0) dt \quad (2.3)$$

where $P(t)$ defines the variation of the absolute pressure with time, and P_0 is the ambient pressure of undisturbed air. The value can be obtained for a known scaled distance Z from Figure 2.5.

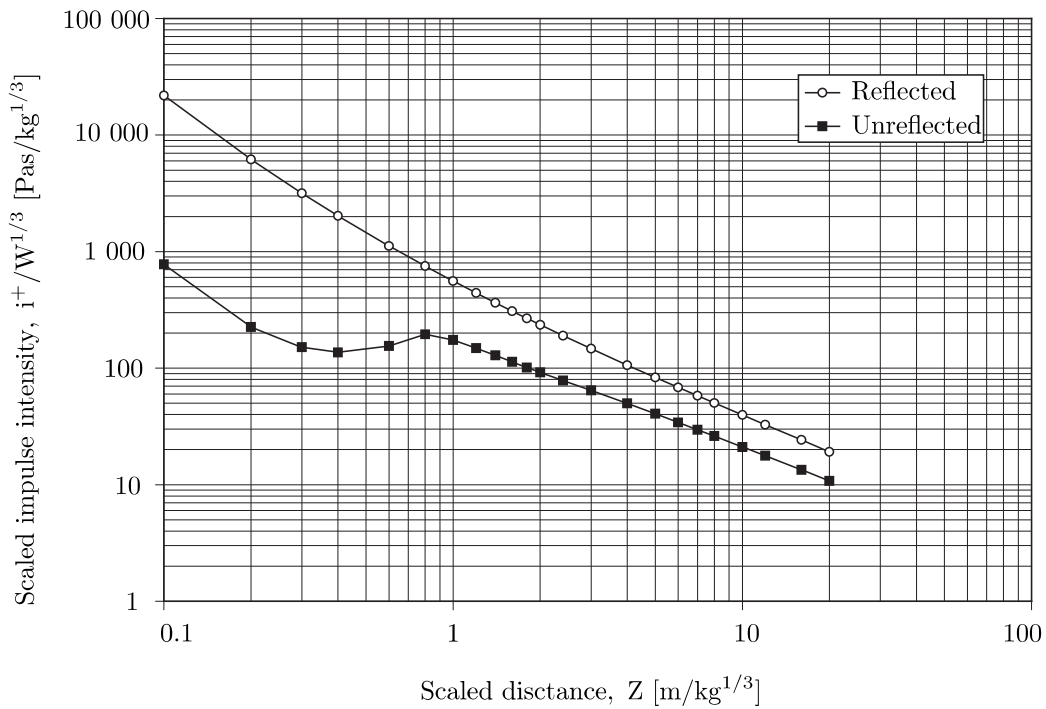


Figure 2.5: *Reflected and unreflected impulse intensity as a function of scaled distance Z. From Johansson et al. (2014).*

- Fictitious duration - t_{Δ}^+

This parameter describes the duration of the simplified idealised shock wave, see Figure 2.6. Note that it is shorter than the duration of idealised shock wave t_a . When blast overpressure P^+ and impulse intensity i^+ are known, the fictitious duration can be calculated as

$$t_{\Delta}^+ = \frac{2i^+}{P^+} \quad (2.4)$$

With all these parameters known, the simplified idealised shock wave can easily be determined, see Figure 2.6.

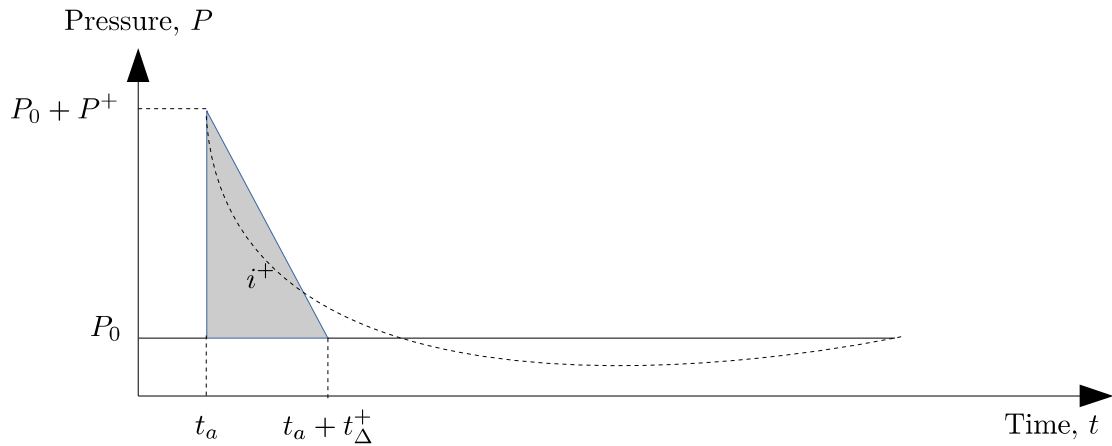


Figure 2.6: *Simplified idealised shock wave.*

2.2 Structural models

2.2.1 General notes

Reinforced concrete structures are of particular interest in this project. Since its response under imposed load is complex, it is preferable to simplify it by adopting suitable response models. Simplified material models result in simplified structural response. The model used in this project is a linear elastic model, although ideally plastic and elastoplastic model are also discussed. The material response of concrete and reinforcing steel is presented for reference in this chapter as well.

2.2.2 Linear elastic

In a linear elastic material model the relationship between stress σ and strain ε is linear. The inclination of stress-strain curve is equal to Young's modulus E . There is also no plastic strain, which means that for increasing stress, strain increases as well (with no limit). It is important to note that when unloaded, the strain will go back to its initial value, which is zero for completely removed load. The stress-strain relationship is presented in Figure 2.7 and can be expressed as:

$$\sigma = E \cdot \varepsilon \quad (2.5)$$

When a displacement u is induced in linear elastic material, a corresponding internal resistance force R is achieved, and the structural response of linear elastic model can be described as:

$$R = k \cdot u \quad (2.6)$$

The inclination of the response curve is k , which can be referred to as the stiffness of the material, see Figure 2.7. In this thesis project, the linear elastic structural model is referred to as just elastic.

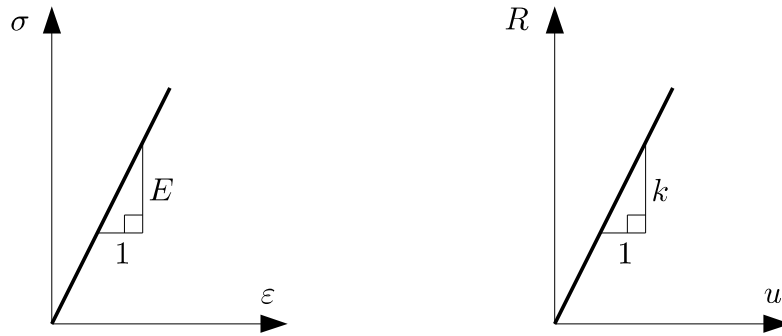


Figure 2.7: *Linear elastic material model.*

2.2.3 Ideally plastic

In an ideally plastic structural model, the strains are zero until the yield stress is reached. Theoretically, the deformations could be infinite for the same value of yield stress, but in practice there are some limits such as ultimate steel strain ϵ_u , or plastic rotation capacity for a structure. The behaviour can be seen in Figure 2.8. For an external force F acting on the structure, the internal resistance force R is defined as

$$R = \begin{cases} F & \text{if } u = 0 \\ R_m & \text{if } u > 0 \end{cases} \quad (2.7)$$

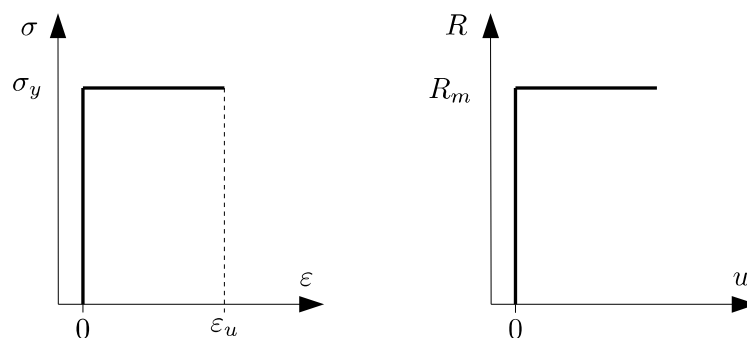


Figure 2.8: *Ideally plastic material model.*

2.2.4 Elastoplastic

An elastoplastic structural model is a hybrid between linear elastic and ideally plastic models. Strains are proportional to the stresses up until the stress reaches the material yield stress σ_y at the deformation of $u_{ep,el}$. After that, plastic strain develops. Even when the load is removed, plastic strains will still be present in the material. On reloading, the material will follow the elastic curve up until the yield stress is reached, which can be seen in Figure 2.9.

For an external force F acting on the body, the internal resistance force R can be defined as

$$R = \begin{cases} ku_{ep,el} & \text{if } u \leq u_{ep,el} \\ R_m & \text{if } u > u_{ep,el} \end{cases} \quad (2.8)$$

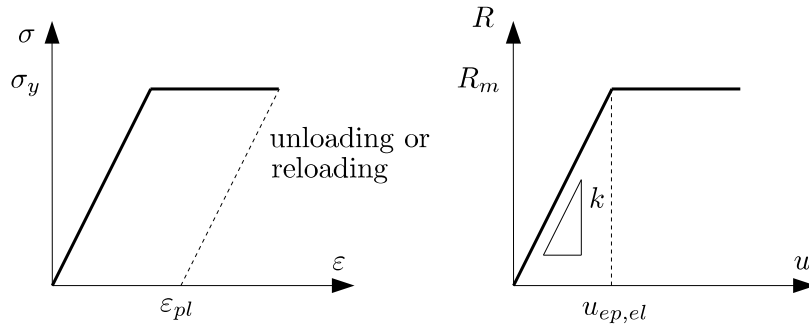


Figure 2.9: *Elastoplastic material model.*

2.2.5 Concrete

The stress-strain behaviour of concrete under load is schematically shown in Figure 2.10. From this it can be seen that concrete has non-linear behaviour in both compression and tension. However, in the initial stage of loading, the material response can be approximated to linear elastic. It should be noted that compressive strength of concrete can be up to 10 times higher than its tensile strength.

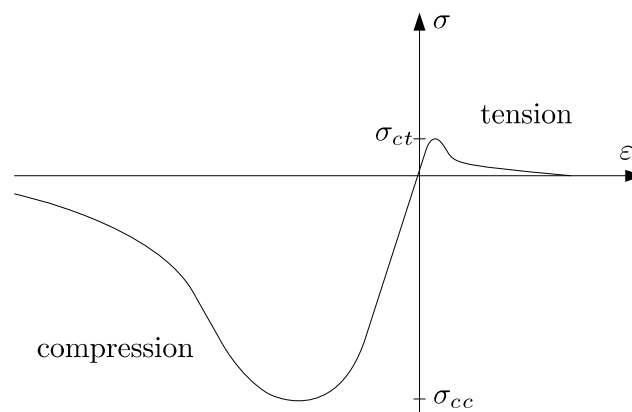


Figure 2.10: *Material response of concrete.*

2.2.6 Reinforcing steel

Steel shows linear elastic behaviour in the beginning of loading, up to the point when the stress reaches the yield strength f_{sy} . After that, the material enters a plastic plateau, when the strain increases without increase of stress. After the plateau phase, strain hardening starts and the strain increases with stress, although in a non-linear manner. After reaching the ultimate tensile stress f_{su} , strains increase until rupture. The behaviour can be seen in Figure 2.11. According to Eurocode 2, CEN (2004), the stress-strain relationship for reinforcing steel can be simplified to an elastoplastic model with or without strain hardening after reaching the yield strength f_{sy} .

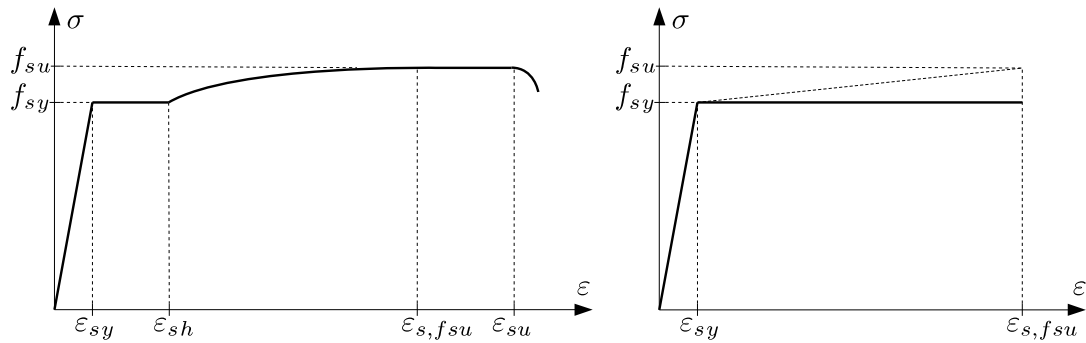


Figure 2.11: *Material response of reinforcing steel according to tests and simplified model in Eurocode 2 (CEN (2004)).*

The amount of plastic deformation before rupture can be directly related to ductility of the reinforcement. If the reinforcement is ductile, it can deform quite much before breaking and therefore it can absorb more energy. Such behaviour is called ductile fracture and is favourable in design, as it can indicate possible failure situations. Hot-rolled steel is ductile. Opposite behaviour is called brittle fracture, and happens when material breaks abruptly without any prior indication. Cold-worked steels are brittle.

Ductility of reinforcement is very important when plastic rotation is needed in the structure. Plastic rotation depends on the ductility of reinforcement, see Section 2.3.3 for more information. Reinforcement comes in Class A, B and C, when ductility is concerned, with class C being the most ductile steel.

2.3 Structural response of beams under load

2.3.1 Response of reinforced concrete cross section under load

The response of a reinforced concrete cross section subjected to a bending moment is non-linear. It is therefore simplified in Eurocode 2, CEN (2004), into three states. A summary of those can be seen in Figure 2.12.

In state I, the section is assumed to be uncracked and the reinforcement does not have much influence. Stresses and strains vary linearly. Moment of inertia I_I and the position of neutral axis can be easily determined.

In state II the concrete is cracked and its influence is disregarded. The position of the neutral axis shifts, and the tensile forces are assumed to be taken entirely by the reinforcing bars. Stresses in concrete are still assumed to vary linearly. The reinforcement can be converted to equivalent concrete areas and sectional constants so that moment of inertia I_{II} can be calculated.

In state III, which can be referred to as the ultimate state, the reinforcement bars are assumed to be yielding, and the stress variation in concrete is no longer linear. The section can fail either by crushing of concrete or rupture of reinforcement. Stress block factors α_R and β_R can be obtained from Engström (2011) depending on the highest concrete strain.

The curvature $\frac{1}{r}$ of the cross section can always be calculated as the inclination of the strain distribution curve (Engström 2011). However, in linear elastic analysis it is more

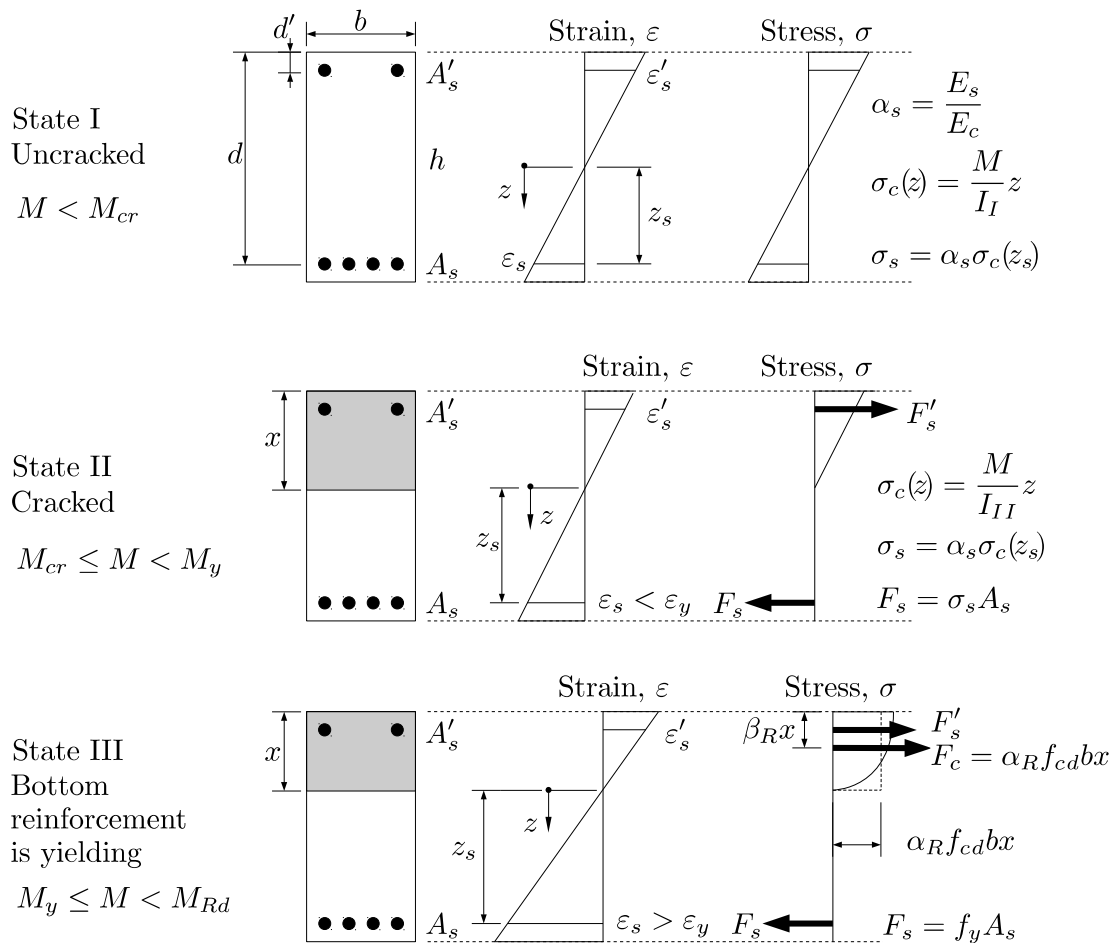


Figure 2.12: Different states in concrete cross section subjected to pure bending.

common to define it as the ratio between bending moment and the flexural rigidity of the cross section, as:

$$\frac{1}{r} = \frac{M}{EI} \quad (2.9)$$

Bending moment acting on the section results in a certain curvature. A typical moment-curvature relationship can be seen in Figure 2.13.

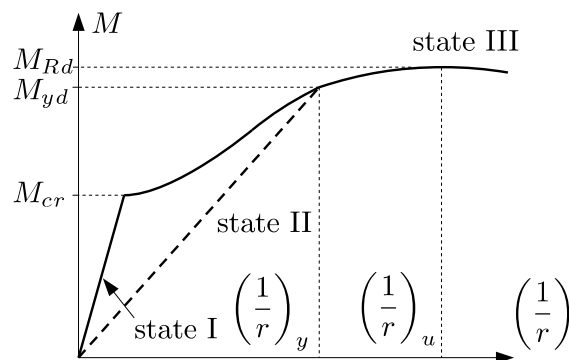


Figure 2.13: Typical moment-curvature relation.

The influence of all states (I to III) can be seen in this curve. First, when the concrete is uncracked, the behaviour is linear, which results in a constant slope (stiffness in state I - EI_I) in the beginning of the diagram. When the cracking moment M_{cr} is reached, the section cracks and loses stiffness at the same time. After that point, the state II model applies. In Figure 2.13 it can be seen that the behaviour in state II is not linear (although this is due to so-called tension stiffening effect, which is not discussed here). Nevertheless, an approximate stiffness in state II - EI_{II} can be calculated. When the curvature $(\frac{1}{r})_y$ is reached, the reinforcement starts to yield. Maximum curvature $(\frac{1}{r})_u$ is achieved when either concrete crushes or reinforcement strain exceeds its strain limit value (plastic rotation capacity exceeded). The corresponding moments - M_{cr} , M_{yd} and M_{Rd} must be obtained from sectional analyses. More information as well as the methodology of the calculation can be found in Engström (2011).

The moment-curvature relation is often simplified to a bi-linear correlation, which can be seen in Figure 2.14. It is clearly visible that the simplification results in slightly smaller overall stiffness, thus giving conservative results. However, according to Engström (2011), this simplification is enough to compute the plastic rotation capacity. It is important to mention that such simplification results in a structural response as shown in Figure 2.9.

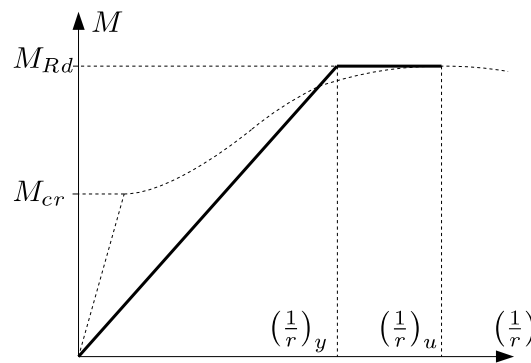


Figure 2.14: *Simplified bi-linear moment-curvature relation.*

2.3.2 Theory of plastic hinges

When a cross section starts yielding, the deformation (and therefore strains) increase when the load remains constant. The whole cross section is assumed to plasticise under the ultimate moment M_y , i.e. the stresses in the cross section will be either σ_y or $-\sigma_y$, changing sign at the neutral axis. The plastic neutral axis is not necessarily situated in the same position as the elastic neutral axis. However, this depends on the shape of the cross section. The position of the elastic neutral axis can be determined by equilibrium of first moments of area at both sides of the axis, while the plastic neutral axis divides the cross section into two equal areas, since the stresses are the same all over the parts. This is illustrated in Figure 2.15.

The plastic section modulus can be calculated as

$$W_{pl} = \frac{A}{2} \cdot z \quad (2.10)$$

where A is the area of the whole cross section.

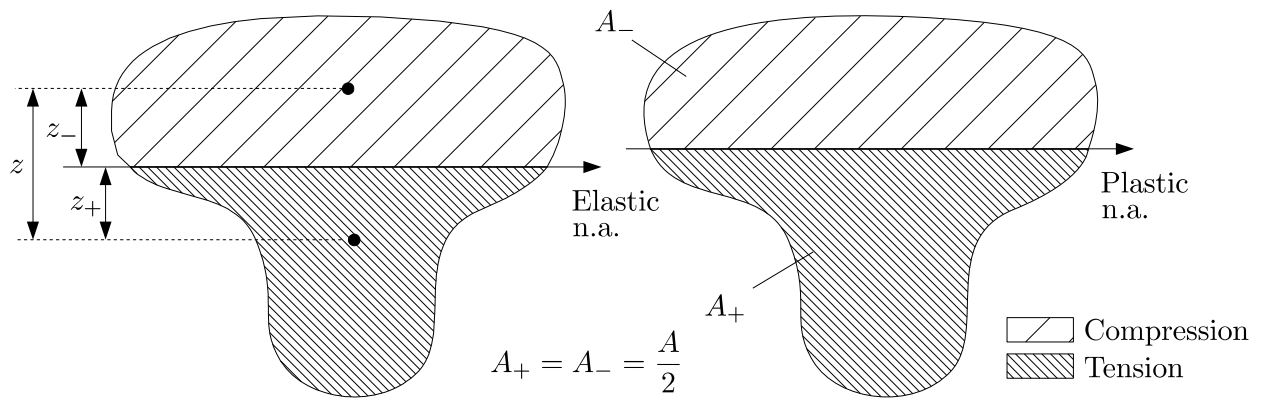


Figure 2.15: Fully plasticised arbitrary cross section.

For example, the plastic section modulus for a rectangular cross section would be

$$W_{pl} = \frac{bh}{2} \cdot \frac{h}{2} = \frac{bh^2}{4}$$

while the elastic section modulus for the same section is

$$W_{el} = \frac{bh^2}{6}$$

Therefore the ratio between plastic and elastic modulus for a rectangular cross section is 1.5. This means that theoretically, the load bearing capacity in a plastic model can be increased with 50 % with regard to the elastic model. This ratio depends on the shape of the cross section.

It is also worth to mention that if the cross section is not symmetric about the neutral axis (elastic or plastic neutral axis), then the section modulus will vary, i.e. the section modulus with respect to top fibres will differ from the one calculated with respect to bottom fibres.

Since according to the theory of plasticity there is no limit to plastic strain, the curvature of a small region of the beam may be much larger than for the rest of the structure. Provided the ductility of reinforcing steel is large enough, this critical section may experience substantial deformation under constant moment M_{Rd} . When this moment is reached, the section is considered to become a so-called plastic hinge. Creation of a plastic hinge does not mean that the load bearing capacity of the beam is reached, rather that the boundary conditions are changed. Provided that the beam was statically indeterminate, it can still take more load, until another plastic hinge (or hinges) develops. A structure that is n times statically indeterminate, can develop $n + 1$ plastic hinges before the collapse mechanism is formed. The principle can be seen in Figure 2.16.

For static load, when the critical number of plastic hinges is reached, the collapse mechanism is formed and the structure collapses. However, for impulse loads, a mechanism is desired. Such mechanism is active until the plastic hinge reaches its plastic rotation capacity (i.e. cannot deform anymore). This is an important difference between static and impulse loading.

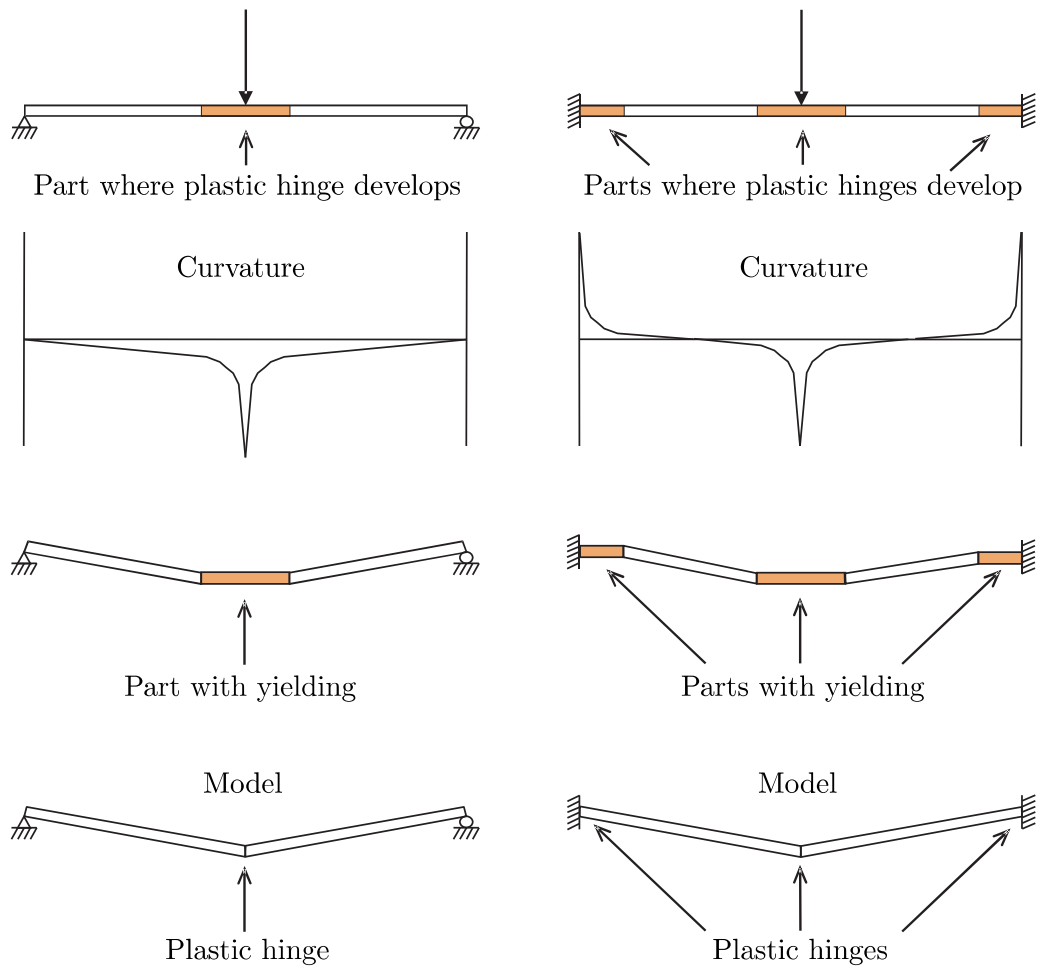


Figure 2.16: *Plastic hinges and collapse mechanisms for simply supported and fixed beam, from Nyström (2006).*

2.3.3 Plastic rotation capacity

According to theory of plasticity, the plastic deformation has no limit. However, this is not the case in real structures. When designing impulse loaded structures, the structure must be able to withstand the largest deformation that the load caused. Normally, it is not a problem to develop a mechanism. However, it can be problematic to maintain the mechanism until desired deformation is reached. For simply supported beam such a mechanism can be seen in Figure 2.17.

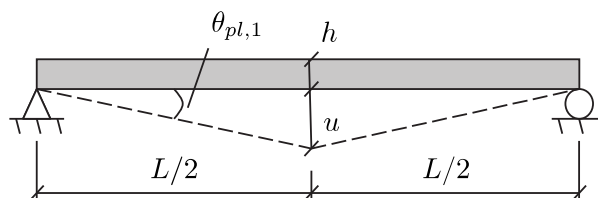


Figure 2.17: *Mechanism shape and plastic rotation for simply supported beam. From Klorek and Sandberg (2013).*

According to Engström (2011), plastic hinges can be classified as single or double. Single plastic hinges are formed at fixed ends or near frame joints. Double plastic hinges are formed in the span or over intermediate support. For the simply supported beam, the plastic hinge will develop in the place, where the maximum bending moment is present. Depending on loading conditions, it does not need to be in the mid-span, but it is often so. In such a case the total plastic rotation is $\theta_{pl} = \theta_{pl,1} + \theta_{pl,2}$, see Figure 2.18.

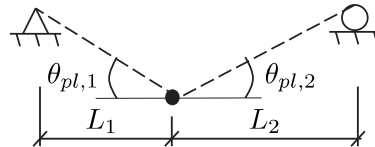


Figure 2.18: Double plastic hinge in the span. From Engström (2011).

The plastic rotation itself can be determined in many different ways. In this project, the provisions included in Eurocode 2, CEN (2004), were used. By using the graph in Figure 2.19, the basic value of allowable rotation θ_{pl} can be obtained. It depends on the ductility class of the reinforcement and the ratio of the compressive zone height to effective depth - $\frac{x}{d}$.

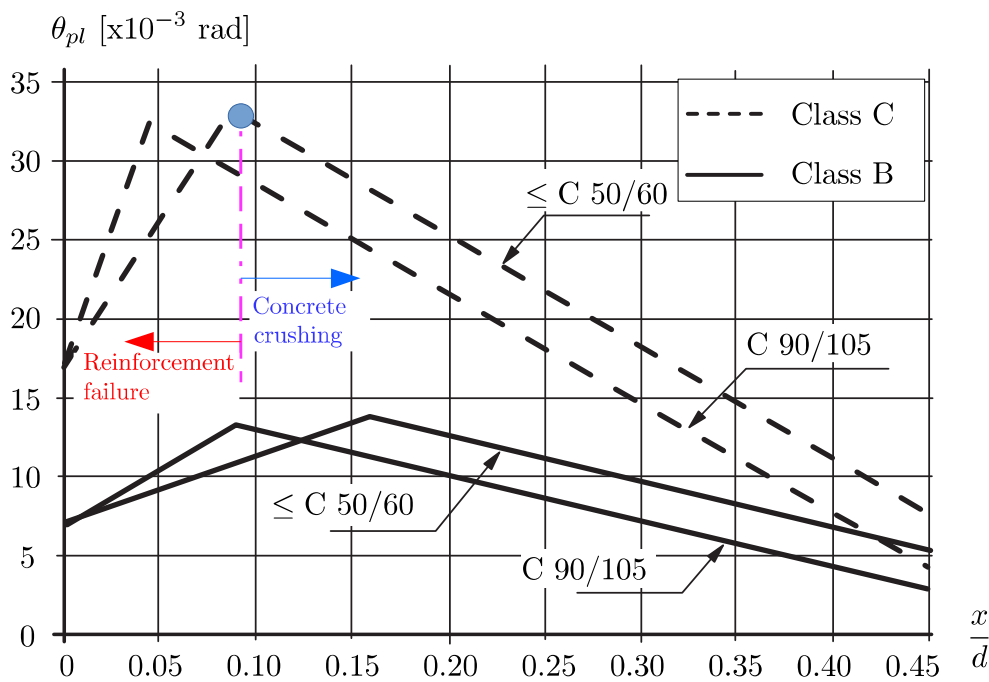


Figure 2.19: Relation between basic value of allowable rotation and $\frac{x}{d}$ ratio.

Furthermore, the received value must be multiplied with a correction factor k_λ , which can be expressed as

$$k_\lambda = \sqrt{\frac{\lambda}{3}} \quad (2.11)$$

where λ is a function of L_0 - distance between respective plastic hinge and adjacent zero

moment section, and d - effective depth.

$$\lambda = \frac{L_0}{d} \quad (2.12)$$

Eventually, the rotation capacity of the plastic hinge can be defined as

$$\theta_{rd} = k_\lambda \cdot \theta_{pl} \quad (2.13)$$

According to Johansson and Laine (2012b), the values in Figure 2.19 correspond to the rotation at one side of the plastic hinge. When the plastic hinge develops in the mid-span, the allowable plastic rotation read from the graph, θ_{pl} , can be doubled. The maximum possible deformation that the structure can withstand can be expressed as a function of the plastic rotation capacity, θ_{rd} . For a simply supported beam with a uniformly distributed load or point load in the mid-span, the maximum deformation as seen in Figure 2.17 can be calculated as:

$$u_{rd} = \frac{\theta_{rd} \cdot L}{2} \quad (2.14)$$

where θ_{rd} is the rotation capacity of the plastic hinge. This expression takes into account the provisions included in Johansson and Laine (2012b), i.e. that the allowable rotation read from Eurocode 2 can be doubled.

It can be seen from Figure 2.19 that for low values of x/d the member will fail with rupture of reinforcement bars. For higher values of x/d the failure will be caused by crushing of concrete. Reinforcement class C is much more ductile than class B, therefore this type is preferable in structures subjected to explosion loads.

2.4 Work and energy

2.4.1 Fundamental parameters

In order to better understand the design approach for dynamically loaded structures, some basic notions must first be defined.

- Velocity

Velocity is a vector quantity which defines the rate of change of position of an object. If the change of position is denoted as Δu , and the time required for this shift to take place is denoted as Δt , then the velocity of the body can be defined as

$$v = \lim_{\Delta t \rightarrow 0} \frac{\Delta u}{\Delta t} = \frac{du}{dt} = \dot{u} \quad (2.15)$$

- Acceleration

Acceleration is a vector quantity describing the rate of change of velocity of a body. If the change of velocity is denoted as Δv , and the time required for this shift to take place is denoted as Δt , then the acceleration of the body can be defined as

$$a = \lim_{\Delta t \rightarrow 0} \frac{\Delta v}{\Delta t} = \frac{dv}{dt} = \ddot{u} \quad (2.16)$$

- Force

Force is a vector quantity, and according to Newton's Second Law, the net force acting on a body is equal to its mass times its acceleration.

$$F = m \frac{dv}{dt} = ma \quad (2.17)$$

- Pressure

Pressure is a scalar quantity, and it can be defined as force distributed over an area on which this force is acting.

$$P = \frac{F}{A} \quad (2.18)$$

- Momentum

Momentum is a vector quantity, and it is a product of the mass of a body and its velocity.

$$p = mv \quad (2.19)$$

The law of conservation of momentum implies that for a closed system, which is not affected by external forces, the total momentum of the system cannot change.

- Impulse

If a force F is applied to the body for the time interval Δt , the momentum of the body changes as

$$\Delta p = F \Delta t \quad (2.20)$$

If the force is time dependent, then the resulting momentum change from time t_1 to time t_2 can be defined as

$$\Delta p = \int_{t_1}^{t_2} F(t) dt = I \quad (2.21)$$

where I is the resulting impulse. Equation (2.21) can be rewritten using relations from Equations (2.16) and (2.17) as

$$I = \int_{t_1}^{t_2} ma(t) dt = m \int_{t_1}^{t_2} a(t) dt = mv \quad (2.22)$$

Explosion shock waves are measured in pressure. Therefore by using Equation (2.18) in Equation (2.21), an expression for impulse as a function of pressure can be obtained:

$$I = A \int_{t_1}^{t_2} P(t) dt \quad (2.23)$$

- Impulse intensity

Impulse intensity is the ratio of the magnitude of impulse to the area on which it is acting.

$$i = \frac{I}{A} = \int_{t_1}^{t_2} P(t) dt \quad (2.24)$$

Therefore the intensity of the impulse can be understood as the area under the pressure-time curve, see Figure 2.20.

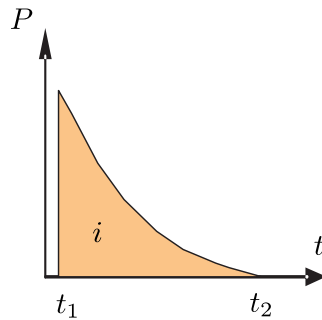


Figure 2.20: *Impulse intensity as the area under pressure-time curve.*

2.4.2 Characteristic impulse

There are two extreme cases of an impulse. Either the impulse is infinitely large for an infinitesimally small time, or there is a smaller force acting for an infinitely long time. The first case is called the characteristic impulse I_k , see Figure 2.21a and Figure 2.21b.

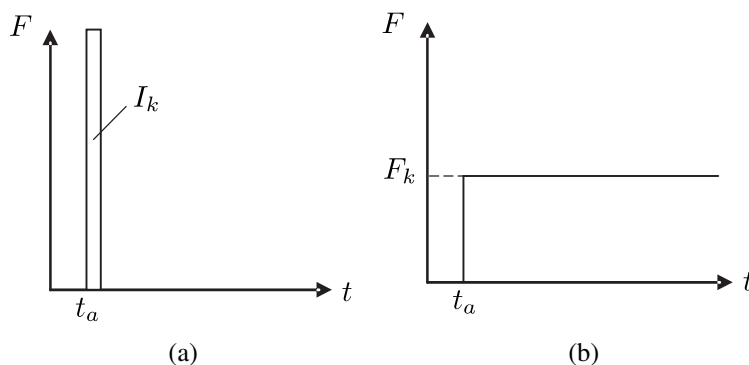


Figure 2.21: *Extreme cases for an impulse - (a) characteristic impulse I_k and (b) characteristic pressure load F_k .*

If the structure has zero resistance (i.e. $R = 0$), then there is no difference in what does $F(t)$ look like. As long as the same impulse I is transferred to the body, the final response will be the same, because the transferred energy is the same in every case. If the structure resistance is non-zero ($R \neq 0$), this does not apply any more, and the shape of $F(t)$ has influence on the final response. If an impulse I approaches the value of a characteristic impulse I_k , the significance of resistance being different than zero diminishes, and for $I = I_k$ the same final response is obtained as if there was no resistance in the structure (i.e. $R = 0$). External work and energy expressions defined in Section 2.4 are valid for characteristic impulse I_k . For impulses other than characteristic, a way of modifying an arbitrary impulse into equivalent characteristic impulse is needed. An arbitrary impulse can be transformed to the characteristic one with the correction factor γ_I , defined as:

$$I_k = \frac{I_1}{\gamma_I} \quad (2.25)$$

The procedure is thoroughly described in Johansson and Laine (2012b). The correction factor is a function of the type of impulse load, see Figure 2.22. The three types of impulse load are described by the equation:

$$F(t) = F_I \left(1 - \frac{t}{t_1}\right)^n \quad (2.26)$$

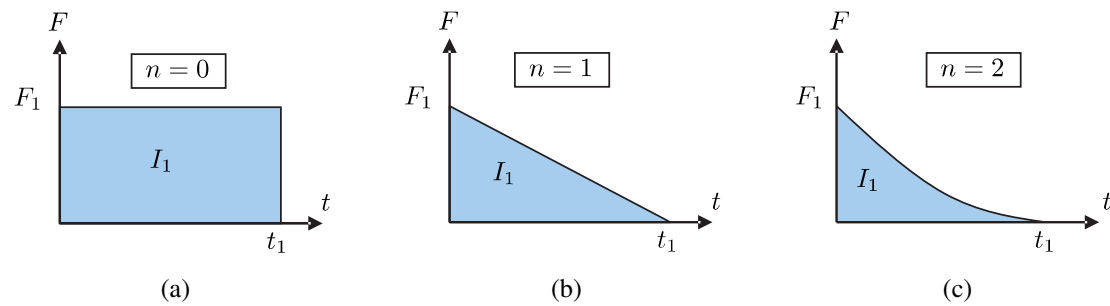


Figure 2.22: Types of impulse loads - (a) rectangular load, (b) triangular load, (c) quadratic decreasing load. From Johansson et al. (2014).

Elastic model

In case of elastic response, the correction factor γ_I is also a function of the fundamental period of the system, which can be described as

$$T = \frac{2\pi}{\omega} \quad (2.27)$$

where ω is the fundamental angular frequency of the system. The ratio between the maximum load F_1 and the characteristic load F_k is denoted as

$$\gamma_F = \frac{F_1}{F_k} \quad (2.28)$$

According to Johansson and Laine (2012b), the correction factor γ_I can be obtained from Table 2.2.

Table 2.2: Relation between the error δ_{el} , the ratio $\frac{T}{t_1}$, and the impulse load correction factor γ_I for load types according to Figure 2.22. From Johansson et al. (2014).

δ_{el} [%]	γ_I [-]	$\frac{T}{t_1} = \pi \cdot \frac{\gamma_F}{\gamma_I}$ $n = 0$	$\frac{T}{t_1} = \frac{\pi}{2} \cdot \frac{\gamma_F}{\gamma_I}$ $n = 1$	$\frac{T}{t_1} = \frac{\pi}{3} \cdot \frac{\gamma_F}{\gamma_I}$ $n = 2$
1	1.01	12.89	10.60	8.84
2	1.02	9.22	7.45	6.13
3	1.03	7.51	6.10	5.00
4	1.04	6.52	5.33	4.35
5	1.05	5.86	4.75	3.90
10	1.10	4.20	3.41	2.78
15	1.15	3.48	2.82	2.29
20	1.20	3.06	2.47	1.98
25	1.25	2.78	2.23	1.77
50	1.50	2.10	1.56	1.18
75	1.75	1.80	1.23	0.91
100	2.00	1.57	1.02	0.74

For example, for a ratio of $T/t_1 = 3.41$ and the impulse type that corresponds to $n = 1$, Table 2.2 gives $\gamma_I = 1.10$. Therefore, the characteristic impulse is calculated as $I_k = I_1/1.10$.

Plastic model

In case of plastic response, the correction factor γ_I is a function of parameter γ_F , which is defined as the ratio between the maximum load F_1 and internal resistance R .

$$\gamma_F = \frac{F_1}{R} \quad (2.29)$$

According to Johansson and Laine (2012b), the correction factor γ_I can be obtained from Table 2.3.

Table 2.3: *Relation between the error δ_{el} , the load factor γ_F , and the impulse load correction factor γ_I for load types according to Figure 2.22. From Johansson et al. (2014).*

δ_{el} [%]	γ_I [-]	$\gamma_F = \frac{F_1}{R}$ $n = 0$	$\gamma_F = \frac{F_1}{R}$ $n = 1$	$\gamma_F = \frac{F_1}{R}$ $n = 2$
1	1.005	100	-	-
2	1.010	52	70	77
3	1.015	35	46	52
4	1.020	27	35	39
5	1.025	21	29	32
10	1.049	11	15	17
15	1.072	7.7	10	12
20	1.095	6.0	8.0	9.0
25	1.118	5.0	6.7	7.5
50	1.225	3.0	4.0	4.5
75	1.323	2.3	3.1	3.5
100	1.414	2.0	2.7	3.0

For example, for a ratio of $F_1/R = 15$ and the impulse type that corresponds to $n = 1$, Table 2.3 gives $\gamma_I = 1.049$. Therefore the characteristic impulse is calculated as $I_k = I_1/1.049$.

2.4.3 External work

Work defines the change of energy. Since according to energy conservation rule, no energy can vanish, work is needed to transform energy from one kind to another. External work is the amount of energy that is released and acts on the structure due to an explosion. It is denoted here by W_e .

According to Section 2.4.1, the increase in momentum of a body is equal to the impulse that acts on that body. Before the explosion, the body has no velocity. The explosion load can be simplified to a characteristic impulse, I_k (see Section 2.4.2). The momentum of the system must be preserved, from definition of impulse in Equation (2.22), the velocity of the body is

$$v = \frac{I_k}{m} \quad (2.30)$$

The amount of external kinetic energy transferred to the structure is then

$$E_k = \frac{mv^2}{2} = \frac{I_k^2}{2m} \quad (2.31)$$

If the impulse is the characteristic impulse, i.e. it acts over infinitely short time, then it might be assumed that the external energy is fully converted to the kinetic energy of

the structure. If the impulse acts over a longer time, then the structure will transform part of the external energy into the internal energy (as it deforms under load, i.e. the internal resistance of structure $R \neq 0$), even if the value of impulse is the same as the characteristic one. This means, that the external work applied on the body can be equal to the external kinetic energy only in the case of characteristic impulse. Transformation of arbitrary impulse into characteristic impulse is presented in Section 2.4.2. Influence of the impulse duration on external work can be seen in Figure 2.23.

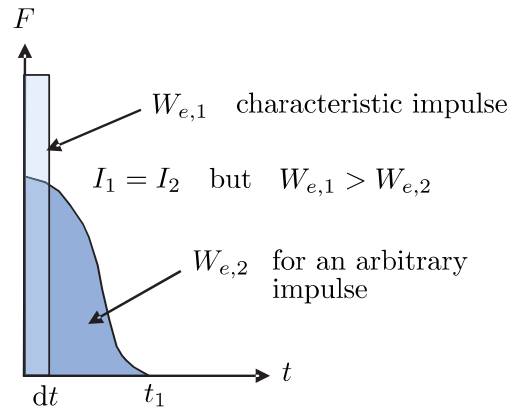


Figure 2.23: *Influence of impulse duration on the value of external work. From Klorek and Sandberg (2013).*

In the case of a characteristic impulse, it can be stated that the external work applied on the structure is

$$W_e = E_k = \frac{I_k^2}{2m} \quad (2.32)$$

2.4.4 Internal work

If the structure is subjected to an action of external work, it will start to deform. These deformations will cause the energy to be stored as potential energy (spring and mass analogy). If energy losses due to e.g. friction are disregarded, the element will deform as long as the whole kinetic energy is converted into potential energy, or until it collapses. Dynamically loaded structures vibrate about the equilibrium position. This means that after the whole energy has been stored as potential energy in the form of deformations, the structure will start to sway back (provided that there is elastic energy stored in the body), losing this energy and converting it to kinetic energy again. This process is recurring and as long as there is no damping or other forms of energy losses, it will continue. The change of potential energy of the structure is described by the internal work W_i and is studied in this section for different material response models.

Elastic model

The response of an elastic model can be seen in Figure 2.24, with the work being the area under the force-displacement diagram.

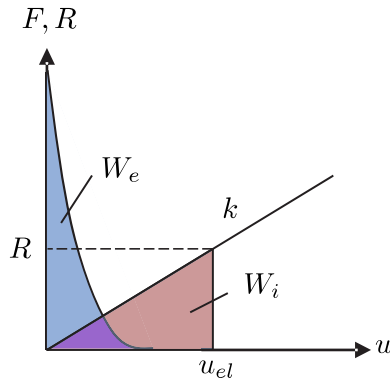


Figure 2.24: *Internal and external work in elastic response. From Johansson and Laine (2012b).*

The internal work in this case can be expressed as:

$$W_i = \frac{ku_{el}^2}{2} \quad (2.33)$$

From the conservation of energy law, i.e. $W_i = W_e$, we get:

$$\frac{I_k^2}{2m} = \frac{ku_{el}^2}{2} \quad (2.34)$$

After substituting $\omega = \sqrt{\frac{k}{m}}$ in Equation (2.34), the correlation for the maximum deformation may be expressed as:

$$u_{el} = \frac{I_k}{m\omega} \quad (2.35)$$

Plastic model

The response of a perfectly plastic model can be seen in Figure 2.25.

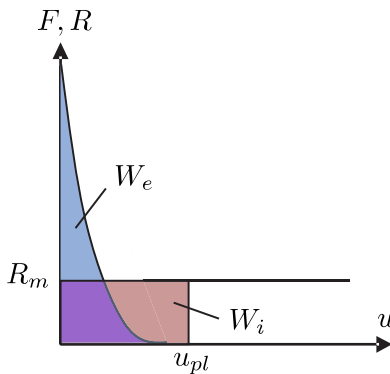


Figure 2.25: *Internal and external work in plastic response. From Johansson and Laine (2012b).*

The internal work in this case can be expressed as:

$$W_i = R_m u_{pl} \quad (2.36)$$

From the conservation of energy law, i.e. $W_i = W_e$, we get:

$$\frac{I_k^2}{2m} = R_m u_{pl} \quad (2.37)$$

The maximum deformation for a perfectly plastic material response is

$$u_{pl} = \frac{I_k^2}{2mR_m} \quad (2.38)$$

Elastoplastic model

The elastoplastic response is the most complex of the three models considered. The work equilibrium can be seen in Figure 2.26.

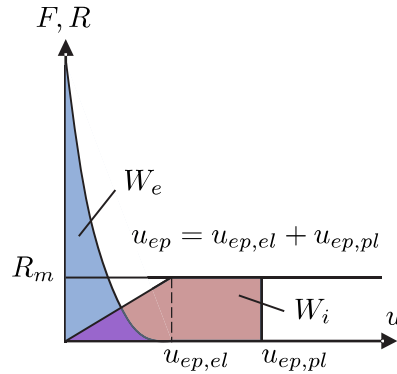


Figure 2.26: *Internal and external work in elastoplastic response. From Johansson and Laine (2012b).*

where the total deformation u_{ep} is a sum of total elastic deformation $u_{ep,el}$ and total plastic deformation $u_{ep,pl}$.

Internal work for this response can be written as

$$W_i = \frac{R_m u_{ep,el}}{2} + R_m u_{ep,pl} = \frac{R_m}{2} (u_{ep,el} + 2u_{ep,pl}) \quad (2.39)$$

From the conservation of energy law, i.e. $W_i = W_e$, we get:

$$\frac{I_k^2}{2m} = \frac{R_m}{2} (u_{ep,el} + 2u_{ep,pl}) \quad (2.40)$$

Hence, by inserting Equation (2.38) into Equation (2.40)

$$u_{ep,pl} = \frac{I_k^2}{2mR_m} - \frac{u_{ep,el}}{2} = u_{pl} - \frac{u_{ep,el}}{2}$$

Note: u_{pl} from Equation (2.38) is not the same plastic deformation as $u_{ep,pl}$.

The maximum total deformation for elastoplastic case can be therefore defined as

$$u_{ep} = u_{ep,el} + u_{ep,pl} = u_{pl} + \frac{u_{ep,el}}{2} = \frac{R_m}{2k} + \frac{I_k^2}{2mR_m} \quad (2.41)$$

2.5 Transformation into equivalent SDOF/2DOF system

2.5.1 Introduction

Continuous structures like beams or slabs have infinitely many degrees of freedom. Computational discretization of the results in model with a finite number of degrees of freedom, which can be solved using for instance finite element method. When designing against explosion, a continuous structure is often transformed into a Single Degree of Freedom (SDOF) system of mass on a spring. Such a system has one degree of freedom, and can move only in one direction. The concept of transformation can be seen in Figure 2.27.

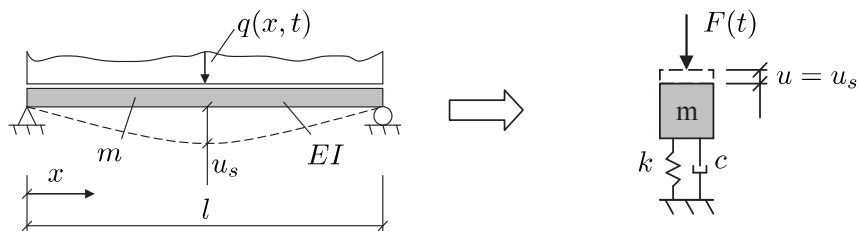


Figure 2.27: *The concept of transformation into equivalent SDOF system. From Johansson and Laine (2012b).*

In order to conduct the transformation, a system point representing the structure must be chosen. It is the vibration of this single point, that the mass-spring SDOF system will simulate. The system point can be arbitrary, but usually the point in the centre of the beam or slab is chosen. Another alternative is to choose a point where the displacement reaches its maximum, as it may not coincide with the centre for different types of boundary conditions.

When a structural system consisting of slab on beams or beam on beams is studied, it is possible to capture its behaviour in a better way by adopting a transformation into a Two Degrees of Freedom system (2DOF), consisting of two masses on two springs. The idea here is to treat each structural part (upper beam/slab or lower beam) as a separate mass with distinctive stiffness. The principle of the transformation can be seen in Figure 2.28.

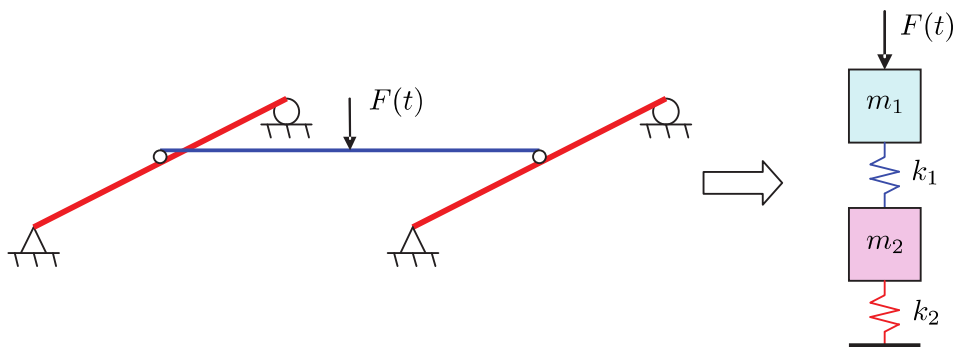


Figure 2.28: *The concept of transformation into equivalent 2DOF system.*

2.5.2 Single Degree of Freedom system

A typical Single Degree of Freedom system (SDOF) consisting of a mass m on a spring with stiffness k and a damper with damping c is studied. The system and its free body diagram can be seen in Figure 2.29. The force in the damper is proportional to the body's velocity and the force in the spring is proportional to the displacement of the mass. The external force acting on the body is referred to as $F(t)$.

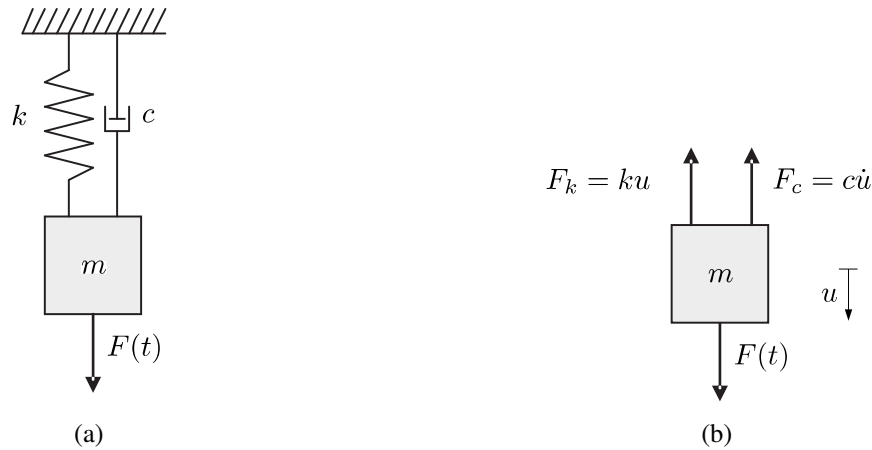


Figure 2.29: *Single Degree of Freedom system (a) and free body diagram (b).* According to Newton's second law, following relationship can be established:

$$m\ddot{u} = F(t) - F_k - F_c = F(t) - ku - c\dot{u}$$

Consequently, the governing equation of motion can be expressed as:

$$m\ddot{u} + c\dot{u} + ku = F(t) \quad (2.42)$$

And the eigenfrequency of the body's vibration (when disregarding damping) is expressed as:

$$\omega = \sqrt{\frac{k}{m}} \quad (2.43)$$

The Single Degree of Freedom system can be numerically solved for displacement with Central Difference Method (CDM), which is described in Appendix A.

2.5.3 Two Degrees of Freedom system

A typical Two Degrees of Freedom system (2DOF) consisting of masses m_1 and m_2 on springs with stiffnesses k_1 and k_2 and dampers with damping c_1 and c_2 is studied. The system and its free body diagram can be seen in Figure 2.30. Forces in the dampers are proportional to the relative velocity of the mass and the forces in the springs are proportional to the relative displacement of the body. The external force acting on the body is referred to as $F(t)$.

The forces acting on the bodies are

$$F_{k1} = k_1(u_1 - u_2) \quad F_{c1} = c_1(\dot{u}_1 - \dot{u}_2) \quad F_{k2} = k_2 u_2 \quad F_{c2} = c_2 \dot{u}_2$$

Second Newton's law for the first mass gives

$$m_1 \ddot{u}_1 = F(t) - k_1 u_1 + k_1 u_2 - c_1 \dot{u}_1 + c_1 \dot{u}_2 \quad (2.44)$$

and for the second mass

$$m_2 \ddot{u}_2 = k_1 u_1 - k_1 u_2 + c_1 \dot{u}_1 - c_1 \dot{u}_2 - k_2 u_2 - c_2 \dot{u}_2 \quad (2.45)$$

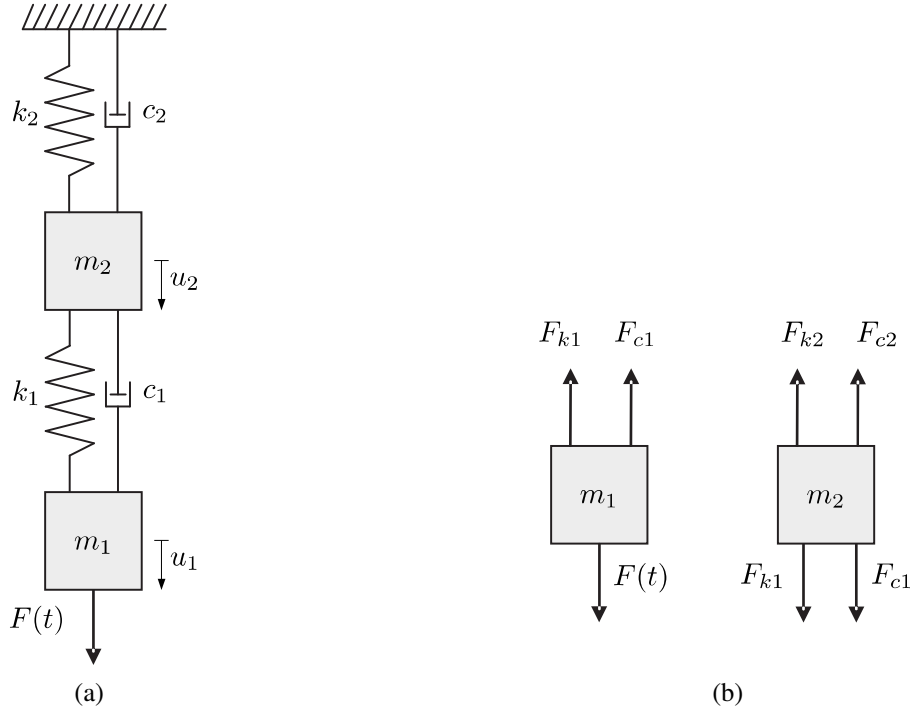


Figure 2.30: Two Degrees of Freedom system (a) and free body diagrams (b).

By rewriting equations (2.44) and (2.45) into matrix form, the system of equations of motion is obtained

$$\begin{bmatrix} m_1 & 0 \\ 0 & m_2 \end{bmatrix} \begin{bmatrix} \ddot{u}_1 \\ \ddot{u}_2 \end{bmatrix} + \begin{bmatrix} c_1 & -c_1 \\ -c_1 & c_1 + c_2 \end{bmatrix} \begin{bmatrix} \dot{u}_1 \\ \dot{u}_2 \end{bmatrix} + \begin{bmatrix} k_1 & -k_1 \\ -k_1 & k_1 + k_2 \end{bmatrix} \begin{bmatrix} u_1 \\ u_2 \end{bmatrix} = \begin{bmatrix} F(t) \\ 0 \end{bmatrix} \quad (2.46)$$

Equation (2.46) can be written in algebraic form as

$$\mathbf{M}\ddot{\mathbf{u}} + \mathbf{C}\dot{\mathbf{u}} + \mathbf{K}\mathbf{u} = \mathbf{F} \quad (2.47)$$

where \mathbf{M} is the mass matrix, \mathbf{C} is the damping matrix, \mathbf{K} is the stiffness matrix of the system, and \mathbf{F} is the force vector.

Damping reduces the amplitude of vibration over time. Since in design of structures subjected to explosion loads, only the maximum amplitude of vibration is usually of interest and damping will therefore be disregarded in this study as well, as recommended in Johansson and Laine (2012b).

In order to determine the eigenfrequencies of the system, an eigenvalue problem must be solved. The non-trivial solution of this problem can be expressed as

$$\det(\mathbf{K} - \lambda\mathbf{M}) = 0 \quad (2.48)$$

where λ is a vector containing the angular eigenfrequencies ω_i^2 :

$$\lambda = \begin{bmatrix} \omega_1^2 \\ \omega_2^2 \end{bmatrix} \quad (2.49)$$

An explicit form of the eigenfrequency for each body is then solved as

$$\omega_1 = \sqrt{\frac{r + k_1 m_1 + k_1 m_2 + k_2 m_1}{2m_1 m_2}} \quad (2.50)$$

$$\omega_2 = \sqrt{\frac{k_1 m_1 - r + k_1 m_2 + k_2 m_1}{2m_1 m_2}} \quad (2.51)$$

where

$$r = \sqrt{k_1^2 m_1^2 + 2k_1^2 m_1 m_2 + k_1^2 m_2^2 + 2k_1 k_2 m_1^2 - 2k_1 k_2 m_1 m_2 + k_2^2 m_1^2} \quad (2.52)$$

The eigenvector ϕ_i (modal shape) of the system can be solved for each eigenfrequency as

$$(\mathbf{K} - \lambda_i \mathbf{M}) \phi_i = 0 \quad (2.53)$$

The 2DOF system can be solved numerically for displacements $u_1(t)$ and $u_2(t)$ with Central Difference Method, which is described in Appendix A. Octave code for solving an arbitrary 2DOF system with different material response of individual elements, as well as with different properties of the elements in different directions is included in Appendix C.

2.5.4 Transformation factors

As already described in Section 2.5.1, a beam or slab can be transformed into an equivalent SDOF mass-spring system. Starting from Equation (2.42) and adopting subscript e as to indicate that this is an equivalent system, one gets:

$$m_e \ddot{u} + c_e \dot{u} + k_e u = F_e(t) \quad (2.54)$$

where m_e is the equivalent mass, c_e is the equivalent damping, k_e is the equivalent stiffness and $F_e(t)$ is the equivalent force. Based on provisions described in Section 2.5.3, the damping contribution is disregarded. Denoting the mass of the structure as m , its stiffness in the system point as k , and the force acting on it as $F(t)$, the equivalent parameters can be expressed as:

$$m_e = \kappa_m m \quad (2.55)$$

$$k_e = \kappa_k k \quad (2.56)$$

$$F_e = \kappa_F F \quad (2.57)$$

The parameters κ_m , κ_k and κ_F are called transformation factors. According to Biggs (1964), the following relation is fulfilled

$$\kappa_k = \kappa_F \quad (2.58)$$

The equation of motion can be then written as:

$$\kappa_m m \ddot{u} + \kappa_k k u = \kappa_F F(t) \quad (2.59)$$

After division by κ_F , one gets

$$\frac{\kappa_m}{\kappa_F} m \ddot{u} + \frac{\kappa_k}{\kappa_F} k u = F(t) \quad (2.60)$$

And using equation (2.58) in equation (2.60) results in:

$$\frac{\kappa_m}{\kappa_F} m \ddot{u} + k u = F(t) \quad (2.61)$$

The ratio $\frac{\kappa_m}{\kappa_F}$ is defined as

$$\kappa_{mF} = \frac{\kappa_m}{\kappa_F} \quad (2.62)$$

The final form of the equation of motion for the transformed system is then

$$\kappa_{mF} \cdot m \ddot{u} + k u = F(t) \quad (2.63)$$

The transformation factors are derived from energy conservation rules. For more details and for complete derivations, the reader is referred to Johansson and Laine (2012b).

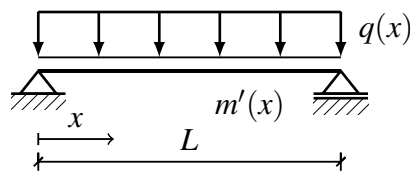


Figure 2.31: Notations used in derivation of transformation factors κ .

For a simply supported beam of length L with mass distribution $m'(x)$ (according to Figure 2.31), the mass transformation factor κ_M is defined as:

$$\kappa_m = \int_0^L \frac{m'(x) \cdot u(x)^2}{m \cdot u_s^2} dx \quad (2.64)$$

The force transformation factor κ_F is defined as:

$$\kappa_F = \int_0^L \frac{q(x) \cdot u(x)}{F \cdot u_s} dx \quad (2.65)$$

And the stiffness transformation factor, κ_k can be expressed as:

$$\kappa_k = \int_0^L \frac{M(x) \cdot u''(x)}{F \cdot u_s} dx \quad (2.66)$$

Provided that the mass distribution and uniformly distributed load are constant along the beam (i.e. $m'(x) = m'$ and $q(x) = q$), the expressions take the form:

$$\kappa_m = \frac{1}{L} \int_0^L \frac{u(x)^2}{u_s^2} dx \quad (2.67)$$

$$\kappa_F = \frac{1}{L} \int_0^L \frac{u(x)}{u_s} dx \quad (2.68)$$

where $u(x)$ is the deflection shape and $u_s(x)$ is the displacement of the system point. It depends on boundary conditions and whether the assumed response is elastic or plastic, see Figure 2.32.

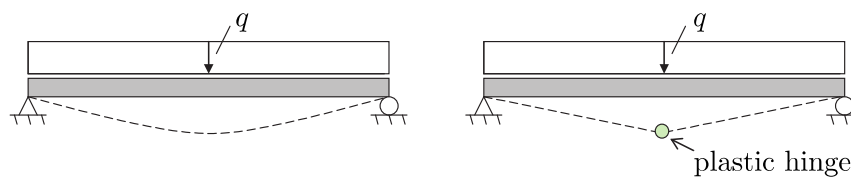


Figure 2.32: *Difference in the shape of deflection for elastic and plastic response. From Johansson and Laine (2012b).*

In the case of a simply supported beam from Figure 2.31 subjected to uniformly distributed load q , which has a system point in the middle, the maximum displacement of this point is

$$u_s = \frac{5qL^4}{384EI} \quad (2.69)$$

and the deflection shape $u(x)$ can be expressed as:

$$u(x) = \frac{qL^3}{24EI} \left(x - \frac{2x^3}{L^2} + \frac{x^4}{L^3} \right) \quad (2.70)$$

The transformation factors are summarised for beams with different boundary conditions, load case and type of material response in Table 2.4 and 2.5.

Table 2.4: Transformation factor for a beam subjected to a point load. From Johansson and Laine (2012b).

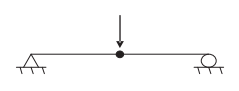
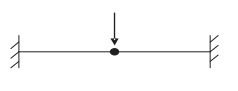
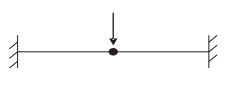
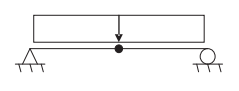
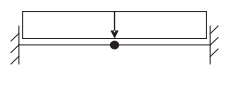
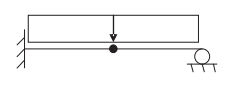
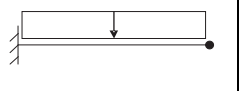
Point load on beam element				
				
Elastic deformation curve				
κ_m	0.486	0.371	0.455	0.236
κ_F	1.000	1.000	1.000	1.000
κ_{mF}	0.486	0.371	0.446	0.236
Plastic deformation curve				
κ_m	0.333	0.333	0.333	0.333
κ_F	1.000	1.000	1.000	1.000
κ_{mF}	0.333	0.333	0.333	0.333

Table 2.5: Transformation factor for a beam subjected to an uniformly distributed load. From Johansson and Laine (2012b).

Uniformly distributed load on beam element				
				
Elastic deformation curve				
κ_m	0.504	0.406	0.483	0.257
κ_F	0.640	0.533	0.600	0.400
κ_{mF}	0.788	0.762	0.805	0.642
Plastic deformation curve				
κ_m	0.333	0.333	0.333	0.333
κ_F	0.500	0.500	0.500	0.500
κ_{mF}	0.667	0.667	0.667	0.667

2.6 Equivalent static load

2.6.1 General notes

In order to make the design against explosion loads easier, it is possible to convert the impulse loading into an equivalent static load. According to Johansson and Laine (2012b), handling of such loads becomes more instinctive for structural engineers. The concept here is to find such a static load Q , for which the work it does corresponds to the work done by the impulse load on the structure. To do this, energy balance equations are used. Namely, the external work (Equation (2.32)) done by the impulse must be equal to the internal work done by the force Q . The magnitude of equivalent static load depends on the constitutive model used.

In general, the force Q can be expressed as

$$Q = \int q(x) dx \quad (2.71)$$

2.6.2 Elastic model

For the elastic model, the force Q acting in the system point of simply supported beam (i.e. in the mid-span) results in internal work according to

$$W_i = \frac{Q u_{el}}{2} \quad (2.72)$$

The maximum elastic displacement from Equation (2.35) is used instead of u_{el} in this relation, giving

$$W_i = \frac{Q I_k}{2 m \omega} \quad (2.73)$$

From the work balance (external work - Equation (2.32)):

$$\frac{Q I_k}{2 m \omega} = \frac{I_k^2}{2 m} \quad (2.74)$$

Thus the equivalent static load for elastic response can be defined as

$$Q = I_k \omega \quad (2.75)$$

2.6.3 Plastic model

For the plastic model, the force Q acting in the mid-span of the simply-supported beam results in internal work according to

$$W_i = Q u_{pl} \quad (2.76)$$

The maximum elastic displacement from Equation (2.38) is used instead of u_{pl} in this relation, giving

$$W_i = \frac{Q I_k^2}{2 m R_m} \quad (2.77)$$

From the work balance (external work - Equation (2.32)):

$$\frac{Q I_k^2}{2 m R_m} = \frac{I_k^2}{2 m} \quad (2.78)$$

Thus the equivalent static load for elastic material response can be defined as

$$Q = R_m \quad (2.79)$$

2.6.4 Elastoplastic model

For the elastoplastic model, the equivalent static force Q is obtained in the same manner as for the plastic model. Therefore

$$Q = R_m \quad (2.80)$$

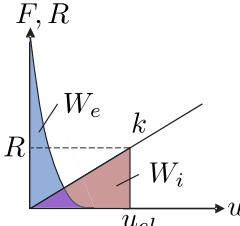
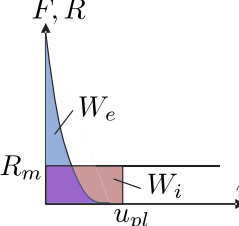
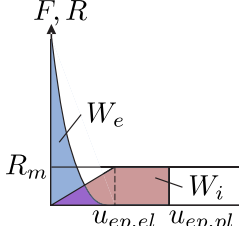
However, in this model, the resistance R_m is defined with respect to the stiffness k and elastic part of the deformation $u_{ep,el}$

$$R_m = ku_{ep,el} \quad (2.81)$$

2.7 Summary of SDOF system loaded with characteristic impulse

A summary of fundamental parameters for Single Degree of Freedom system under characteristic impulse can be seen in Table 2.6.

Table 2.6: Expressions for external and internal work, displacements and equivalent static load for SDOF system loaded with a characteristic impulse I_k . From Johansson et al. (2014).

Notion	Elastic	Plastic	Elastoplastic
			
External work	$W_e = E_k = \frac{I_k^2}{2m}$	$W_e = E_k = \frac{I_k^2}{2m}$	$W_e = E_k = \frac{I_k^2}{2m}$
Internal work	$W_i = \frac{ku_{el}^2}{2}$	$W_i = R_m u_{pl}$	$W_i = \frac{R_m}{2} (u_{ep,el} + 2u_{ep,pl})$
Total deformation	$u_{tot} = u_{el}$	$u_{tot} = u_{pl}$	$u_{tot} = u_{pl} + \frac{u_{ep,el}}{2}$
Elastic deformation	$u_{el} = \frac{I_k}{m\omega}$	-	$u_{ep,el} = \frac{R_m}{k}$
Plastic deformation	-	$u_{pl} = \frac{I_k^2}{2mR_m}$	$u_{ep,pl} = u_{pl} - \frac{u_{ep,el}}{2}$
Equivalent static load	$Q = I_k \omega$	$Q = R_m$	$Q = R_m$
Angular frequency	$\omega = \sqrt{\frac{k}{m}}$	-	-

3 Parametric study - beam on spring supports

3.1 Introduction

The response of a structural system consisting of a beam resting on two beams depends not only on the stiffness and mass of the beam that is directly exposed to the explosion load, but also on the flexibility and mass of the supporting elements. For better understanding, as well as in order to achieve a smooth transition between a beam structure transformed into a SDOF system, and such structural system described by a 2DOF system, an intermediate study was carried out first. The aforementioned structural system is simplified to a beam on spring supports, as seen in Figure 3.1. The lower beams are transformed to springs with the same stiffness, k_2 , and no mass, while the upper beam remains unchanged, with the stiffness k_1 and the mass m_1 .

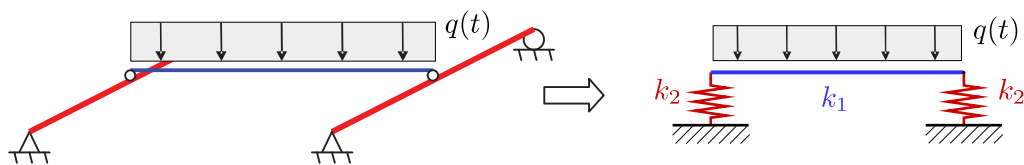


Figure 3.1: *Intermediate simplification of structural system.*

The goal of this study was to develop a modified SDOF model that is able to describe the displacement of a beam on spring supports, as well as the total displacement of the beam and spring system. It was also of big interest to evaluate its response, and determine reasonable limits stating for which stiffness ratios k_1/k_2 it is needed to consider the flexibility of lower beams, and when it could be safely disregarded.

The beam on spring supports was modelled in the commercial FE software ADINA (2014). The modified SDOF model's response was solved in GNU Octave (2014) using the Central Difference Method. For the sake of simplicity, only linear elastic response was studied.

3.2 Outline of the study

3.2.1 Parametric beams, springs and load case

The subjects of the study were three different fictitious concrete beams and three different spring supports. Since in this study it was not of high importance to keep practical cross section's dimensions of the beams, but rather to have reasonable parameters such as eigenfrequency (after transformation into SDOF), the cross section was in each case adjusted to achieve the desired parameters. Each beam had the length L of 4 m and the mass m_{beam} of 1000 kg. Young's modulus for the concrete was chosen as $E = 33$ GPa. Concrete density was chosen as $\rho = 2400$ kg/m³. The procedure of determining the cross section dimensions (height h and width b) was as follows:

1. The frequency (in Hz), f , of an equivalent SDOF system (transformed from a simply supported beam) (in Hz) is chosen.
2. The stiffness of the beam is calculated as

$$k_1 = m_1 \omega^2 = 4\pi^2 \kappa_{mF} m_{beam} f^2 \quad (3.1)$$

In this case, a frequency of an equivalent SDOF system was chosen. The system was created from a simply supported beam subjected to an evenly distributed load - hence the transformation factor $\kappa_{mF} = 0.788$.

3. The moment of inertia is calculated as

$$I = \frac{5k_1 L^3}{384E} \quad (3.2)$$

4. The cross sectional area A is determined from

$$A = \frac{m_{beam}}{\rho b h L} \quad (3.3)$$

5. The height is obtained as

$$h = \sqrt{\frac{12I}{A}} \quad (3.4)$$

6. The width is obtained as

$$b = \frac{A}{h} \quad (3.5)$$

List of studied beams can be seen in Table 3.1:

Table 3.1: *Parametric beams used in the study.*

Beam	f_i [Hz]	$k_{1,i}$ $\left[\frac{\text{N}}{\text{m}}\right]$	h_i [m]	b_i [m]
Beam 1	8	1 990 975	0.0761	1.369
Beam 2	16	7 963 902	0.152	0.683
Beam 3	4	497 744	0.0381	2.738

With the beam stiffness denoted as $k_{1,i}$, and the spring stiffness denoted as $k_{2,j}$, the choice of the three parametric springs and their stiffness ratios with respect to beam 1 can be seen in Table 3.2 and the beam-to-spring stiffness ratios used in this study can be seen in Table 3.3.

Table 3.2: *Parametric springs used in the study.*

Spring	Stiffness $k_{2,j}$ $\left[\frac{\text{N}}{\text{m}} \right]$	Spring to beam stiffness ratio $\frac{k_{2,j}}{k_{1,1}}$
Spring 1	1 990 975	1
Spring 2	995 488	1/2
Spring 3	331 829	1/6

Table 3.3: *Beam to spring stiffness ratios used in the study.*

$\frac{k_{1,i}}{k_{2,j}}$	Spring 1	Spring 2	Spring 3
Beam 1	1	2	6
Beam 2	4	8	24
Beam 3	0.25	0.5	1.5

The load case in the study was chosen to be a line load of the same value for every beam. A triangular impulse was chosen, with the maximum force being $q_{max} = 25$ kN/m during the time $t_1 = 2$ ms. This is a reasonably low value of an explosion load, but for the parametric study it is not that important.

3.2.2 Modelling in ADINA

In the model, 3-D beam elements were used. The beam consisted of 30 elements along the length. Material type for the concrete beam was modelled as linear elastic, with specified Young's modulus, Poisson's ratio and the density, which can be seen in Table 3.4.

Table 3.4: *Material parameters used in the FE analysis.*

Parameter	Value
E	33 GPa
ν	0.2
ρ	2400 kg/m ³

For modelling supports, there are two alternatives. The first alternative involves the use of spring elements. Their length was set to one metre and the corresponding stiffness was assigned to them. The second alternative involves the modelling of 1-D truss elements and assign them such length, cross sectional area and Young's modulus, that the resulting stiffness corresponds to the desired spring stiffness. The stiffness of the truss element in its longitudinal direction can be expressed as

$$k = \frac{EA}{L} \quad (3.6)$$

In this case, the length of this element was chosen as $L = 1$ m, and the cross sectional area was decided to be $A = 1$ m². A linear elastic material with the needed Young's modulus was created and assigned to the truss elements.

Both models were tested, and the results agreed with each other. The alternative with spring elements was eventually chosen to conduct the rest of the study, as it required less work. As for outputs, the vertical displacement of the mid-span of the beam was recorded, as well as the vertical displacement of the beam's end (i.e. spring elongation/contraction).

According to Carlsson and Kristensson (2012), the time increments for the implicit analysis need to be carefully chosen. The time function assigned to the load in ADINA was specified so that the load increment from 0 to 1 happens during the first 0.2 ms, and then drops to 0 at 2 ms and stays there. In the dynamic analysis, a total of 1500 time steps were used, each one with the duration of 0.2 ms, giving the total time of analysis of 0.3 s. The shape of the time function can be seen in Figure 3.2.

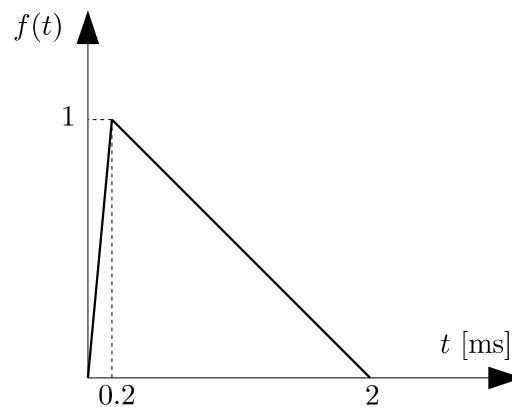


Figure 3.2: *Time function used to describe the load.*

3.3 Modified transformation factors

3.3.1 General notes

When transforming the structure into an equivalent SDOF system, transformation factors, κ_F and κ_m , are needed, and as already mentioned in Section 2.5.4, those depend on the deformation shape. Due to flexible supports, the deformation shape of the beam is now not the same as it was earlier, i.e. for simply supported beam. Therefore the transformation factors listed in Section 2.5.4 are not valid anymore and cannot be used in an analysis with the Central Difference Method; new transformation factors must be derived. The only entity that changes is the deformation shape, as it must take the spring flexibility into account. Apart from it, the procedure is the same as presented in Johansson et al. (2014).

3.3.2 Beam subjected to uniformly distributed load

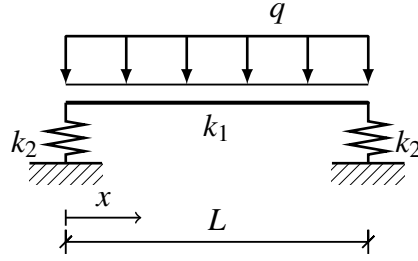


Figure 3.3: *Beam on spring supports subjected to uniformly distributed load.*

For the beam presented in Figure 3.3, the deformation shape is the sum of the simply supported beam deformation and the spring contraction, and therefore it can be expressed as

$$u(x) = \frac{qL^3}{24EI} \left(x - \frac{2x^3}{L^2} + \frac{x^4}{L^3} \right) + \frac{qL}{2k_2} \quad \text{for } 0 \leq x \leq \frac{L}{2} \quad (3.7)$$

The system point is again chosen in the mid-span of the beam, and its deflection can be expressed in a similar manner.

$$u_s = \frac{5qL^4}{384EI} + \frac{qL}{2k_2} \quad (3.8)$$

The beam stiffness is denoted k_1 and is in this case equal to

$$k_1 = \frac{384EI}{5L^3} \quad (3.9)$$

The transformation factors are defined in Section 2.5.4. If the uniformly distributed load and distributed mass are constant along the beam (i.e. $q(x) = q$ and $m'(x) = m$), then the integrals can be expressed and simplified as

$$\begin{aligned} \kappa_F(k_1, k_2) &= \frac{1}{L} \int_0^L \frac{u(x)}{u_s} dx = \frac{2}{L} \int_0^{L/2} \frac{u(x)}{u_s} dx = \frac{2}{L} \int_0^{L/2} \frac{\frac{qL^3}{24EI} \left(x - \frac{2x^3}{L^2} + \frac{x^4}{L^3} \right) + \frac{qL}{2k_2}}{\frac{5qL^4}{384EI} + \frac{qL}{2k_2}} dx = \\ &= \frac{16(k_2L^3 + 60EI)}{5(5k_2L^3 + 192EI)} = \dots = \frac{k_1 + \frac{32k_2}{25}}{k_1 + 2k_2} \end{aligned} \quad (3.10)$$

$$\begin{aligned} \kappa_m(k_1, k_2) &= \frac{1}{L} \int_0^L \frac{u^2(x)}{u_s^2} dx = \frac{2}{L} \int_0^{L/2} \frac{u^2(x)}{u_s^2} dx = \frac{2}{L} \int_0^{L/2} \frac{\left(\frac{qL^3}{24EI} \left(x - \frac{2x^3}{L^2} + \frac{x^4}{L^3} \right) + \frac{qL}{2k_2} \right)^2}{\left(\frac{5qL^4}{384EI} + \frac{qL}{2k_2} \right)^2} dx = \\ &= \frac{128(90720(EI)^2 + 3024EIL^3k_2 + 31L^6k_2^2)}{315(5k_2L^3 + 192EI)^2} = \dots = \frac{k_1^2 + \frac{64k_1k_2}{25} + \frac{15872k_2^2}{7875}}{(k_1 + 2k_2)^2} \end{aligned} \quad (3.11)$$

It is therefore possible to compute the modified transformation factors for varying spring stiffness k_2 . These can be seen in Figure 3.4, Figure 3.5 and Figure 3.6, which present the variation of κ_F , κ_m and κ_{mF} for varying beam-to-support stiffness ratio k_1/k_2 .

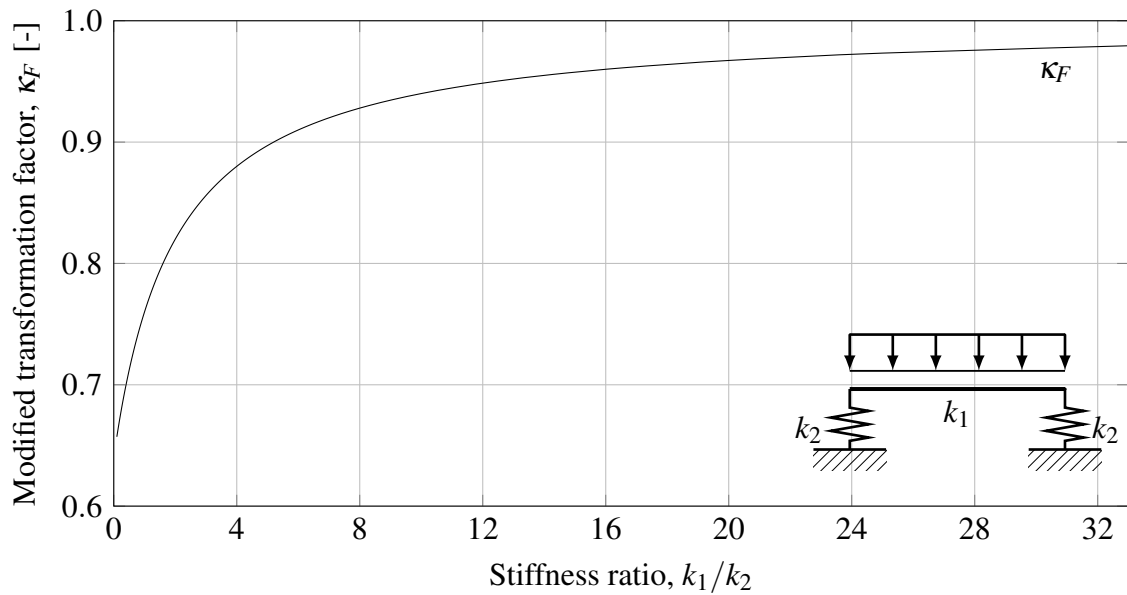


Figure 3.4: Modified transformation factor, κ_F , for varying beam-to-support stiffness ratio, k_1/k_2 . Beam subjected to uniformly distributed load.

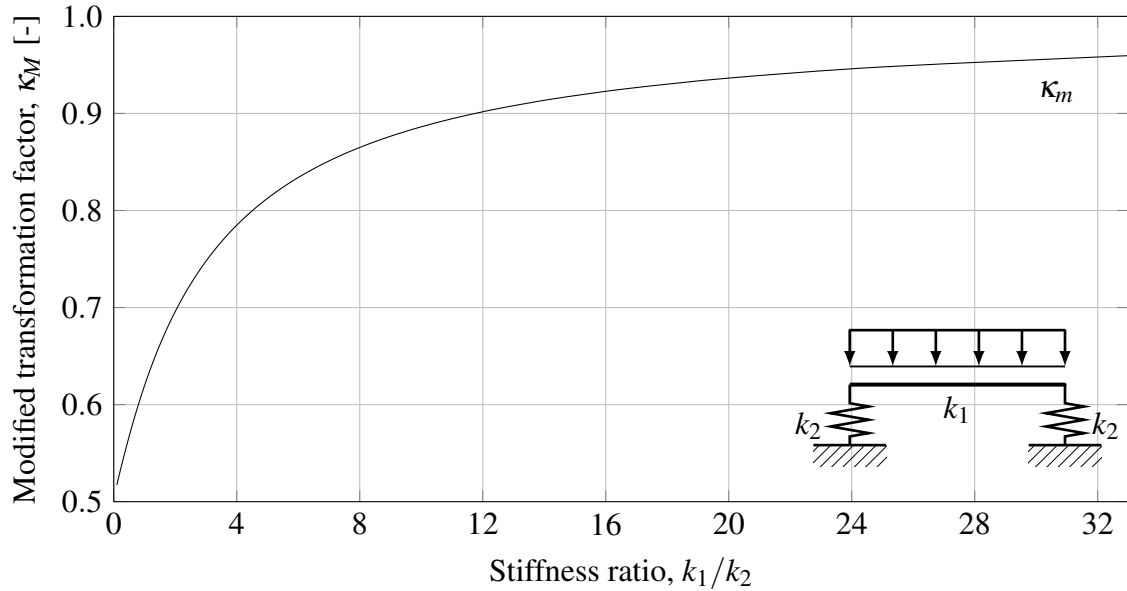


Figure 3.5: Modified transformation factor, κ_m , for varying beam-to-support stiffness ratio, k_1/k_2 . Beam subjected to uniformly distributed load.

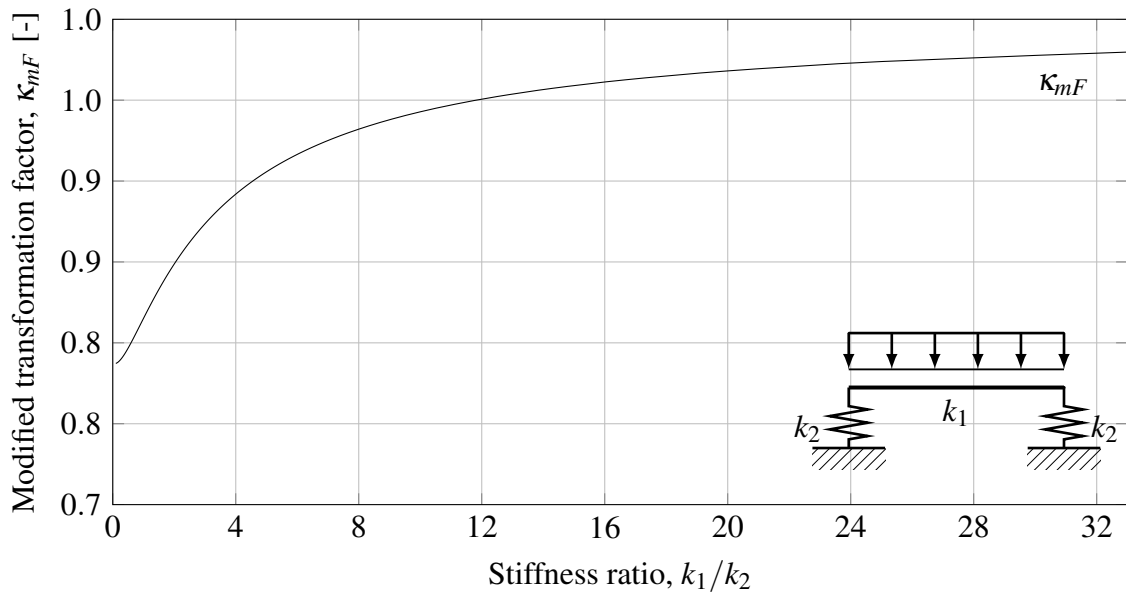


Figure 3.6: Modified transformation factor, κ_{mF} , for varying beam-to-support stiffness ratio, k_1/k_2 . Beam subjected to uniformly distributed load.

3.3.3 Beam subjected to point load

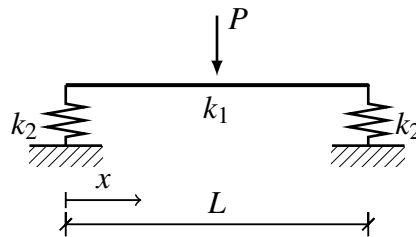


Figure 3.7: Beam on spring supports subjected to point load.

For the beam presented in Figure 3.7, the deformation shape is the sum of the simply supported beam deformation and the spring contraction, and therefore it can be expressed as

$$u(x) = \frac{PL^2}{48EI} \left(3x - \frac{4x^3}{L^2} \right) + \frac{P}{2k_2} \quad \text{for } 0 \leq x \leq \frac{L}{2} \quad (3.12)$$

The system point is chosen in the mid-span of the beam, and its deflection can be expressed in a similar manner.

$$u_s = \frac{PL^3}{48EI} + \frac{P}{2k_2} \quad (3.13)$$

The beam stiffness is denoted k_1 and is in this case equal to

$$k_1 = \frac{48EI}{L^3} \quad (3.14)$$

For the beam subjected to a point load, the transformation factors are defined in Section 2.5.4. If the distributed mass is constant along the beam (i.e. $m'(x) = m$), then the

integral can be expressed and simplified as

$$\begin{aligned}\kappa_m(k_1, k_2) &= \frac{1}{L} \int_0^L \frac{u^2(x)}{u_s^2} dx = \frac{2}{L} \int_0^{L/2} \frac{u^2(x)}{u_s^2} dx = \frac{2}{L} \int_0^{L/2} \frac{\left(\frac{PL^2}{48EI} \left(3x - \frac{4x^3}{L^2} \right) + \frac{P}{2k_2} \right)^2}{\left(\frac{PL^3}{48EI} + \frac{P}{2k_2} \right)^2} dx = \\ &= \frac{20160(EI)^2 + 1050EIL^3k_2 + 17L^6k_2^2}{35(k_2L^3 + 24EI)^2} = \dots = \frac{k_1^2 + \frac{5k_1k_2}{2} + \frac{68k_2^2}{35}}{(k_1 + 2k_2)^2}\end{aligned}\quad (3.15)$$

It is therefore possible to compute the modified transformation factors for varying spring stiffness k_2 . These can be seen in Figure 3.8, which presents the variation of $\kappa_m = \kappa_{mF}$ for varying beam to support stiffness ratio k_1/k_2 .

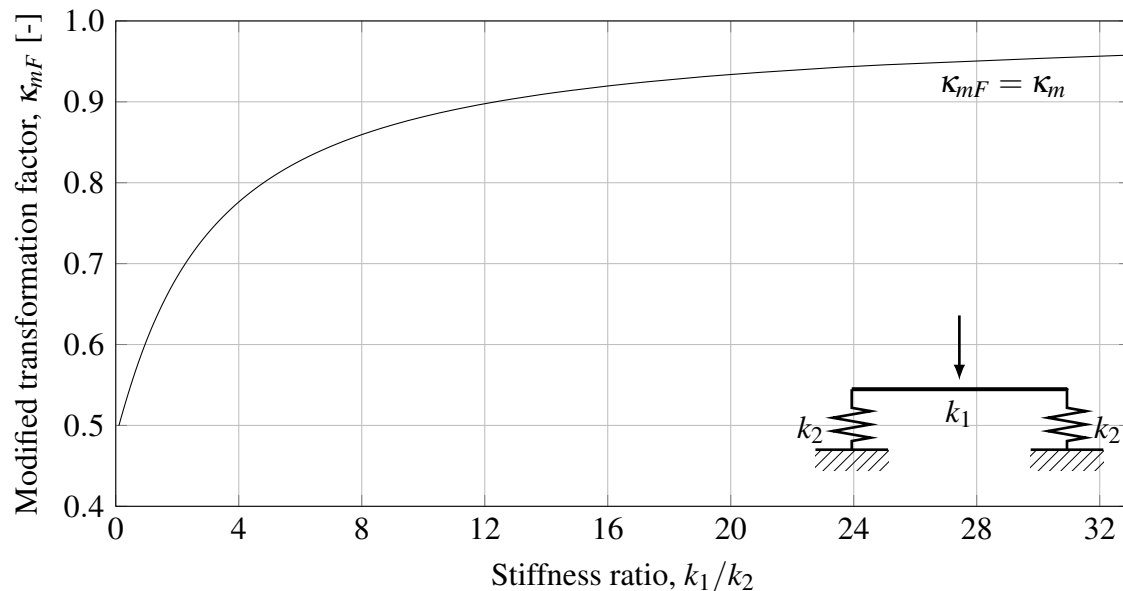


Figure 3.8: Modified transformation factor, κ_{mF} , for varying beam-to-support stiffness ratio, k_1/k_2 . Beam subjected to a point load.

3.3.4 Discussion

It can be seen in Figure 3.4, that when the spring is much stiffer than the beam (i.e. $k_1/k_2 \approx 0$), the behaviour of the beam is close to a simply supported beam, i.e. the deformation form of a soft beam on stiff supports can be compared to the deformation form of a simply supported beam. The transformation factor for a simply supported beam is $\kappa_F = 0.504$, and it can be seen that this value is reached when $k_1/k_2 = 0$. The same applies for κ_m and κ_{mF} , which reach the values $\kappa_m = 0.504$ and $\kappa_{mF} = 0.788$ when the ratio k_1/k_2 tends to zero.

For a beam subjected to point load, the situation is analogous. Although κ_m and κ_{mF} have the same values (due to $\kappa_F = 1$ from definition), it can be seen that for a soft beam

on stiff supports, the values reach $\kappa_M = \kappa_{mF} = 0.486$, which is the solution for a simply supported beam.

For higher values of stiffness ratio, it is evident that all transformation factors converge to 1.0 as the beam becomes stiffer. If the beam is very stiff (compared to the supports), then its movement can be compared to a rigid body motion; i.e. there will be vertical deformations (due to spring movement), but the beam itself would hardly bend regardless of the type of loading due to very high stiffness.

For the stiffness ratios from Table 3.3, the corresponding transformation factor, κ_{mF} , can be seen in Table 3.5. They are then used in hand calculations, as well as in Octave for solving the SDOF system with the Central Difference Method.

Table 3.5: Transformation factors, κ_{mF} , for the studied cases.

κ_{mF}	Spring 1	Spring 2	Spring 3
Beam 1	0.815	0.849	0.916
Beam 2	0.892	0.932	0.970
Beam 3	0.789	0.797	0.830

3.4 Modified SDOF system

3.4.1 Description of the system

Beam on spring supports can easily be transformed into an equivalent SDOF system. The concept of transformation is presented in Figure 3.9.

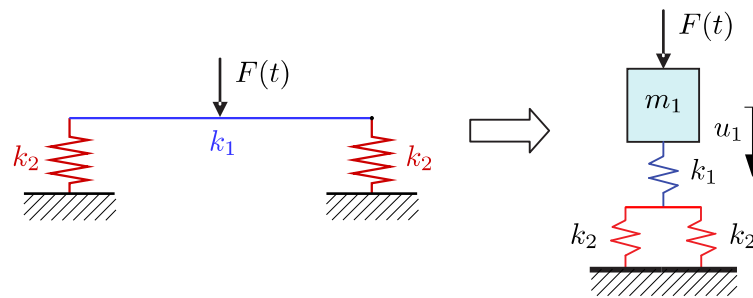


Figure 3.9: The concept of transformation into an equivalent SDOF system.

The main difference now (compared to a case with stiff supports) is the presence of additional springs with stiffness k_2 , otherwise the procedure is analogous to that given in Section 2.5.2. The group of springs is replaced with one spring with an equivalent stiffness k_e . Since the springs are connected both in parallel and in series, therefore the following correlation is true:

$$\frac{1}{k_e} = \frac{1}{k_1} + \frac{1}{2k_2} \quad (3.16)$$

Hence the equivalent stiffness can be expressed as:

$$k_e = \frac{2k_1k_2}{2k_2 + k_1} \quad (3.17)$$

After employing the Central Difference Method, the deformation $u_1(t)$ can be obtained. It is an overall system deformation. However, the displacement of the beam only is often of interest, as it is transferred directly to bending moment and can be used in design. To find the deformation of the beam is to find the elongation/contraction of the first spring with stiffness k_1 . The force in the fictitious equivalent spring can be calculated as

$$F_s(t) = k_e u_1(t) \quad (3.18)$$

The two springs connected in parallel can be treated as one spring with stiffness $2k_2$. Then the system takes the form of a mass on two springs connected in series, with stiffnesses k_1 and $2k_2$ respectively. Since those springs are connected in series, the force in each of them is the same. Therefore the deformation of the lower spring, $u_L(t)$, can be expressed as

$$u_L(t) = \frac{F_s(t)}{2k_2} = \frac{k_e u_1(t)}{2k_2} \quad (3.19)$$

The resulting elongation/contraction of the upper spring, $u_U(t)$, is then the difference between the overall system deformation and the deformation of the lower spring, i.e.

$$\begin{aligned} u_U(t) &= u_1(t) - u_L(t) = u_1(t) - \frac{k_e u_1(t)}{2k_2} = u_1(t) \left(1 - \frac{k_e}{2k_2} \right) = \\ &= u_1(t) \left(1 - \frac{2k_1 k_2}{2k_2(2k_2 + k_1)} \right) = u_1(t) \left(1 - \frac{k_1}{2k_2 + k_1} \right) = u_1(t) \frac{2k_2}{2k_2 + k_1} \end{aligned} \quad (3.20)$$

3.4.2 Hand calculations

Simple hand calculations can be performed for this modified SDOF system in order to estimate the response of the structure. Knowing the equivalent stiffness, the angular frequency of the system can be calculated as:

$$\omega_{SDOF} = \sqrt{\frac{k_e}{\kappa_{mF} m_{beam}}} \quad (3.21)$$

Finally, the total elastic deformation of the structure (together with springs' movement) can be determined with

$$u_{max,SDOF} = \frac{I_k}{\kappa_{mF} m_{beam} \omega_{SDOF}} \quad (3.22)$$

where I_k denotes the characteristic impulse and $\kappa_{mF} = \kappa(k_1, k_2)$ represents the aforementioned modified transformation factor.

If only the beam deformation (without springs' movement) is of interest, the procedure can be slightly modified to obtain an estimate. The angular frequency of the beam is calculated as

$$\omega_b = \sqrt{\frac{k_1}{\kappa_{mF} m_{beam}}} \quad (3.23)$$

and the total elastic deformation can be determined with

$$u_{U,max,SDOF} = \frac{I_k}{\kappa_{mF} m_{beam} \omega_b} \quad (3.24)$$

where I_k denotes the characteristic impulse and $\kappa_{mF} = \kappa(k_1, k_2)$ represents the aforementioned modified transformation factor.

3.5 Discussion and conclusions

3.5.1 Results of the parametric study

Selected results of the analysis are presented in Figure 3.10 to Figure 3.12, which correspond to the cases where $k_1/k_2 = 0.25$, $k_1/k_2 = 2$ and $k_1/k_2 = 24$, respectively. These figures represent the relative deformation η as a function of time t . The parameter η is defined as the ratio between the actual deformation of interest and the maximum total deformation of the structure obtained in the FE analysis. It can be expressed as

$$\eta(t) = \frac{u(t)}{u_{max,ADINA}} \quad (3.25)$$

For results of the remaining cases, the reader is referred to Appendix B.

There are three pairs of lines in each graph. In each pair one line signifies the total relative deformation of the structure (i.e. deformation of the beam along with contraction/elongation of the spring supports), while the other corresponds to the deformation of the beam alone. The solid lines indicate numerical results from the Finite Element Analysis in ADINA, while the dashed lines denote the numerical solution of a SDOF system from Octave, using the Central Difference Method. Dash-dotted lines represent the results of hand calculations, i.e. using Equation (3.22) and (3.24). In ADINA, the displacements of the mid-span point and end support were stored. The aforementioned "beam only" displacement is in this case the difference between those two deformations.

It can be seen that in each case, the SDOF system displacement fits quite well to the actual vibration obtained from FEM. The inconsistency in eigenfrequencies is rather small, and there are no secondary oscillations. Furthermore, the maximum deformation are close to each other, which proves that the results are good. However, when looking at the vibration of the beam only, one can see secondary oscillations which are not captured by the equivalent SDOF system. This is believed to be the influence of higher eigenmodes, which are present in the structure, and are taken into account in the FE analysis, but not in the SDOF system. Even though those peaks and valleys are not preserved in the SDOF model, the overall behaviour and amplitude seem to fall reasonably as an average value, and the results are therefore deemed reasonable.

As for the results of the hand calculations, it can be seen that for low stiffness ratios, the results are not on the safe side for the whole structure as well as for the beam only. As the stiffness ratio increases, the result of the hand calculation for the beam begins to be on the safe side, which is a good indication.

The beam-to-support stiffness ratio has a large influence on the relation between the beam and overall deformation. When the ratio k_1/k_2 is small (close to 0), it means that the beam is relatively flexible (or the support is much stiffer than the beam). Therefore, the energy coming from the explosion will be consumed mainly on the movement of the beam, as it either deforms easily or has stiff supports and acts like a simply supported beam. Then the total deformation and beam deformation are expected to be reasonably close to each other, and this indeed is the case, which can be seen in Figure 3.10. The total deformation comprises almost only the beam deformation, since the supports are relatively stiff and not expected to deform much.

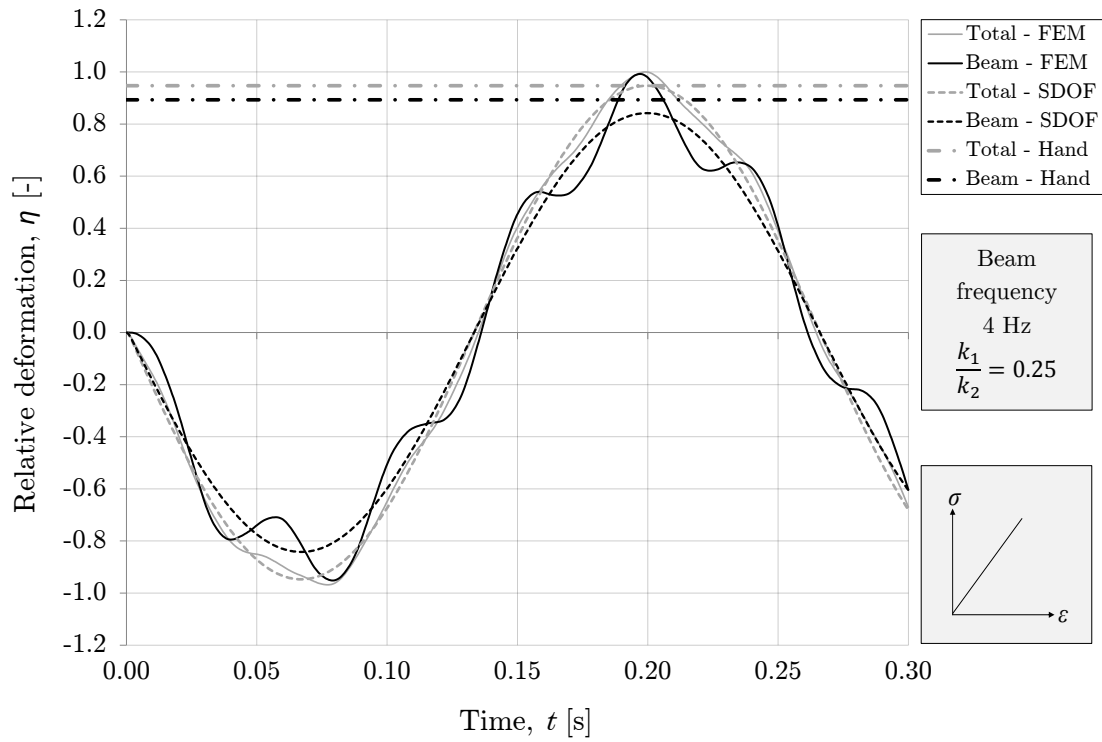


Figure 3.10: Relative vertical displacement as a function of time. Beam subjected to uniformly distributed load. Stiffness ratio $k_1/k_2 = 0.25$.

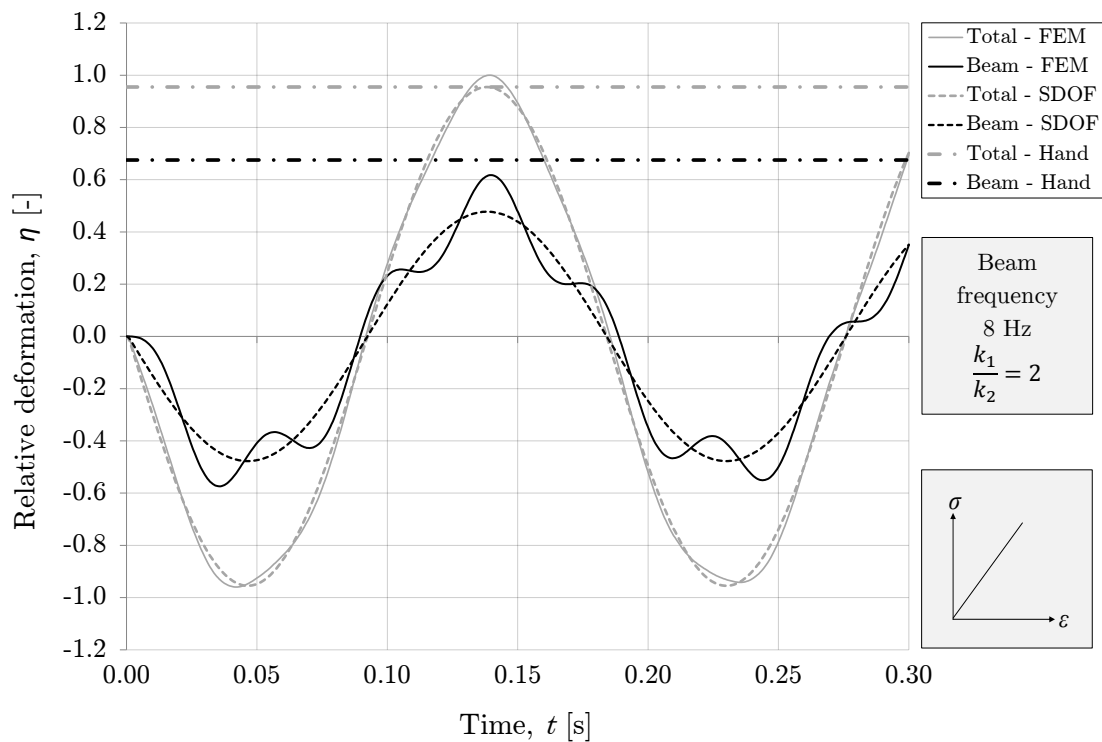


Figure 3.11: Relative vertical displacement as a function of time. Beam subjected to uniformly distributed load. Stiffness ratio $k_1/k_2 = 2$.

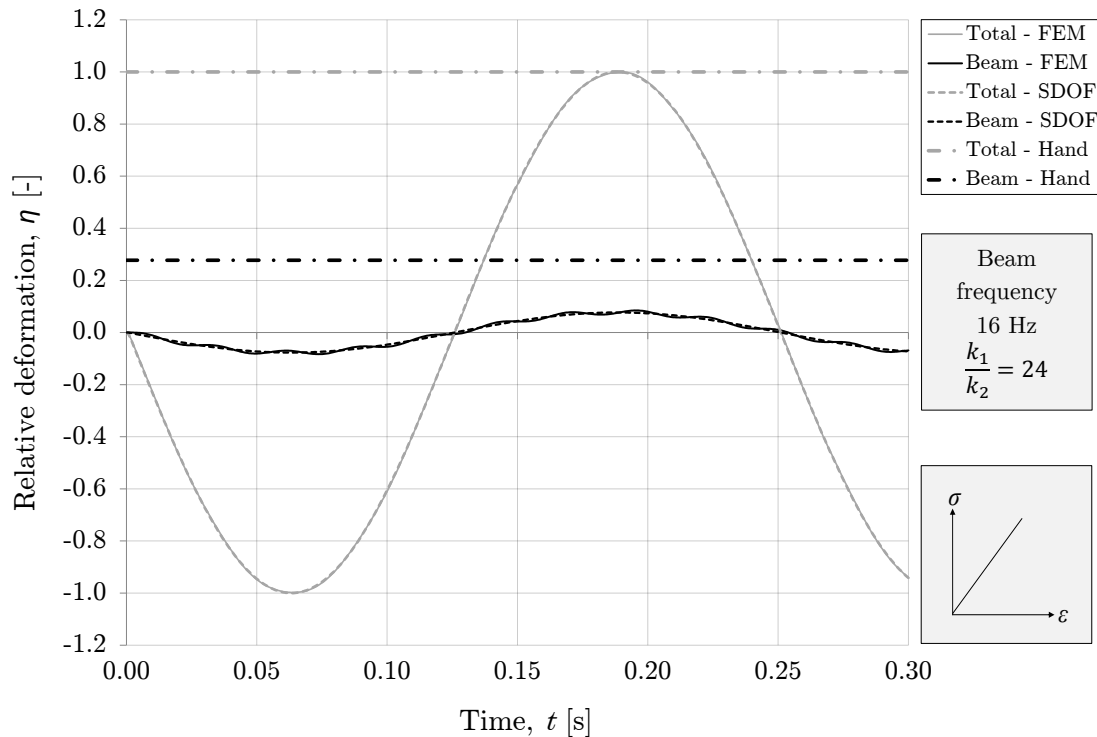


Figure 3.12: *Relative vertical displacement as a function of time. Beam subjected to uniformly distributed load. Stiffness ratio $k_1/k_2 = 24$.*

As the stiffness ratio grows, the beam becomes relatively stiffer (or the supports are becoming more flexible). This means, that there will be no definite predominance of neither beam nor support in deformation. It can be seen in Figure 3.11 and Figure 3.12, that the higher the stiffness ratio gets, the greater the discrepancy between beam and support deformation.

In the other extreme case illustrated by Figure 3.12, the beam-to-support stiffness ratio is $k_1/k_2 = 24$. This means, that the beam is much stiffer than the support (or relatively that the support is very flexible in comparison with the beam). In such a case, the expected response is mainly due to support movement. The beam should react as a rigid body, and undergo a rigid body motion, but should not be greatly influenced by bending. This is indeed the case now, since it can be seen that the amplitude of the beam vibration is approximately 10 % of the total deformation in the structure. It is also worth to mention that, the higher the stiffness ratio, the less influence of secondary oscillations there is, and the SDOF model becomes more accurate compared to the FEM response.

As far as the hand calculation results are concerned, it can be seen that the total deformation is not always on the safe side, but reasonably close in each case. However, the deformation of the beam only calculated by hand, starts to deviate from the actual deformation value even at rather small changes of k_1/k_2 . Even though for low stiffness ratios, k_1/k_2 , the results agree to a reasonable extent, this concurrence ceases quickly. From the rest of results included in Appendix B, a conclusion can be drawn; the higher the stiffness ratio is, the more the deviation of the hand result from the actual value. The beam's deformation is of particular interest, because it is further used to estimate the design bending moment, which can govern the design process.

The relative deformation of the beam, η_b , is defined as:

$$\eta_b = \frac{u_{U,max,SDOF}}{u_{max,ADINA}} \quad (3.26)$$

Those parameters were gathered for various stiffness ratios, and are presented in Figure 3.13. This graph summarises the conclusions mentioned above and provides a quick reference on the relevance of the stiffness of the support on the deformation of the beam.

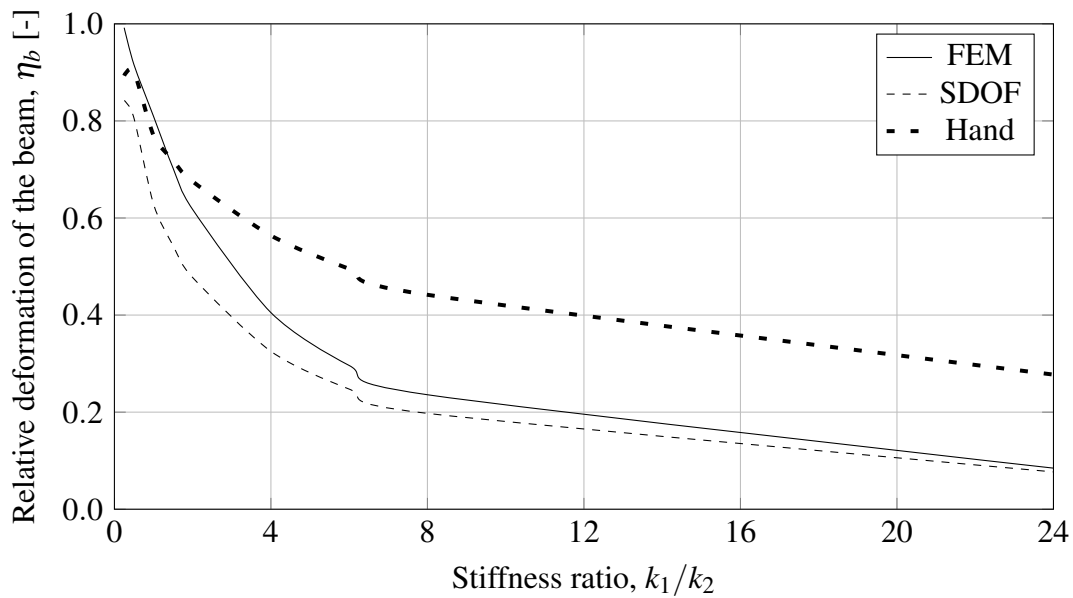


Figure 3.13: *Relative deformation of the beam, η_b , as a function of the stiffness ratio k_1/k_2 .*

3.5.2 Preliminary conclusions

The study included in this chapter is to be considered as an intermediate step between a SDOF simplified model and a structure represented with a 2DOF system. Granted that such model corresponds well to the reality and is efficient, a preliminary conclusion could be drawn already now. There is not much expected to be gained (in terms of total deformations) by expanding the analysis into a 2DOF system for a structure (structural system) with a low stiffness ratio. On the other hand, a structure with a high stiffness ratio, k_1/k_2 , could preferably be analysed using a 2DOF model, since the expectations in terms of lower deformations are high. However, it should be noted that this analysis was carried out only for a linear elastic material response, and not much can be said about the ideally plastic or elastoplastic response.

4 Transformation into 2DOF system

4.1 Introduction

As a next step in the process, a structural system consisting of a beam resting on two beams is studied. The response of such system cannot be easily analysed using a SDOF model, since it was already proved in Chapter 3 that the response of the structure depends on the structural properties of individual members. In the study carried out in that chapter, only the influence of the member's stiffness was considered, since the spring supports were assumed to have no mass. Now, on the other hand, both parts of the structure have both stiffness and mass, and it is believed that not only the stiffness ratio k_1/k_2 , but also the mass ratio m_1/m_2 has influence on the response. Furthermore, it is also reasoned that the angular frequency ratio, ω_1/ω_2 plays also an important role on the response.

The idea here is to transform the structure into an equivalent 2DOF system, so that each part has its own degree of freedom and therefore such system is believed to be able to describe the vibration of the whole structural system. The concept can be seen in Figure 4.1.

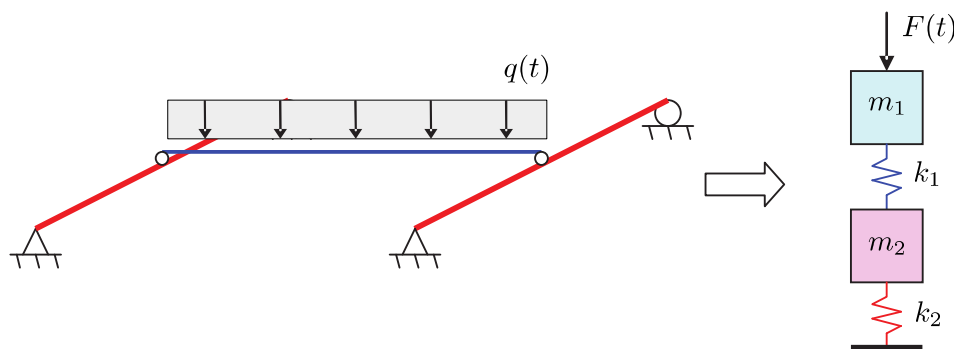


Figure 4.1: *The concept of transformation into an equivalent 2DOF system.*

The aim of this study was to develop a 2DOF model, that can describe the vibrations of both parts of the structure (upper and lower beam). It was also of big interest to compare the response of such structure (especially the upper beam) and a simply supported beam with the same properties. This way it can be determined if, when, and to what extent the deformation is overestimated by a SDOF model.

The structural system consisting of a beam resting on two beams was modelled in the commercial FE software ADINA (2014). The 2DOF system was solved using the Central Difference Method in GNU Octave (2014). For the sake of simplicity, only the linear elastic response was studied.

4.2 Outline of the study

4.2.1 Parametric beams and the load case

In order to achieve a wide sweep of stiffness ratios, a total of 13 reinforced concrete beams were created, where the three parametric beams used in Chapter 3 were treated as a starting point. The rest of the beams was created according to the procedure described

in Section 3.2.1. However, in this study the stiffness is a very important parameter, hence it was the main parameter for beam creation. Each beam was 4 m long and the cross section was adjusted so that it weighted 1000 kg. The stiffness and mass of the upper beam is denoted as k_1 and m_1 , while the stiffness and mass of a single lower beam is referred to as k_2 and m_2 , respectively.

It is assumed, that the upper beam is subjected to a uniformly distributed load coming from an explosion. Moreover, it is assumed to be simply supported on the two lower beams. Hence the stiffness of this beam can be expressed as

$$k_1 = \frac{384EI}{5L^3} \quad (4.1)$$

The lower beams are simply supported, and are assumed to be subjected only to a point load in the mid-span (which comes from the upper beam). The stiffness of one such beam can therefore be calculated as

$$k_2 = \frac{48EI}{L^3} \quad (4.2)$$

A list of the studied beams can be seen in Table 4.1, and beam-to-beam stiffness ratios can be seen in Table 4.2.

Table 4.1: *Parametric beams used in the study.*

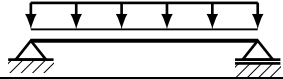
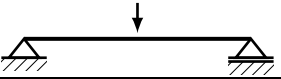
Beam no.	Stiffness, $k_1 = \frac{384EI}{5L^3} \left[\frac{\text{N}}{\text{m}} \right]$ 	Stiffness, $k_2 = \frac{48EI}{L^3} \left[\frac{\text{N}}{\text{m}} \right]$ 	Height [m]	Width [m]
Beam 1	1 990 975	1 244 359	0.07611	1.36873
Beam 2	7 963 902	4 977 439	0.15221	0.68346
Beam 3	497 744	311 090	0.03805	2.73746
Beam 4	996 488	622 805	0.05381	1.93562
Beam 5	331 829	207 393	0.03107	3.35267
Beam 6	4 977 440	3 110 900	0.12033	0.86566
Beam 7	5 972 928	3 733 080	0.13182	0.79024
Beam 8	10 618 528	6 636 580	0.17576	0.59268
Beam 9	13 273 160	8 295 725	0.19650	0.53011
Beam 10	15 927 792	9 954 870	0.21526	0.48392
Beam 11	21 237 056	13 273 160	0.24856	0.41909
Beam 12	23 891 688	14 932 305	0.26363	0.39512
Beam 13	31 855 584	19 909 740	0.30442	0.34218

Table 4.2: *Stiffness ratios for the parametric beams used in this study. Valid for beams of equal mass, i.e. $m_1/m_2 = 1$.*

$\frac{k_1}{k_2}$	B1	B2	B3	B4	B5	B6	B7	B8	B9	B10	B11	B12	B13
B1	1.60	0.40	6.40	3.20	9.60	0.64	0.53	0.30	0.24	0.20	0.15	0.13	0.10
B2	6.40	1.60	25.60	12.79	38.40	2.56	2.13	1.20	0.96	0.80	0.60	0.53	0.40
B3	0.40	0.10	1.60	0.80	2.40	0.16	0.13	0.08	0.06	0.05	0.04	0.03	0.03
B4	0.80	0.20	3.20	1.60	4.80	0.32	0.27	0.15	0.12	0.10	0.08	0.07	0.05
B5	0.27	0.07	1.07	0.53	1.60	0.11	0.09	0.05	0.04	0.03	0.03	0.02	0.02
B6	4.00	1.00	16.00	7.99	24.00	1.60	1.33	0.75	0.60	0.50	0.38	0.33	0.25
B7	4.80	1.20	19.20	9.59	28.80	1.92	1.60	0.90	0.72	0.60	0.45	0.40	0.30
B8	8.53	2.13	34.13	17.05	51.20	3.41	2.84	1.60	1.28	1.07	0.80	0.71	0.53
B9	10.67	2.67	42.67	21.31	64.00	4.27	3.56	2.00	1.60	1.33	1.00	0.89	0.67
B10	12.80	3.20	51.20	25.57	76.80	5.12	4.27	2.40	1.92	1.60	1.20	1.07	0.80
B11	17.07	4.27	68.27	34.10	102.40	6.83	5.69	3.20	2.56	2.13	1.60	1.42	1.07
B12	19.20	4.80	76.80	38.36	115.20	7.68	6.40	3.60	2.88	2.40	1.80	1.60	1.20
B13	25.60	6.40	102.40	51.15	153.60	10.24	8.53	4.80	3.84	3.20	2.40	2.13	1.60

For beams with equal mass, i.e. $m_1/m_2 = 1$, the angular frequency ratio can be easily calculated, i.e.

$$\frac{\omega_1}{\omega_2} = \sqrt{\frac{k_1}{k_2} \cdot \frac{m_2}{m_1}} = \sqrt{\frac{k_1}{k_2}} \quad (4.3)$$

Beams 8-12 in Table 4.1 result in very high stiffness ratios for some cases (up to $k_1/k_2 = 153.6$). When the length or the cross section dimensions are changed for the beam, its mass and stiffness changes as well. If analysis of different mass ratios m_1/m_2 are of interest, it is easy to just increase or decrease the width of the cross section, as the stiffness and mass of the beam change with the same factor. If the length is changed, the stiffness changes in a cubic manner, for instance for a beam two times shorter, the stiffness is eight times higher and the mass is two times lower. This provides a very wide range of potential results for different stiffness and mass ratios. In this study, the analyses were made up to the case where $k_1/k_2 = 36$ (in most cases), since it was deemed a reasonable limit of interest. There is also a possibility of changing the Young's modulus, E , if other stiffness is desired. However, this alteration causes deviations in the wave propagation velocity ($c = \sqrt{\frac{E}{\rho}}$), which is not desired (Carlsson and Kristensson 2012).

For example, an analysis with the mass ratio of $m_1/m_2 = 0.25$ and an intermediate stiffness ratio is needed. The subject of the analysis is chosen to be Beam 6 resting on Beam 5 (two Beams 5 actually). From Table 4.2, the stiffness ratio k_1/k_2 for such a case is 24. However, this ratio is valid only when the masses of the beams are the same. Beam 5 is needed to be four times heavier, and thus the width of its cross section is increased four times and its length is kept constant. This results in four times greater stiffness, resulting in the actual stiffness ratio $k_1/k_2 = 24/4 = 6$ and the actual mass ratio $m_1/m_2 = 0.25$.

The explosion load used in this study is the same as the one used in Chapter 3. The uniformly distributed force with the magnitude of 25 kN/m is applied as a line load on the upper beam only. The duration of the load is 2 ms. For a visual reference, see Figure 4.3.

4.2.2 Modelling in ADINA

The model consisted of three beams, each one 4 meters long, see Figure 4.2. Material type was set to linear elastic, with specified Young's modulus, Poisson's ratio and density, see Table 3.4. The cross section dimensions are specified according to Table 4.1. For representation of the beams, 3-D beam elements were used, and each beam was divided into 30 elements. The model can be seen in Figure 4.2.

The boundary conditions at points B and C were set so that the translation in X, Y and Z direction was locked at point C, and in X and Z direction at point B. Rotational degrees of freedom at both points were kept intact, with the exception of rotation around the Y axis at points C. This rotation was locked in order to prevent torsion of the lower beams. Moreover, only small deformations were considered, so that Euler's beam theory can be applied.

The upper beam shares a node with each lower beam at their mid-span. At these points, an end release is specified in order to assure that the upper beam is working as simply supported. End release in ADINA is set for the bending moment about the Y axis. Therefore, no moment can be transferred between the two beams at the support, and the upper beam can be expected to work as a simply supported beam.

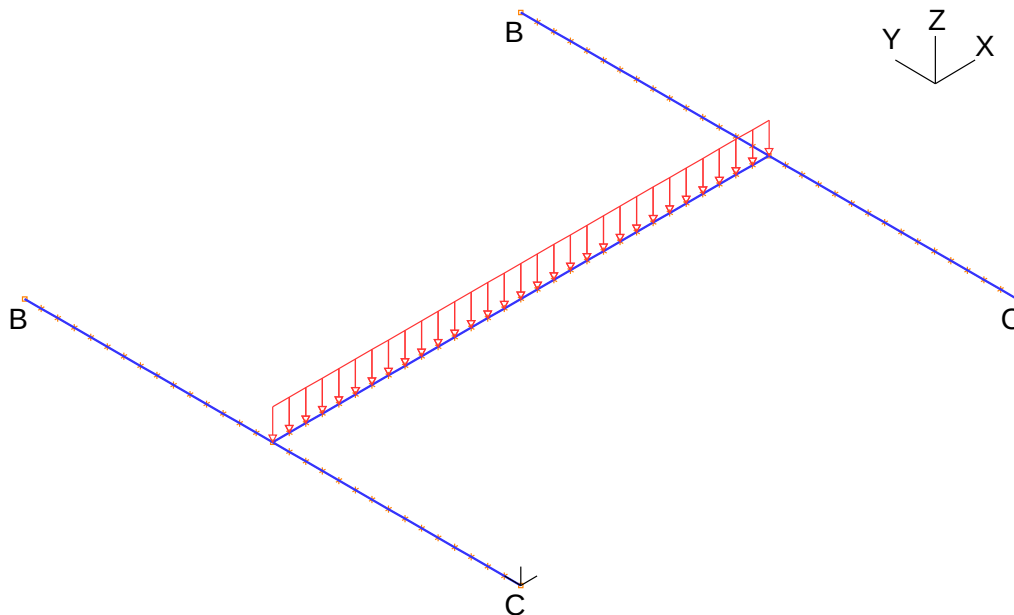


Figure 4.2: *Model of the structure in ADINA.*

The time function for the load was created, so that the initial increment from 0 to 1 happens during first 0.2 ms. This is to avoid computational errors, according to Carlsson and Kristensson (2012). After this initial peak, the function is linearly decreasing until the time is 2 ms, as can be seen in Figure 4.3. This results in a triangular impulse type,

which sufficiently described the intended load case. The time step used in these analyses was 0.2 ms, and there were a total of 4500 time steps, resulting in the total time of response being 900 ms.

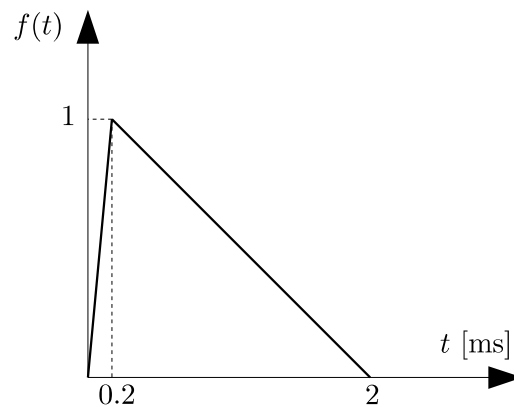


Figure 4.3: *Time function for the load used in ADINA.*

Two types of analyses were run in ADINA for the model; a modal analysis, which finds the eigenfrequencies and eigenmodes of the structure, and a dynamic direct integrated implicit analysis, which gets the deformation of the structure over time.

In the output, two specific displacements are of particular interest. The displacement of the upper beam in mid-span (denoted further as $u_{1A}(t)$) and the displacement of the mid-span in the lower beam (denoted further as $u_{2A}(t)$). Since the displacement $u_{1A}(t)$ is the total displacement of the structure, it is later post-processed into the deflection of the upper beam only - $u_{UA}(t)$:

$$u_{UA}(t) = u_{1A}(t) - u_{2A}(t) \quad (4.4)$$

The deflection of the lower beam $u_{LA}(t)$ is equal to the deformation $u_{2A}(t)$ and can be obtained directly from ADINA.

$$u_{LA}(t) = u_{2A}(t) \quad (4.5)$$

An illustration of this reasoning can be seen in Figure 4.4.

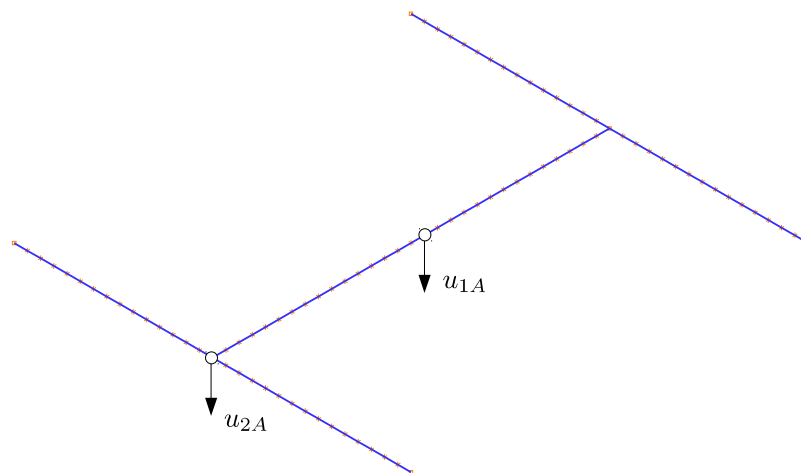


Figure 4.4: *Deformations obtained as a result of the analysis.*

4.3 Response of 2DOF model - transformation factors

4.3.1 Differential equation system

As derived in Section 2.5.3 and Section 2.5.4, the differential equations of motion for the 2DOF system are

$$\begin{bmatrix} \kappa_{mF_1} m_1 & 0 \\ 0 & 2\kappa_{mF_2} m_2 \end{bmatrix} \begin{bmatrix} \ddot{u}_1 \\ \ddot{u}_2 \end{bmatrix} + \begin{bmatrix} k_1 & -k_1 \\ -k_1 & k_1 + 2k_2 \end{bmatrix} \begin{bmatrix} u_1 \\ u_2 \end{bmatrix} = \begin{bmatrix} F(t) \\ 0 \end{bmatrix} \quad (4.6)$$

where k_1 and m_1 are the stiffness and mass respectively of the upper beam, while k_2 and m_2 denote the stiffness and mass of one lower beam. The transformation factors κ_{mF_1} and κ_{mF_2} can be obtained for each beam from Table 2.4 and Table 2.5, depending on the loading conditions. It is assumed here, that the beams' supports are not susceptible to deformation, i.e. the beams can be treated as simply supported.

The upper beam is subjected to a uniformly distributed load, therefore the transformation factor κ_{mF_1} from the table Table 2.4 is

$$\kappa_{mF_1} = 0.788 \quad (4.7)$$

The lower beams are considered to be subjected to point load (reaction from upper beam), hence the transformation factor κ_{mF_2} obtained from Table 2.5 is

$$\kappa_{mF_2} = 0.486 \quad (4.8)$$

This equation system is solved using the Central Difference Method in GNU Octave (2014). The outputs are the displacements $u_1(t)$ and $u_2(t)$. Since the deformation u_1 is the overall deformation of the system in the mid-span, the upper beam deflection $u_U(t)$ can be calculated as

$$u_U(t) = u_1(t) - u_2(t) \quad (4.9)$$

The deflection of the lower beam u_L can be obtained directly from the solution as

$$u_L(t) = u_2(t) \quad (4.10)$$

The number and duration of time steps is the same as the one specified in ADINA. This was done in order to assure, that at each time the same force acts on the body, so that the comparison is easier.

In this section, when referred to the 2DOF model, the model using the ordinary transformation factors κ_{mF_i} is meant.

4.3.2 Results and conclusions

For the first attempt, the response of the structure consisting of beam no. 1 supported on beams no. 1, see Table 4.1, is studied. The mass of the upper and lower beam is the same, therefore the mass ratio $m_1/m_2 = 1$. Even though both of the beams are the same, the loading situation causes a change in their stiffness. The stiffness ratio can then be obtained directly from Table 4.2, which gives $k_1/k_2 = 1.6$. The results can be seen in Figure 4.5. The top part of the graph represents the relative displacement of the mid-span

of the upper beam, while in the bottom part of the graph the relative deformation of the mid-span in the lower beam is plotted. The solid line indicates the equivalent 2DOF system solution, and the dashed line is the solution from ADINA.

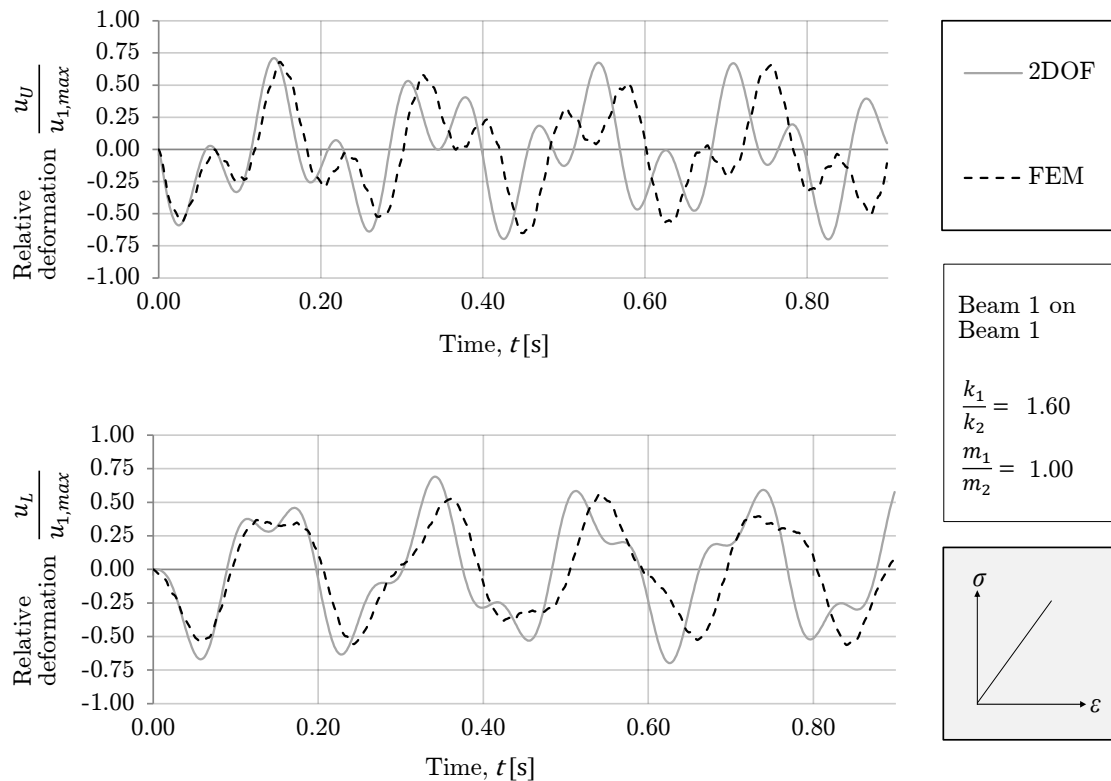


Figure 4.5: *Relative deformation of the upper (top) and lower beam (bottom) over time. Beam no. 1 resting on beams no. 1 according to Table 4.1.*

It can be seen in the graph, that the upper beam's initial response (first two-three sways) according to the 2DOF model agrees reasonably with the FE results both in terms of the amplitude and frequency. However, the shift in frequencies becomes clearly visible later on. The same applies for the lower beam, with the initial shape and frequency of displacement agreeing between the model. However, the shift in frequencies is also present, and the amplitudes of the 2DOF solution are somewhat higher than the actual response.

It is worth to note that this is an intermediate stiffness ratio case. By looking at the maximum amplitudes of both beams, it can be said that their movement is comparable, i.e. both of them deflect up to 50-70% of the total deformation of the system. There is no part of the structure, in which the movement governs the overall system behaviour; no dominating frequency can be seen. The 2DOF model possesses two eigenfrequencies, and neither of them is clearly visible here. It means that both eigenmodes represent the energy of the movement, see Section 4.4.2.

Another case of interest is a structure comprising beam no. 11 resting on beams no. 7 with a chosen mass ratio of $m_1/m_2 = 4$. The length of the beams is kept unchanged and therefore the width of beam no. 11 (upper beam) must be increased four times in ADINA. At the same time, it also implies a four times greater stiffness. From Table 4.2

it can be read, that for a case where beam no. 11 rests on beams no. 7 the stiffness ratio is 5.69. However, since the upper beam is in reality four times stiffer, the actual ratio will be $k_1/k_2 = 4 \cdot 5.69 = 22.76$, which is a rather high ratio. The results are presented in Figure 4.6.

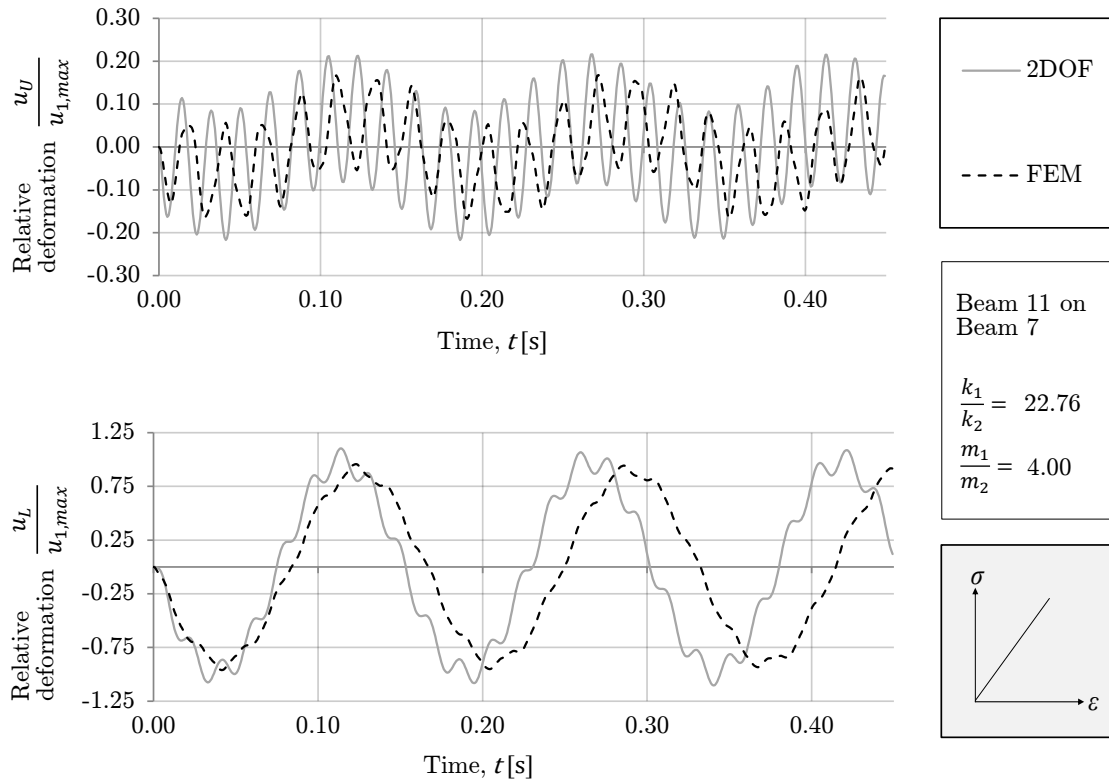


Figure 4.6: *Relative deformation of the upper (top) and lower beam (bottom) over time. Beam no. 11 resting on beams no. 7 according to Table 4.1.*

For clarity, the results are presented for half the run time, i.e. up until 0.45 s. The shift in frequencies between the FEM and 2DOF model is still present and is clearly visible for both the lower and the upper beam. At the same time, the amplitudes of the lower beam's motion according to both models seems to agree with each other quite well, with the 2DOF solution being on the safe side. The same can be said for the upper beam. The amplitudes according to the 2DOF model seem to match the FE model, being a bit on the safe side. However, the shift in the frequencies is still present and visible.

This is a high stiffness ratio case, and based on the conclusions from Chapter 3, the movement of the lower beams should be dominant here. This is indeed the case, and it can be seen by looking at the values of displacement for both parts of the structure. The movement of the upper beam constitutes about 20 % of the overall movement of the whole structure. The lower beam vibrates with a lower frequency, and the secondary oscillations in this beam do not pose a significant influence. At the same time, the behaviour of the upper beam is opposite. It vibrates mainly in the higher eigenfrequency, but there is also a secondary vibration (with a longer period) at the lower eigenfrequency. However, this secondary vibration does not influence the movement greatly. Therefore, it can be concluded that the behaviour of the structure (in term of the magnitude of

displacements) is governed by the vibration of the lower beams, and this is confirmed by both models.

For the third case, a structure consisting of beam no. 1 placed on beams no. 6 is studied. A mass ratio of $m_1/m_2 = 0.25$ is chosen, hence the width of the cross section of the lower beams must be increased four times in ADINA. Table 4.2 states that the stiffness ratio for this case is 0.64, but since the lower beam is now four times stiffer, the actual stiffness ratio for this case is $k_1/k_2 = 0.64/4 = 0.16$, which is a low ratio. Results from both models are presented in Figure 4.7.

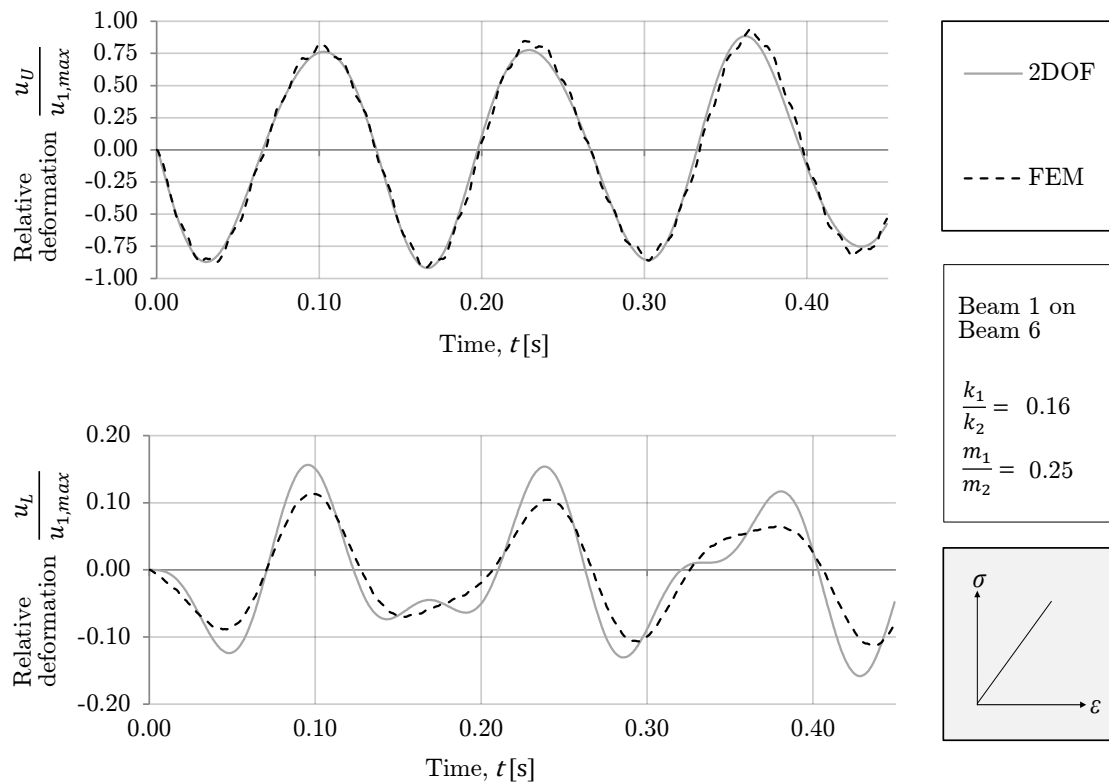


Figure 4.7: *Relative deformation of the upper (top) and lower beam (bottom) over time. Beam no. 1 resting on beams no. 6 according to Table 4.1.*

For clarity, the results are again presented for the half of the run time, i.e. up until 0.45 s. The first thing that is conspicuous when comparing the graphs, is that the response of the upper beam according to the 2DOF model agrees very well with the FE solution both in terms of frequency and amplitude. It cannot be clearly stated if the 2DOF model is on the safe or unsafe side though. However, there is a discrepancy between the models' response for the lower beam. On the other hand, the lower beam's movement is just a fraction of the overall structural movement, and hence is not that significant. The equivalent 2DOF model seems to result in higher amplitudes, giving results on the safe side. The overall shape of the lower beam's deformation seems to match between the models.

Since this is a low stiffness ratio case, one could expect that the overall movement of the structure will comprise mainly the motion of the upper beam, as it is resting on relatively stiff supports. By looking at Figure 4.7 it can be seen that this is indeed the case. By

considering the absolute values of the deformation, it can be said that the vibration of the upper beam is dominating. It is vibrating at a lower frequency, with no evident secondary oscillations. Lower beams' deformation constitute about 10 % of the overall structure movement. The supporting beams also seem to vibrate at the same main frequency as the upper beam.

As an overall conclusion, it can be said that for extreme cases (very high or very low stiffness ratio), the behaviour of the 2DOF model seem to capture the behaviour of the dominating beam quite well, while the behaviour of the remaining part needs improvements both in terms of frequency and amplitude. For an intermediate case (medium value of stiffness ratio), where no part of the structure clearly dominates in the movement, this 2DOF model has problem describing either the upper or lower beam (in terms of frequency and amplitude), and ameliorating measures can be taken.

4.4 Calibration of the 2DOF model - frequency

4.4.1 General notes

It was shown in Section 4.3, that the 2DOF model using traditional transformation factors κ_{mFi} could be improved in order to better describe the behaviour of the whole structure, not only part of it. This is especially the case for intermediate stiffness ratios, where there is no distinctive domination in the movement between the respective parts of the structure. In this section, the 2DOF model described in Section 4.3 is calibrated with respect to frequencies.

4.4.2 Frequency domain and eigenmodes

It could be seen in the figures in Section 4.3, that the eigenfrequencies in the 2DOF model do not always match (there is room for improvement) the frequencies of the vibration of the model in FE analysis.

The model in ADINA has several degrees of freedom, which means that it will also have several eigenfrequencies. Not all of them are of interest though, and not all of them play significant role in the structure's behaviour. In order to assess which modes are the most important, a spectrum analysis was performed. The displacement function of both the upper and lower beams - $u_{UA}(t)$ and $u_{LA}(t)$ were converted from the time domain into the frequency domain. Such operation can be done by using Fast Fourier Transform (FFT) algorithm in GNU Octave (function `fft`), which results in a frequency spectrum. In other words, if the movement of the structure is in reality a sum of all major and minor vibrations at each eigenfrequency, the Fourier transform provides a way to evaluate the influence of specific eigenfrequencies on the overall movement. More information about the Fast Fourier Transform algorithm can be found in Duhamel and Vetterli (1990).

To illustrate, the Fourier transforms of the displacements (from FE response) for the case in which beam no. 1 rests on beams no. 1, see Figure 4.5, is presented in Figure 4.8. According to the frequency spectrum, the structure (or at least part of it) vibrates at two distinct frequencies. In order to illustrate this, a modal analysis was performed in ADINA for each studied case, and the eigenmodes corresponding to the frequencies obtained from the spectrum analysis were picked out. The two eigenmodes that influence the behaviour of the structure the most, are presented in Figure 4.9.

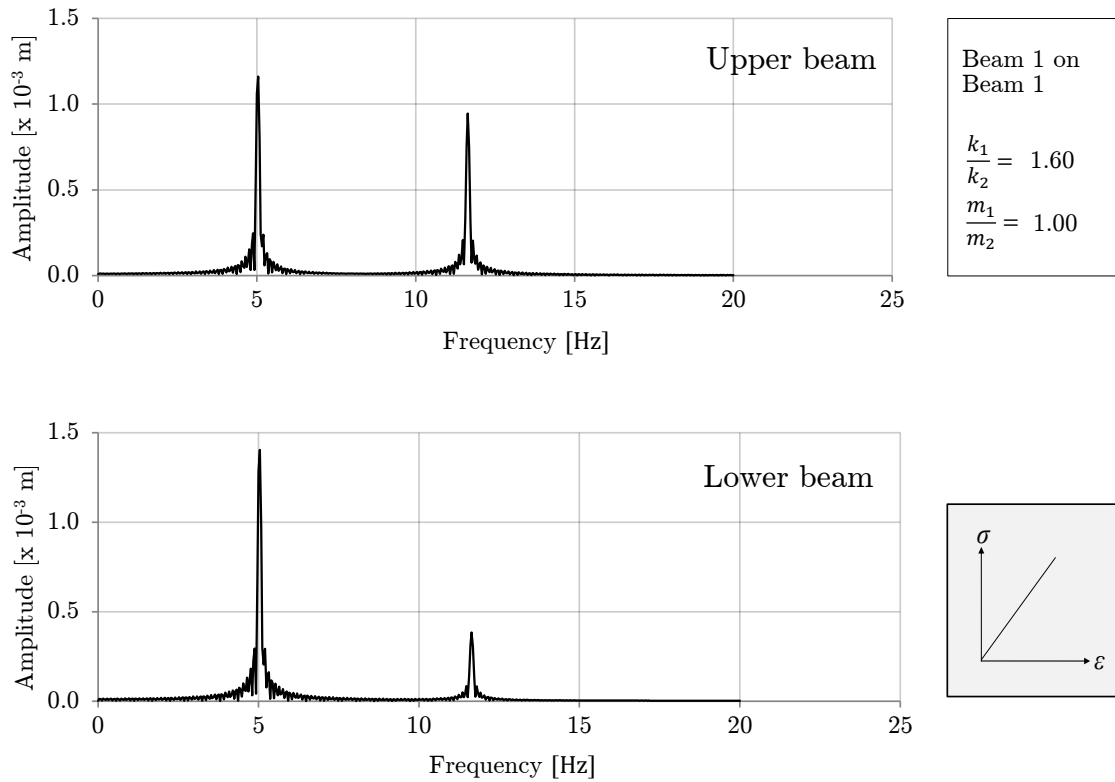


Figure 4.8: *Fourier transform of the displacements of upper (top) and lower beam (bottom) - see Figure 4.5. Beam no. 1 resting on beams no. 1 according to Table 4.1.*

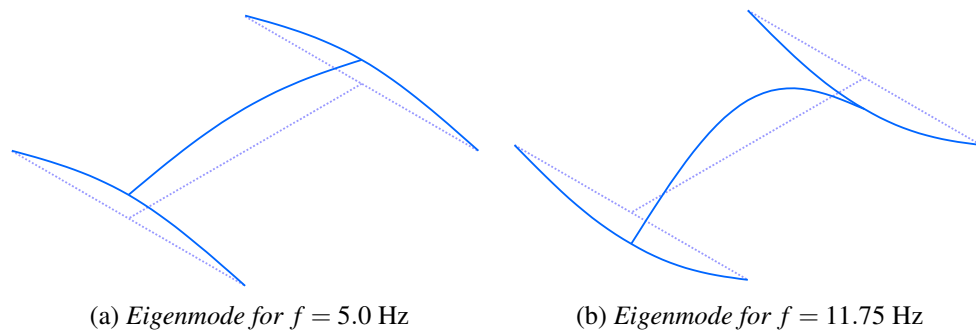


Figure 4.9: *Two main eigenmodes of the structure. Dotted line signifies the equilibrium position.*

In Figure 4.8, two distinct peaks can be seen for the upper beam, as well as for the lower beam; one at 5.0 Hz and one at 11.75 Hz. This means that the movement of the top beam is almost equally influenced by both of these two frequencies, while the lower beam is influenced mainly by the lower frequency and not so much by the higher one. Moreover, the magnitude of the movement of the upper beam and lower beam are comparable, see Figure 4.5. To compare, the eigenfrequencies obtained by solving the 2DOF system (according to Section 2.5.3) were 5.2 Hz and 12.4 Hz. This difference in eigenfrequencies is what causes the shift between the solutions. Hence, if the frequencies used in the 2DOF model had been the same as in FE analysis, the shift would have been

smaller.

In the modal analysis the eigenfrequencies and eigenvectors are obtained. In the case of the FE model, each eigenvector has the same length as the number of degrees of freedom in the model. By treating the eigenvector's components as the translational and rotational displacement of the structure, a modal shape can be plotted. In case of an equivalent 2DOF system, eigenvectors are also obtained, however now they only have two components. Nevertheless, some general consistency can be checked. The system points of the structure are located in the mid-span of the upper and lower beam. For the first eigenmode, the eigenvector's components have the same sign, which means that both of the masses (system points) move in the same direction. This also agrees with the modal shape presented in Figure 4.9a. For the second eigenmode, the entries in the eigenvector are of opposite sign. This means, that while the system point of the upper beam moves upward (or downward), the other system point will move downward (or upward). This relation can also be seen in Figure 4.9b.

Although there were many more modes in between those two, they were either antisymmetric (which were deemed to be unable to capture the vibration energy, and therefore were omitted) or of rather rotational nature (which is believed to be caused by insufficient locking of the degrees of freedom in ADINA).

The Fourier transforms for the next case, see Figure 4.6, which is beam no. 11 resting on beams no. 7 (with mass ratio of 4) can be seen in Figure 4.10.

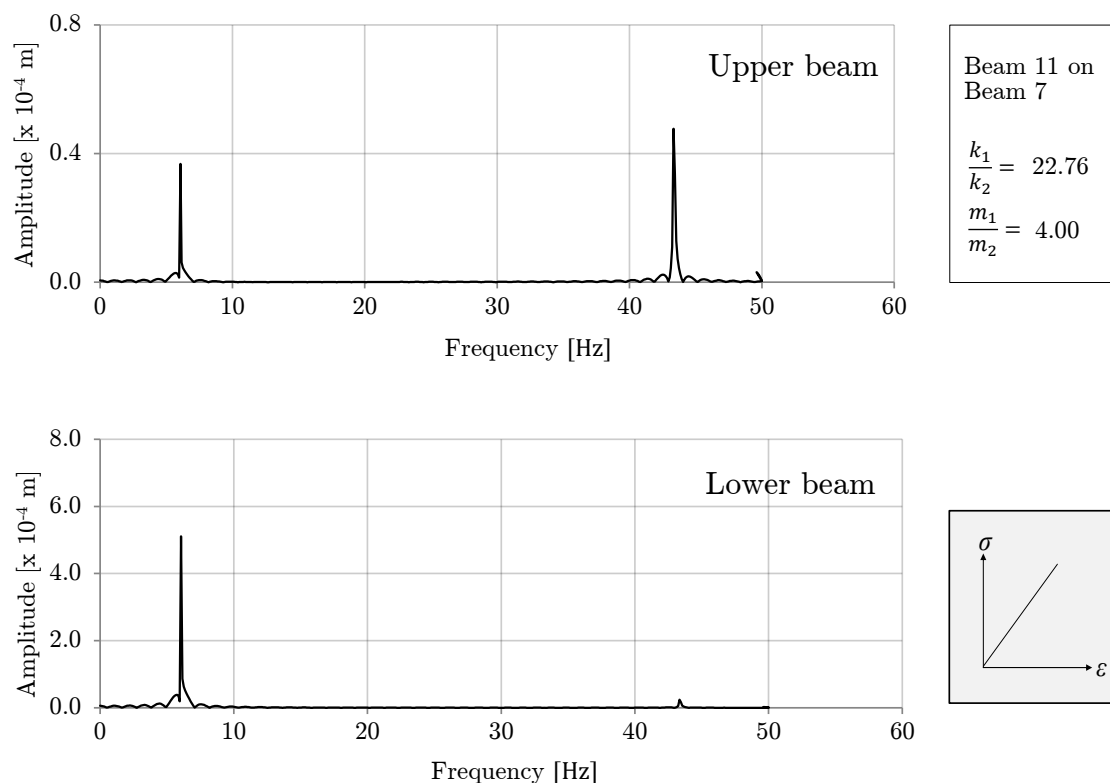


Figure 4.10: *Fourier transform of the displacements of upper (top) and lower beam (bottom) - see Figure 4.6. Beam no. 11 resting on beams no. 7 according to Table 4.1. Note the difference in unit of vertical axis.*

By comparing Figure 4.10 with Figure 4.6, it can be seen that the upper beam indeed vibrates at two distinct frequencies, and that their influence is comparable. On the other hand, the lower beam vibrates mainly with the lower frequency, and the influence of the higher eigenfrequency is very small. By comparing the amplitude, it can be seen that the movement of the lower beam is much greater in magnitude. This concurs with the conclusions drawn in Section 4.3.2. For this high stiffness ratio, the movement of the upper beam more or less corresponds to rigid body motion, and not so much to bending. The lower beams' movement constitutes the most of the overall movement of the structure.

For comparison, the eigenfrequencies obtained from the spectrum analysis are 6.0 Hz and 43.3 Hz. It is worth to add, that those eigenfrequencies result in the same modal shapes as presented earlier in Figure 4.9. At the same time, the eigenfrequencies obtained from the equivalent 2DOF system are 6.6 Hz and 55.2 Hz. The lower frequencies are close to each other, which results in better agreement (for the longer wave) in Figure 4.6. However, the difference between the higher frequencies is greater, and therefore the upper beam's secondary oscillations are out of phase from those obtained in ADINA.

The Fourier transforms for the last case, see Figure 4.7, which is beam no. 1 placed on beams no. 6 (with mass ratio of 0.25) are presented in Figure 4.11.

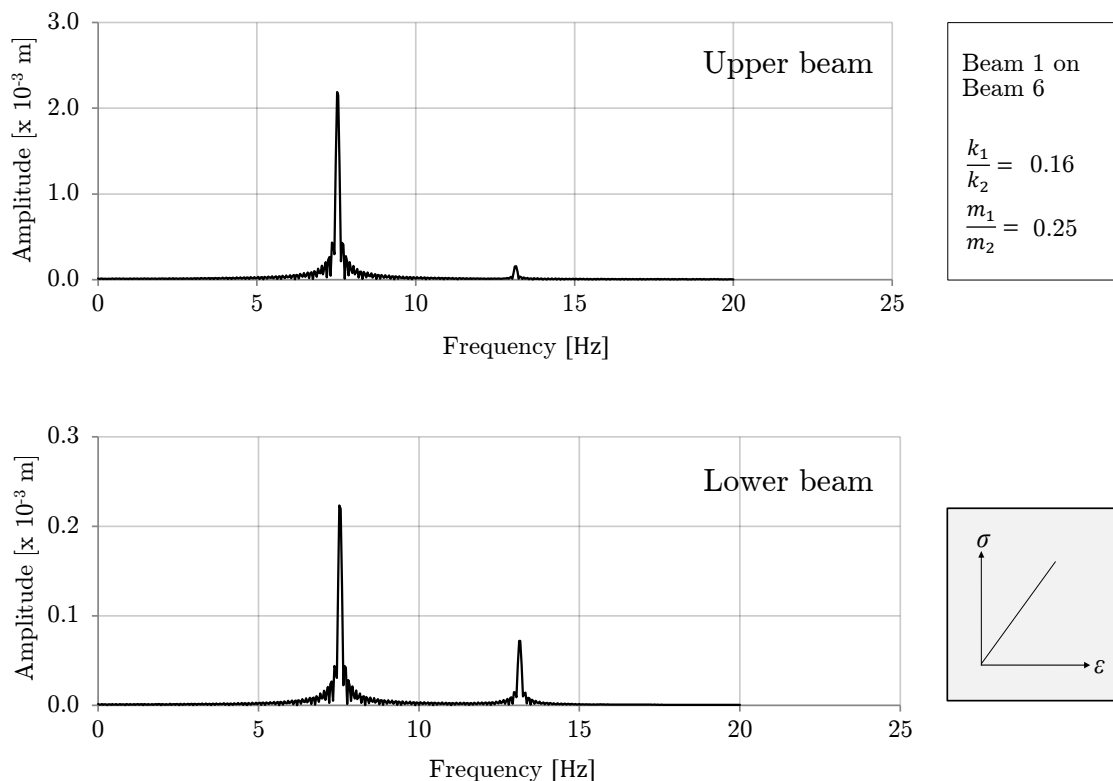


Figure 4.11: *Fourier transform of the displacements of upper (top) and lower beam (bottom) - see Figure 4.7. Beam no. 1 resting on beams no. 6 according to Table 4.1.*

In this case the situation is reversed - it is the lower beam which is influenced more by both frequencies. The eigenfrequencies of interest can be identified at 7.5 Hz and 12.9 Hz. Similarly, the frequencies obtained from an equivalent 2DOF system were received as

7.5 Hz and 13.5 Hz. The lower frequencies in FEM and 2DOF agree very well with each other, and the result of it can be seen in Figure 4.7, where the displacements are very much in phase. However, only the low frequency has significant influence on the upper beam behaviour, which results in little (or close to none) secondary oscillations. At the same time, those oscillations can be seen in the movement of the lower beam.

By looking at the amplitudes in Figure 4.11, it can be seen that the majority of the movement is coming from the upper beam, which is relatively much more flexible, and therefore bends easier. Similarly in this case, the modal shapes from ADINA resemble those presented in Figure 4.9. More detailed comparison of eigenmodes, the reader is referred to Chapter E.

To summarise, a few conclusions can be drawn from the Fourier transforms. Firstly, it is the stiffer beam which is usually affected by the secondary oscillations at the higher eigenfrequency. In the case of intermediate stiffness ratios, both beams are affected. Secondly, for extreme stiffness ratios (where one of the beams dominates) the response of an equivalent 2DOF system will always be a superposition of the two modes, whereas in reality the higher frequency vibrations are of little importance on the stiffer element. This may lead to slight disagreements between the motion of the structure and the equivalent 2DOF system. Lastly, the presented eigenmodes were recurring in the analyses, and are believed to be the main modal shapes of the structure. The 2DOF system should be adjusted to them.

4.4.3 Mass adjustment factors

In this section, the eigenfrequencies of the equivalent 2DOF system are adjusted to match those from ADINA. As already shown in Section 2.5.3, the frequencies of a 2DOF system depend both on the masses m_1 , m_2 and on the stiffnesses k_1 , k_2 . There are therefore many ways to obtain the desired values. However, there are four unknown parameters and only two equations for the frequencies, which means some of the parameters must become fixed. It was decided that the stiffnesses k_1 and k_2 will be kept fixed, while the masses m_1 and m_2 can vary. The eigenvalue problem of the system, from Equation (2.48) states that

$$\det(\mathbf{K} - \lambda\mathbf{M}) = 0 \quad (4.11)$$

After solving this equation, the vector of eigenvalues λ is obtained. By expanding (and disregarding for the moment the transformation factors κ_{mF}), we receive:

$$\left| \begin{bmatrix} k_1 & -k_1 \\ -k_1 & k_1 + 2k_2 \end{bmatrix} - \lambda \begin{bmatrix} m_{a1} & 0 \\ 0 & m_{a1} + 2m_{a2} \end{bmatrix} \right| = 0 \quad (4.12)$$

where m_{a1} and m_{a2} are the adjusted masses. Let's suppose that the desired eigenfrequencies f_1 and f_2 are known from the Fourier transform; they can be converted into the eigenvalues as

$$\lambda_1 = (2\pi f_1)^2 \quad (4.13)$$

$$\lambda_2 = (2\pi f_2)^2 \quad (4.14)$$

From there, the respective determinant for each eigenvalue can be calculated as

$$\begin{vmatrix} k_1 - m_{a1}\lambda_1 & -k_1 \\ -k_1 & k_1 + 2k_2 - 2m_{a2}\lambda_1 \end{vmatrix} = 2k_1k_2 - k_1m_{a1}\lambda_1 - 2k_1m_{a2}\lambda_1 - 2k_2m_{a1}\lambda_1 + \\ + 2m_{a1}m_{a2}\lambda_1^2 \quad (4.15)$$

$$\begin{vmatrix} k_1 - m_{a1}\lambda_2 & -k_1 \\ -k_1 & k_1 + 2k_2 - 2m_{a2}\lambda_2 \end{vmatrix} = 2k_1k_2 - k_1m_{a1}\lambda_2 - 2k_1m_{a2}\lambda_2 - 2k_2m_{a1}\lambda_2 + \\ + 2m_{a1}m_{a2}\lambda_2^2 \quad (4.16)$$

Setting Equation (4.15) and Equation (4.16) equal to zero, the unknown masses m_{a1} and m_{a2} can be solved, giving:

$$m_{a1} = \frac{2k_1k_2\lambda_1 - k_1 \left(k_2\lambda_1 - \sqrt{k_2^2\lambda_1^2 - 2k_2^2\lambda_1\lambda_2 + k_2^2\lambda_2^2 - 2k_1k_2\lambda_1\lambda_2 + k_2\lambda_2} \right) + 2k_1k_2\lambda_2}{k_1\lambda_1\lambda_2 + 2k_2\lambda_1\lambda_2} \quad (4.17)$$

$$m_{a2} = \frac{k_2\lambda_1 - \sqrt{k_2^2\lambda_1^2 - 2k_2^2\lambda_1\lambda_2 + k_2^2\lambda_2^2 - 2k_1k_2\lambda_1\lambda_2 + k_2\lambda_2}}{2\lambda_1\lambda_2} \quad (4.18)$$

The mass adjustment γ_{mF_1} and γ_{mF_2} factors can then be expressed as

$$\gamma_{mF_1} = \frac{m_{a1}}{m_1} \quad (4.19)$$

$$\gamma_{mF_2} = \frac{m_{a2}}{m_2} \quad (4.20)$$

where m_1 and m_2 are the original masses of each beam.

During the calculations, it was discovered that if a faulty frequency f_2 was given as input (wrong choice of eigenmode), the result of Equation (4.17) and Equation (4.18) gave complex numbers. In the beginning, the eigenmodes were picked out directly from the modal analysis in ADINA. However, due to aforementioned multitude of the modal shapes, it was not always clear which one to choose. When performing the Fourier transform on the displacement functions (as described in Section 4.4.2) and picking out the second frequency from it, the resulting mass adjustment factors were real and positive numbers. It was usually the second eigenfrequency that caused the problem, as it may be quite high for some cases. The first eigenfrequency and modal shape from the Fourier transform usually came as first or close to the first in the modal analysis in ADINA. As already mentioned, both eigenfrequencies resulted in the modal shapes similar to those presented in Figure 4.9 for each case of interest (see Appendix E for more information).

A total of 97 different analyses with various stiffness and mass ratios were run in ADINA. The mass ratios of interest were $m_1/m_2 = [0.25, 0.5, 1, 2, 4]$, while the stiffness ratios usually varied from 0 to 36. For each case, both implicit dynamic analysis and modal

analysis were carried out. On the displacement variations in time obtained in ADINA, the Fourier transform was performed and the dominating eigenfrequencies were stored. Next, for each case the two mass adjustment factors γ_{mF_1} and γ_{mF_2} were calculated. The results were plotted in 5 different graphs, depending on the mass ratio, and are presented in Figure 4.12 to Figure 4.16.

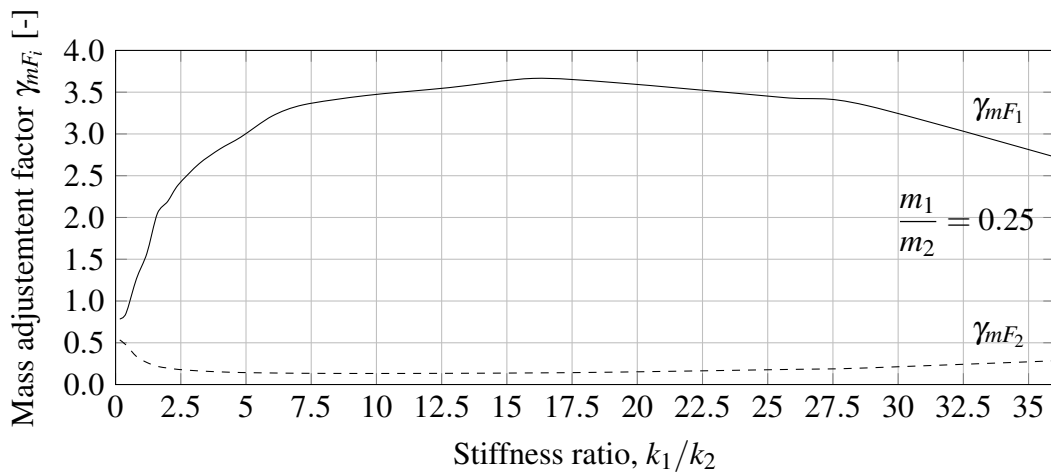


Figure 4.12: Mass adjustment factors γ_{mF_1} and γ_{mF_2} for $m_1/m_2 = 0.25$.

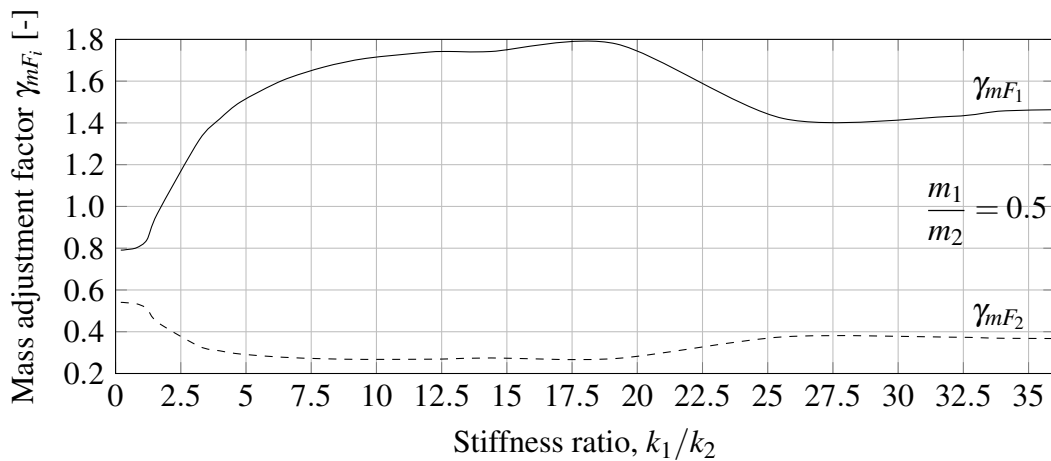


Figure 4.13: Mass adjustment factors γ_{mF_1} and γ_{mF_2} for $m_1/m_2 = 0.5$.

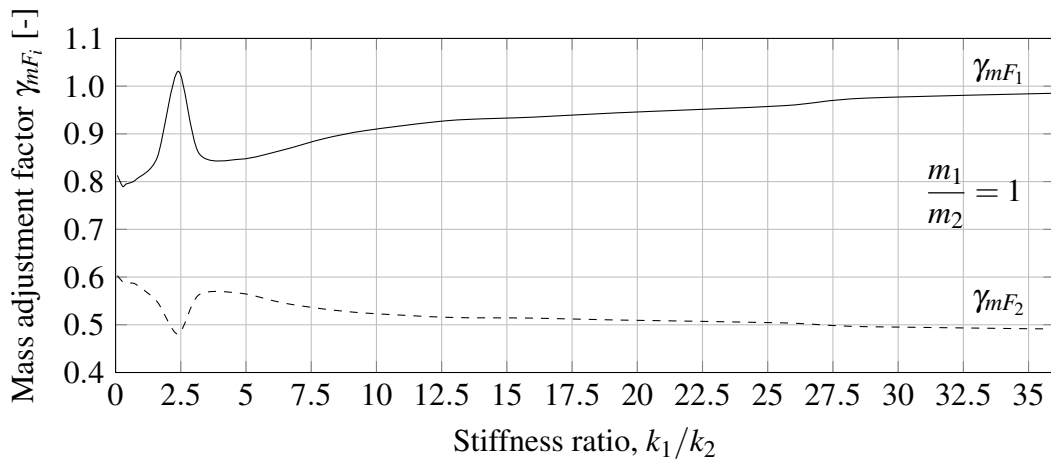


Figure 4.14: Mass adjustment factors γ_{mF_1} and γ_{mF_2} for $m_1/m_2 = 1$.

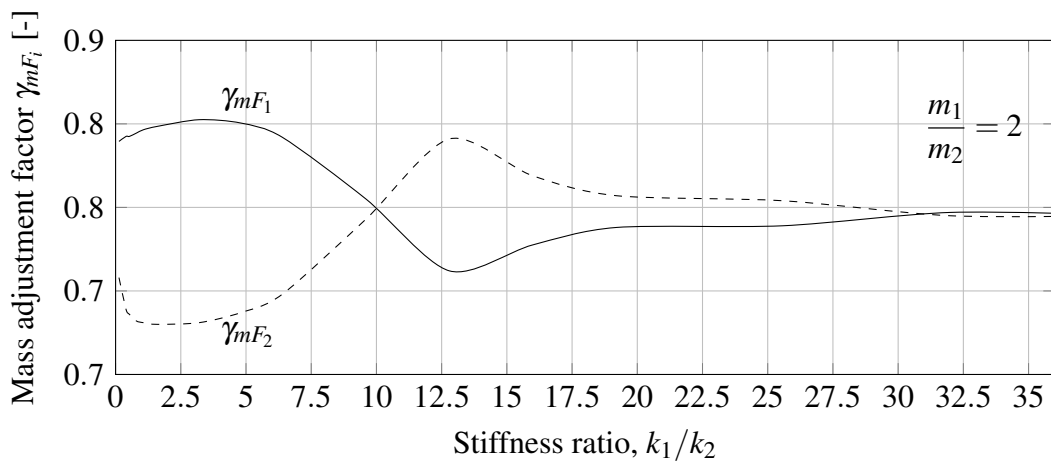


Figure 4.15: Mass adjustment factors γ_{mF_1} and γ_{mF_2} for $m_1/m_2 = 2$.

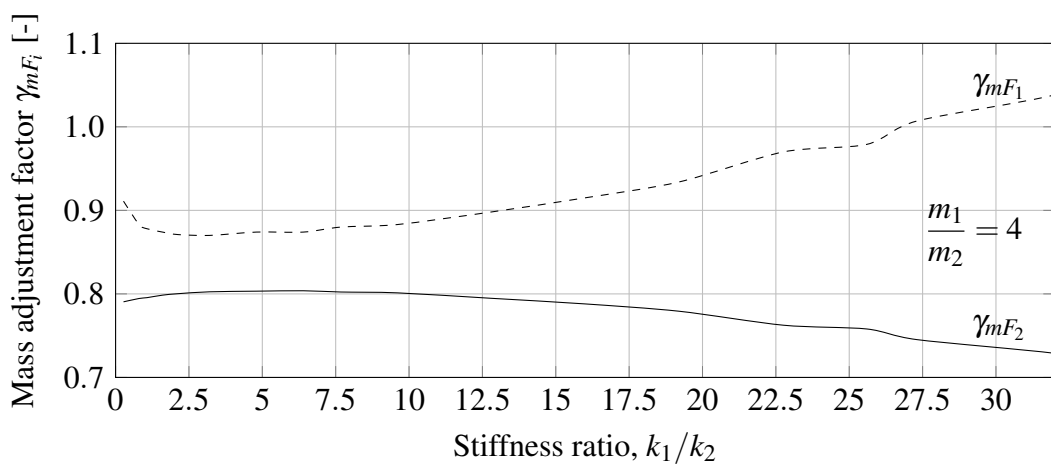


Figure 4.16: Mass adjustment factors γ_{mF_1} and γ_{mF_2} for $m_1/m_2 = 4$.

4.4.4 Response of the 2DOF model calibrated with mass adjustment factors

Based on the results in Section 4.4.3, the system of differential equations can be now expressed as

$$\begin{bmatrix} \gamma_{mF_1} m_1 & 0 \\ 0 & 2\gamma_{mF_2} m_2 \end{bmatrix} \begin{bmatrix} \ddot{u}_1 \\ \ddot{u}_2 \end{bmatrix} + \begin{bmatrix} k_1 & -k_1 \\ -k_1 & k_1 + 2k_2 \end{bmatrix} \begin{bmatrix} u_1 \\ u_2 \end{bmatrix} = \begin{bmatrix} F(t) \\ 0 \end{bmatrix} \quad (4.21)$$

where γ_{mF_1} and γ_{mF_2} are previously derived mass adjustment factors (see Equation (4.19) and Equation (4.20), respectively). For mass ratios lying in between those depicted in Section 4.4.3, linear interpolation can be employed in order to obtain an estimate of the mass adjustment factors. Such estimate was discovered to provide reasonable results.

The procedure of solution is now exactly the same as it was in Section 4.3, for the 2DOF model with regular transformation factors κ_{mF} . The system of equations (4.21) is solved in GNU Octave using the Central Difference Method, and the functions of system points' displacements in time are received as output. Those displacements are then converted into the displacements of respective beams (as explained in Section 4.3.1). The only thing that changes now is the incorporation of mass adjustment factors, γ_{mF_1} and γ_{mF_2} , in the place of the old transformation factors, κ_{mF_1} and κ_{mF_2} .

The same cases as in Section 4.3 were solved, so that a direct comparison is possible. Let's start with the situation, when beam no. 1 is placed on beams no. 1. The resulting stiffness ratio is in this case $k_1/k_2 = 1.6$, while the mass ratio is kept at $m_1/m_2 = 1$. The mass adjustment factors can be obtained from Figure 4.14, and are for this case $\gamma_{mF_1} = 0.851$ and $\gamma_{mF_2} = 0.548$. The response of the 2DOF model can be seen in Figure 4.17.

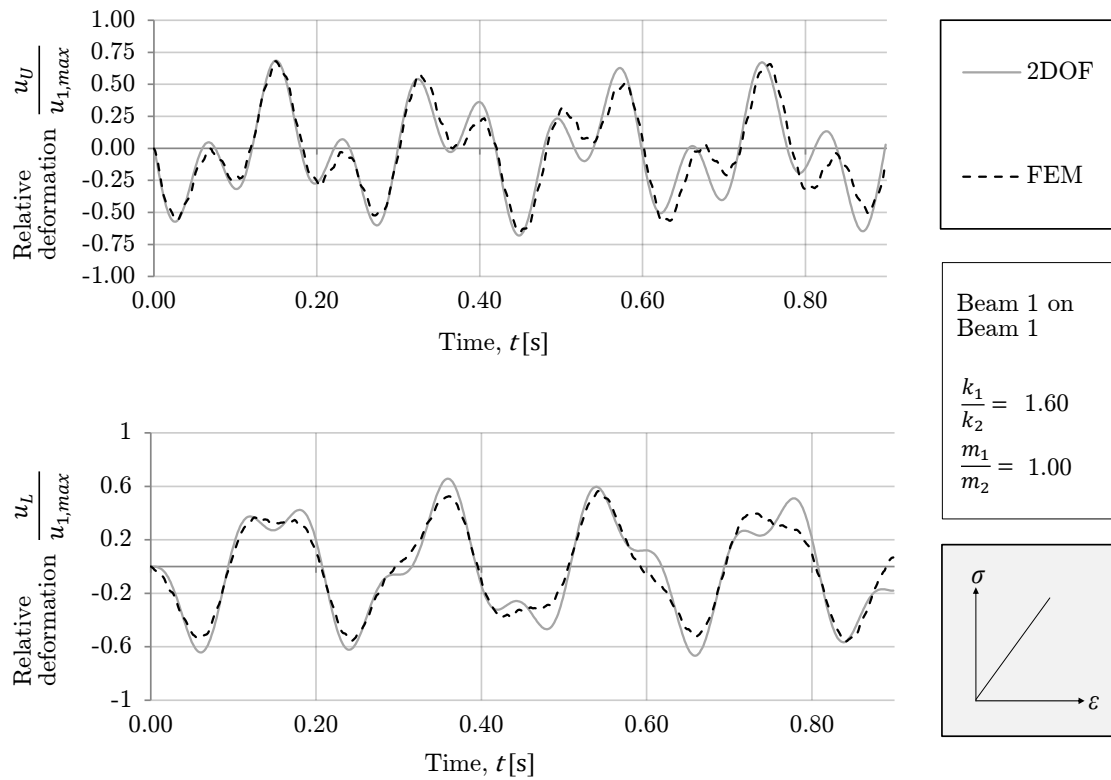


Figure 4.17: *Relative deformation of the upper (top) and lower beam (bottom) over time. Beam no. 1 resting on beams no. 1 according to Table 4.1. 2DOF model with mass adjustment factors.*

Comparing Figure 4.17 with Figure 4.5, one can see that the shift in eigenfrequencies is no longer present, which was also intended. Apart from that, the shape of the upper beam displacement agrees well for both of the models. However, the secondary oscillation of the lower beam is still somewhat larger in the 2DOF model than in ADINA. This is believed to be caused by low influence of the higher eigenfrequency on the lower beam (see Figure 4.8). The amplitudes according to the 2DOF model are now too high in comparison to the actual FE response. The difference varies with time, but usually a 20 -30 % greater displacement is obtained from the 2DOF system for both beams. Since the magnitude of displacements is comparable for both beams (due to intermediate stiffness ratio), this is considered a serious issue, and will be investigated and mitigated later.

The results for the next structure, namely beam no. 11 resting on beams no. 7 can be seen in Figure 4.18. The stiffness ratio now is $k_1/k_2 = 22.76$, while the mass ratio for the structure is $m_1/m_2 = 4$. For such a case, the mass adjustment factors can be read from Figure 4.16, and are equal to $\gamma_{mF_1} = 0.763$ and $\gamma_{mF_2} = 0.970$.

By looking at the graphs, it can be seen that the frequencies agree very well with each other, which was the intention. For the upper beam, the lower and higher frequencies also agree well. This is the result of having two distinct frequencies in the spectrum (see Figure 4.10), which the 2DOF model will capture. For the lower beam, the lower frequency is dominating, but the secondary oscillations at the higher eigenfrequency are also easily noticeable for the 2DOF model response. The FE response does not possess such clear secondary vibrations, since the lower beam vibrates mainly at the lower eigenfrequency.

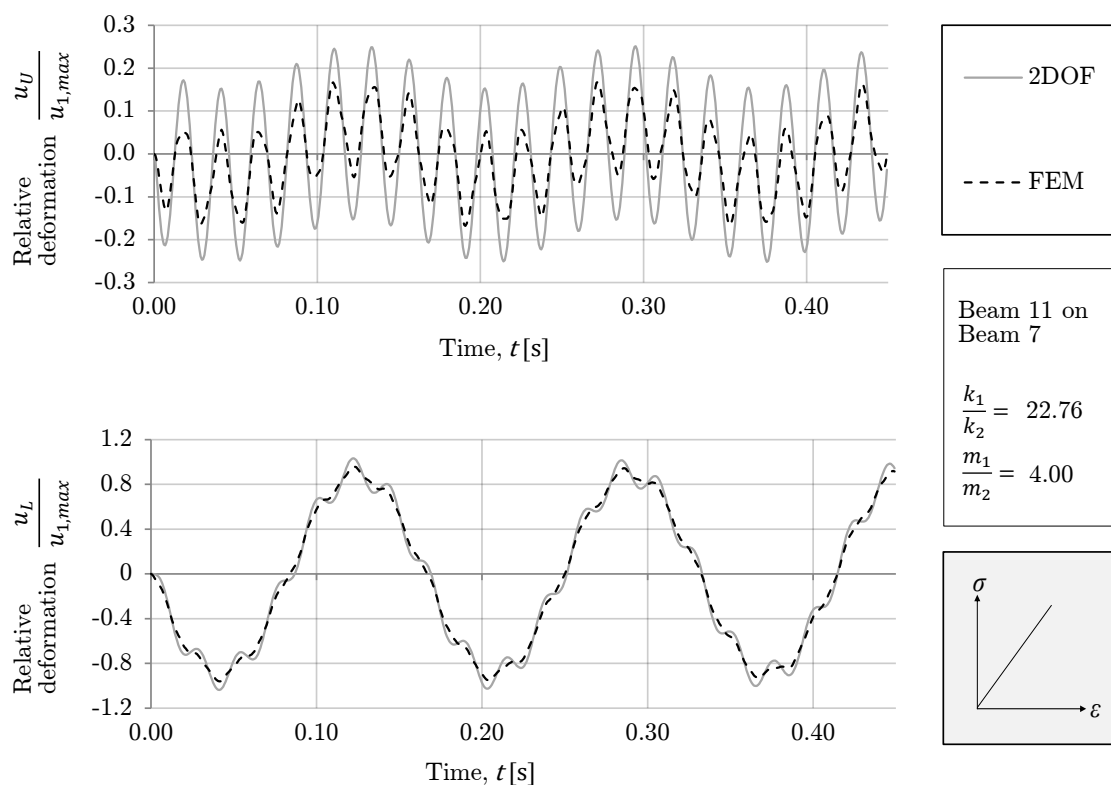


Figure 4.18: *Relative deformation of the upper (top) and lower beam (bottom) over time. Beam no. 11 resting on beams no. 7 according to Table 4.1. 2DOF model with mass adjustment factors.*

The other thing of interest here is the amplitude. Displacement of the lower beam, u_L agrees quite well between the models, but the upper beam's movement amplitude varies considerably between 2DOF and FEM. However, it is on the safe side for both cases. The large discrepancy in amplitude for the upper beam can reach up to 20-30 %, while the difference for the lower beam is 5-10 %. Comparing Figure 4.18 and Figure 4.6, it can be concluded that the responses are now in phase, but at the same time there is a difference in amplitudes, and hence the model could be further refined.

The last case studied here is the structure comprising beam no. 1 supported on beams no. 6. This structure has a low stiffness ratio of $k_1/k_2 = 0.16$, a mass ratio of $m_1/m_2 = 0.25$. For this kind of structure, the mass adjustment factor can be obtained from Figure 4.12 and are equal to $\gamma_{mF_1} = 0.786$ and $\gamma_{mF_2} = 0.534$. The results for both models are presented in Figure 4.19.

When looking at the graphs, it can be seen that for the upper beam, which poses the majority of the structure's movement, the response of both models agree well when it comes to frequency. The lower eigenfrequency is dominating for this beam (see Figure 4.11). There are some differences in amplitude, approximately 10 % discrepancy between the models. In contrast now, the response of the 2DOF model is on the unsafe side, which is not favourable.

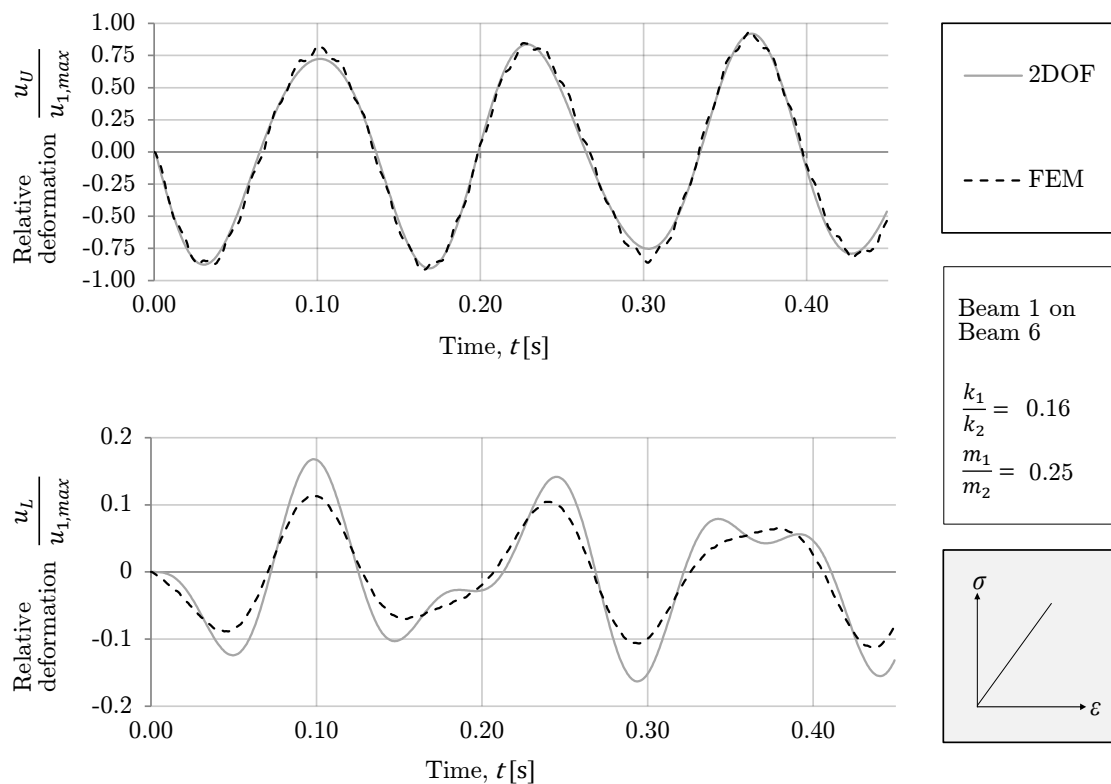


Figure 4.19: *Relative deformation of the upper (top) and lower beam (bottom) in time. Beam no. 1 resting on beams no. 6 according to Table 4.1. 2DOF model with adjusted mass adjustment factors.*

For the lower beam, despite good agreement in frequencies between the model, the amplitudes deviate even more. There is approx. 40-60 % between the models. This time, the 2DOF response is on the safe side. The response of both models shows that the beam vibrates at two distinct frequencies (according also to Figure 4.11), and the 2DOF model captures them both. It should be noted that the lower beam is much stiffer in relation to the upper one, and therefore its movement does not play a big role in the overall movement of the structure.

To conclude this part of the calibration of the 2DOF model, it can be said that it is possible and simple to assure that the response agrees with the actual behaviour (FEM)

in terms of the frequency. As long as the right frequencies are decided to be captured by the 2DOF model, the mass adjustment factors result overall in better correlation between the models. However, a new problem with amplitudes was created. It was shown that the amplitudes deviate between the models. Moreover, it cannot be directly said in which direction they will deviate (safe or unsafe side). Therefore, a way to calibrate the model further with respect to amplitudes only is needed.

4.5 Calibration of the 2DOF model - amplitude

4.5.1 General notes

As it was shown in Section 4.4.4, the 2DOF model can be further calibrated, so that not only the right frequency is captured, but also the right amplitude. Hence in this section an optimisation procedure is carried out in order to find the best fit of the 2DOF model response to the actual ADINA structural behaviour. There are many methods of optimisation, but in this case unconstrained nonlinear optimisation was used. In particular, the Nelder-Mead simplex algorithm was employed. Function `fminsearch` in GNU Octave uses this method for finding a minimum of a function. For more information about the Nelder-Mead method, the reader is referred to Lagarias et al. (1998). In this section, the calibrated 2DOF model (with respect to the amplitudes) will be referred to as the optimised 2DOF model.

4.5.2 Optimisation procedure and constraints

The goal in this section was to find such parameters that can be used in the differential equation system (as in Equation (4.6) or Equation (4.21)), which result in the response of the 2DOF system matching the actual FE response as close as possible. One type of such adjusting parameters are the mass adjustment factors γ_{mF_i} , which were described in Section 4.4.3. In that case, only the mass matrix entries were changed as a result. Now, there is no such limitation. It means that there can be adjustment factors which pertain to both mass and stiffness matrix, as well as to the force vector.

The simplex method finds the minimum of an objective function, which is a function of the sought parameters. This function can be constructed in various ways, as well as different constraints can be used to assure that boundary conditions are fulfilled.

The algorithm also needs an initial guess value, from which it starts the search. It is vital that the initial guess values provide approximately good results, otherwise local minima of the objective function can be found instead of the desired result. The more parameters are involved in the optimisation procedure, the more important it is to use a proper guess value.

The optimisation was performed for each of the studied cases (see Section 4.2.1), and the results were then analysed and evaluated. A good fit between the curves was however not achieved for every stiffness ratio k_1/k_2 and mass ratio m_1/m_2 . If the resultant adjustment parameters were deemed unreasonable, another attempt with different objective function or constraints was carried out. It was an iterative process, and a total of 5 attempts were made.

Attempt 1

For the first try, the components of the force vector were unconstrained, meaning they can attain any value. Therefore two adjustment factors γ_{F1} and γ_{F2} could be computed. At the same time, the mass adjustment factors γ_{mFi} from section Section 4.4.3 were applied to the mass matrix, and were constrained at these values. Also, the stiffness matrix remained unchanged. The system of differential equation used in this attempt was

$$\begin{bmatrix} \gamma_{mF_1} m_1 & 0 \\ 0 & 2\gamma_{mF_2} m_2 \end{bmatrix} \begin{bmatrix} \ddot{u}_1 \\ \ddot{u}_2 \end{bmatrix} + \begin{bmatrix} k_1 & -k_1 \\ -k_1 & k_1 + 2k_2 \end{bmatrix} \begin{bmatrix} u_1 \\ u_2 \end{bmatrix} = \begin{bmatrix} \gamma_{F1} F(t) \\ \gamma_{F2} F(t) \end{bmatrix} \quad (4.22)$$

- Objective function: sum of the differences between maximum displacements (for upper and lower beam) from ADINA and 2DOF.

$$L = (u_{UA}^{max} - u_U^{max}) + (u_{LA}^{max} - u_L^{max}) \quad (4.23)$$

- Guess values: $\gamma_{F1} = 1.0$, $\gamma_{F2} = 0.2$.
- Constraints: none
- Sought parameters: γ_{F1} , γ_{F2}
- Results: Not so good visual fit between curves. Often negative value for γ_{F2} . Decided to go further to next iteration.

Attempt 2

In this attempt, the force vector was chosen to be constant. The sought parameters were both for adjustment of mass and stiffness matrix. Starting value was set again from the frequency calibrated 2DOF model. The system of equations in this case can be expressed as

$$\begin{bmatrix} \gamma_{m_1} m_1 & 0 \\ 0 & 2\gamma_{m_2} m_2 \end{bmatrix} \begin{bmatrix} \ddot{u}_1 \\ \ddot{u}_2 \end{bmatrix} + \begin{bmatrix} \gamma_{k_1} k_1 & -\gamma_{k_1} k_1 \\ -\gamma_{k_1} k_1 & \gamma_{k_1} k_1 + 2\gamma_{k_2} k_2 \end{bmatrix} \begin{bmatrix} u_1 \\ u_2 \end{bmatrix} = \begin{bmatrix} F(t) \\ 0 \end{bmatrix} \quad (4.24)$$

- Objective function: sum of the squares of differences between displacement (for upper and lower beam) from ADINA and 2DOF in each time step.

$$L = \sum_{t=0}^{t_{end}} ((u_{UA} - u_U)^2 + (u_{LA} - u_L)^2) \quad (4.25)$$

- Guess values: $\gamma_{m_1} = \gamma_{mF_1}$, $\gamma_{m_2} = \gamma_{mF_2}$, $\gamma_{k_1} = 1$, $\gamma_{k_2} = 1$
- Constraints: none
- Sought parameters: γ_{m_1} , γ_{m_2} , γ_{k_1} , γ_{k_2}
- Results: Better visual fit between curves, but still not good enough. Decided to go further to next iteration.

Attempt 3

The third attempt is very similar to the previous one. The only difference now is that the second component of the force vector becomes unconstrained. The system of differential equation takes the form:

$$\begin{bmatrix} \gamma_{m_1} m_1 & 0 \\ 0 & 2\gamma_{m_2} m_2 \end{bmatrix} \begin{bmatrix} \ddot{u}_1 \\ \ddot{u}_2 \end{bmatrix} + \begin{bmatrix} \gamma_{k_1} k_1 & -\gamma_{k_1} k_1 \\ -\gamma_{k_1} k_1 & \gamma_{k_1} k_1 + 2\gamma_{k_2} k_2 \end{bmatrix} \begin{bmatrix} u_1 \\ u_2 \end{bmatrix} = \begin{bmatrix} \gamma_{F_1} F(t) \\ \gamma_{F_2} F(t) \end{bmatrix} \quad (4.26)$$

- Objective function: sum of the squares of differences between displacement (for upper and lower beam) from ADINA and 2DOF in each time step.

$$L = \sum_{t=0}^{t_{end}} ((u_{UA} - u_U)^2 + (u_{LA} - u_L)^2) \quad (4.27)$$

- Guess values: $\gamma_{m_1} = \gamma_{m_{F_1}}$, $\gamma_{m_2} = \gamma_{m_{F_2}}$, $\gamma_{k_1} = 1$, $\gamma_{k_2} = 1$, $\gamma_{F_2} = 0.2$
- Constraints: $\gamma_{F_1} = 1$
- Sought parameters: γ_{m_1} , γ_{m_2} , γ_{k_1} , γ_{k_2} , γ_{F_2}
- Results: Even better visual fit between curves, but for high k_1/k_2 ratios, the sought force factor γ_{F_2} was unreasonably larger than $\gamma_{F_1} = 1$ (more than 10^3 times greater). Decided to go further to next iteration.

Attempt 4

In this attempt, the sum of the components in the force vectors is chosen to be always $F(t)$ so that the overall force acting on the structure is preserved. Furthermore, the objective function is normalized, so that the beam which has smaller displacement and the beam with larger displacement both have significant influence on the end result. The system of differential equation is in this case the same as in Equation (4.26).

$$\begin{bmatrix} \gamma_{m_1} m_1 & 0 \\ 0 & 2\gamma_{m_2} m_2 \end{bmatrix} \begin{bmatrix} \ddot{u}_1 \\ \ddot{u}_2 \end{bmatrix} + \begin{bmatrix} \gamma_{k_1} k_1 & -\gamma_{k_1} k_1 \\ -\gamma_{k_1} k_1 & \gamma_{k_1} k_1 + 2\gamma_{k_2} k_2 \end{bmatrix} \begin{bmatrix} u_1 \\ u_2 \end{bmatrix} = \begin{bmatrix} \gamma_{F_1} F(t) \\ \gamma_{F_2} F(t) \end{bmatrix} \quad (4.28)$$

- Objective function: sum of the squares of differences between displacement (for upper and lower beam) from ADINA and 2DOF in each time step. Function is normalized to the maximum displacement for each beam

$$L = \sum_{t=0}^{t_{end}} \left(\frac{u_{UA} - u_U}{u_{UA}^{max}} \right)^2 + \left(\frac{u_{LA} - u_L}{u_{LA}^{max}} \right)^2 \quad (4.29)$$

- Guess values: $\gamma_{m_1} = \gamma_{m_{F_1}}$, $\gamma_{m_2} = \gamma_{m_{F_2}}$, $\gamma_{k_1} = 1$, $\gamma_{k_2} = 1$, $\gamma_{F_1} = 0.8$, $\gamma_{F_2} = 0.2$. The search is done in three steps, so that the most of the shape of the function is captured. The end result of each step becomes the guess value of the next step.
- Constraints: $\gamma_{F_1} + \gamma_{F_2} = 1$
- Sought parameters: γ_{m_1} , γ_{m_2} , γ_{k_1} , γ_{k_2} , γ_{F_1} , γ_{F_2}
- Results: Good visual fit. However, the resulting amplitudes have been differing up to 20 % on the unsafe side from the actual ADINA displacements. Decided to go further with next iteration.

Attempt 5

The final attempt used the same idea as in attempt 4. The only thing that changed is the definition of error. In order to force the 2DOF response to be even closer or at least on the safe side, the displacement located at the unsafe side was weighted with an additional factor 2. The system of the differential equation of motion for the system is kept unchanged, i.e

$$\begin{bmatrix} \gamma_{m_1} m_1 & 0 \\ 0 & 2\gamma_{m_2} m_2 \end{bmatrix} \begin{bmatrix} \ddot{u}_1 \\ \ddot{u}_2 \end{bmatrix} + \begin{bmatrix} \gamma_{k_1} k_1 & -\gamma_{k_1} k_1 \\ -\gamma_{k_1} k_1 & \gamma_{k_1} k_1 + 2\gamma_{k_2} k_2 \end{bmatrix} \begin{bmatrix} u_1 \\ u_2 \end{bmatrix} = \begin{bmatrix} \gamma_{F1} F(t) \\ \gamma_{F2} F(t) \end{bmatrix} \quad (4.30)$$

- Objective function: sum of the squares of differences between displacement (for upper and lower beam) from ADINA and 2DOF in each time step. Function is normalized to the maximum displacement for each beam. If the displacement lies on the unsafe side, it is additionally weighted with factor 2 to force the result to be on the safe side and so that it comes even closer to the real ADINA response.

$$L = \sum_{t=0}^{t_{end}} \left(\frac{u_{UA} - u_U}{u_{UA}^{max}} \right)^2 + \left(\frac{u_{LA} - u_L}{u_{LA}^{max}} \right)^2 + 2 \left\langle \frac{|u_{UA}| - |u_U|}{u_{UA}^{max}} \right\rangle^2 + 2 \left\langle \frac{|u_{LA}| - |u_L|}{u_{LA}^{max}} \right\rangle^2 \quad (4.31)$$

Note: In order to distinguish safe and unsafe side, the Macaulay bracket function is used here. This function is also called a ramp function, and is defined as:

$$\langle x \rangle = \begin{cases} 0 & \text{if } x < 0 \\ x & \text{if } x \geq 0. \end{cases} \quad (4.32)$$

- Guess values: Same as in attempt 4
- Constraints: $\gamma_{F1} + \gamma_{F2} = 1$
- Sought parameters: $\gamma_{m_1}, \gamma_{m_2}, \gamma_{k_1}, \gamma_{k_2}, \gamma_{F1}, \gamma_{F2}$
- Results: Very good visual fit. Results seem to agree very well between the models. However, a divergence of up to 10 % on the unsafe side is present. Decided to stop the iteration.

4.5.3 Optimisation factors

An example result of the final iterations - the optimisation factors $\gamma_{m_1}, \gamma_{m_2}, \gamma_{k_1}, \gamma_{k_2}, \gamma_{F1}, \gamma_{F2}$ is presented in Figure 4.20. The remaining results - optimisation factors for different mass ratios along with tabulated values can be found in Figure D.1 - Figure D.5 and Table D.1 - Table D.5 in Appendix D.

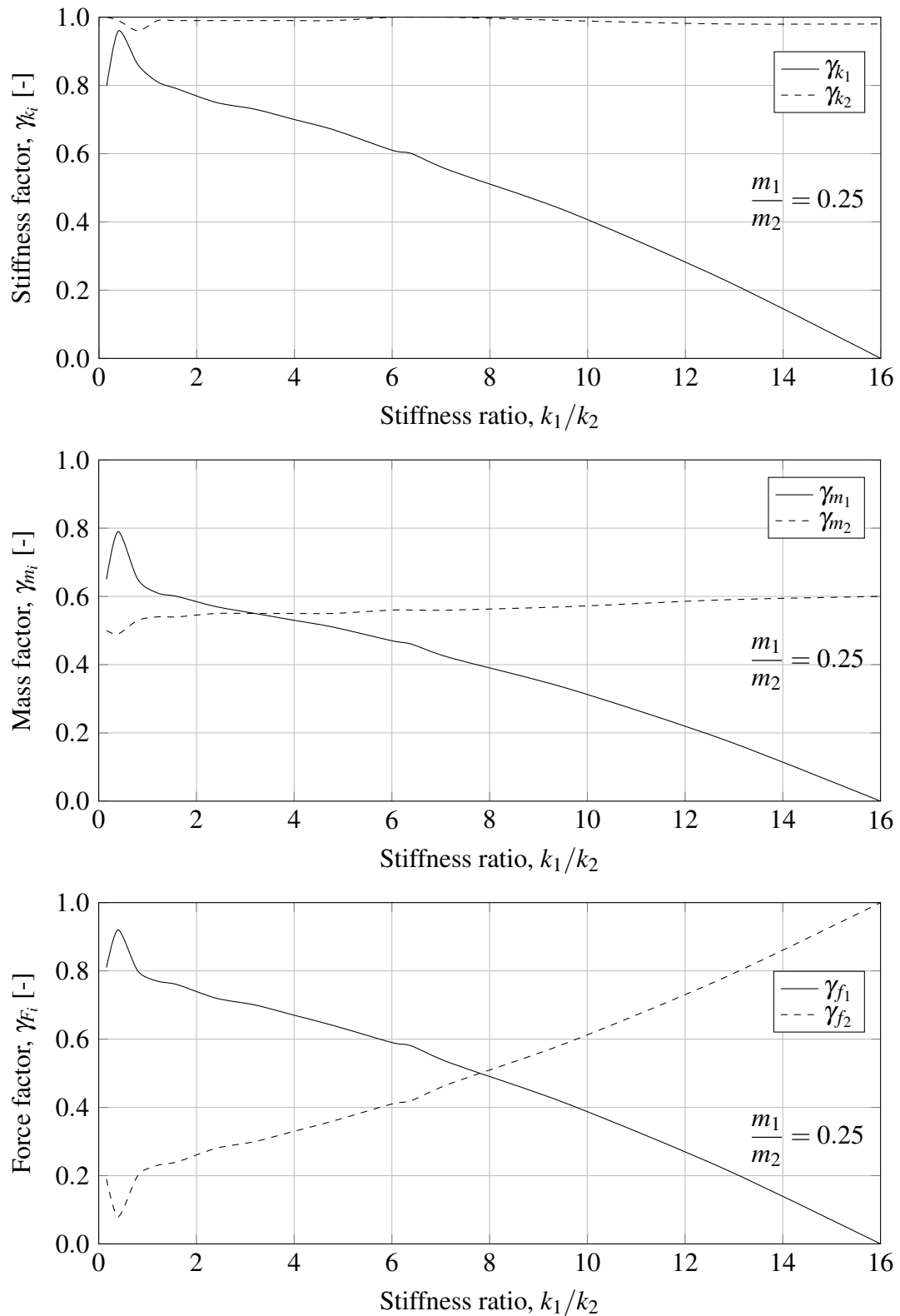


Figure 4.20: Optimisation factors as a function of stiffness ratio k_1/k_2 . Valid for mass ratio of $m_1/m_2 = 0.25$

4.6 Response of the optimised 2DOF model

4.6.1 General notes

With obtained optimisation factors from Section 4.5.3, the response of the equivalent 2DOF system can now be generated. If the structure of interest has a mass ratio that lies in between the studied cases, it is advised to perform linear interpolation in order to obtain an estimate of the factors. The system of differential equation, solving of which results in the 2DOF response can be expressed as:

$$\begin{bmatrix} \gamma_{m_1} m_1 & 0 \\ 0 & 2\gamma_{m_2} m_2 \end{bmatrix} \begin{bmatrix} \ddot{u}_1 \\ \ddot{u}_2 \end{bmatrix} + \begin{bmatrix} \gamma_{k_1} k_1 & -\gamma_{k_1} k_1 \\ -\gamma_{k_1} k_1 & \gamma_{k_1} k_1 + 2\gamma_{k_2} k_2 \end{bmatrix} \begin{bmatrix} u_1 \\ u_2 \end{bmatrix} = \begin{bmatrix} \gamma_{F_1} F(t) \\ \gamma_{F_2} F(t) \end{bmatrix} \quad (4.33)$$

where γ_i are the optimisation factors.

The 2DOF model modified with the aforementioned optimisation factors is further referred to as the optimised 2DOF model. Again, the same three structures were analysed and the results of these analyses are presented for easy comparison.

4.6.2 Deformation

The structure consisting of beam no. 1 placed on beams no. 1 was studied first. Again, the stiffness ratio for it is $k_1/k_2 = 1.6$ and the mass ratio is $m_1/m_2 = 1$. The results can be seen in Figure 4.21.

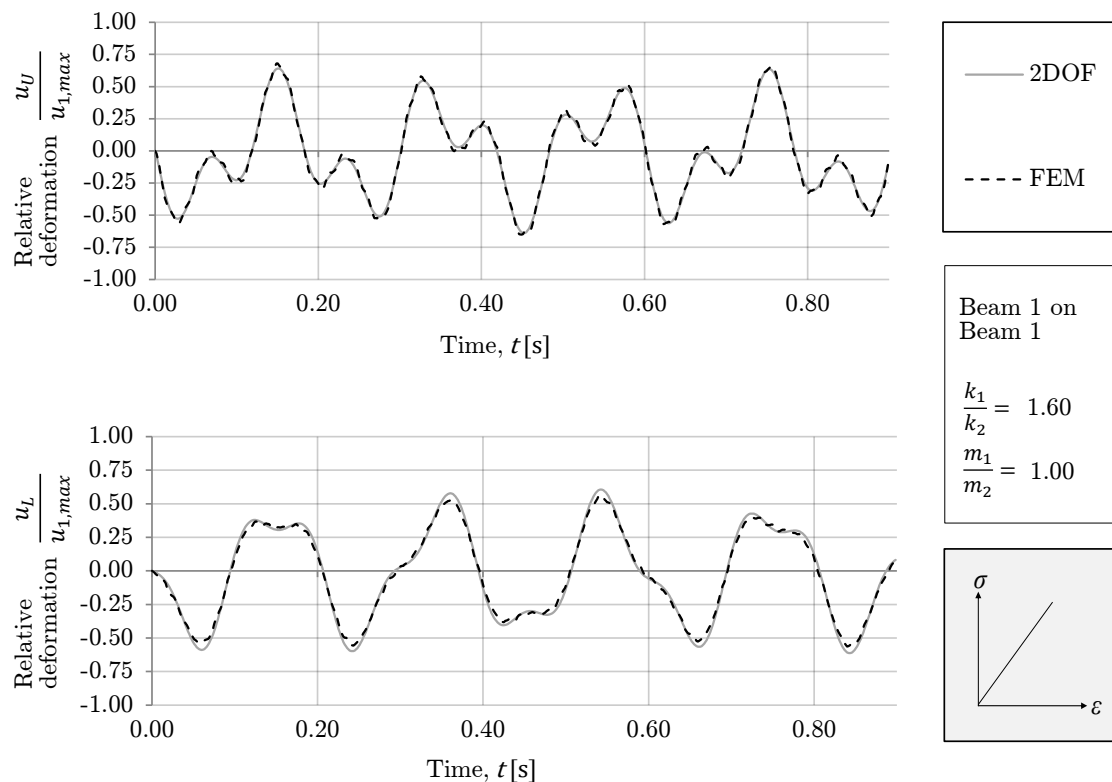


Figure 4.21: Response of the upper (top) and lower beam (bottom) for both FE model and optimised 2DOF model. The structure consists of beam no. 1 placed on beams no. 1 according to Table 4.1.

By looking at the graphs, a very good correlation between displacements can be seen, for both the upper and the lower beam. Both frequencies and amplitudes seem to match well. When looking at the maximum amplitudes, it can be said that for the lower beam the 2DOF model underestimates the response by 5.9 %, while the lower beam's deformation is overestimated by 8.3 % at maximum. The error from the previous model (in Section 4.4.4) has been reduced or converted into an overestimation, which is on the safe side. This is a structure with an intermediate stiffness ratio, which means that the movement of both beams has much influence on the overall motion of the structure. Hence it is important to capture as much as possible of the deformation for both of the beams.

For the next studied case, a structure built from beam no. 11 resting on beams no. 7 was chosen, where the lower beam was four times heavier than the upper one. The resulting stiffness ratio is $k_1/k_2 = 22.76$ and the mass ratio is $m_1/m_2 = 4$. The results are presented in Figure 4.22.

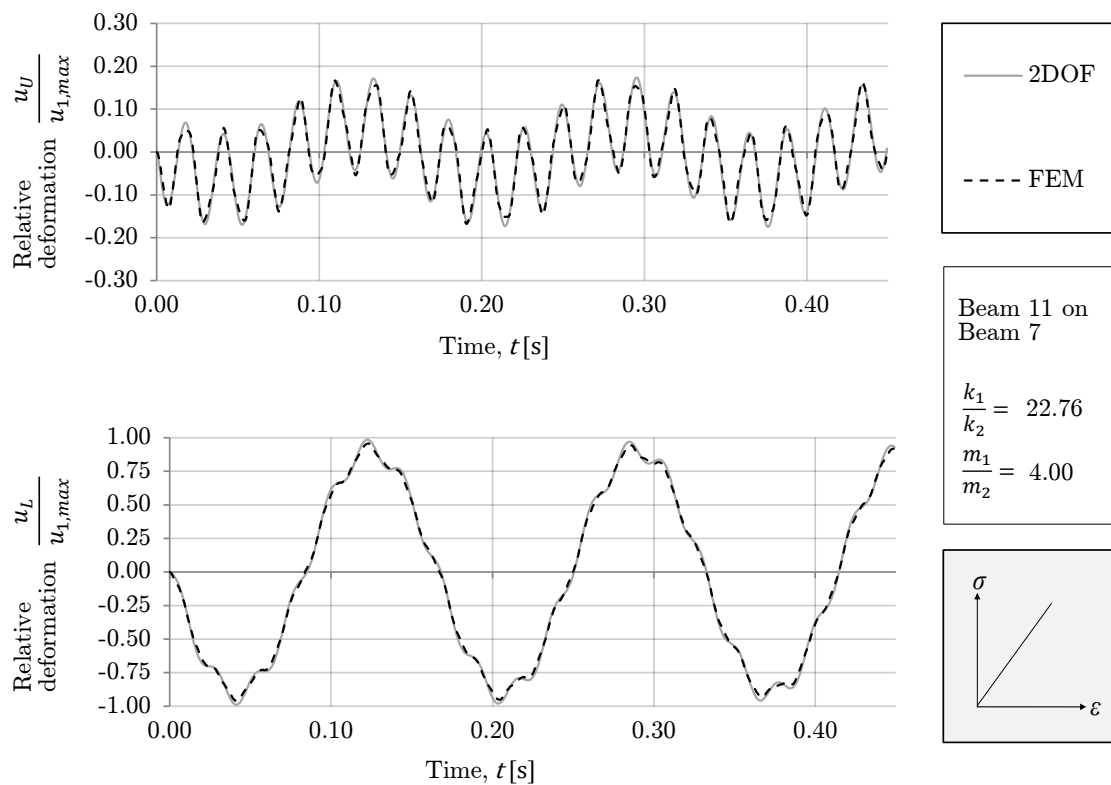


Figure 4.22: Response of the upper (top) and lower beam (bottom) for both FE model and optimised 2DOF model. The structure consists of beam no. 11 placed on beams no. 7 according to Table 4.1.

Both primary and secondary oscillations are well captured by the 2DOF model. No visible shift in the frequencies can be noticed. For the upper beam, the 2DOF model underestimated the response by 2.9 %, while the deformation of the lower beam is overestimated by 3.0 %. To remind the reader, this is a structure with relatively high stiffness ratio, which means that most of the movement will come from the lower beams. Just as in the previous case shown in Figure 4.21, the optimised 2DOF model resulted in

reduced difference in amplitudes (especially for the upper beam), and is believed overall to provide a better description of the behaviour of this structure.

The last studied case encompassed a structure composed of beam no. 1 supported on beams no. 6, which are four times heavier. This resulted in the stiffness ratio of $k_1/k_2 = 0.16$ and the mass ratio of $m_1/m_2 = 0.25$. Plots of upper and lower beam's deformation are presented in Figure 4.23.

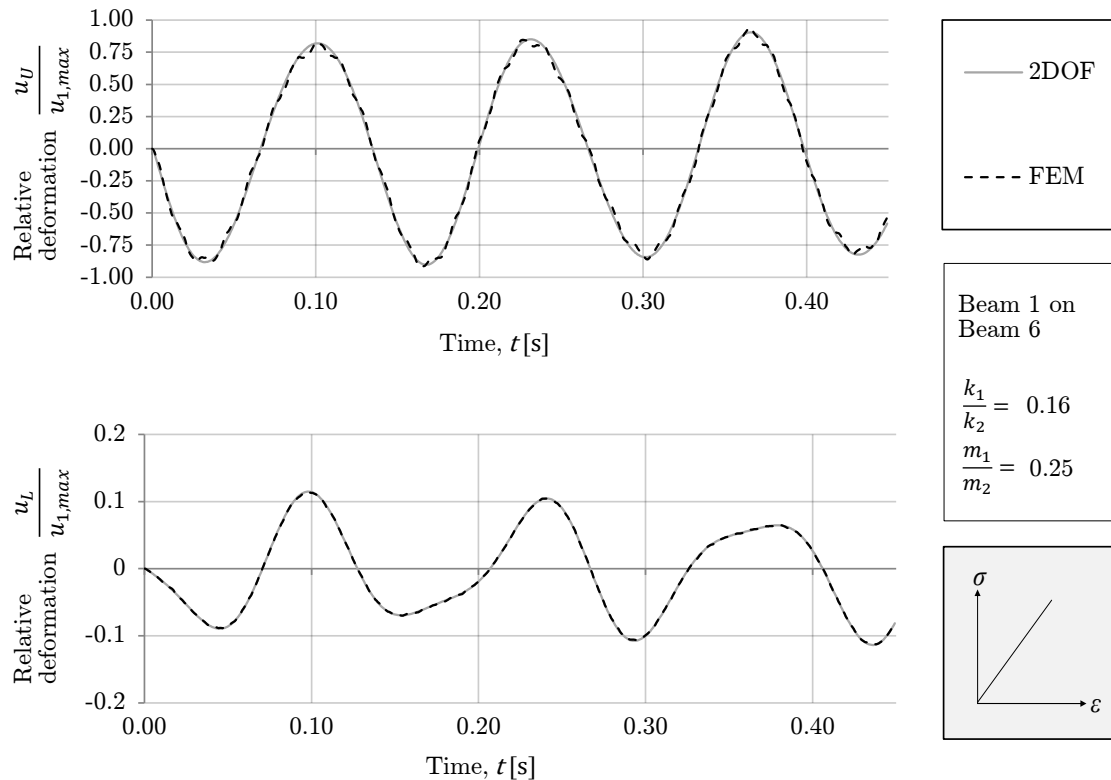


Figure 4.23: *Response of the upper (top) and lower beam (bottom) for both FE model and optimised 2DOF model. The structure consists of beam no. 1 placed on beams no. 6 according to Table 4.1.*

This time, the correlation between the models is very good as well. The optimised 2DOF model follows the FE response very well, capturing not only primary but also secondary vibration in the lower beam. The amplitudes are also placed close to each other now. The maximum deformation of the upper beam is underestimated by 5.7 % with the 2DOF model, while the lower beam's deflection is underestimated by 0.1 %. The optimisation reduced the error and provided overall a better approximation of the structure behaviour.

4.6.3 Amplitude error

In order to show the accuracy of the model, the discrepancy between the 2DOF and ADINA displacement was examined. For each studied case, the ratio between the maximum displacement in the optimised 2DOF system and the corresponding ADINA solution was calculated. The results are presented in Figure 4.24 and Figure 4.25.

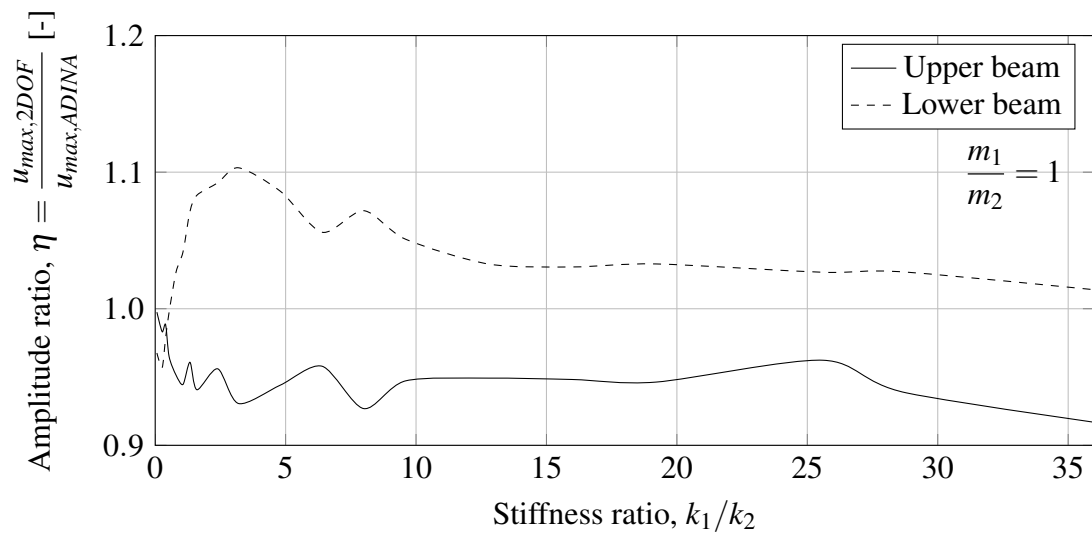
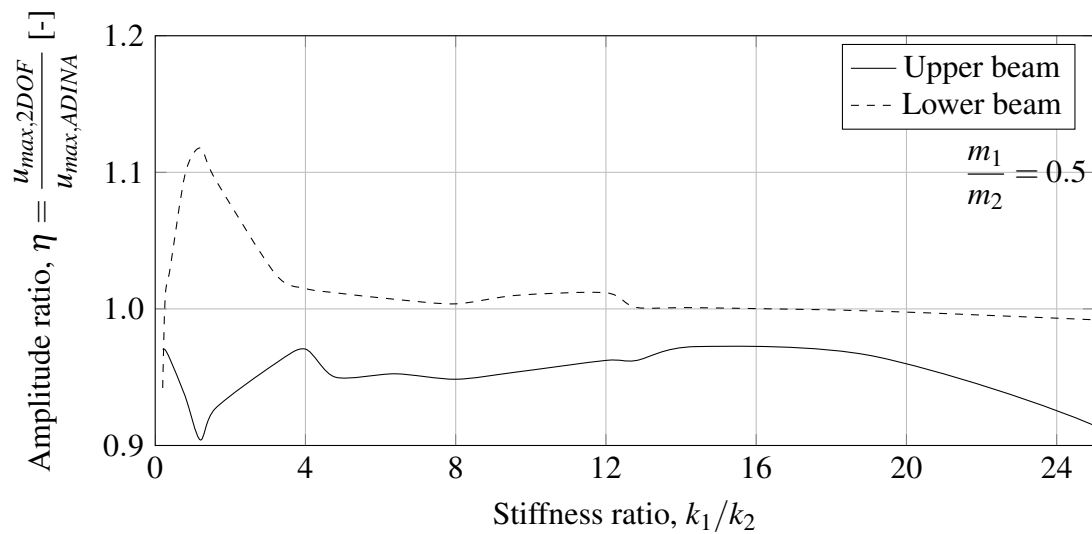
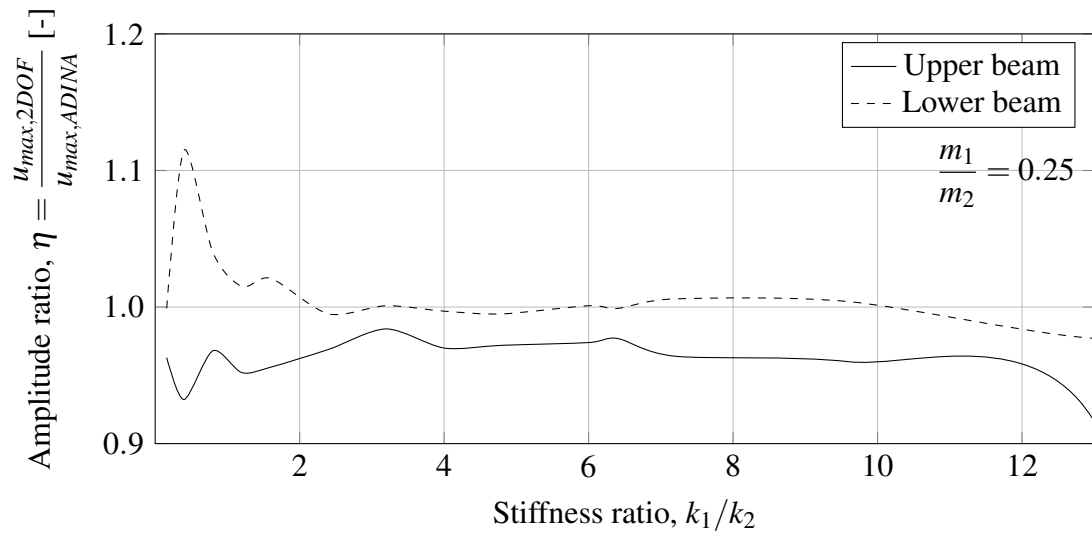


Figure 4.24: Difference between the optimised 2DOF model response and the actual FE solution.

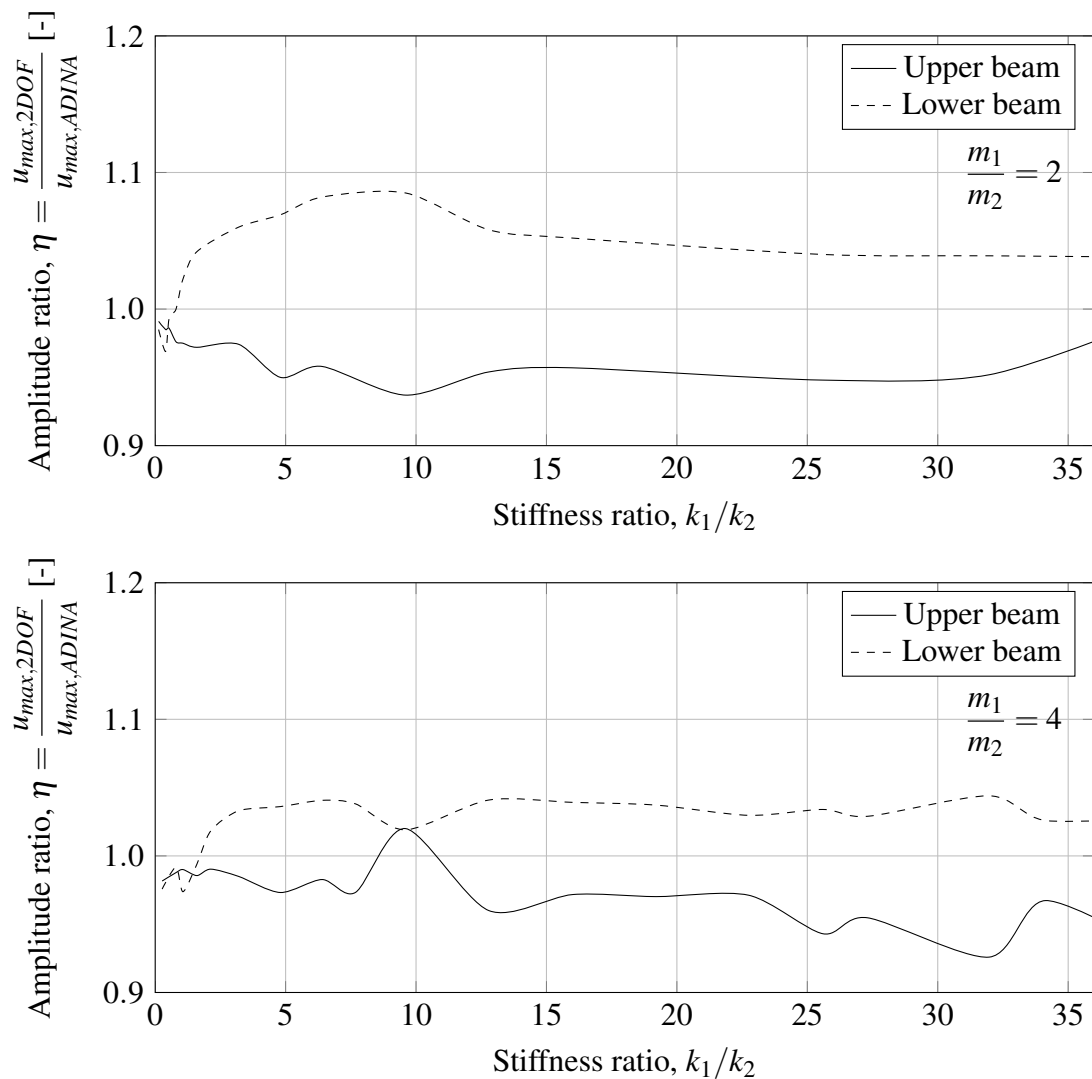


Figure 4.25: *Difference between the optimised 2DOF model response and the actual FE solution.*

It can be noticed by studying the graphs, that the displacement of the lower beam is often somewhat overestimated, especially for low stiffness ratios, where there can be up to 12-13 % overestimation. On the other hand, the upper beam tends to be somewhat underestimated by the 2DOF model, however not by more than 10 %.

To summarise, the optimisation of the 2DOF model resulted in better fitting. The response is closer to the actual FE solution for both parts of the structure. The discrepancy between displacements present in both the 2DOF model with traditional transformation factors (Figure 4.5 - Figure 4.7) as well as in the frequency calibrated 2DOF model (Figure 4.17 - Figure 4.19) is now reduced. It is believed that the optimised 2DOF system is able to describe the deformation of both parts of the real structure in a good way, and the results should be close to the actual FE response. It should however be noted, that this calibration and optimisation was developed only for the linear elastic material response. Moreover, only one load case was tested, and it could be a topic of further research to test the model for explosion loads of other duration, i.e. ones that do not resemble a characteristic impulse load.

4.6.4 Bending moment

It is also of interest to check how the optimised 2DOF model describes the internal forces in both beams, as this is an important design parameter. In this section, the bending moment and shear force will be analysed and compared to the actual FE response.

First, the bending moment in the mid-span is analysed. The procedure of obtaining the moment-time function is exactly the same as for the SDOF system, see Carlsson and Kristensson (2012) for reference. For the upper beam, the function can be expressed as

$$M_U(L_1/2, t) = \frac{k_1 u_U(t) \cdot L_1}{8} \quad (4.34)$$

where $k_1 = \frac{384EI_1}{5L_1^3}$ and L_1 is the length of the upper beam.

For the lower beam, the function takes different form, since this beam is subjected to a point load.

$$M_L(L_2/2, t) = \frac{k_2 u_L(t) \cdot L_2}{4} \quad (4.35)$$

In this formula, the stiffness k_2 is equal to $k_2 = \frac{48EI_2}{L_2^3}$, where the length of the lower beam is denoted as L_2 .

Because the moment, according to the 2DOF solution, is directly proportional to the mid-span displacement, the shape of it in time is going to be the same as the shape of the deformation. The moment distribution in time for the structure consisting of beam no.1 supported on beams no. 1 is presented in Figure 4.26.

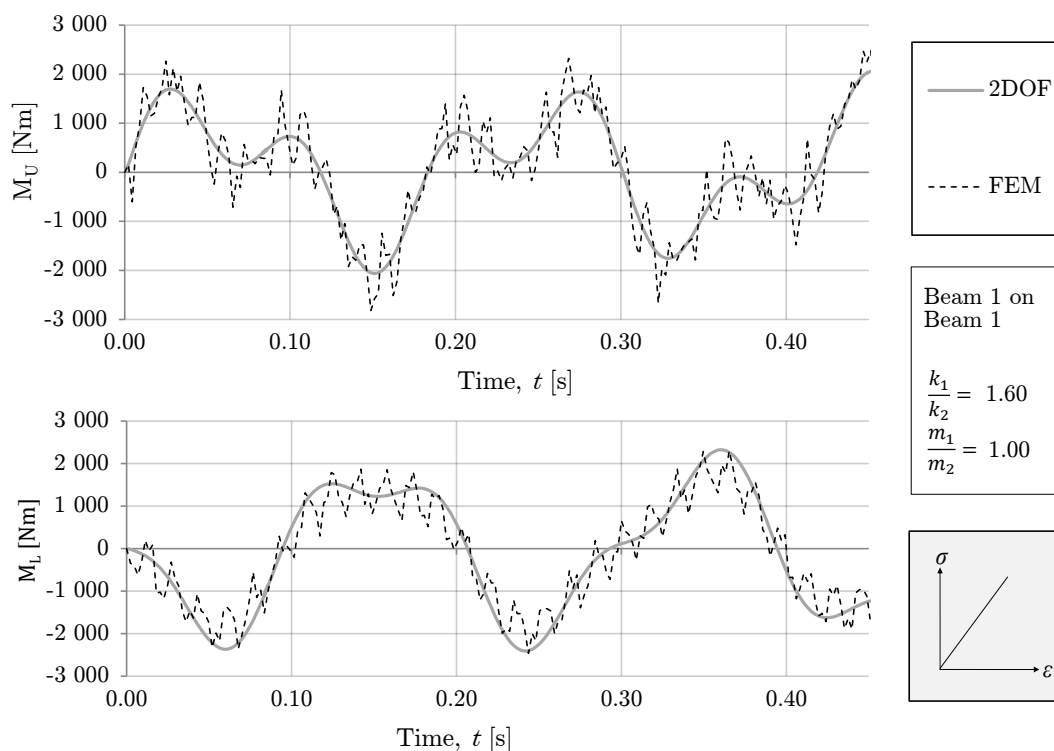


Figure 4.26: *Beding moment in the mid-span of upper and lower beam as a function of time.*

In this figure, the solid line depicts the bending moment received from the 2DOF model, while the dashed line is the result from ADINA. It is clearly seen, that there are secondary oscillations at higher frequencies for both beams, but the overall vibration at the lower frequencies is preserved. In order to further investigate this phenomenon, a Fourier transform of the bending moment for both beam was carried out, and the resulting frequency spectrum can be seen in Figure 4.27.

The first two peaks signify the eigenfrequencies given by the 2DOF model. They also have the largest impact on the final result. The later peaks also represent higher eigenmodes. The secondary oscillations of the bending moments are caused by the higher eigenfrequencies, and cannot be captured by the 2DOF model; more degrees of freedom is needed for that purpose. This phenomenon was also shown by Carlsson and Kristensson (2012) for a SDOF model. The oscillations were present also there, and it was concluded that a higher number of eigenmodes influence the bending moment. The modal shapes of the structure that correspond to eigenfrequencies $f_1 - f_5$ can be seen in Figure 4.28.

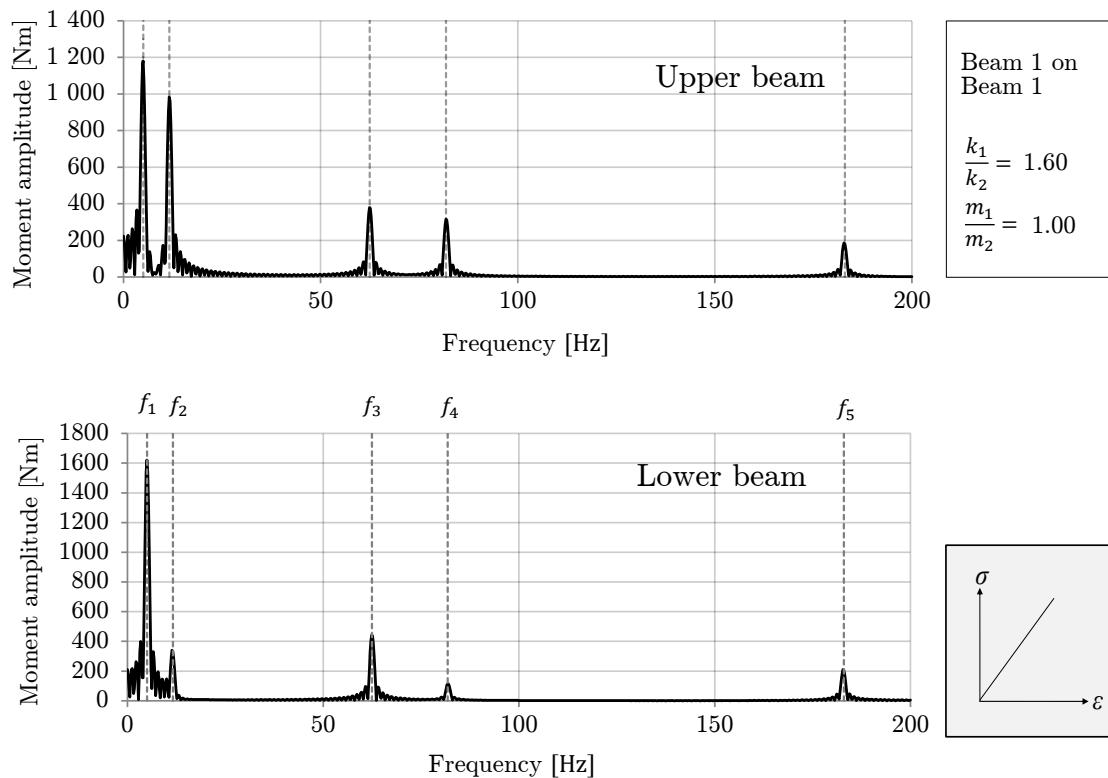


Figure 4.27: Frequency spectrum of the bending moment for upper (top) and lower beam (bottom).

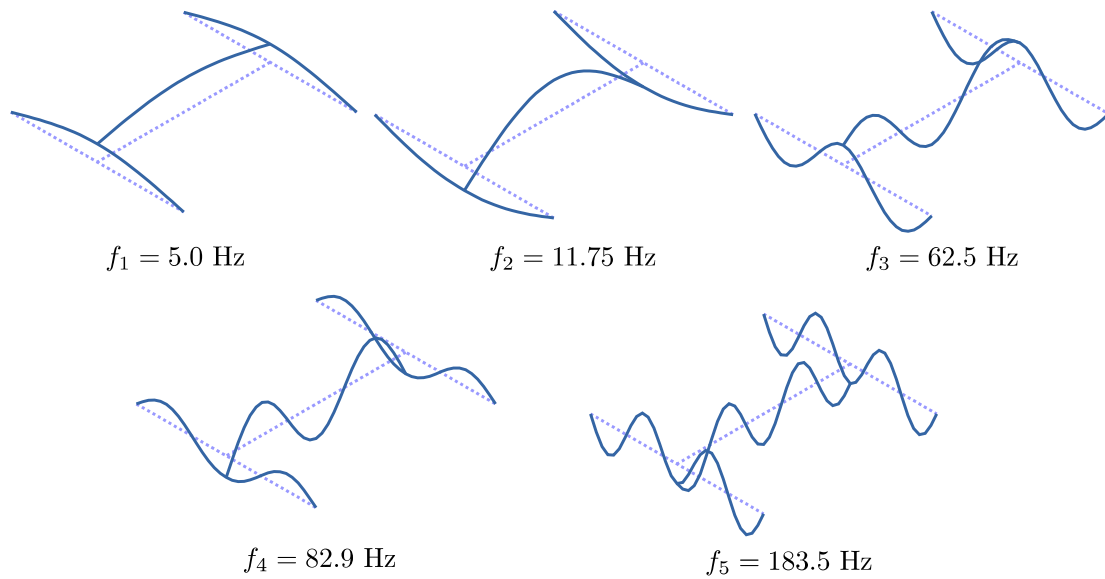


Figure 4.28: *Eigenmodes influencing the bending moment in the upper and lower beam. System consisting of beam no.1 resting on beams no.1 according to Table 4.1.*

Another thing investigated here was the bending moment distribution along the beams. Remembering that the equivalent static load is a load that results in the same deflection as the dynamic load, it can easily be calculated for these beams since the maximum deformations are known. From this equivalent static load, a moment distribution along the beam can be obtained. It is presented for both beams in Figure 4.29.

Since the upper beam is subjected to a uniformly distributed load, the shape of the moment envelope (from the 2DOF solution) is parabolic. The envelope can be obtained directly from ADINA, by taking the maximum value of the bending moment in time for each point along the beam, i.e. $M(x) = \max(M(x,t))$. The ADINA response shows that the shape of the bending moment is a combination of more than one mode shape. A discrepancy between the models exists, with the largest difference in moments in the mid-span. This was also the case for an equivalent SDOF model response, and has also been shown elsewhere; e.g. Carlsson and Kristensson (2012) and Andersson and Karlsson (2012). Therefore it is considered reasonable. The lower beam is subjected to a point load in the mid-span, thus the expected moment distribution is triangular. Similarly, the FE envelope is again a combination of several mode shapes. Overall, the correlation between the models is considered to be reasonably well, even though a small difference between the moments are still present and the equivalent static load provides results on the unsafe side.

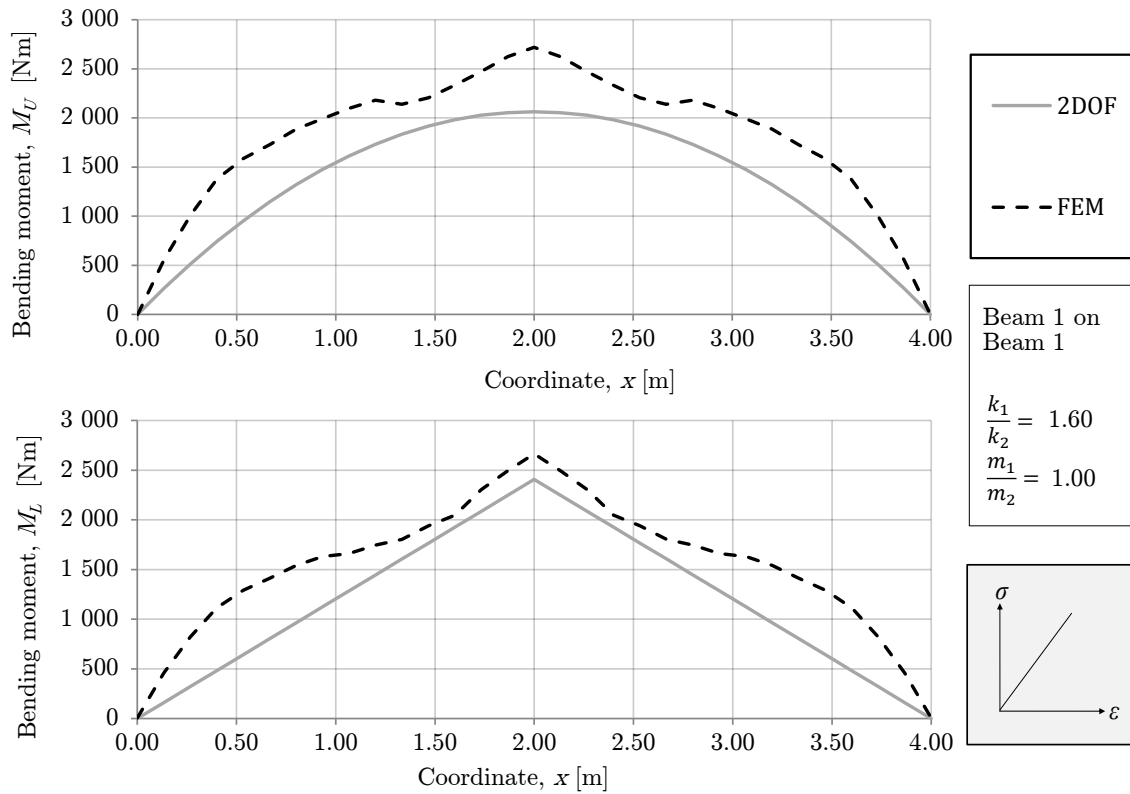


Figure 4.29: *Bending moment envelope for the upper (top) and lower beam (bottom). System consists of beam no. 1 resting on beams no. 1 according to Table 4.1.*

4.6.5 Shear force

For the shear force, the comparison is made at the contact point of the structural system, i.e. the support point of the upper beam, which is also the mid-span point of the lower beams. Shear is a more complex phenomenon than bending moment, and the description of it by the equivalent SDOF model is also needed to be improved. For more reference on this topic, the reader is referred to Andersson and Karlsson (2012).

The resulting shear distribution in time and its comparison is presented in Figure 4.30. For the ADINA result, the shear force is taken directly at the end of the upper beam. The 2DOF solution is obtained as the reaction at the support. According to Andersson and Karlsson (2012), the dynamic reaction of a simply supported beam subjected to a uniformly distributed load and under linear elastic material response can be expressed as:

$$V(t) \approx 0.4R(t) + 0.1F(t) \quad (4.36)$$

where $R(t)$ is the internal resistance of the beam, i.e.

$$R(t) = \frac{k_1 \cdot u_U(t)}{2} \quad (4.37)$$

and $F(t)$ is the external dynamic load, i.e. $F(t) = q(t) \cdot L$.

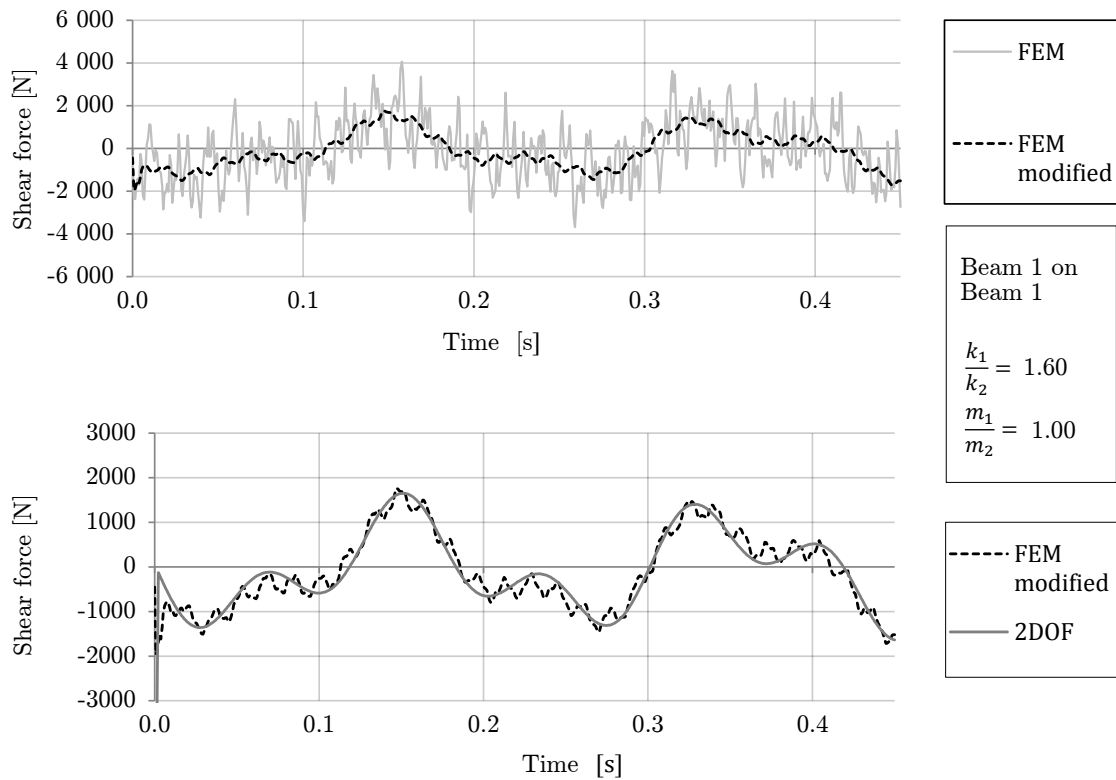


Figure 4.30: *Distribution of shear force over time at the contact point of the system.*

The dynamic reaction reaches very high values (of the order of 10000 N) in the initial phase of the response (first 2 ms - not presented explicitly in the graphs due to visual reasons). This is caused by the magnitude of external loading. Moreover, the behaviour of the shear force is very complex (FEM solution, upper graph), and cannot be easily compared with the 2DOF solution. Therefore, the curve needed to be smoothened. In order to achieve this, a moving average of 100 values before and after the sought point was calculated for each time step, i.e. an average value within 20 ms was computed. The resulting curve (called FEM modified) is shown as well in the figure. In order to investigate the matter further, a Fourier transform of the shear force was carried out, and is presented in Figure 4.31.

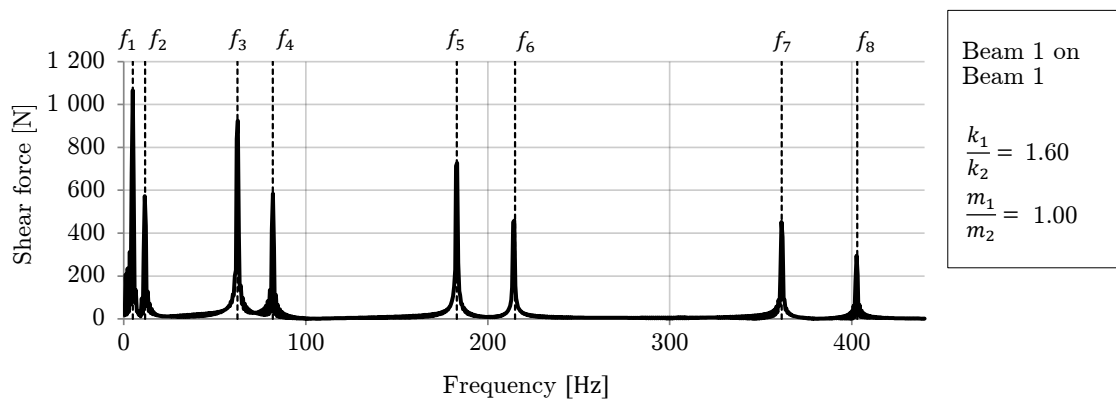


Figure 4.31: *Frequency spectrum of the shear force.*

It is easy to see, that more eigenmodes are needed if the shear force behaviour is needed to be correctly captured. The first five eigenfrequencies correspond to the same modes, that were presented in Figure 4.28. The remaining modal shapes can be seen in Figure 4.32. Moreover, the influence of higher modes may be even higher than the influence of the lower modes (e.g. mode 3 and 5 contribute more than mode 2 and 4).

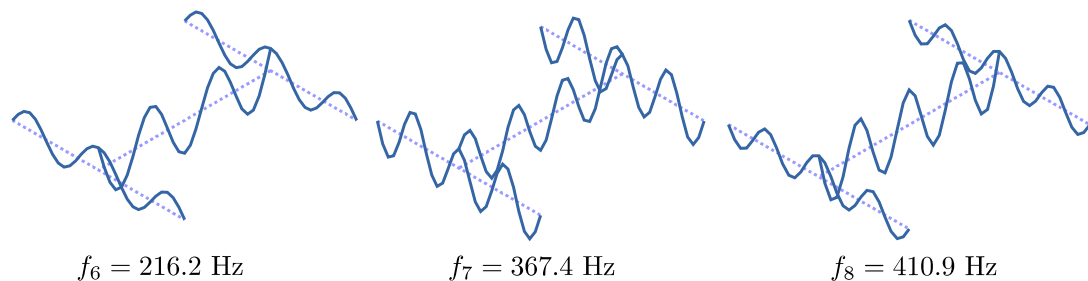


Figure 4.32: *Remaining eigenmodes present in the frequency spectrum for the shear force. System composed of beam no. 1 resting on beams no. 1 according to Table 4.1.*

Nevertheless, the 2DOF model can work with only two modes. The overall shape of the shear force is preserved by the model, but it cannot be said that the correlation between the models is very good, since the shear phenomenon is more complex in reality.

4.7 Influence of beam length and load case

4.7.1 Different lengths

Up until now, the structural system consisted of beams which had the same length. The length of the beam influences its stiffness and mass, which results in a unique stiffness and mass ratio for the system. The 2DOF system obtains its optimisation factors depending on k_1/k_2 and m_1/m_2 . Therefore, for a structural system consisting of beams with different lengths, but with the same values of masses and stiffnesses as before (thus stiffness and mass ratio are also the same), the response of the 2DOF system will be the same.

However, it is not obvious if the Finite Element Method responses of such systems are the same, since there might be some unforeseen factors influencing the behaviour. In order to investigate that, a couple of analyses were carried out in ADINA.

The main focus was to alter the lengths of the beams, but keeping their stiffness and mass the same as before. Hence, the cross section dimensions had to be changed in order to reflect the desired change in length. For example, if a beam was needed to be 2 times longer, the cross section area, A , needs to be reduced twice if the mass is to remain unchanged. Knowing the old value of the stiffness, k , and the new length, L , the new moment of inertia, I , can be found. Knowing both the cross section and the moment of inertia, the height h and width b of the new cross section can be calculated. As a result, a new beam with the same properties (stiffness and mass) is generated, but its length is now different. The appearance of the structural system is altered, but its descriptive parameters remain the same.

Three new structural systems were studied. The first one stems from the structure consisting of beam no. 1 resting on beams no. 1. The length of the lower beam was kept at 4 m, while the upper beam's length was increased twice; to 8 m. The cross section dimensions of the upper beam were adjusted so that the beam had the same stiffness and mass as before, and therefore the stiffness and mass ratios remained unchanged, i.e. $k_1/k_2 = 1.6$ and $m_1/m_2 = 1$. The line load was reduced by half (to 12.5 kN/m), therefore keeping the total impulse load unchanged. The response of the new and old system's upper and lower beam according to ADINA can be seen in Figure 4.33.

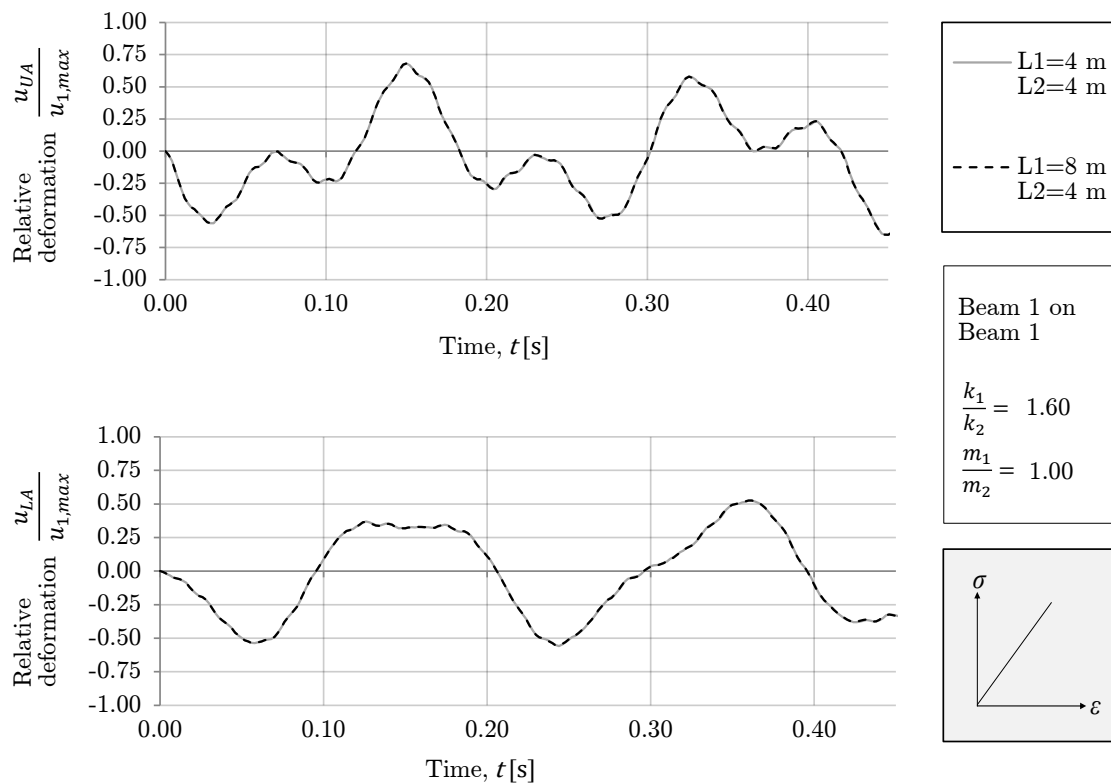


Figure 4.33: *FE response of the old system ($L_1 = L_2 = 4$ m) and the new system ($L_1 = 2L_2 = 8$ m).*

It can be noticed that the two systems behave in the same way, i.e. the correlation between the deformations is very good. This means that for this structure, changing the length of the lower beam does not induce any unforeseen phenomena. The behaviour of the system can be described only with stiffness and masses of the respective members.

For the next case, a system originating from a structure consisting of beam no. 11 supported on beams no. 7 was analysed. That system had a stiffness ratio of $k_1/k_2 = 22.76$ and the mass ratio of $m_1/m_2 = 4$. This time the length of the lower beam was increased from 4 m to 8 m, while the upper beam's span was kept at 4 m. New cross section dimensions were found for the lower beam, so that its mass and stiffness corresponds to the mass and stiffness of beam no. 11. Therefore the stiffness and mass ratios did not change. The relative deformation for the new and old structural system are presented in Figure 4.34.

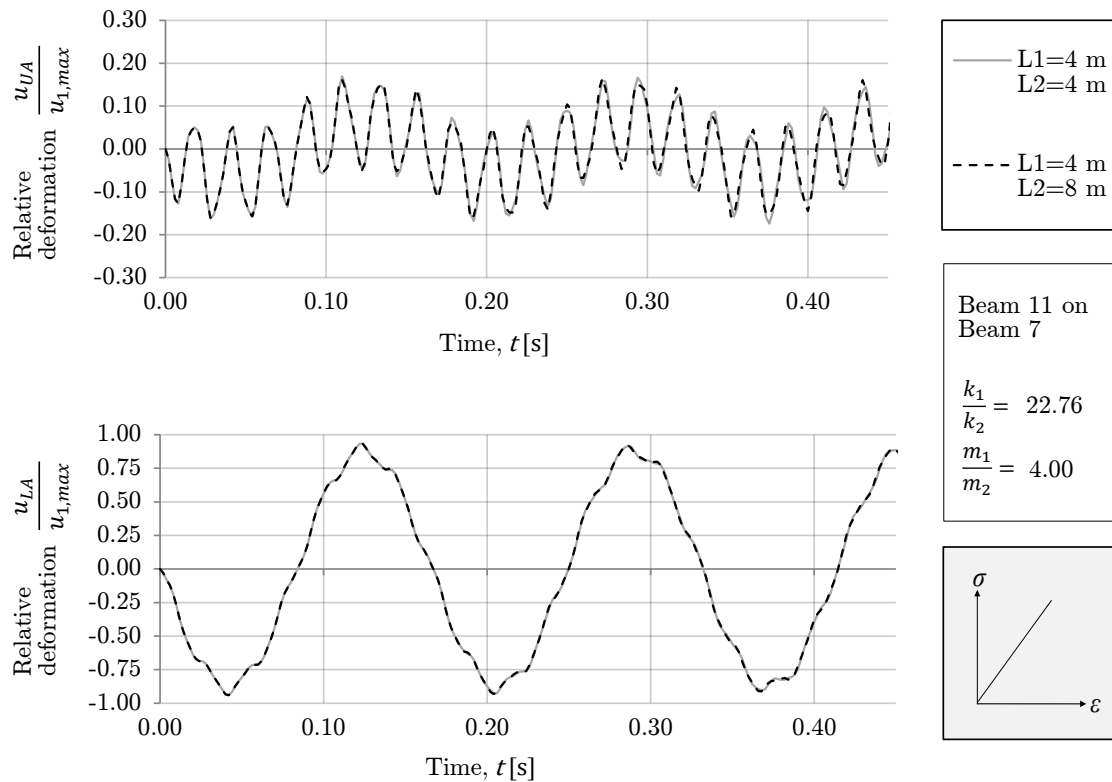


Figure 4.34: FE response of the old system ($L_1 = L_2 = 4$ m) and the new system ($L_1 = 0.5L_2 = 4$ m).

Like in the previous case, see Figure 4.33, the behaviour of both systems is the same. In the deformations of the lower beam, which is the dominating member in these structures, no visible discrepancy can be seen between the responses. Some minor differences can be perceived for the upper beam (later in time), but the movement of this member is not of big interest if the whole structure is considered. The conclusion drawn for the previous system obtains. It is possible also for this structure to describe its behaviour only with the stiffness and mass of the members.

The last studied case originates from a structural system consisting of beam no. 1 resting on beams no. 6. The original system was described by the stiffness and mass ratios of $k_1/k_2 = 0.16$ and $m_1/m_2 = 0.25$. The length of the upper beam is increased 3 times - from 4 to 12 m, while the length of the lower beam is kept unchanged at 4 m. New cross section dimension were found for the upper beam, so that the stiffness and mass were kept at the same values. Therefore the mass and stiffness ratios of the new system correspond to the ones stated above. The relative deformation of upper and lower beam can be seen in Figure 4.35.

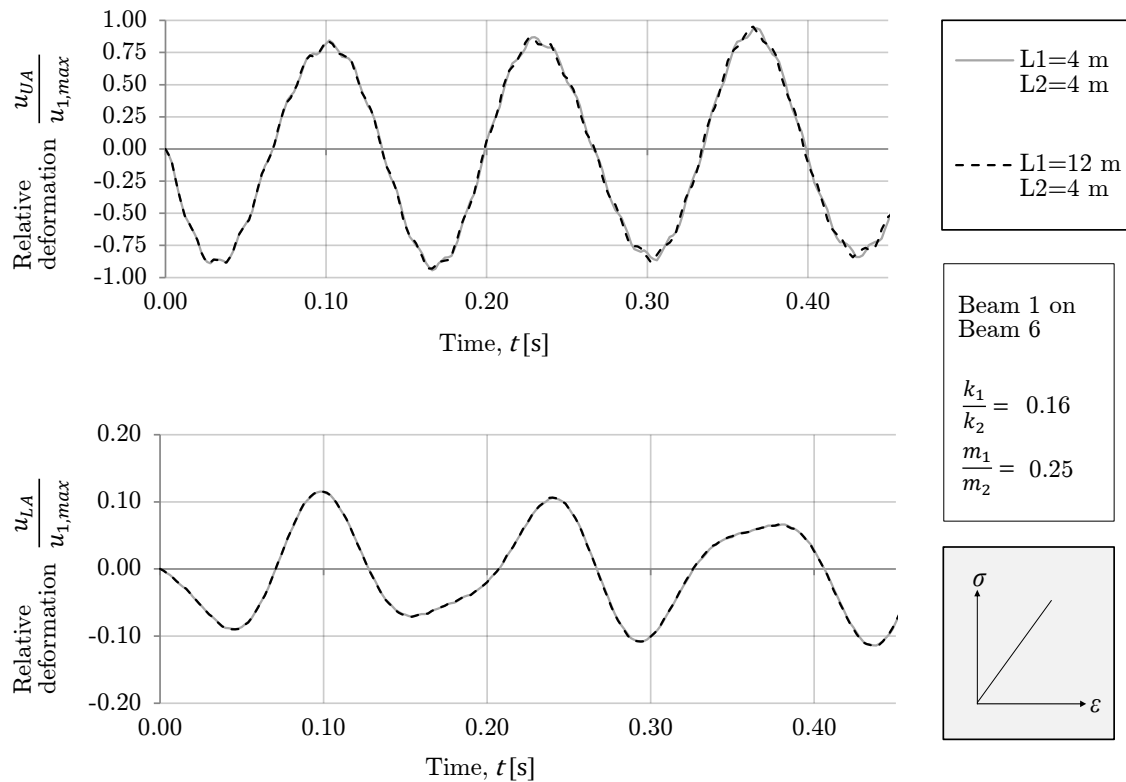


Figure 4.35: FE response of the old system ($L_1 = L_2 = 4$ m) and the new system ($L_1 = 3L_2 = 12$ m).

By looking at the graphs, it can be seen that the deformations coincide with each other for both systems, and no visible discrepancy is present. Even though the response of the optimised 2DOF system was not plotted, it corresponds to the one plotted in Figure 4.21 - Figure 4.23, since the stiffness and the mass of both parts of the structure is the same. This means that the stiffness and mass ratios are also the same, and therefore the optimisation factors do not change. Hence, the response of the 2DOF system cannot differ if no parameter in Equation (4.33) is changed.

To conclude, it can be stated that no unforeseen phenomena are taking place in the structure when the lengths of its constitutive members are altered. Varying the length does not seem to result in any secondary repercussions other than changing the stiffness and mass of the member. Based on the results of the analyses carried out in this section, it is believed that the optimised 2DOF system developed in Section 4.5 is capable of describing structural systems consisting of beams of various lengths.

4.7.2 Different load cases

Up until now, the only load case that was used in the study was a triangular impulse with a duration of 2 ms, see Figure 4.3 for the time function used in specification of load in ADINA. Since it is a very short impulse, it can be said that it corresponds to a characteristic impulse. This is advantageous when hand calculations are to be used, since the formulas there are derived from the energy conservation principles, which are valid for the characteristic impulse. However, explosions lasting longer also occur, and it is of interest to be able to describe the response of a body subjected to a load with a longer duration. In order to check if the optimised 2DOF system is capable of analysing the system subjected to a load with longer duration, three cases were studied, see Table 4.3 for details.

The key parameter used in this study is the impulse duration, t_i . The time function used in ADINA when specifying the load has for each load case the same initial inclination, so that numerical errors are avoided. The function can be seen in Figure 4.36.

Table 4.3: *Parameters for the study.*

Beam case	B1 on B1	B11 on B7	B1 on B6
Stiffness ratio, k_1/k_2 [-]	1.6	22.76	0.16
Mass ratio, m_1/m_2 [-]	1	4	0.25
Impulse duration, t_i [ms]	4	20	50
T/t_i [-]	50	8.33	2.67
Correction factor, γ_I [-]	1.0	1.02	1.17

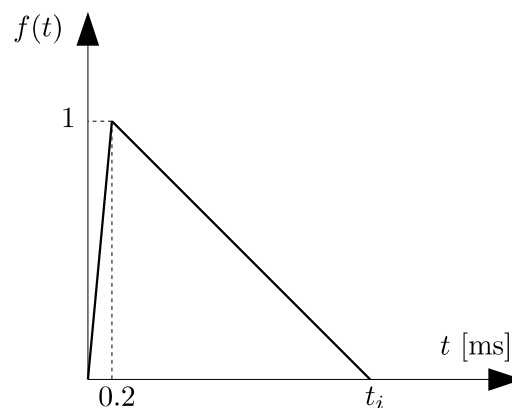


Figure 4.36: *Time function for the load used in ADINA.*

For each load case, the structure was first solved in ADINA, and then the optimised 2DOF system was solved in Octave by using the Central Difference Method. Both deformations were then recalculated to relative deformations, so that the influence of each part of the structure on the overall movement can be easily noticed. For the first case, a structure consisting of beam no. 1 supported on beams no. 1 (with the mass ratio $m_1/m_2 = 1$) was studied. The explosion load corresponded to an impulse load with

duration of 4 ms, which is twice the duration used earlier. Results for both parts of the structure can be seen in Figure 4.37.

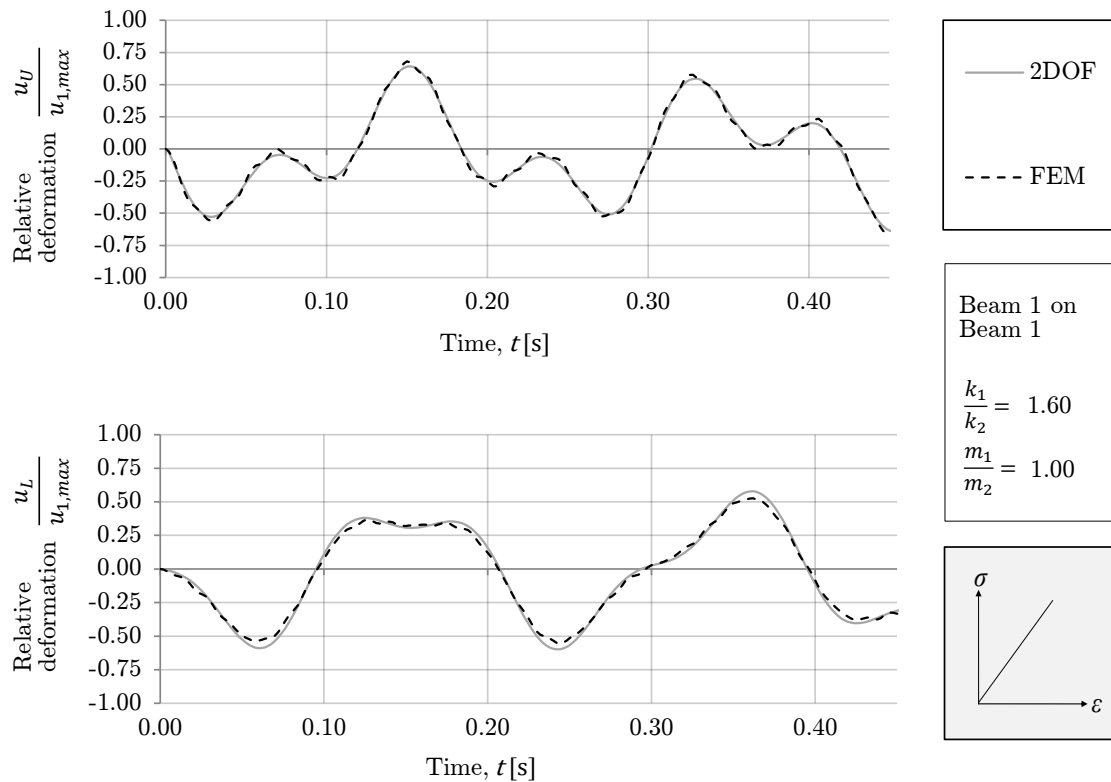


Figure 4.37: Relative deformation of the upper and lower beam over time. Duration of the impulse - 4 ms. Structure consisting of beam no. 1 resting on beams no. 1.

When looking at the figure, a good correlation between the models can be noticed. This is an intermediate stiffness ratio case, thus the movement of both members plays a big role on the resultant behaviour of the structure. The 2DOF model is a bit on the safe side for the lower beam. However, the upper beam's deformation is slightly underestimated by it. Both frequencies seem to be captured, and no visible shift in time between the models can be noticed. It can be stated, that twice longer duration of the impulse is described well by the 2DOF model, and no unforeseen phenomena related to the duration of the load occur in the FE model.

For the next case, a structure consisting of beam no. 11 resting on beams no. 7 (with the mass ratio $m_1/m_2 = 4$) was analysed. The initial duration of the impulse (2 ms) was increased 10 times, i.e. an impulse load lasting 20 ms was applied on the structure. It should be noted, that this impulse does not really correspond to the characteristic impulse, and if hand calculations need to be used, it must be transformed in to the characteristic impulse with correction factor γ_I (see Table 2.2). The results are presented in Figure 4.38.

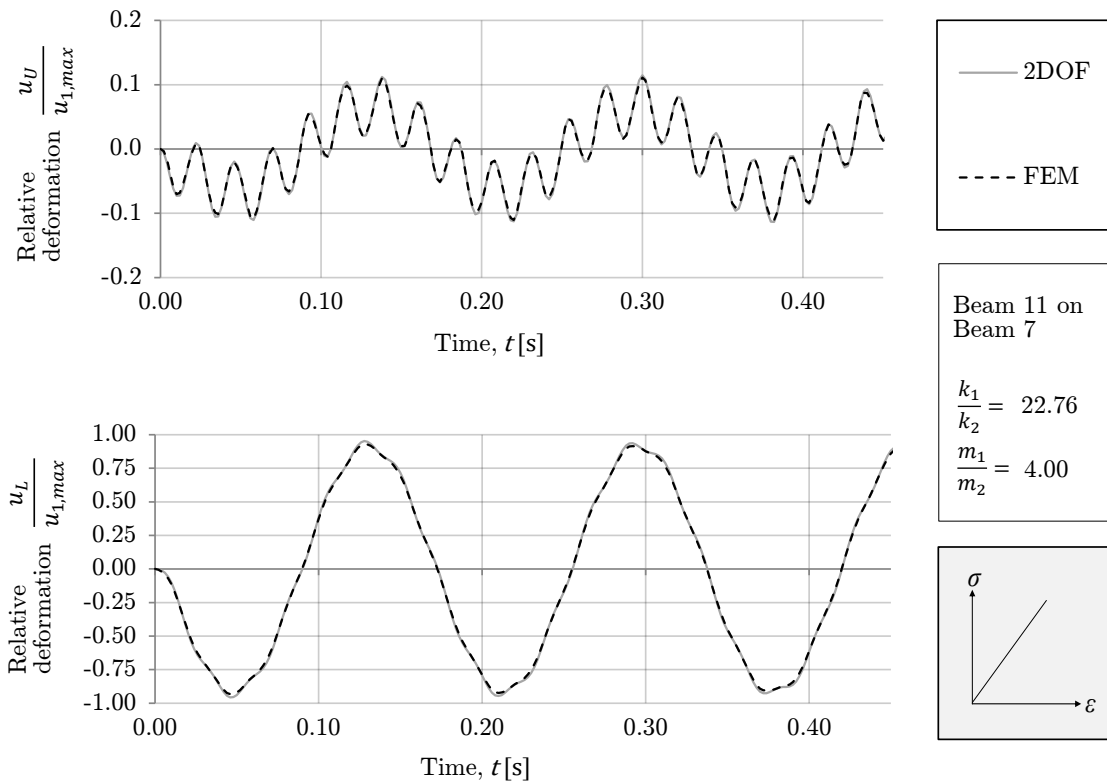


Figure 4.38: *Relative deformation of the upper and lower beam over time. Duration of the impulse - 20 ms. Structure consisting of beam no. 11 resting on beams no. 7.*

Good accordance between the models can be noticed when looking at the graphs. This is a high stiffness ratio case, thus the movement of the lower beam dominated in the overall behaviour of the structure. The 2DOF model seem to fit the ADINA response even better than in the previous case, i.e. for impulse duration of 4 ms. No visible overestimation or underestimation can be noticed. The optimised 2DOF model was able to describe the behaviour under load with ten times longer duration, which is a good indication.

The last analysed case was a structure consisting of beam no. 1 supported on beams no. 6 with the mass ratio of $m_1/m_2 = 0.25$. The duration of the impulse used in this study was 50 ms. As in the previous case, it needs to be transformed into a characteristic impulse, if the use of hand calculations is desired. In this case, the impulse can hardly correspond to a characteristic one. The relative deformations of the upper and lower beam according to FE analysis and numerical 2DOF solution are presented in Figure 4.39.

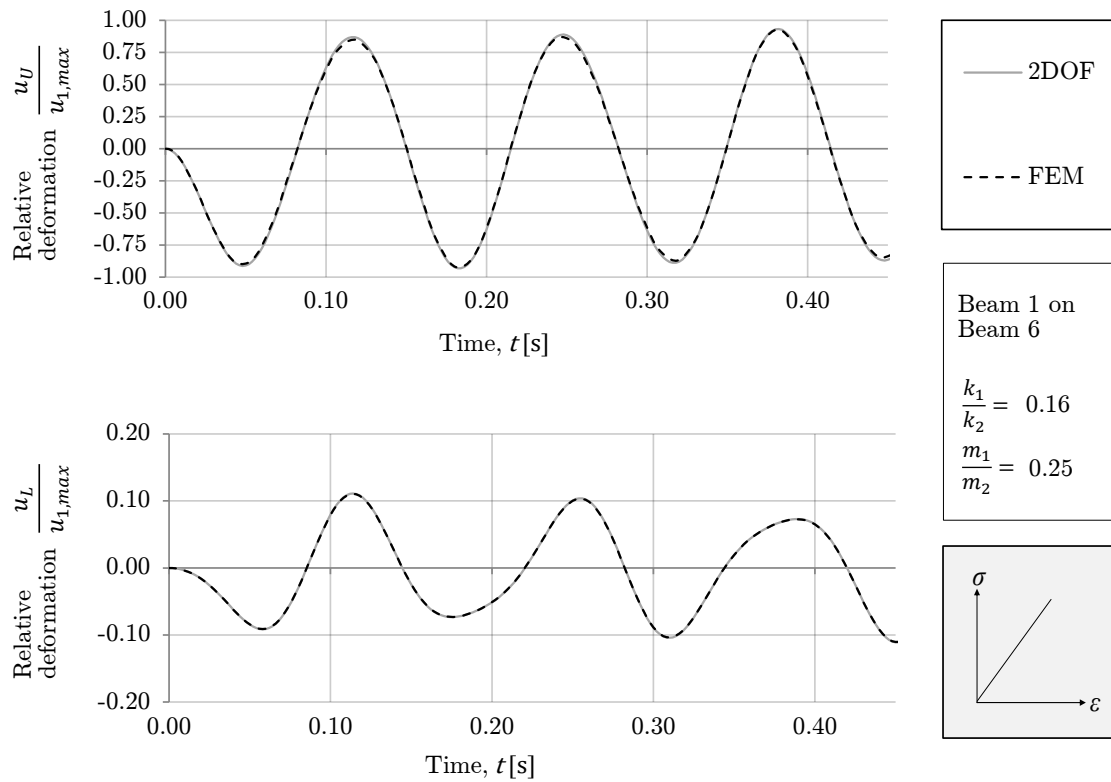


Figure 4.39: *Relative deformation of the upper and lower beam over time. Duration of the impulse - 50 ms. Structure consisting of beam no. 1 resting on beams no. 6.*

No distinctive discrepancy between the responses can be noticed for either upper or lower beam. This is a low stiffness ratio case, meaning that the movement of the upper part of the structure will dominate.

To sum up, by looking at Figure 4.37 - Figure 4.39 some conclusions can be drawn. According to the results of these analyses, it can be said that the optimised 2DOF model works well when describing the behaviour of a structural system subjected to a longer impulse. Moreover, it is possible to see that the longer the impulse, the better the agreement between the model's response and the behaviour in ADINA.

4.8 Response of a structural system - calculation example

4.8.1 Introduction

In this section, an arbitrary structural system consisting of a beam supported on two beams is solved step by step in order to show the procedure explicitly. The example encompasses the creation of the optimised 2DOF system, comparison with ADINA results and quick comparison with a SDOF solution (only hand calculation). Only displacements of the upper and lower beams are of interest, and only the linear elastic material behaviour is studied.

The chosen structure consists of two types of reinforced concrete beams, see Figure 4.40. The upper beam has a rectangular cross-section with 660 mm of height and 300 mm of width. The length of this beam is 3 m. The lower beams have a square cross-section with the width (height) of 500 mm, while their length is 4 m for each beam.

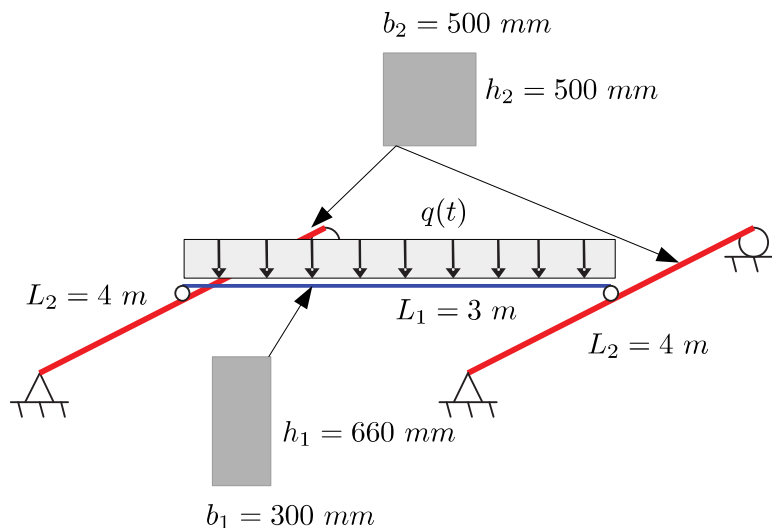


Figure 4.40: *The analysed structural system.*

The load coming from the explosion is assumed to act only on the upper beam as a uniformly distributed line load. The magnitude of this load is 2500 kN/m and it has a triangular shape in time. After 2 ms there is no more load. As for material parameters, the density of concrete is $\rho = 2400 \text{ kg/m}^3$, and the Young's modulus is $E = 33 \text{ GPa}$.

4.8.2 Stiffness and mass ratios

First, the stiffness and mass ratios are calculated. In order to do that, moments of inertia of both cross-sections are to be determined.

$$I_1 = \frac{b_1 h_1^3}{12} = 7.187 \cdot 10^{-3} \text{ m}^4 \quad (4.38)$$

$$I_2 = \frac{b_2 h_2^3}{12} = 5.208 \cdot 10^{-3} \text{ m}^4 \quad (4.39)$$

Keeping in mind that the upper beam is subjected to a uniformly distributed load, while the lower beam is subjected to a point load only, the stiffnesses of the beams can be computed. Masses of the beams can as well be determined.

$$k_1 = \frac{384EI_1}{5L_1^3} = \frac{384 \cdot 33 \text{ GPa} \cdot 7.8178 \cdot 10^{-3} \text{ m}^4}{5 \cdot (3 \text{ m})^4} = 6.75 \cdot 10^8 \frac{\text{N}}{\text{m}} \quad (4.40)$$

$$k_2 = \frac{48EI_2}{L_2^3} = \frac{48 \cdot 33 \text{ GPa} \cdot 5.208 \cdot 10^{-3} \text{ m}^4}{(4 \text{ m})^4} = 1.29 \cdot 10^8 \frac{\text{N}}{\text{m}} \quad (4.41)$$

$$m_1 = b_1 h_1 L_1 \rho = 0.3 \text{ m} \cdot 0.66 \text{ m} \cdot 3 \text{ m} \cdot 2400 \text{ kg/m}^3 = 1426 \text{ kg} \quad (4.42)$$

$$m_2 = b_2 h_2 L_2 \rho = 0.5 \text{ m} \cdot 0.5 \text{ m} \cdot 4 \text{ m} \cdot 2400 \text{ kg/m}^3 = 2400 \text{ kg} \quad (4.43)$$

Having all these quantities, the stiffness and mass ratio of the structure can be calculated.

$$k_r = \frac{k_1}{k_2} = 5.234 \quad (4.44)$$

$$m_r = \frac{m_1}{m_2} = 0.594 \quad (4.45)$$

4.8.3 Creation of the optimised 2DOF model

The system of differential equations for the optimised 2DOF model can be expressed as:

$$\begin{bmatrix} \gamma_{m_1} m_1 & 0 \\ 0 & 2\gamma_{m_2} m_2 \end{bmatrix} \begin{bmatrix} \dot{u}_1 \\ \dot{u}_2 \end{bmatrix} + \begin{bmatrix} \gamma_{k_1} k_1 & -\gamma_{k_1} k_1 \\ -\gamma_{k_1} k_1 & \gamma_{k_1} k_1 + 2\gamma_{k_2} k_2 \end{bmatrix} \begin{bmatrix} u_1 \\ u_2 \end{bmatrix} = \begin{bmatrix} \gamma_{F_1} F(t) \\ \gamma_{F_2} F(t) \end{bmatrix} \quad (4.46)$$

where the optimisation factors γ_i must be obtained either from Figure D.1 to Figure D.5 or from Table D.1 to Table D.5.

The factors can be interpolated for intermediate mass ratios, which is clearly this case. For the stiffness ratio of 5.234 and the mass ratio of 0.5, they are equal to:

$$\begin{aligned} \gamma_{k_{1.05}} &= 0.802 \\ \gamma_{k_{2.05}} &= 0.990 \\ \gamma_{m_{1.05}} &= 0.595 \\ \gamma_{m_{2.05}} &= 0.595 \\ \gamma_{F_{1.05}} &= 0.742 \\ \gamma_{F_{2.05}} &= 1 - \gamma_{F_1} = 0.258 \end{aligned}$$

For the stiffness ratio of 5.234 and the mass ratio of 1, the resulting factors are:

$$\begin{aligned}\gamma_{k_{1,1}} &= 0.960 \\ \gamma_{k_{2,1}} &= 0.980 \\ \gamma_{m_{1,1}} &= 0.805 \\ \gamma_{m_{2,1}} &= 0.555 \\ \gamma_{F_{1,1}} &= 0.907 \\ \gamma_{F_{2,1}} &= 1 - \gamma_{F_1} = 0.093\end{aligned}$$

Having the factors for the two nearest mass ratios, the optimisation factors for the actual mass ratio of 0.594 can be interpolated. Here, a linear interpolation is carried out.

$$\begin{aligned}\gamma_{k_1} &= \gamma_{k_{1,05}} + \frac{\gamma_{k_{1,1}} - \gamma_{k_{1,05}}}{1 - 0.5} \cdot (m_r - 0.5) = 0.832 \\ \gamma_{k_2} &= \gamma_{k_{2,05}} + \frac{\gamma_{k_{2,1}} - \gamma_{k_{2,05}}}{1 - 0.5} \cdot (m_r - 0.5) = 0.988 \\ \gamma_{m_1} &= \gamma_{m_{1,05}} + \frac{\gamma_{m_{1,1}} - \gamma_{m_{1,05}}}{1 - 0.5} \cdot (m_r - 0.5) = 0.634 \\ \gamma_{m_2} &= \gamma_{m_{2,05}} + \frac{\gamma_{m_{2,1}} - \gamma_{m_{2,05}}}{1 - 0.5} \cdot (m_r - 0.5) = 0.227 \\ \gamma_{F_1} &= \gamma_{F_{1,05}} + \frac{\gamma_{F_{1,1}} - \gamma_{F_{1,05}}}{1 - 0.5} \cdot (m_r - 0.5) = 0.773 \\ \gamma_{F_2} &= 1 - \gamma_{F_1} = 0.227\end{aligned}$$

The last component, which is to be calculated before the equation system from Equation (4.46) can be solved, is the value of the point force $F(t)$. This one is easily received, as it is just the line load converted into a point load. Therefore

$$F(t) = 2500 \frac{\text{kN}}{\text{m}} \cdot 3 \text{ m} = 7500 \text{ kN} \quad (4.47)$$

With this value obtained, every component of the differential equation system is now known, and the Central Difference Method can be employed to solve it.

4.8.4 Deformation

The optimised 2DOF model was solved for displacements. The resulting $u_1(t)$ and $u_2(t)$ were used to get the resulting displacement $u_U(t)$ (upper beam) and $u_L(t)$ (lower beam) in the mid-spans, according to the expressions:

$$u_U(t) = u_1(t) - u_2(t) \quad (4.48)$$

$$u_L(t) = u_2(t) \quad (4.49)$$

The structure was then modelled in ADINA following the procedure described in Section 4.2.2. It was then solved with the dynamic implicit procedure, taking 4500 time steps, each one 0.2 ms long. The output of the analysis was chosen to be the absolute displacement of the mid-span of the upper beam ($u_{1A}(t)$) and the absolute displacement

of the mid-span of the lower components of the structure ($u_{2A}(t)$). Those can be further converted into the relative beams' displacements ($u_{UA}(t)$ and $u_{LA}(t)$), expressed as

$$u_{UA}(t) = u_{1A}(t) - u_{2A}(t) \quad (4.50)$$

$$u_{LA}(t) = u_{2A}(t) \quad (4.51)$$

The results are presented in Figure 4.41.

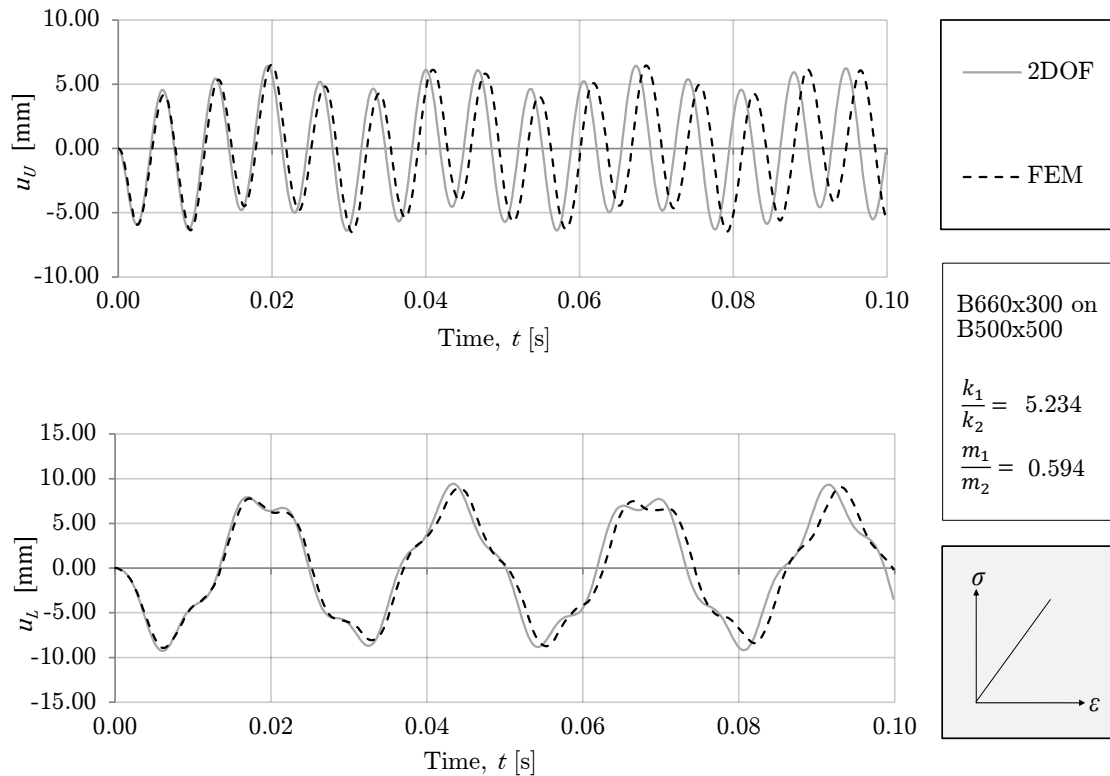


Figure 4.41: *Deformation of the mid-span of the upper and lower beam from optimised 2DOF system and the FE solution.*

By looking at the graphs, it can be said that the response for both the upper and lower beam agrees very well in the beginning, but later a slight shift in time is noticeable. This is believed to be caused by the linear interpolation of the optimisation factors used in the 2DOF model. Other types of interpolation might provide better results, but this was not checked. Another conspicuous thing is the very high frequency of the upper beam's secondary oscillations, which causes the slight frequency shift to be more noticeable. In order to assess the severity of the shift, the eigenfrequencies can be obtained from the 2DOF model and compared with the spectrum analysis of the structure. However, due to the nature of this example it was not done here.

As far as the amplitudes are concerned, one might notice good agreement between the models. For both parts of the structure the 2DOF response is on the safe side, but this is believed to be more of a coincidence than a tendency. The upper beam's maximum deformation predicted by the 2DOF model is 2 % higher than the one in ADINA. For

the lower beam the same direction of the error is present, however now the difference between the models is at around 4 % at the maximum.

The analysed structure had an intermediate stiffness ratio ($k_1/k_2 = 5.234$), which means that no part of the structure was definitely dominating in the motion. This can also be assessed by looking at the magnitude of the deformation for both beams and noticing that they are of similar size.

4.8.5 Hand calculations according to SDOF model

To further illustrate the difference between the behaviour of a structural system and its individual parts, simplified hand calculations were carried out. The upper and lower beams are now treated separately with the SDOF model approach. The goal of the calculations is the maximum elastic deformation for both beams.

Upper beam

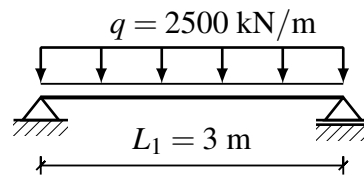


Figure 4.42: Schematic of the upper beam.

The eigenfrequency of the beam can be calculated as:

$$\omega_1 = \sqrt{\frac{k_1}{m_1}} = \sqrt{\frac{6.75 \cdot 10^8 \text{ N/m}}{1426 \text{ kg}}} = 688 \text{ rad/s} \quad (4.52)$$

As already stated in Section 2.4.2, the fundamental period can be determined as

$$T_1 = \frac{2\pi}{\omega_1} = \frac{2\pi}{688 \text{ rad/s}} = 9.133 \cdot 10^{-3} \text{ s} \quad (4.53)$$

Keeping in mind that the duration of the impulse load is $t_1 = 2 \text{ ms}$ and its shape can be described with parameter $n = 1$ according to Figure 2.22, the ratio T_1/t_1 is:

$$\frac{T_1}{t_1} = \frac{9.133 \cdot 10^{-3} \text{ s}}{2 \cdot 10^{-3} \text{ s}} = 4.567 \quad (4.54)$$

For this value, a load correction factor γ_l can be interpolated by using the values from Table 2.2.

$$\gamma_{l1} = 1.05 + \frac{1.1 - 1.05}{4.2 - 5.86} (4.567 - 5.86) = 1.089 \quad (4.55)$$

The characteristic impulse can be calculated as the area under the force-time graph. It must be corrected with the load correction factor γ_l .

$$I_{k1} = \frac{0.5 \cdot 2500 \text{ kN/m} \cdot 3 \text{ m} \cdot 2 \text{ ms}}{1.089} = 6887 \text{ Ns} \quad (4.56)$$

Finally, the elastic deformation can be calculated (note: the transformation factor κ_{mF} for a simply supported beam subjected to uniformly distributed load must be used).

$$u_{el1} = \frac{I_{k1}}{\kappa_{mF} m_1 \omega_1} = \frac{6887 \text{ Ns}}{0.788 \cdot 1426 \text{ kg} \cdot 688 \text{ rad/s}} = 8.9 \text{ mm} \quad (4.57)$$

The ratio between the displacement of the upper beam treated as a part of a structure (from ADINA solution) and the displacement of the same beam treated separately is then:

$$\frac{6.52 \text{ mm}}{8.9 \text{ mm}} = 0.733 \quad (4.58)$$

In other words, the influence of the rest of the structure on the upper beam results in a deformation, which is 73 % of the deformation this beam would reach when treated as a separate structure.

Lower beam

The lower beam is loaded by a point force, coming from a reaction of the upper beam under impulse loading. The magnitude of the force is

$$P = \frac{2500 \text{ kN/m} \cdot 3 \text{ m}}{2} = 3750 \text{ kN} \quad (4.59)$$

and the beam can schematically be seen in Figure 4.43.

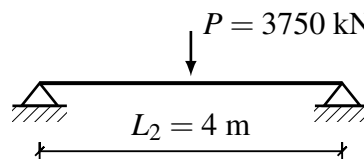


Figure 4.43: Schematic of the lower beam.

The eigenfrequency of the beam can be calculated as:

$$\omega_2 = \sqrt{\frac{k_2}{m_2}} = \sqrt{\frac{1.29 \cdot 10^8 \text{ N/m}}{2400 \text{ kg}}} = 232 \text{ rad/s} \quad (4.60)$$

As already stated in Section 2.4.2, the fundamental period can be determined as

$$T_2 = \frac{2\pi}{\omega_2} = \frac{2\pi}{231.756 \text{ rad/s}} = 27.1 \cdot 10^{-3} \text{ s} \quad (4.61)$$

Keeping in mind that the duration of the impulse load is $t_1 = 2$ ms and its shape can be described with parameter $n = 1$ according to Figure 2.22, the ratio T_2/t_1 is:

$$\frac{T_2}{t_1} = \frac{27.1 \cdot 10^{-3} \text{ s}}{2 \cdot 10^{-3} \text{ s}} = 13.556 \quad (4.62)$$

According to Table 2.2, no load correction is needed for this time ratio. Hence

$$\gamma_l = 1.0 \quad (4.63)$$

The characteristic impulse can then be computed as

$$I_{k2} = \frac{0.5 \cdot 3750 \text{ kN} \cdot 2 \text{ ms}}{1.0} = 3750 \text{ Ns} \quad (4.64)$$

Finally, the elastic deformation can be determined (note: the transformation factor, κ_{mF} , for a simply supported beam subjected to point load in the mid-span must be used).

$$u_{el2} = \frac{I_{k2}}{\kappa_{mF} m_2 \omega_2} = \frac{3750 \text{ N} \cdot \text{s}}{0.486 \cdot 2400 \text{ kg} \cdot 232 \text{ rad/s}} = 13.9 \text{ mm} \quad (4.65)$$

The ratio between the displacement of the lower beam treated as a part of a structure (from ADINA solution) and the displacement of the same beam treated separately is then:

$$\frac{9.1 \text{ mm}}{13.9 \text{ mm}} = 0.65 \quad (4.66)$$

In other words, the influence of the rest of the structure on the lower beam results in a deformation, which is 65 % of the deformation this beam would reach when treated as a separate structure.

It can be seen that treating the elements as a part of a larger structure can have significant effects, namely smaller deformation than it would have been if the elements had been treated separately. Those values are however approximate, as the hand calculations were used.

4.9 Discussion and conclusions

4.9.1 Two degrees of freedom model

In this chapter it was shown that the optimised 2DOF model is capable of describing the behaviour of a structural system consisting of a beam simply supported on two beams, with arbitrary stiffness and mass ratio. The produced response might not be absolutely correct, but it is believed to be reasonably good, since the predicted maximum displacements are located close to those obtained in ADINA. Even though a slight shift in frequency might still exist for structures with mass ratios lying in between the analysed cases, the initial response (first few sways) is captured quite well. In reality, every structure has a certain damping, which will reduce the amplitudes with time, and therefore the initial response is of particular interest. However, it should be noted that this model was validated only for linear elastic material response, which might be far from reality if the structure develops plastic response.

4.9.2 Comparison with SDOF models

It was already mentioned in Section 4.8.5 that the response of a structural system is different than the response of its separate elements. It was therefore decided to investigate this matter further, in order to come up with an idea, for which structures the reduction or appreciation in displacements is the largest.

To do so, new analyses were carried out. Along with the structural systems consisting of the parametric beams described in Section 4.2.1, the same beams were studied in ADINA, but this time as separate structures. The upper beams were loaded by a uniformly distributed load, while the lower beams were loaded by a point force (following the procedure shown in Section 4.8.5). The output of the analyses were the mid-span displacements. Next, the maximum displacements were compared with the deformation of the examined structural beam-on-beams systems. The ratio between the upper (or lower) beam displacement when it was a part of a structure and the displacement of a separate beam was calculated for each studied case. It is believed that such ratio is a function of the stiffness and mass ratio, hence the results were gathered, plotted and extrapolated for intermediate values of stiffness and mass ratios.

The resulting contour plots for the upper beam can be seen in Figure 4.44. Both plots present the same data, however the scale of the horizontal axis is different, due to high congestion of data for low stiffness ratios. From the plots, it can be seen that for very low stiffness ratios (less than 0.5) and high mass ratios it is even possible to gain deformation when analysing the upper beam as a part of a structure. However, apart from this extreme case, it is conspicuous that the deformation is usually smaller if the beam is treated as a component, not a separate entity. Hence, there is much to be saved (in terms of deformation) especially for high stiffness ratios, which was also pointed out in Chapter 3.

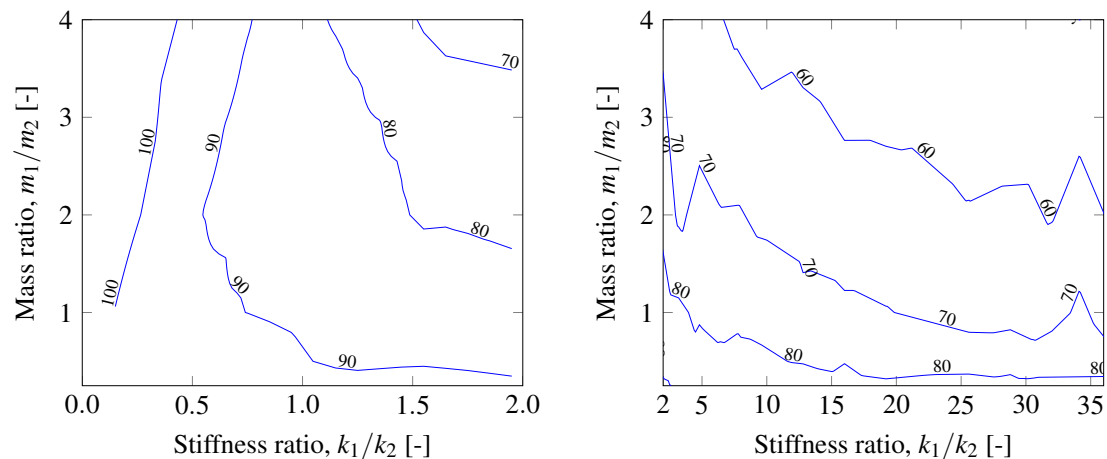


Figure 4.44: *Quotient of the maximum elastic deformation (in %) of the upper beam treated as a part of the structure, and the upper beam's maximum deformation when the beam is treated separately.*

The contour plots for the lower beam are presented in Figure 4.45. Like previously, the same data is presented at both of them, however the scale of horizontal axis is different due to a concentration of curves. For this beam, it is possible to gain relative deformation when analysed as a component for low mass ratios and intermediate stiffness ratios (0.25 - 2). Apart from this extreme case, it can be seen that usually the deformation is much overestimated if the lower beam is calculated as a separate structure.

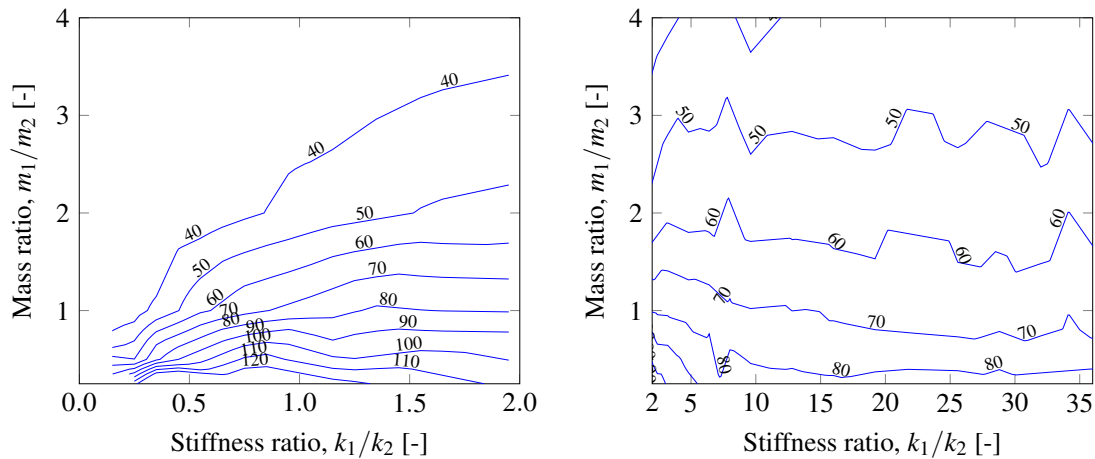


Figure 4.45: *Quotient of the maximum elastic deformation (in %) of the lower beam treated as a part of the structure, and the lower beam's maximum deformation when the beam is treated separately.*

When studying the example from Section 4.8, it turned out that the relative displacement of the upper beam (component vs separate structure) was 73 %, while for the lower beam the value was 65 %. For the corresponding stiffness ratio of 5.234 and the mass ratio of 0.594, it can be seen that these values do not agree with the contour plots, which say that the reduction should be at around 80 %. The reason of this discrepancy is not known, but it is believed that the eigenfrequency of individual beams might play a role here. All of the examined parametric beams had low eigenfrequencies, up to 28 Hz at most. The beams used in the example had much higher eigenfrequencies (109 Hz and 37 Hz). Those matters can be concluded later, as a part of a further studies in the subject.

5 Enhanced SDOF systems

5.1 Introduction

In Chapter 4 it was shown that the response of a structural system consisting of a beam supported on beams can be analysed numerically with the help of an optimised 2DOF system. Even though it produces reasonable result, the process of its construction and solution with Central Difference Method may be considered lengthy and laborious. Moreover, the 2DOF system cannot be easily analysed with hand calculations to get the maximum deformation, as is the case for SDOF systems. Therefore, it was desired to modify the existing SDOF system for the upper and lower beam in order to construct reasonable systems. These systems would be able to describe the behaviour (in terms of the largest deformation) of the respective constitutive elements of the structure, at least within a limited range of the spectrum.

The concept of the transformation can be seen in Figure 5.1. The two systems are considered independent of each other. One of them is describing the movement of the upper beam, while the other treats the lower beam.

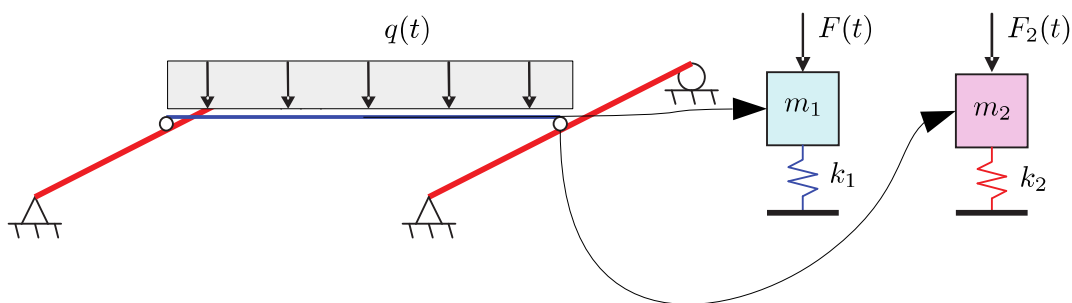


Figure 5.1: *The concept of transformation into two independent SDOF systems.*

Since a SDOF system vibrates with only one frequency, it is evident that it will not describe well the actual behaviour of a structure vibrating in more eigenfrequencies, i.e. a system in which both elements dominate the motion. Therefore it can be stated that the behaviour of structures in intermediate stiffness ratios will not be reflected well by SDOF systems.

Furthermore, even if the movement of one element dominates the movement of the whole structure, there is also a slight influence of higher eigenmodes, which will not be captured by a SDOF system. However, the reason behind developing new SDOF systems is to facilitate and expedite getting estimated results for the deformation. Therefore it is assumed, that the shape of the motion is not of great importance, but rather that the maximum deformation is of secondary relevance.

In this chapter, a method of estimating the maximum deformation of each constitutive element of the structure with simplified SDOF systems is presented, as well as the approximate range of the application of those systems.

5.2 Lower beam

5.2.1 Simply supported beam

The first option is to consider the lower beam as an ordinary simply supported beam, which can be seen in Figure 5.2.

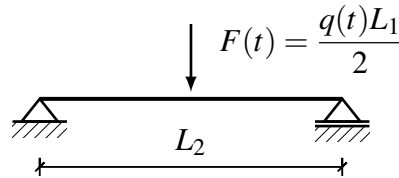


Figure 5.2: Simply supported beam subjected to point load.

The beam has stiffness k_2 and mass m_2 - the reader is referred to Section 4.2.1 for more information about these parameters. The transformation factor κ_{mF} for this beam can be obtained directly from Table 2.4, and in this case it is equal to

$$\kappa_{mF} = 0.486 \quad (5.1)$$

The angular frequency of this system can be expressed as

$$\omega = \sqrt{\frac{k_2}{\kappa_{mF}m_2}} \quad (5.2)$$

And finally, the maximum deformation of the beam can be calculated as

$$u_{max,SDOF} = \frac{I_k}{\kappa_{mF}m_2\omega} \quad (5.3)$$

where I_k is the characteristic impulse corresponding to the load $F(t)$. For more information, the reader is referred to Section 2.4.2.

When solving this SDOF system with the Central Difference Method, a sine curve with the amplitude $u_{max,SDOF}$ and the angular frequency ω is obtained. The result was computed for each of the studied cases (from Chapter 4). If the maximum deformation of the lower beam obtained from ADINA, $max(u_{LA})$, is denoted as $u_{L,max,ADINA}$, then an accuracy factor η can be calculated, i.e.

$$\eta = \frac{u_{max,SDOF}}{u_{max,ADINA}} \quad (5.4)$$

If the accuracy factor is 1, then the response of the SDOF system is the same as in ADINA (in terms of deformation), which is desired. If the factor is higher than 1, the system overestimates the deformation. Subsequently, when $\eta < 1$, the system underestimates the deformation of the lower beam. The resultant η for the whole spectrum of analysed structures can be seen in Figure 5.3.

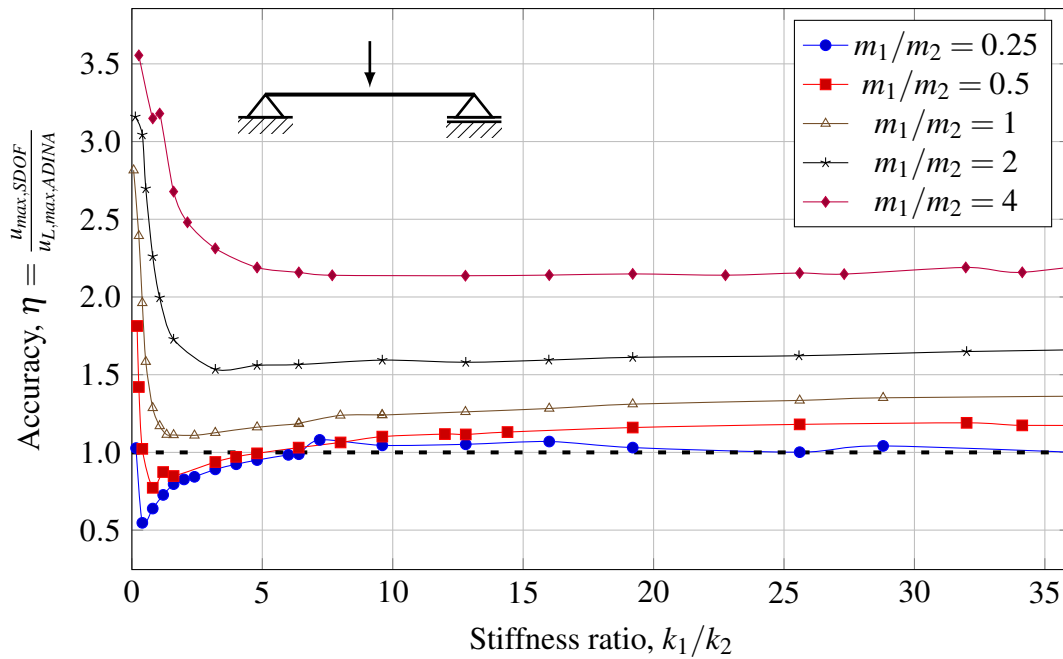


Figure 5.3: Accuracy of the SDOF model for the lower beam. Beam treated as a simply supported beam.

It can be seen in the graph, that the deformation of the lower beam is largely overestimated with this SDOF model. The beginning of each curve is not very important, since the response of a structural system with a low stiffness ratio is mainly governed by the oscillation of the upper beam. Therefore it will not be described well by a simple SDOF system. On the other hand, the response of the system with a high stiffness ratio is mainly due to the motion of the lower beam, and it should be possible to describe it approximately by a simple SDOF model. For the low mass ratios (i.e. up to $m_1/m_2 = 1$) the deformation is overestimated, but still within a reasonable range. For higher mass ratios, the overestimation grows unreasonably, and therefore it is concluded that this model is insufficient to describe the movement of the lower beam.

5.2.2 Simply supported beam with a point mass

Another option is to take into consideration, that there is some mass of the upper beam which may influence the behaviour of the lower beam. Therefore, a beam with a point mass in the mid-span can be constructed, see Figure 5.4. The beam has the stiffness k_2 , mass m_2 and the point mass in the mid-span, m_{point} .

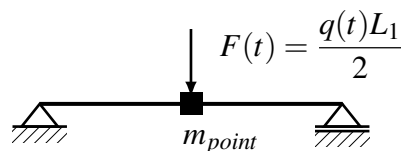


Figure 5.4: Simply supported beam with a point mass in mid-span subjected to point load.

The transformation factor κ_F is still equal to 1, since the structure is subjected to a point force in the system point.

$$\kappa_{F,mod} = 1 \quad (5.5)$$

However, the transformation factor κ_m will change now, since an additional mass m_{point} is present at the system point. The overall mass of the structure is denoted m and is the sum of the mass of the beam m_2 and the point mass m_{point} . If the beam's mass per length is constant (i.e. $m'_2(x) = m_2$) and the transformation factor for a beam without point mass is denoted as κ_m , then the new transformation factor $\kappa_{m,mod}$ can be calculated as

$$\begin{aligned} \kappa_{m,mod} &= \frac{1}{m} \int_0^L \frac{m'(x)u(x)^2}{u_s^2} dx = \frac{1}{m} \int_0^L \frac{m'_{point}(x)u(x)^2}{u_s^2} dx + \frac{1}{m} \int_0^L \frac{m'_2(x)u(x)^2}{u_s^2} dx \\ &= \frac{1}{m} \frac{m_{point} \cdot u \left(\frac{L_2}{2} \right)^2}{u_s^2} + \frac{1}{m} m_2 \kappa_m = \frac{1}{m} m_{point} \cdot 1 + \frac{1}{m} m_2 \kappa_m = \frac{m_{point} + m_2 \kappa_m}{m_{point} + m_2} \end{aligned} \quad (5.6)$$

After calculating κ_m , the transformation factor κ_{mF} can be obtained as before, i.e.

$$\kappa_{mF,mod} = \frac{\kappa_{m,mod}}{\kappa_F} \quad (5.7)$$

The value of the point mass was assumed to be half of the weight of the upper beam, so

$$m_{point} = \frac{m_1}{2} \quad (5.8)$$

The angular frequency and the maximum deformation of the structure can be now computed as:

$$\omega = \sqrt{\frac{k_2}{\kappa_{mF,mod} \left(m_2 + \frac{m_1}{2} \right)}} \quad (5.9)$$

$$u_{max,SDOF} = \frac{I_k}{\kappa_{mF,mod} \left(m_2 + \frac{m_1}{2} \right) \omega} \quad (5.10)$$

The SDOF system was solved for each analysed case, and the accuracy coefficient η was calculated. The results can be seen in Figure 5.5.

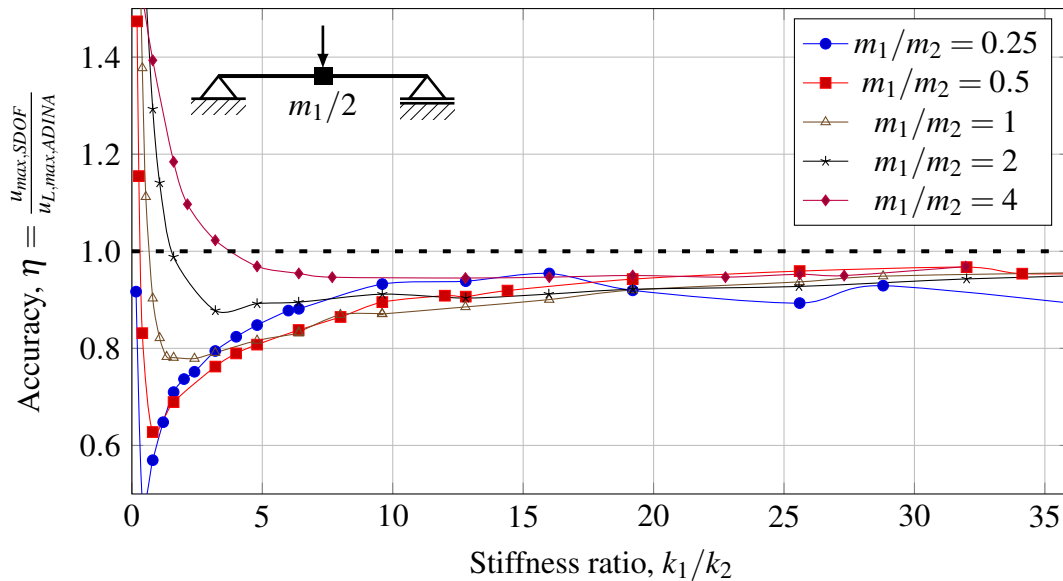


Figure 5.5: Accuracy of the SDOF model for the lower beam. Beam treated as a simply supported beam with a point mass in the mid-span.

The discrepancy between structures with different mass ratio cannot be seen now. The response of the SDOF model tends to $\eta = 1$ as the stiffness ratio increases. The results for low stiffness ratios are not of interest, since the lower beams hardly move in such structures. The model gives results on the unsafe side, underestimating the response by 10-20 % in the tentative range of application (which is assumed to be when $k_1/k_2 \geq 8$). This is because there is no influence of higher eigenmodes in this simplified model. To conclude, the deformation of the lower beam can easily be estimated with reasonable accuracy with the SDOF model created from a simply supported beam with a point mass in the mid-span. However, the obtained results will be somewhat non-conservative.

5.3 Upper beam

5.3.1 Simply supported beam

The easiest alternative is to consider the upper beam as an ordinary simply supported beam subjected to a uniformly distributed load, which can be seen in Figure 5.6

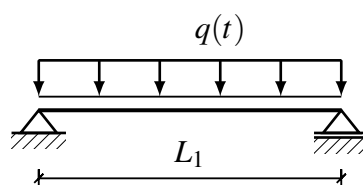


Figure 5.6: Simply supported beam subjected to a uniformly distributed load.

The beam has stiffness k_1 and mass m_1 - the reader is referred to Section 4.2.1 for more information about these parameters. The transformation factor κ_{mF} for this beam can be obtained directly from Table 2.5, and in this case it is equal to

$$\kappa_{mF} = 0.788 \quad (5.11)$$

The angular frequency of this system can be expressed as

$$\omega = \sqrt{\frac{k_1}{\kappa_{mF} m_1}} \quad (5.12)$$

And finally, the maximum deformation of the beam can be calculated as

$$u_{max,SDOF} = \frac{I_k}{\kappa_{mF} m_1 \omega} \quad (5.13)$$

where I_k is the characteristic impulse corresponding to the load $F(t) = q(t)L_1$. For more information, the reader is referred to Section 2.4.2.

The maximum deformation received from this SDOF system is denoted $u_{max,SDOF}$. From the FE solution, the maximum deformation of the upper beam, $max(u_{UA})$ is referred to as $u_{U,max,ADINA}$. The accuracy coefficient, η , can be computed for each studied case, i.e.

$$\eta = \frac{u_{max,SDOF}}{u_{max,ADINA}} \quad (5.14)$$

The resultant accuracy of the system is presented in Figure 5.7.

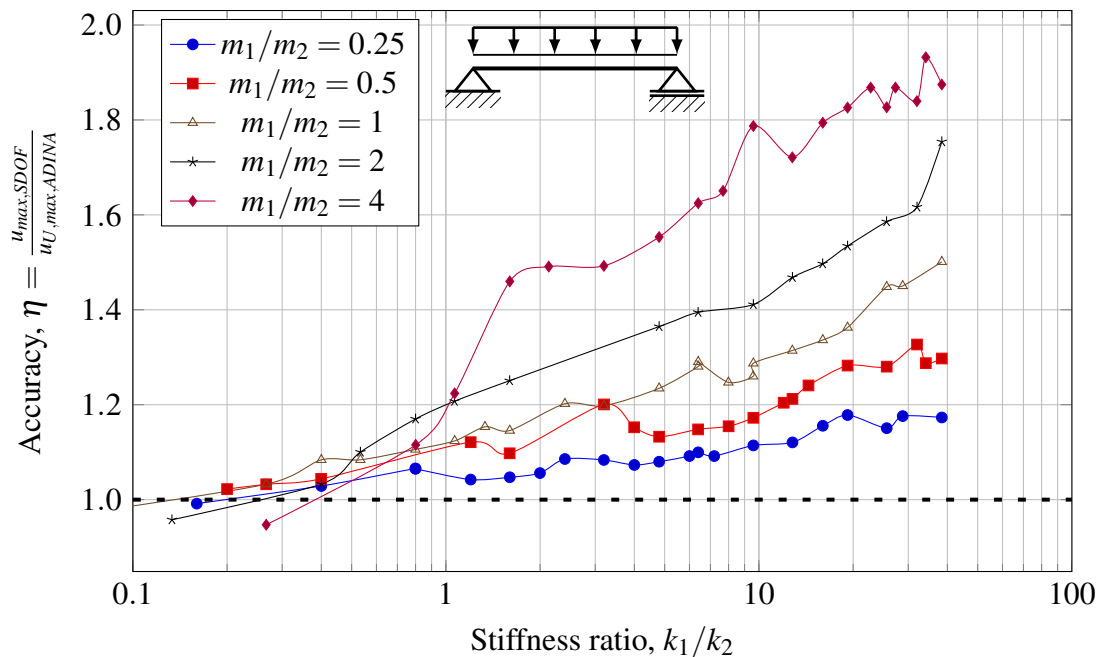


Figure 5.7: Accuracy of the SDOF model for the upper beam. Beam is treated as a simply supported beam subjected to a uniformly distributed load.

The behaviour of a structural system with a low stiffness ratio will be dominated by the vibration of the upper beam. Therefore it can be anticipated, that if this SDOF model gave good results, it would be in the range of the low stiffness ratios, hence the graph was shown in logarithmic scale. It can be seen that this model overestimates the deformation in virtually every case. The higher the mass ratio, the higher the overestimation, which can reach up to 80 % on the safe side for a structure with both high stiffness and mass ratio. The range of acceptable results can be deemed until the stiffness ratio $k_1/k_2 = 1$. This is clearly not a good SDOF model, and should be improved.

5.3.2 Beam on spring supports

Another alternative is to realise that the beam in reality is resting on another beam - thus the stiffness of the support is not infinite. Therefore a model consisting of a beam on spring supports can be adopted to reflect the flexibility of the lower beams. A schematic layout of such model is shown in Figure 5.8.

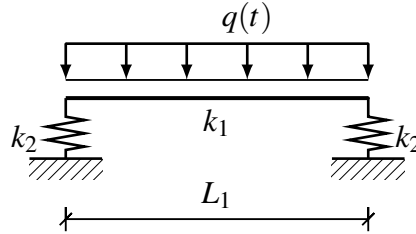


Figure 5.8: *Beam on spring supports subjected to a uniformly distributed load.*

The stiffness of the spring supports was chosen to be k_2 in order to reflect the flexibility of the lower beams. The springs are massless, while the mass of the beam is m_1 . The transformation factors for this beam can be calculated according to Section 3.3. The creation of the SDOF system can be performed according to Section 3.4. The equivalent stiffness of the structure can be calculated as:

$$k_e = \frac{2k_1k_2}{2k_2 + k_1} \quad (5.15)$$

The angular frequency is obtained as

$$\omega = \sqrt{\frac{k_e}{\kappa_{mF}m_1}} \quad (5.16)$$

where $\kappa_{mF} = \kappa(k_1, k_2)$ is the modified transformation factor for a beam on spring supports subjected to a uniformly distributed load, see Figure 3.6.

The maximum deformation of this SDOF system is then

$$u_{max,SDOF} = \frac{I_k}{\kappa_{mF,mod}m_1\omega} \quad (5.17)$$

It should be noted that this is the deformation of the beam along with the contraction/elongation of the spring supports. As already derived in Section 3.4, the pure beam deformation can be expressed as

$$u_{U,max,SDOF} = u_{max,SDOF} \cdot \frac{2k_2}{2k_2 + k_1} \quad (5.18)$$

The accuracy coefficient, η , was calculated for each studied case, and the results are presented in Figure 5.9.

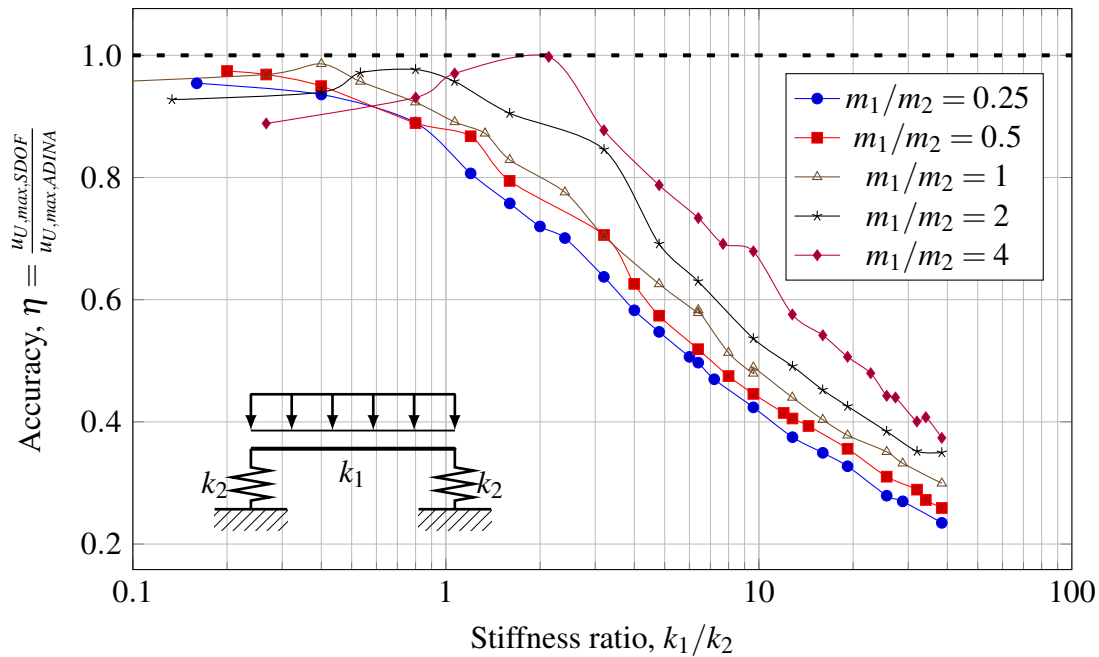


Figure 5.9: Accuracy of the SDOF model for the upper beam. Beam treated as beam on spring supports subjected to a uniformly distributed load.

The graph is shown in logarithmic scale, since it is the low stiffness ratio region that can be expected to give good results. The model behaves now in the opposite way compared to the system in Section 5.3.1, giving results on the unsafe side for the whole spectrum of structures. The results lie in the vicinity of 1 in approximately the same range as before (Figure 5.7). The model gives reasonable estimates of deformation up to 20 % on the unsafe side, if the stiffness ratio $k_1/k_2 \leq 1.0$. However, its performance is still rather poor, and the model could possibly be improved, so that the range of application widens.

5.3.3 Optimised SDOF model for the upper beam

An alternative approach to the simplified SDOF model for the upper beam was tried. This time, an optimisation procedure was employed to create a SDOF model, which can describe the response of the upper beam in terms of the maximum deformation and the first eigenfrequency. The basis for this model was a beam on spring supports (presented in Figure 5.10), but now some adjusting parameters depending on stiffnesses and masses of the constitutive elements are also present. The optimisation procedure is described in Appendix F.

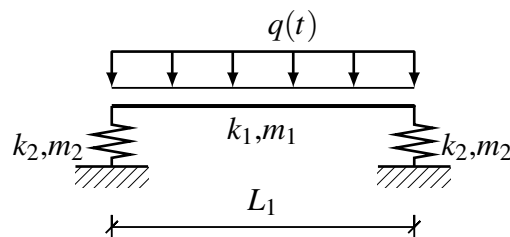


Figure 5.10: Beam on spring supports subjected to a uniformly distributed load.

The differential equation of motion for this optimised SDOF system has the form:

$$\gamma_m m_e \ddot{u}_U + \gamma_k k_e u_U = F(t) \quad (5.19)$$

The system uses equivalent mass and stiffness, which can be expressed with following equations.

$$m_e = m_1 + 2m_2 \quad (5.20)$$

$$k_e = \frac{2k_1 k_2}{2k_2 + k_1} \quad (5.21)$$

Furthermore, these properties are adjusted with adjustment factors, γ_m and γ_k , so that they reflect the behaviour of the upper beam within a longer range than before. Moreover, they were optimised in such a way, that the angular frequency of the SDOF system matches the first eigenfrequency of the structural system. The angular frequency can be calculated as

$$\omega_{SDOF} = \sqrt{\frac{\gamma_k k_e}{\gamma_m m_e}} \quad (5.22)$$

where the adjustment factors, γ_m and γ_k can be computed as

$$\gamma_m = \left(0.0288 + 0.1697 \left(\frac{m_1}{m_2} \right) - 0.0233 \left(\frac{m_1}{m_2} \right)^2 \right) \cdot \left(\frac{k_1}{k_2} + 1.3023 \right) \quad (5.23)$$

$$\gamma_k = 0.9961 + \left(0.1767 + 0.1853 \ln \left(\frac{m_1}{m_2} \right) \right) \cdot \frac{k_1}{k_2} \quad (5.24)$$

For a detailed procedure of how those expressions were obtained, the reader is referred to Appendix F.

The maximum deformation of the upper beam according to this model can be computed as

$$u_{U,max,SDOF} = \frac{I_k}{\gamma_m m_e \omega_{SDOF}} \quad (5.25)$$

where I_k is the characteristic impulse.

To check how well the model works for different stiffness ratios, the accuracy coefficient, η , can be calculated for each studied case. The definition of this coefficient remains as before, i.e. it is the ratio of the maximum deformation of the upper beam obtained from the SDOF model and the maximum deformation of the upper beam taken from ADINA.

$$\eta = \frac{u_{U,max,SDOF}}{u_{U,max,ADINA}} \quad (5.26)$$

For each studied case the accuracy coefficient was calculated, and the results can be seen in Figure 5.11.

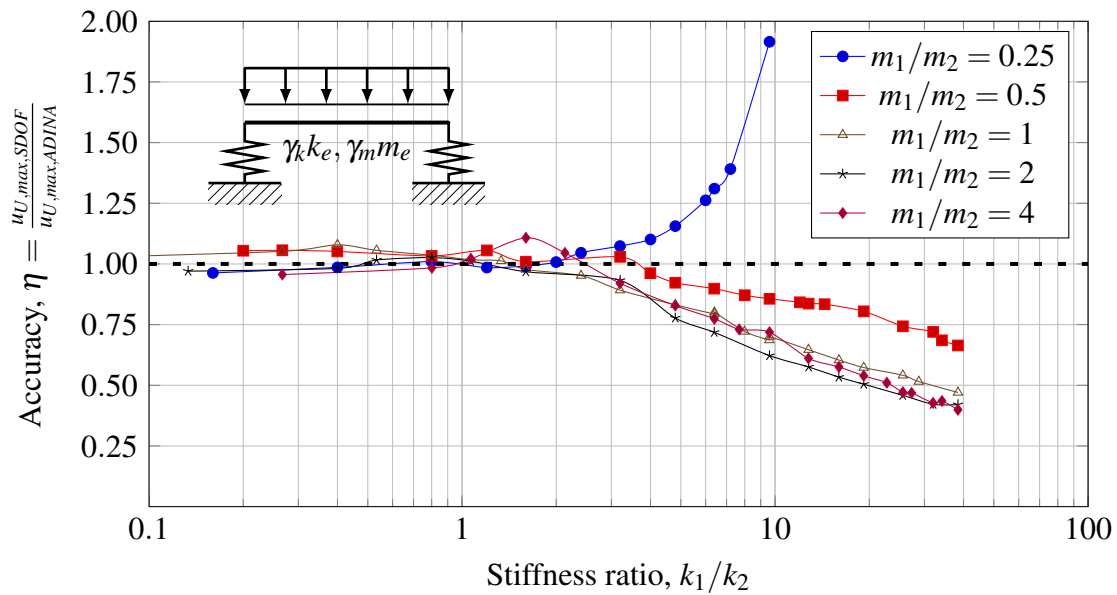


Figure 5.11: Accuracy of the optimised SDOF model for the upper beam.

It can be seen, that the model provides reasonable results up to the stiffness ratio of 3, which is a notable improvement compared to that obtained in Section 5.3.1 and Section 5.3.2. and The results start to diverge after that, e.g. for the lowest mass ratio an overestimation of the deformation is received, while for all the other mass ratios the model is underestimating the deformation. The reason behind it is unclear, but it is believed, that this is caused by the numerical nature of the optimisation process. Moreover, for a structural system with a high stiffness ratio, the movement of the upper beam is rather small in comparison to the lower elements, and therefore it can be accepted.

Even though this optimised SDOF model is capable of approximating the deformation of the upper beam up to the stiffness ratio of 3, it should be noted that for structures with this ratio, the lower beam's movement can also pose a considerable role in the vibration of the total structure.

5.4 Discussion and conclusions

5.4.1 Alternative approach to the upper beam

From the beginning, the upper beam was intended to be simplified in another way. Namely, a beam on spring supports and point masses at the ends subjected to a uniformly distributed load was believed to reflect the behaviour of this part of the structure in the best way. Such a beam is presented in Figure 5.12.

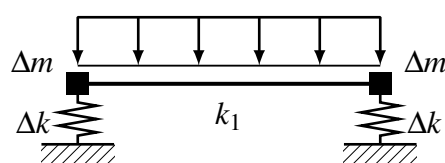


Figure 5.12: Beam on spring supports with point masses at ends.

The simple model of a beam on spring supports with the stiffness of the supports being equal to the stiffness of the lower beam did not give good results, see Section 5.3.2. Therefore it was suspected that the support's stiffness has a different value, depending on the structural properties of one or even both of the constitutive elements of the structure. Therefore it was chosen to use a support with a flexibility of Δk , which can be a function of the properties of both elements. A similar approach was reasoned for the point masses at the ends, Δm . It was believed that during the vibrations, the upper beam might "receive" a part of the mass from the lower supporting elements and vice versa.

This beam was studied extensively in order to find the relations and expressions for Δk and Δm , but the survey was not successful. When modelled numerically, such a structure vibrates with two distinctive frequencies, therefore it has two clear eigenmodes. One in which the beam bends upwards (downwards) and the springs elongate (contract), and one with an opposite behaviour - namely the beam bends downwards (upwards) accompanied by the elongation (contraction) of the springs. Efforts were put to adopt such point masses and spring supports, so that the eigenfrequencies correspond to the eigenfrequencies of the structure, and the amplitudes for the respective modes reflect the amplitudes received in the FE analysis. Unfortunately, this search did not provide good results. For instance, negative masses, Δm , were received, and the flexibilities, Δk , did not follow any reasonable trend. Moreover, it was not clear how the transformation factors κ should be treated in this case. In the end this approach was abandoned.

5.4.2 Lower beam with point mass and the optimised SDOF system for the upper beam

The response of the constitutive elements of a beam-on-beams structural system can be obtained approximately by using the modified SDOF systems. For describing the behaviour of the lower beam, the SDOF model based on a simply supported beam with a point mass in the middle can be recommended, see Section 5.2.2. However, it was shown that this model describes the displacement of the lower beam on the unsafe side, increasing the accuracy as the stiffness ratio of the structure, k_1/k_2 , increases. It is hard to set a definite limit, as to when the system is successful, but it is believed that for structures with stiffness ratio higher than 8, the behaviour of the lower beam can be estimated by this model with 80-90 % accuracy. Since the model underestimates the actual response, it is advisable to use a safety factor in design taking this deviation into account.

For describing the behaviour of the upper beam, an optimised SDOF system based on a beam on spring supports can be used, see Section 5.3.3. This system was adjusted so that the response of the simplified beam and the actual FE response are similar. Nevertheless, some inaccuracy exists, and should be accounted for in the design of such beams. It is believed that the limit of application for this model is a structure with a stiffness ratio, $k_1/k_2 \leq 3$. In this range, the model can describe the movement of the upper beam with the accuracy of 80-90 %. It cannot be clearly said whether the model underestimates or overestimates the response, hence a safety factor should be used in design.

It should be noted, that for a beam-on-beams structural system with a stiffness ratio in the range of 1 to 3, the movement of the upper beam is no longer dominating the total motion of the structure. As it was shown in Chapter 4, even for a structure with a stiffness ratio of 1.6, the lower beam's movement can constitute even 50 % of the total amplitude of vibration. It is therefore advised to check the behaviour of the lower beam as well for the structures in the intermediate stiffness ratio region ($1 \leq k_1/k_2 \leq 8$). However, no simplified SDOF system was developed for this purpose.

6 Discussion

6.1 General discussion

This thesis project consists of three main sub-studies, namely the study of beam on spring supports, the study of an equivalent 2DOF system, and finally a modification of existing SDOF models in order to estimate the response of a compound structure. Detailed discussions for each sub-part are included in the respective chapters. Nevertheless, some general remarks which summarise the whole project are presented in this chapter.

In terms of accuracy of the results, some primary assumptions and limitations should be reminded. First of all, all studies were limited to linear elastic response. Therefore the resultant response of the structure might be misleading. As far as the FE model is concerned, the boundary conditions used are also a simplification of reality. Namely, the connection between the upper and lower beams is simplified to a simple support. Since the considered structural system is just a simplification of a continuous beam grid, there exists some kind of restraint between the two elements, and it should also be taken into account when judging the credibility of the analysis. The results of the Fast Fourier Transform depend greatly on the sampling time; the longer the time of the recorded response, the better the accuracy of the received amplitudes and eigenfrequencies. In order to save computational time, the sampling time was not considered to be a very important output, therefore the results of the FFT may be also slightly misleading.

Nevertheless, the outcomes of the sub-studies solve the research problems stated in the beginning of this thesis; a beam-on-beams structural system can be transformed into a 2DOF system, and the sought deformations, and eigenfrequencies can be obtained. If the procedure is considered too complicated, and the structure has a stiffness ratio in certain limits, the response of one of its elements can be estimated with easier SDOF models and even hand calculations.

6.2 Limitations of the 2DOF system

Apart from the limitations stated in Section 1.3 and in the respective discussion chapters, a concluding survey was done to show why the optimisation factors could not be received for all stiffness and mass ratios in the same limits. It was pointed out, that the angular frequency ratio might have a large influence on the response of individual members of the structure. Therefore, for all studied cases, the results of the Fast Fourier Transform were analysed once more. Namely, the amplitude of respective eigenmode was related to the maximum amplitude of the structure's vibration. The angular frequencies of separate members were calculated as:

$$\omega_1 = \sqrt{\frac{k_1}{m_1}} \quad (6.1)$$

$$\omega_2 = \sqrt{\frac{k_2}{m_2}} \quad (6.2)$$

Thus, the resultant angular frequency ratio can be computed as:

$$\frac{\omega_1}{\omega_2} = \sqrt{\frac{k_1}{k_2} \cdot \frac{m_2}{m_1}} \quad (6.3)$$

When presenting the results with respect to the varying angular frequency ratio, ω_1/ω_2 , an interesting pattern can be seen. The results related to the upper beam for the whole spectrum of studied structures can be seen in Figure 6.1, while the results belonging to the lower beam can be seen in Figure 6.2.

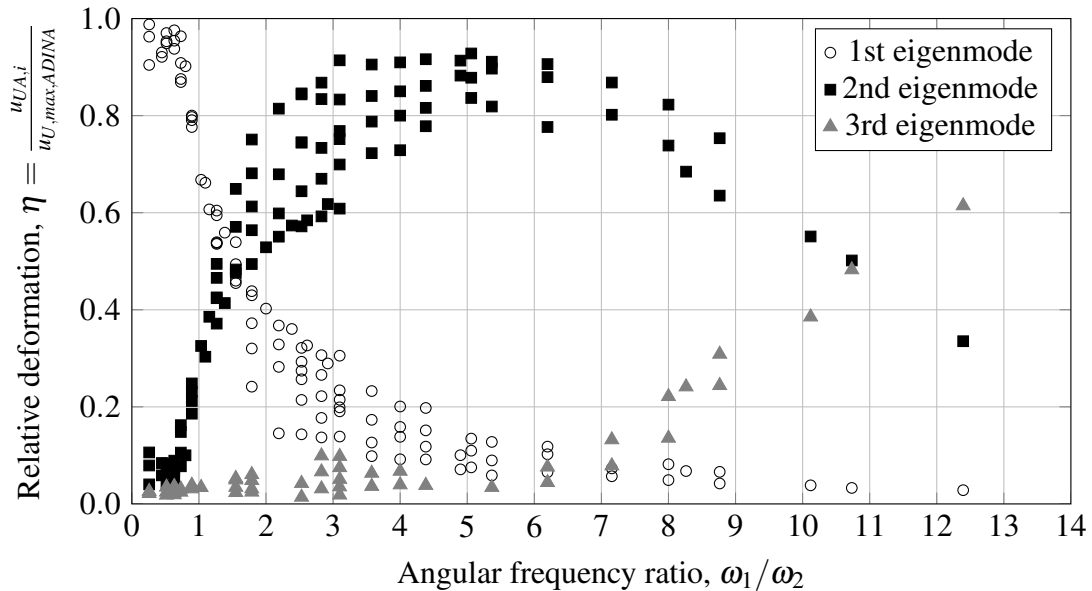


Figure 6.1: Influence of the eigenmodes on the total amplitude of the upper beam's deformation.

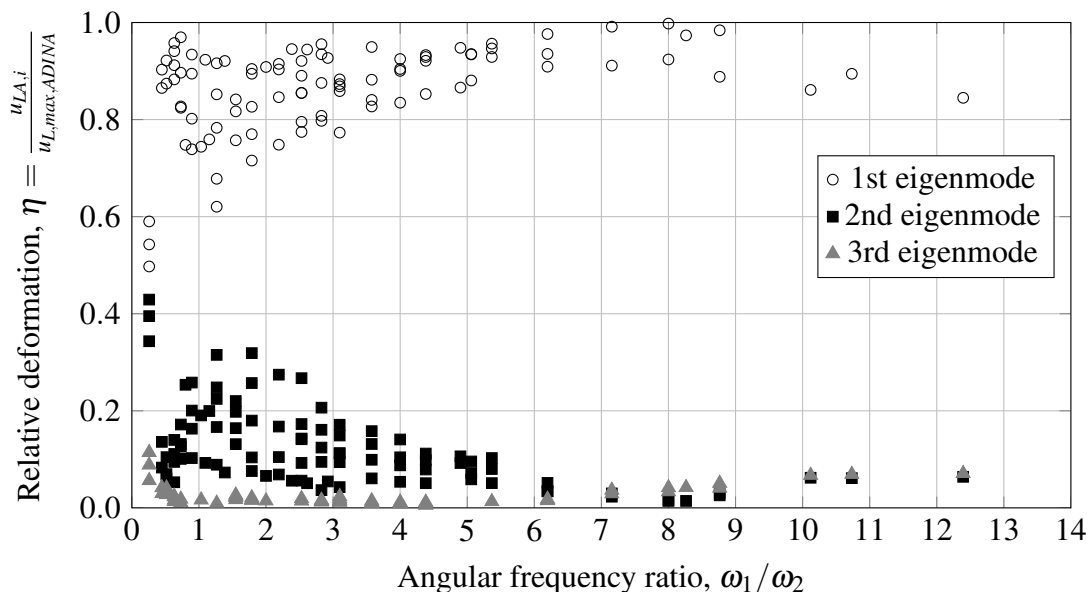


Figure 6.2: Influence of the eigenmodes on the total amplitude of the lower beam's deformation.

As far as the upper beam's behaviour is concerned, for low frequency ratios the first eigenmode dominates the total movement, while the second eigenmode has very little influence. This relation changes as the ratio increases. Once the ratio passes approximately 1.5, the amplitude of the second eigenmode starts to dominate in the movement of the

upper beam. For high angular frequency ratios, the third mode starts to play a big role, and this is the reason that not all the structures were able to be successfully analysed with a simple 2DOF system. It is still possible to analyse the structural system with a 2DOF system, but other eigenfrequencies must be used in the calibration process. In this thesis, only the first two eigenfrequencies were used, and from Figure 6.1 it can be seen that with those two, the 2DOF system can be successful up to the frequency ratio of approximately 6-7. After that, the influence of the third eigenmode will noticeably affect the result. This is believed to be the reason why complex numbers were sometimes received in the calibration process, and why the optimisation factors for a structure with a low mass ratio and high stiffness ratio could not be obtained. High stiffness ratio and low mass ratio result in a high angular frequency ratio, and therefore for those ratios the model should be calibrated to the second and third eigenfrequency, rather than to the first and the second, as it was done for the whole spectrum.

As far as the lower beam is concerned, the prevalence of the first eigenmode can be seen almost throughout the whole spectrum. However, for low frequency ratios the influence of second eigenmode can be high. With increasing angular frequency ratio the influence of third eigenmode increases as well, although it is still of minor magnitude (about 10 %). Overall, it can be seen that the behaviour of the lower beam is not affected as much as the behaviour of the upper beam by higher eigenmodes. Therefore it can be deemed that the 2DOF model could describe the lower beam's motion even for high ω_1/ω_2 ratios.

To summarise, the 2DOF system developed and presented in this thesis project can be used as long as the first two eigenmodes play a dominant role, i.e. up to the frequency ratio being approximately 6-7. Above that, the calibration process must be repeated, taking other eigenfrequencies, and possibly using other optimisation factors.

6.3 Summary of results

6.3.1 Response of a structural system

The structural system consisting of beam supported on beams was thoroughly studied in this master's thesis. An optimised 2DOF system was developed in order to be able to describe the response of such a system.

For a structure low stiffness ratio, k_1/k_2 , the response of the structure will be governed by the movement of the upper beam, since the lower beams are much stiffer and act nearly as ideal supports. On the other hand, for a structure with high stiffness ratio, k_1/k_2 , the response of the system will be governed by the movement of the lower beams. Since the upper beam is much stiffer and will undergo movement resembling rigid body motion, meaning that it will hardly bend.

Having in mind the limitations presented in Section 6.2, it can be stated that the optimised 2DOF model can be used to describe the behaviour of the structural system within a wide spectrum of structural properties.

Furthermore, simplified SDOF models were created as well in order to estimate the response in a quick way. The response of the upper beam in a low stiffness ratio structure can be described by the optimised SDOF system which uses adjustment factors γ_m and γ_k and a beam on spring supports. This model proved to give reasonable results up to the stiffness ratio of 3.

On the other hand, the response of the lower beam can be described by a SDOF model which uses a simply supported beam with a point mass in the mid-span. This model proved to give reasonable results from the stiffness ratio $k_1/k_2 = 8$ onwards. A summary of all the models suitable for describing the response of the structural system along with their ranges of application is shown in Figure 6.3.

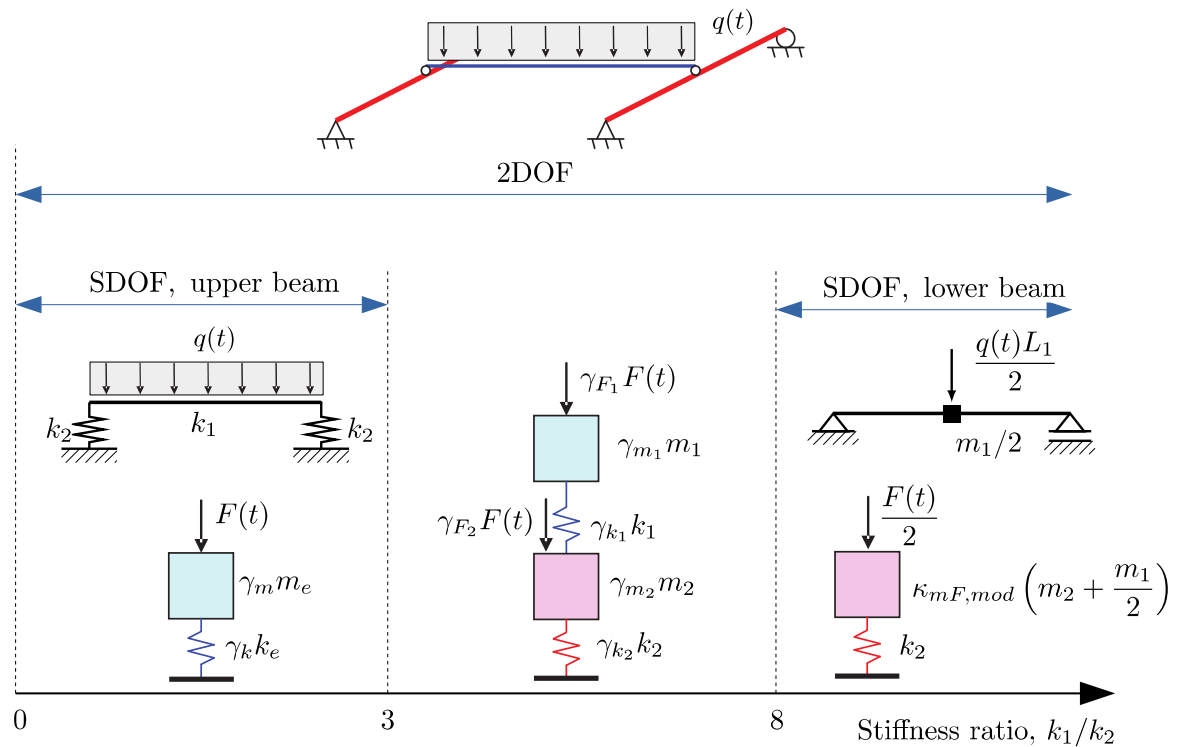


Figure 6.3: Ranges of application of the developed systems.

6.3.2 Influence of the surrounding structure

Another objective in this master's thesis was to investigate the effect the surrounding structure has on the response of its individual elements. In order to examine that, each structural system was divided into two parts. Those two simply supported beams were subjected to the same load (either uniformly distributed load or a point load) as the structural systems before. After dynamic analyses, the maximum deformation for each element was stored and compared with the maximum deformation of the same element in the system consisting of beam on beams. In the end the quotient of the two deformations was computed for each case. The results can be seen in the contour plots in Figure 6.4 and Figure 6.5.

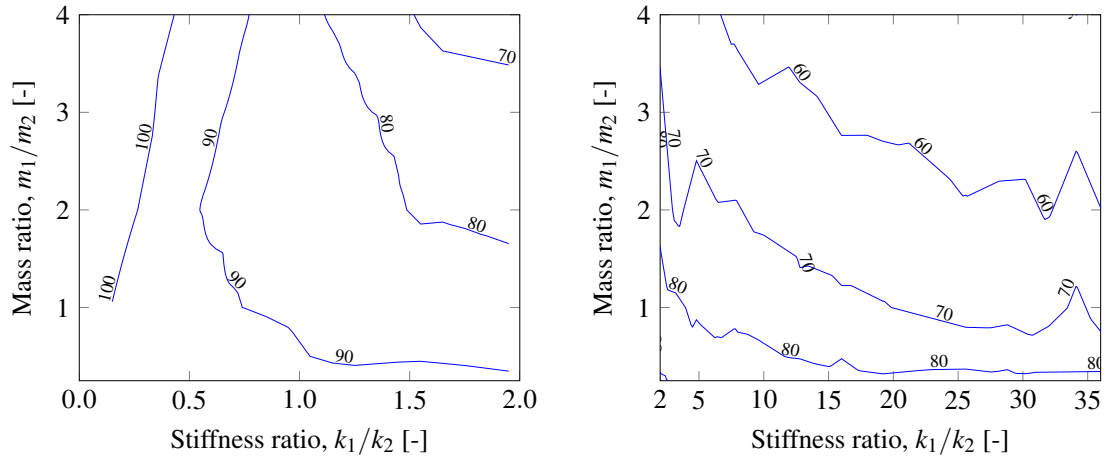


Figure 6.4: *Quotient of the maximum elastic deformation (in %) of the upper beam treated as a part of the structure, and the upper beam's maximum deformation when the beam is treated separately.*

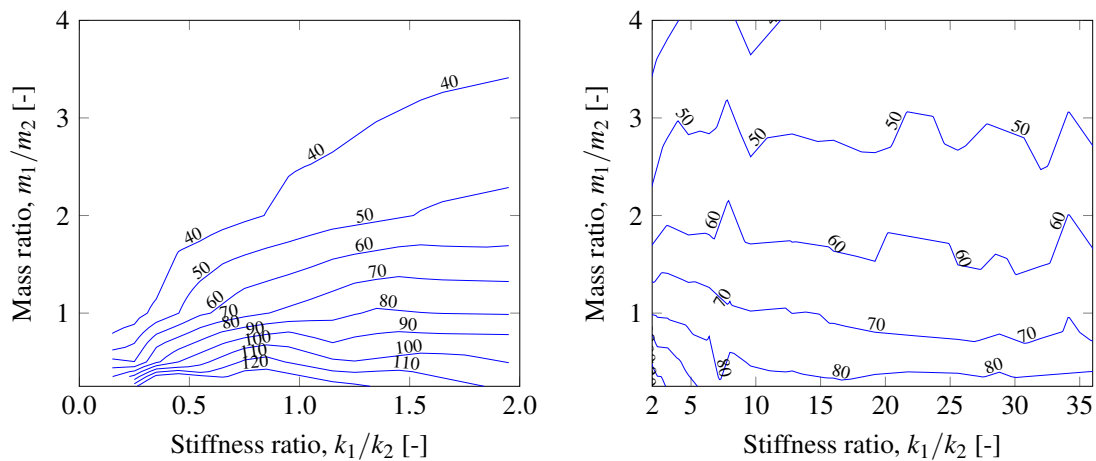


Figure 6.5: *Quotient of the maximum elastic deformation (in %) of the lower beam treated as a part of the structure, and the lower beam's maximum deformation when the beam is treated separately.*

For the upper beam, it can be seen that treating the beam as a separate structure usually overestimates its maximum deformation. For high mass and stiffness ratios, the reduction may be up to 40-50 %. However, for some cases with high mass ratios and low stiffness ratio, treating the upper beam as a separate structure can underestimate its maximum deformation.

Similar conclusions can be drawn by analysing the results for the lower beam. If the beam is treated as a separate structure, its maximum deformation is usually overestimated. For high mass and stiffness ratios as much as 50-60 % in terms of lower deformation can be gained if the surrounding structure is considered. However, for some extreme cases (very low mass ratio and low stiffness ratio) the maximum deformation of the lower beam can be underestimated if the beam is treated separately.

To sum up, it is recommended and worthwhile to consider the influence of the surrounding structure in design of impulse loaded elements.

6.4 Examples of application

The first and most natural example of application of the developed 2DOF model for this structural system is a grid of beams, of which the beam-on-beams system is a repeating representation. Hopefully, it could also be applied in some extent to a floor structure, which is supported on beams. It does not need to be a concrete floor, which is often a slab supported on walls and/or columns. The model works for every elastic material.

The same approach can be applied to roofs. One example of this could be a roof structure, which consists of a concrete slab supported on concrete beams. Even though the analysis of the behaviour of slabs was not carried out in this master's thesis, the slab can be simplified to a strip model, which in turn can be modelled with beams. This results ultimately in the beam-on-beam structural system, which can be analysed with an equivalent 2DOF model.

Roofs of warehouse building can also be assigned to this category. A warehouse building usually consist of main girders supported on columns, placed within a distance to each other. Roof elements span the distance between the girders, with or without purlins. A variety of structural elements can be chosen for roofing. For instance, prefabricated slabs can be laid in between the girders to ensure a stiff roofing. The slabs can be simplified in analysis to simply supported beams which are resting on the girder beams. Therefore, such part of the overall structure can be analysed and designed against explosion with the 2DOF simplification.

Another example of application can be the analysis of multi-storey buildings. This can be construed on different structural levels. First, the wall panels of the building can be subjected to explosion load, as shown in Figure 6.6.

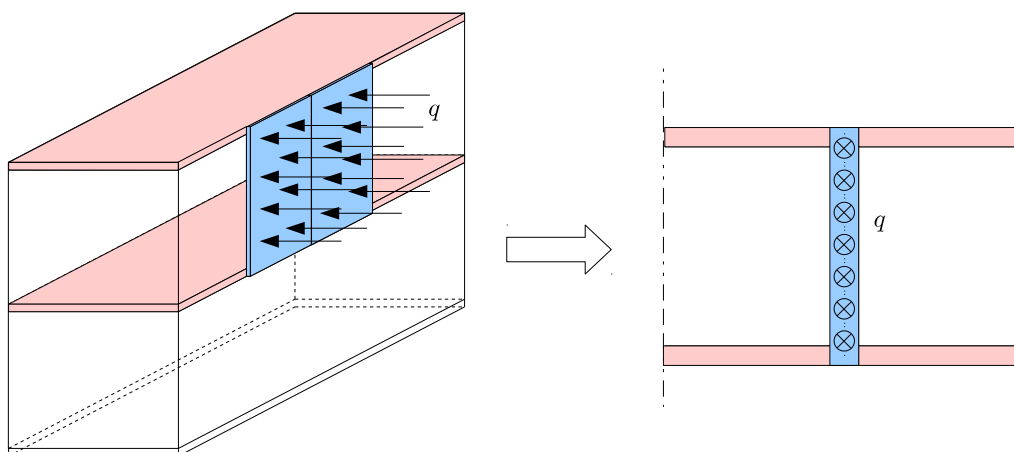


Figure 6.6: Analysis of the wall panel-floor response in a multi-storey building.

The wall panels are connected with the floor and roof elements. Therefore, when looking from the side and simplifying the panel to an equivalent beam, the analogy of beam-on-beams structure can still be used.

When considering the building at a higher structural level, the shear walls can be included, see Figure 6.7.

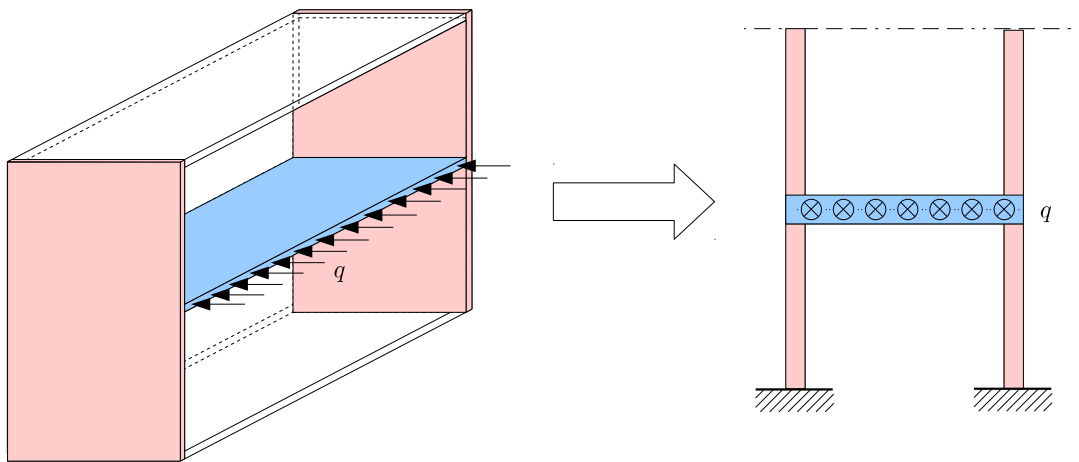


Figure 6.7: *Analysis of the floor-shear wall response in a multi-storey building.*

In this example, the shear walls are considered to be fixed at their base. Therefore, the shear walls and the floor structure can be simplified to a beam-on-beams structural system subjected to explosion. It should be noted, that the stiffness of the floors can be different at different heights of the building, due to the fact that they are connected with the load-bearing structure. The load-bearing structure can resemble a cantilever beam, and therefore its resistance can change with the height; the higher up the load-bearing structure, the less stiffness one could expect. The major difference now are the boundary conditions of the shear walls, which are regarded as cantilever beams instead of simply supported beams. A survey on structural systems with different boundary condition can be regarded as a future research problem.

7 Conclusions

7.1 Response of a structural system

To summarise this thesis project, some final remarks are presented in this chapter. The behaviour of a structural system comprising a beam, simply supported on beams, subjected to an explosion load, will depend on the properties of all members involved. Namely, the stiffness and mass ratios of the individual elements making up the system have great significance. The angular frequency ratio is also of importance. Based on the studies carried out in this thesis, the following conclusions can be drawn:

- For structures with a low stiffness ratio, k_1/k_2 , the response will consist mainly of the movement of the upper beam.
- For structures with a high stiffness ratio the response will consist mainly of the movement of the lower beams.
- The behaviour of a beam-on-beams structural system can be described with the equivalent 2DOF mass-spring system. However, for a structure with high frequency ratio the created 2DOF model might not work, since it is calibrated for other eigenmodes than the ones which are usually predominant for such structures.
- Within certain range of stiffness ratios, it is not necessary to apply a 2DOF model; the response can quickly be estimated with modified SDOF models.
- For a structure with a stiffness ratio lower than 3, the deformation of the upper beam and the first eigenfrequency of the structure can be estimated with an optimised beam-on-springs SDOF model. It should however be kept in mind, that for a structure with a stiffness ratio in the intermediate range (1-3) the movement of the lower beam can also constitute a large part of the total oscillation of the structure.
- For a structure with a stiffness ratio larger than 8, the maximum deformation of the lower beam can be estimated with a SDOF model based on a beam with a point mass in the middle (half of the mass of the upper beam).

7.2 Influence of the surrounding structure

The following conclusions about the influence of the surrounding structure on the response of the individual member can be drawn:

- The surrounding structure has significant influence on the response of its individual elements.
- In the studied stiffness and mass ratios spectrum, the maximum elastic deformation of the upper beam can be reduced by up to 40-50 % if the surrounding structure is considered. However, the magnitude of the reduction is case sensitive and varies for different structures.

- The maximum elastic deformation of the lower beam in the studied spectrum can be reduced by up to 50-60 % if the influence of the surrounding structure is included in the analysis. The actual reduction is case sensitive and varies for different structures.
- For some rare cases (low stiffness ratio and high mass ratio), the maximum elastic deformation of the upper beam can be underestimated when treating the beam as a separate structure.
- For some rare cases (very low mass ratio and a low stiffness ratio), the maximum elastic deformation of the lower beam can be underestimated if the beam is treated as an individual structure.
- Nevertheless, it is recommended and worthwhile to consider the influence of the surrounding structure in design of impulse loaded elements.

7.3 Improvements and further research

To improve the results obtained in this thesis project, several measures could be taken. First of all, a mode superposition analysis could be carried out on the whole spectrum of structures in order to attain a deeper knowledge on the influence of the eigenmodes on the total behaviour of the structural system.

Secondly, the mentioned high frequency ratio structures could be analysed once more in the 2DOF system's calibration process. However, it should be noted that such structures can usually be associated with high stiffness ratio, which means that it is mainly the lower beam which will experience high-amplitude vibrations. Therefore, even if the 2DOF system cannot describe the behaviour of such structures, their behaviour can still be easily approximated with a modified SDOF model for the lower beam, if only its maximum deformation is of interest.

For the further research, there remain many unattended matters. First of all, other material types should be studied, especially an elastoplastic response of the structure, since it is deemed to be much closer to the real response of for example a reinforced concrete structure. The 2DOF system (and possibly the modified SDOF systems) could possibly be modified to reflect the behaviour of the structure for the elastoplastic case.

Another thing would be to develop a simplified hand calculation model for the 2DOF system. The 2DOF model can describe the structure in the whole spectrum of stiffness and mass ratios. Provided that the hand calculation model is sufficiently easy and concise, it could replace the modified SDOF models in estimation of the structure's response.

In this thesis, only the structural system consisting of a beam, simply supported on two beams, was studied. Other structural systems should also be studied, to confirm that the developed 2DOF model is case-sensitive. Perhaps a general 2DOF transformation procedure valid for a variety of structural systems could be found. So far, only the response of a beam was transformed into a 2DOF system. It should be investigated, if similar transformation is valid also for other types of structured, e.g. a slab supported on two beams.

References

- ADINA R &D, I. (2014). *ADINA 900 Nodes Version 9.0*. <http://www.adina.com/>.
- Andersson, S. and H. Karlsson (2012). *Structural Response of Reinforced Concrete Beams Subjected to Explosions, Time dependent transformation factors, support reactions and distribution of section forces*. Institutionen för bygg- och miljöteknik, Chalmers tekniska högskola, no: 2010:38. Göteborg, Sweden.
- Augustsson, R. and M. Härenstam (2010). *Design of reinforced concrete slab with regard to explosions*. Institutionen för bygg- och miljöteknik, Chalmers tekniska högskola, no: 2010:38. Göteborg, Sweden.
- Biggs, J. M. (1964). *Introduction to structural dynamics*. McGraw-Hill College.
- Carlsson, M. and R. Kristensson (2012). *Structural Response with Regard to Explosions - Mode Superposition, Damping and Curtailment*. Division of Construction Sciences, Structural Mechanics, Lund University of Technology, Report TVSM - 5185. Lund, Sweden.
- CEN (2004). *Eurocode 2: Design of Concrete Structures: Part 1-1: General Rules and Rules for Buildings*. European Committee for Standardization. Brussels, Belgium.
- ConWep (1992). *ConWep - Collection of conventional weapons effects calculation based on TM5-855-1, Fundamentals of protective design for conventional weapons*. US Army Engineers Waterways Experimental Station. Vicksburg, USA.
- Duhamel, P. and M. Vetterli (1990). "Fast Fourier transforms: a tutorial review and a state of the art". In: *Signal processing* 19.4, pp. 259–299.
- Eaton, J. W. (2014). *GNU Octave 3.8.2*. <https://www.gnu.org/software/octave/>.
- Ek, K.-J. and P. Mattsson (2009). *Design with Regard to Blast- and Fragment Loading*. Institutionen för bygg- och miljöteknik, Chalmers tekniska högskola, no: 2009:81. Göteborg, Sweden.
- Engström, B. (2011). *Design and analysis of continuous beams and columns*. Division of Structural Engineering, Concrete Structures, Chalmers University of Technology, Report 2007:3. Göteborg, Sweden.
- Johansson, M. and L. Laine (2012a). *Bebyggelsens motståndsförmåga mot extrem dynamisk belastning, Del 1: Last av luftstövåg*. Myndigheten för samhällsskydd och beredskap. Karlstad, Sverige.
- (2012b). *Bebyggelsens motståndsförmåga mot extrem dynamisk belastning, Del 3: Kapacitet hos byggnader*. Myndigheten för samhällsskydd och beredskap. Karlstad, Sweden.
- Johansson, M., J. Leppänen, and B. Ekengren (2014). *MSB:s dokumentserie för beräkning av impulsbelastade konstruktioner*. Myndigheten för samhällsskydd och beredskap. Karlstad, Sverige.
- Klorek, J. and A. Sandberg (2013). *Structural Response of Reinforced Concrete Frames Subjected to Explosions*. Institutionen för bygg- och miljöteknik, Chalmers tekniska högskola, no: 2013:87. Göteborg, Sweden.
- Lagarias, J. C. et al. (1998). "Convergence properties of the Nelder–Mead simplex method in low dimensions". In: *SIAM Journal on optimization* 9.1, pp. 112–147.
- Nyström, U. (2006). *Design with regard to explosions*. Institutionen för bygg- och miljöteknik, Chalmers tekniska högskola, no: 2006:14. Göteborg, Sweden.

Appendix A Central Difference Method

A.1 General Notes

Direct integration methods (also called time step methods) are often used to study the response of initial condition problems described by a system of second-order differential equations. Such equation systems can be written in matrix form, i.e.

$$\mathbf{M}\ddot{\mathbf{u}} + \mathbf{C}\dot{\mathbf{u}} + \mathbf{K}\mathbf{u} = \mathbf{F} \quad (\text{A.1})$$

where \mathbf{M} is the system mass matrix, \mathbf{C} is the system damping matrix, \mathbf{K} is the system stiffness matrix, and \mathbf{F} is the force vector. The displacement vector is denoted \mathbf{u} , the velocity vector is denoted $\dot{\mathbf{u}}$, and the acceleration vector is denoted $\ddot{\mathbf{u}}$.

The total duration of the response of the system can be divided into a finite number of time steps, which length is denoted Δt . Hence, the displacement field at time $t = n\Delta t$ is denoted \mathbf{u}_n . The direct integration methods used in solutions of the dynamic problems can be either explicit or implicit. The Central Difference Method is an explicit integration scheme. Explicit methods are usually conditionally stable, and they express the displacement fields at later times \mathbf{u}_{n+1} in the displacement, velocity and acceleration fields at previous time and at the time step before that, i.e. $\mathbf{u}_{n+1} = f(\mathbf{u}_n, \dot{\mathbf{u}}_n, \ddot{\mathbf{u}}_n, \mathbf{u}_{n-1}, \dot{\mathbf{u}}_{n-1}, \ddot{\mathbf{u}}_{n-1})$.

A.2 Method

An arbitrary displacement-time function is presented in Figure A.1. Three different points can be observed in the figure. The displacement u_{n-1} at time t_{n-1} and the displacement u_n at time t_n are considered to be known. The unknown displacement u_{n+1} at time t_{n+1} is sought. The time steps, Δt used in the method are constant.

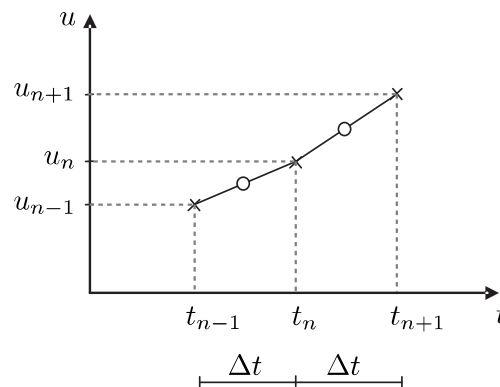


Figure A.1: An arbitrary displacement-time function. From Carlsson and Kristensson (2012).

The velocity of the body is a derivative of its displacement with respect to time. Therefore, at the time t_n , the velocity can be expressed as

$$\dot{\mathbf{u}}_n \approx \frac{\mathbf{u}_{n+1} - \mathbf{u}_{n-1}}{2\Delta t} \quad (\text{A.2})$$

which corresponds to the tangent of the displacement function at point t_n if the time step is sufficiently small.

The acceleration in the Central Difference Method is defined as the derivative of the velocity function with respect to time. However, to derive the acceleration at the time t_n , the difference of mid interval velocities is used (circles in Figure A.1).

$$\ddot{\mathbf{u}}_n \approx \frac{\dot{\mathbf{u}}_{n-1/2} - \dot{\mathbf{u}}_{n+1/2}}{\Delta t} \approx \frac{\frac{(\mathbf{u}_{n+1} - \mathbf{u}_n)}{\Delta t} - \frac{(\mathbf{u}_n - \mathbf{u}_{n-1})}{\Delta t}}{\Delta t} = \frac{\mathbf{u}_{n+1} - 2\mathbf{u}_n + \mathbf{u}_{n-1}}{(\Delta t)^2} \quad (\text{A.3})$$

By inserting Equation (A.3) and Equation (A.2) into Equation (A.1), a system of equations of motion at time t_n can be expressed as

$$\mathbf{M} \frac{\mathbf{u}_{n+1} - 2\mathbf{u}_n + \mathbf{u}_{n-1}}{(\Delta t)^2} + \mathbf{C} \frac{\mathbf{u}_{n+1} - \mathbf{u}_{n-1}}{2\Delta t} + \mathbf{K}\mathbf{u}_n = \mathbf{F}_n \quad (\text{A.4})$$

where \mathbf{F}_n , \mathbf{u}_n and \mathbf{u}_{n-1} are the force vector at the present time, displacement at the present time and the displacement at earlier time respectively. Moreover, those values are assumed to be known. By rewriting Equation (A.4), the following time scheme can be obtained.

$$\left(\frac{\mathbf{M}}{(\Delta t)^2} + \frac{\mathbf{C}}{2\Delta t} \right) \mathbf{u}_{n+1} + \left(\mathbf{K} - \frac{2\mathbf{M}}{(\Delta t)^2} \right) \mathbf{u}_n + \left(\frac{\mathbf{M}}{(\Delta t)^2} - \frac{\mathbf{C}}{2\Delta t} \right) \mathbf{u}_{n-1} = \mathbf{F}_n \quad (\text{A.5})$$

This relation is also often expressed as

$$\hat{\mathbf{k}}\mathbf{u}_{n+1} = \hat{\mathbf{F}}_n \quad (\text{A.6})$$

where

$$\hat{\mathbf{k}} = \frac{\mathbf{M}}{(\Delta t)^2} + \frac{\mathbf{C}}{2\Delta t} \quad (\text{A.7})$$

and

$$\hat{\mathbf{F}}_n = \mathbf{F}_n - \left(\mathbf{K} - \frac{2\mathbf{M}}{(\Delta t)^2} \right) \mathbf{u}_n - \left(\frac{\mathbf{M}}{(\Delta t)^2} - \frac{\mathbf{C}}{2\Delta t} \right) \mathbf{u}_{n-1} \quad (\text{A.8})$$

From this, the sought displacement \mathbf{u}_{n+1} can be calculated as

$$\mathbf{u}_{n+1} = \frac{\hat{\mathbf{F}}_n}{\hat{\mathbf{k}}} \quad (\text{A.9})$$

Equation (A.5) is in the beginning solved for \mathbf{u}_1 using initial conditions in the form of $u(0) = \mathbf{u}_0$ and $\dot{u}(0) = \dot{\mathbf{u}}_0$. In this thesis project, the system is assumed to start from rest, therefore $u(0) = \dot{u}(0) = \mathbf{0}$. However, in order to obtain \mathbf{u}_1 , the displacement at earlier time, \mathbf{u}_{-1} is still needed. This displacement can be obtained from Taylor series expansion and can be expressed as

$$\mathbf{u}_{-1} = \mathbf{u}_0 - \Delta t \dot{\mathbf{u}}_0 + \frac{(\Delta t)^2}{2} \ddot{\mathbf{u}}_0 \quad (\text{A.10})$$

where the unknown acceleration, $\ddot{\mathbf{u}}_0$ can be obtained from Equation (A.1) as

$$\ddot{\mathbf{u}}_0 = \mathbf{M}^{-1} (\mathbf{F}_0 - \mathbf{C}\dot{\mathbf{u}}_0 - \mathbf{K}\mathbf{u}_0) \quad (\text{A.11})$$

In the end, it should be noted that the above derivation is valid only for linear elastic material response. However, the Central Difference Method can be easily modified to include plastic or elastoplastic type of material response.

A.3 Stability and accuracy

As already mentioned, the Central Difference Method is an explicit method, which is conditionally stable. It means that the method will provide credible results as long as the value of the time step, Δt is less than the critical time step Δt_{crit} , expressed as

$$\Delta t_{crit} = \frac{2}{\omega_{max}} \quad (\text{A.12})$$

where ω_{max} is the highest eigenfrequency of the analysed system. If the period corresponding to the highest eigenfrequency is denoted as T_n (it is the shortest vibration period), the stability condition for the Central Difference Method can be given as

$$\frac{\Delta t}{T_n} \leq \frac{1}{\pi} \quad (\text{A.13})$$

In other words, the Central Difference Method is stable as long, as the wave information does not propagate across more than one element in one time step. It should be noted, that for explosions this is seldom a problem, since very small time steps are usually used to capture the behaviour under very short impulse load.

The accuracy aspect also influences the end result. For stable systems, the amplitude error is present. This is caused by numerical damping, which results in certain amplitude decay over time. This is not always a negative phenomenon, since a certain amount of numerical damping will suppress oscillations from inaccurate high frequencies. Apart from the amplitude error, a frequency error also occurs. In this case it can be either contraction or elongation of the period. The Central Difference Method usually experiences period contraction.

Appendix B Results - beam on spring supports

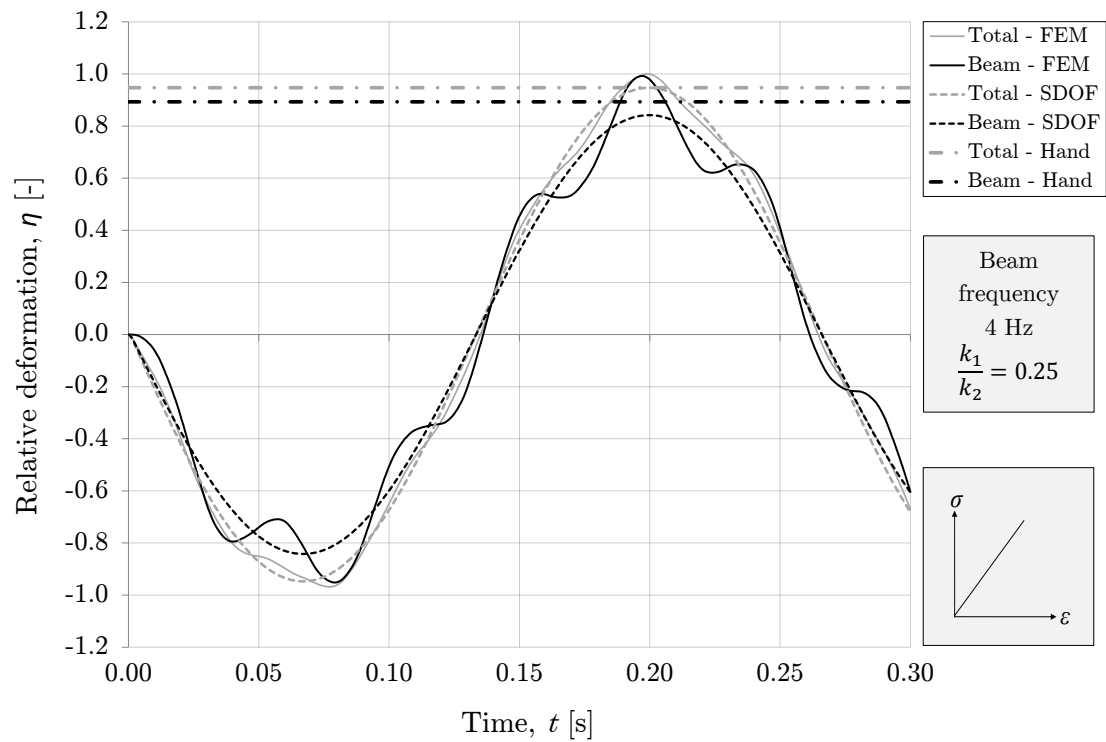


Figure B.1: Relative vertical displacement as a function of time. Beam subjected to uniformly distributed load. Stiffness ratio $k_1/k_2 = 0.25$.

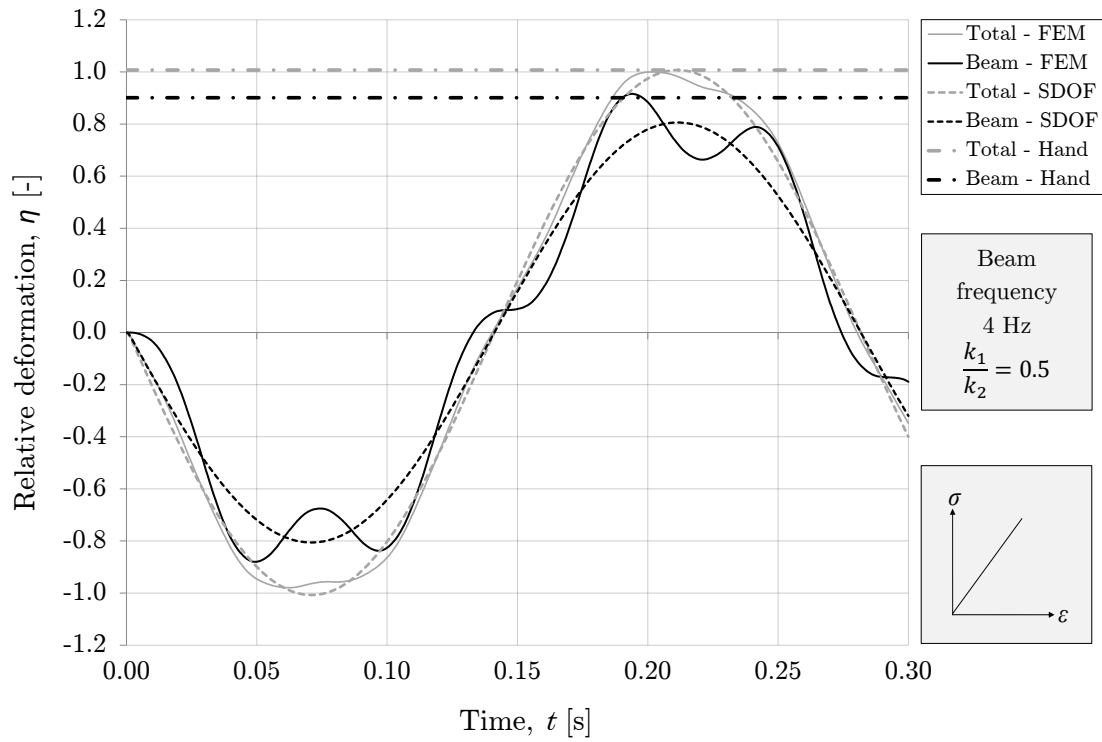


Figure B.2: Relative vertical displacement as a function of time. Beam subjected to uniformly distributed load. Stiffness ratio $k_1/k_2 = 0.5$.

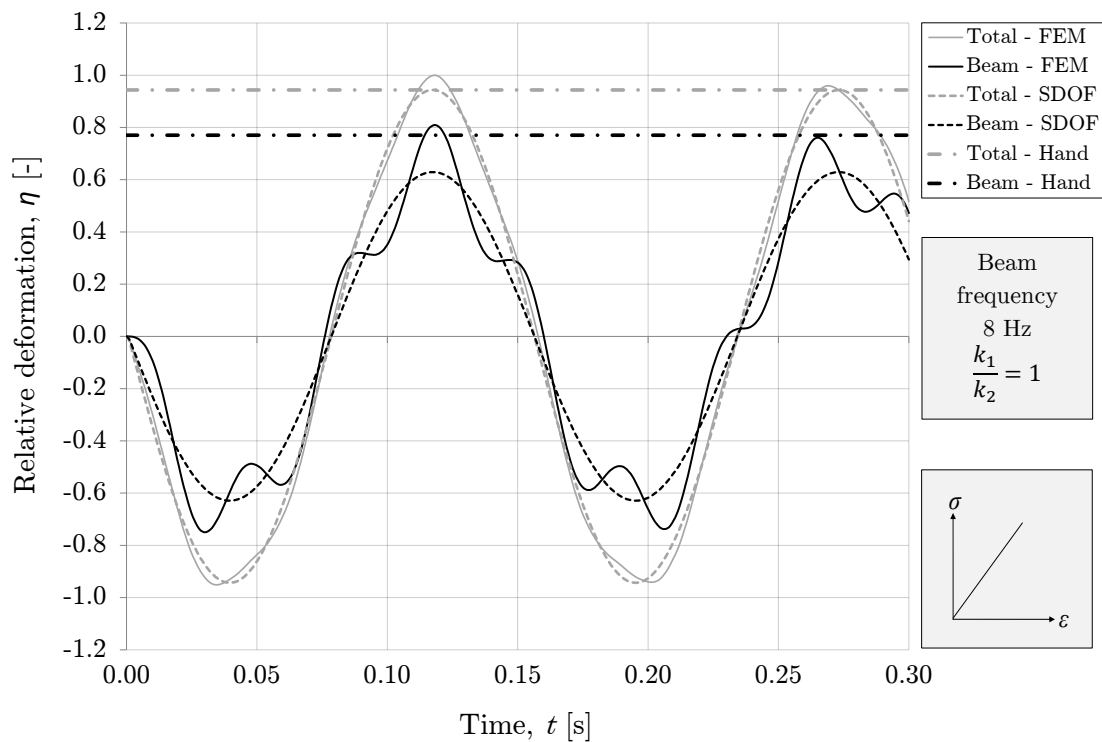


Figure B.3: Relative vertical displacement as a function of time. Beam subjected to uniformly distributed load. Stiffness ratio $k_1/k_2 = 1$.

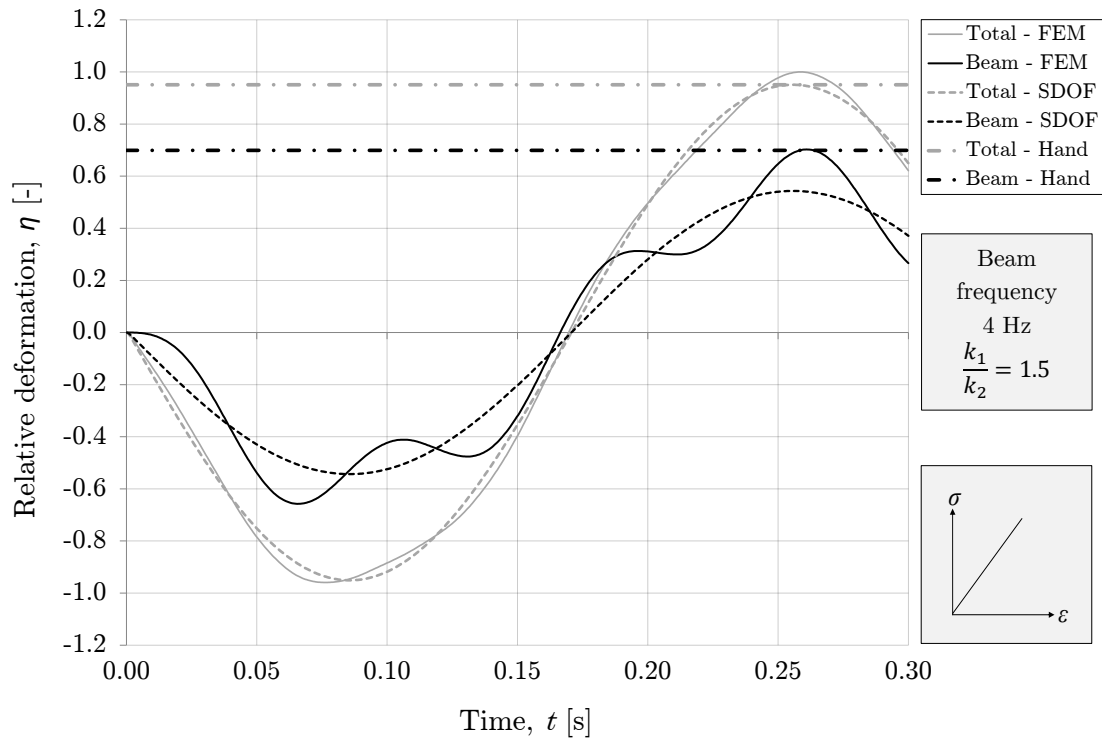


Figure B.4: Relative vertical displacement as a function of time. Beam subjected to uniformly distributed load. Stiffness ratio $k_1/k_2 = 1.5$.

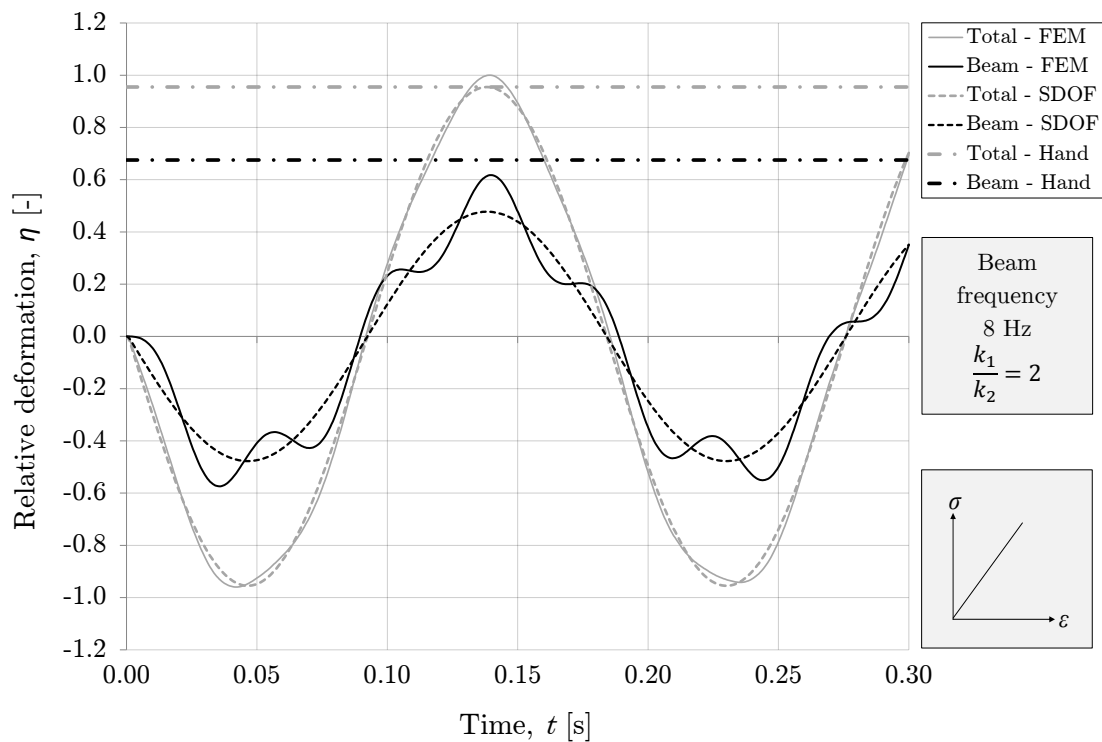


Figure B.5: Relative vertical displacement as a function of time. Beam subjected to uniformly distributed load. Stiffness ratio $k_1/k_2 = 2$.

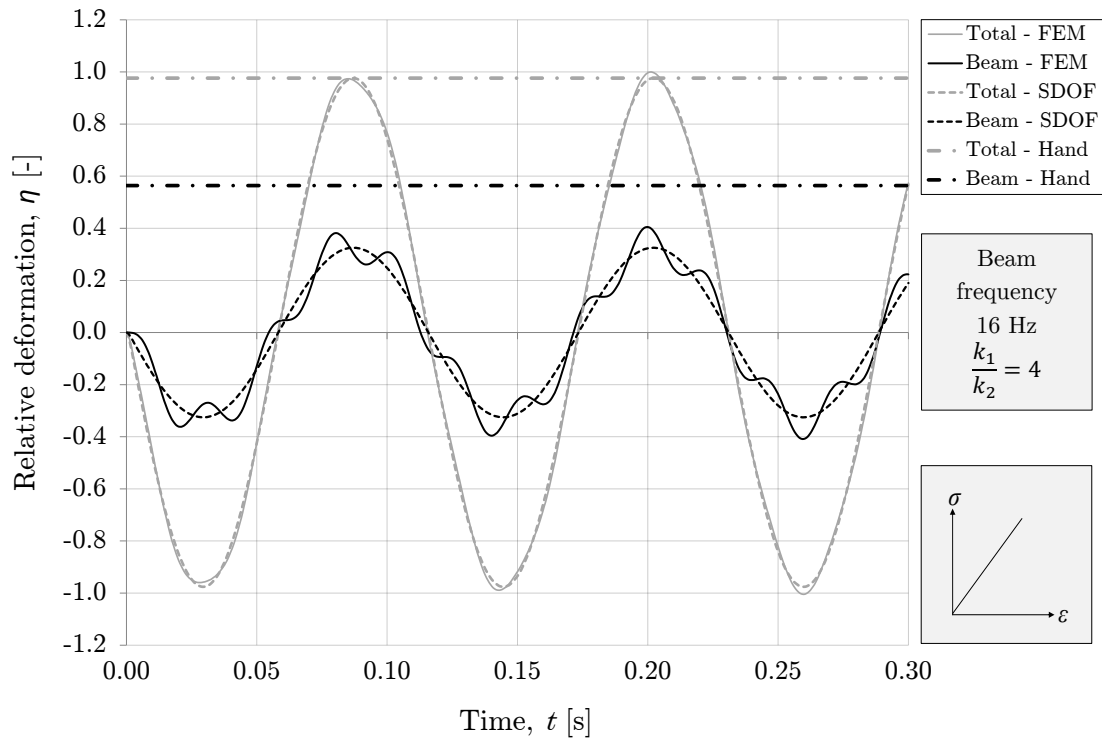


Figure B.6: Relative vertical displacement as a function of time. Beam subjected to uniformly distributed load. Stiffness ratio $k_1/k_2 = 4$.

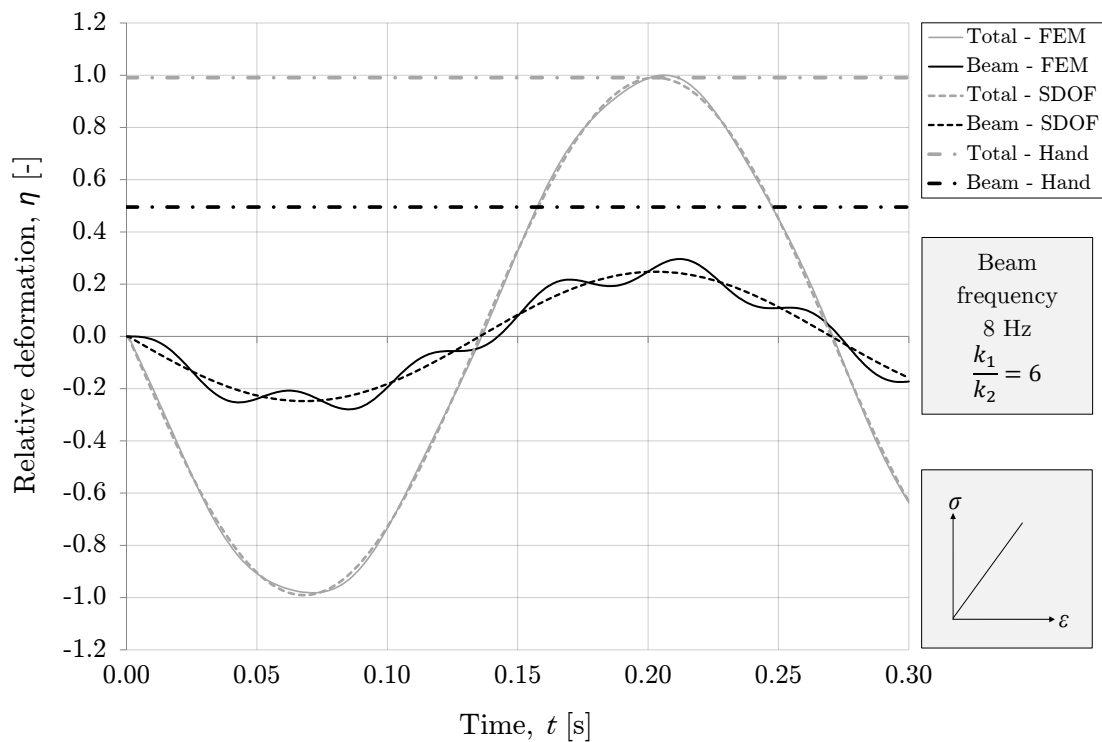


Figure B.7: Relative vertical displacement as a function of time. Beam subjected to uniformly distributed load. Stiffness ratio $k_1/k_2 = 6$.

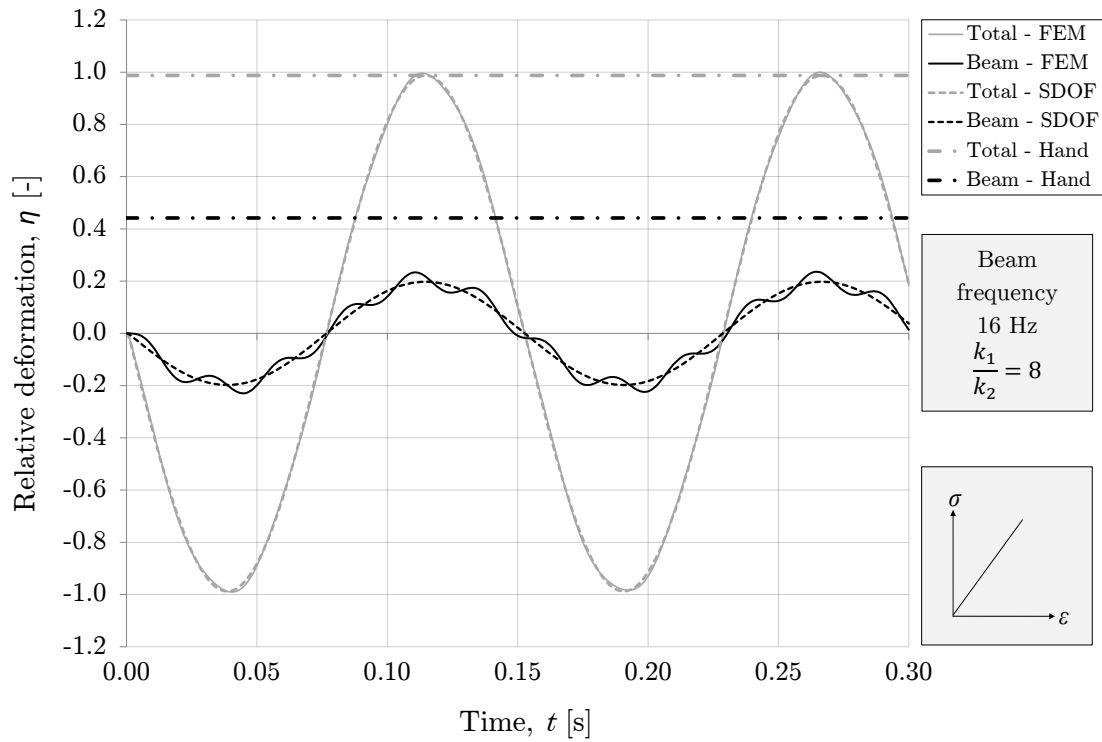


Figure B.8: Relative vertical displacement as a function of time. Beam subjected to uniformly distributed load. Stiffness ratio $k_1/k_2 = 8$.

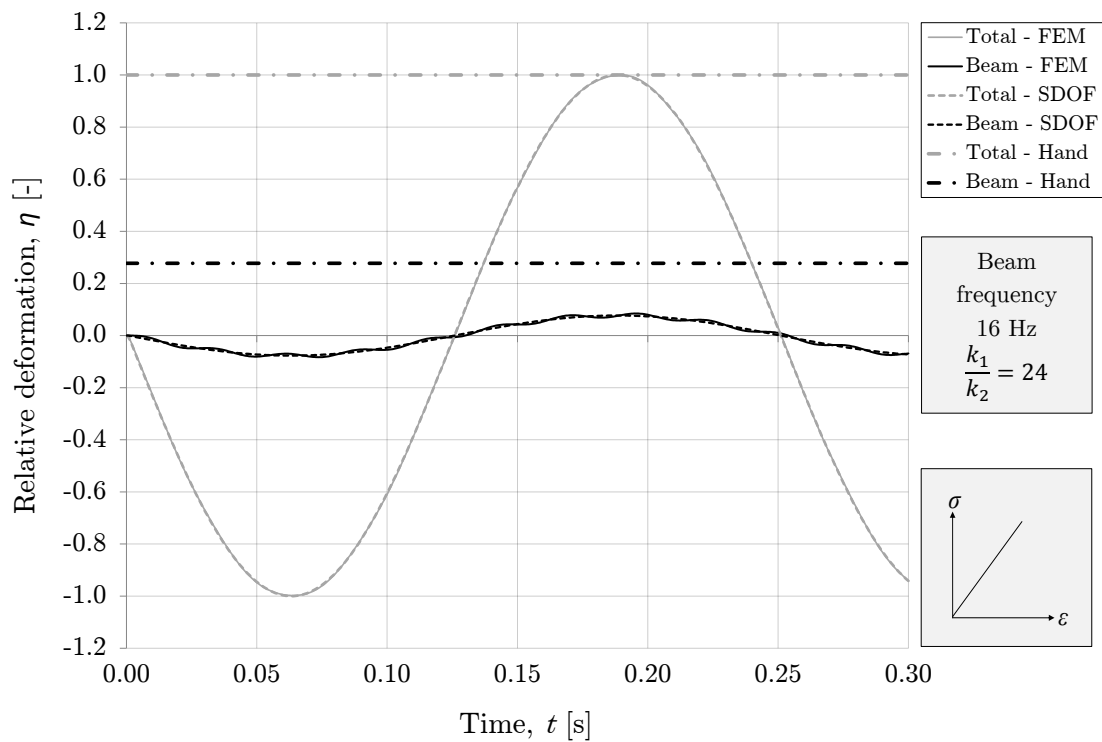


Figure B.9: Relative vertical displacement as a function of time. Beam subjected to uniformly distributed load. Stiffness ratio $k_1/k_2 = 24$.

Appendix C Octave code for solving 2DOF system

```
% Central difference method for solving
% 2DOF system with various material models
clc
close all
clear all

m1=3.21; % Mass #1
m2=2.35; % Mass #2

% Specify parameters in different directions
% k - stiffness, r - resistance, c - damping
k1=[40 20]; % [k-compression k-tension]
k2=[20 18]; % [k-compression k-tension]
r1=[3 -0.8]; % [r-compression r-tension]
r2=[3 -0.8]; % [r-compression r-tension]
c1=0.00*k1(1); % [damping]
c2=0.00*k2(1); % [damping]

h=0.001; % Time increment
T0=0; % Time for the first time step
T_end=6; % Time for the last time step
t_peak=0.001; % Time for peak load (triangular load-time)
t1=0.01; % Time when the load ends
F_peak = 400; % Peak load on 2DOF

% Time dependent force for both bodies.
% [part-on-mass-1; part-on-mass-2]
p=@(t) [1;0]*((t/t_peak)*(t<=t_peak)+...
(1-t/(t1-t_peak))*(t_peak<t & t<t1))*F_peak;

% Building the needed stiffness matrices
K1(:, :, 1)=[1 -1;-1 1]*k1(1); % positive spring load
K1(:, :, 2)=[1 -1;-1 1]*k1(2); % negative spring load
K2(:, :, 1)=[0 0;0 k2(1)]; % positive spring load
K2(:, :, 2)=[0 0;0 k2(2)]; % negative spring load

% Building the needed mass matrix
M=[m1 0;0 m2];

% Building the needed damping matrix
C=[1 -1;-1 1]*c1+[0 0;0 c2];

% Calculate the two vibration periods, using stiffness
% for positive phase and no damping
[~, lambda]=eig(K1(:, :, 1)+K2(:, :, 1), M);
p_time1=2*pi/sqrt(lambda(1));
p_time2=2*pi/sqrt(lambda(4));

% Calculate number of needed time steps and a time-vector
n_step=ceil((T_end-T0)/h)+1;
T=T0:h:(T0+n_step*h-h);

% Setting initial conditions and
% "previous" displacement (only: du=0, u=0)
u0=zeros(2, 1);
du0=zeros(2, 1);
ddu0=M\p(0);
u_m1=u0-h*du0+h^2/2*ddu0;
u=u0;

% Preallocate
u_plastic=zeros(2, 1);
U=zeros(2, n_step);
U_plastic=zeros(2, n_step);
R=zeros(2, n_step);

tic
```

```

% Elastic-Plastic
% Loop for every time step except the last
% Calculating the u for "next" time step.
for i=1:(n_step-1)
    t=T(i);

    % Elastic part for this step
    u_e = u - [1 1;0 1]*u_plastic ;
    k1_d = (1+((-[1 -1]*u_e)<0)) ;
    % 1=spring force +, 2=spring force -
    k2_d = (1+((-[0 1]*u_e)<0)) ;

    % Total displacement for next step
    K=K1(:, :, k1_d)+K2(:, :, k2_d);
    u_p1 = (M/h^2+C/2/h)\(p(t) - K*u_e + 2/h^2*M*u - ...
        (M/h^2-C/2/h)*u_m1) ;

    % Yield criteria, yielding positive direction fi_t=1,
    %yielding negative direction fi_t=2
    % #1 spring-slider
    fi_t1=1*((-[1 -1]*u_p1-u_plastic(1)) > (r1(1)/k1(k1_d)))+ ...
        2*((-[1 -1]*u_p1-u_plastic(1)) < (r1(2)/k1(k1_d)));
    % #2 spring-slider
    fi_t2=1*((u_p1(2)-u_plastic(2)) > (r2(1)/k2(k2_d)))+ ...
        2*((u_p1(2)-u_plastic(2)) < (r2(2)/k2(k2_d)));

    fi=1*(fi_t1~=0)+2*(fi_t2~=0);
    % 0=no yield 1=#1 yields 2=#2 yields 3=both yields

    if fi==1 % r1 plastic, r2 elastic
        u_plastic(1)=[1 -1]*u_p1 - r1(fi_t1)/k1(k1_d) ;
    elseif fi==2 % r1 elastic, 2 plastic
        u_plastic(2)= u_p1(2) - r2(fi_t2)/k2(k2_d) ;
    elseif fi==3 % r1 and r2 plastic
        u_plastic(1)= [1 -1]*u_p1 - r1(fi_t1)/k1(k1_d) ;
        u_plastic(2)= u_p1(2) - r2(fi_t2)/k2(k2_d) ;
    end
    % Store data and prepare for next time step
    R(:,1+i)=[k1(k1_d) -k1(k1_d);0 k2(k2_d)]*u_e;
    u_m1=u ;
    u=u_p1 ;
    U(:,i+1)=u ;
    U_plastic(:,i+1)=u_plastic ;
end
toc

U_1_2=U(1,:)-U(2,:); % Elongation of spring/slider #1
y_range_ep=[min(min(U)) max(max(U))];
y_range_sp=[min(min(R)) max(max(R))];

figure(1)
plot(T,[U;U_1_2;U_plastic]) ;hold on
% plot(p_time1*[1 1],y_range_ep,'k')
% plot(p_time2*[1 1],y_range_ep,'k')
plot([T0 T_end],[0 0],'k')
legend('u_1','u_2','u_1-u_2','u_1-u_2_plastic','u_2_plastic')
xlabel('Time_[s]')
ylabel('Displacement_[m]')
hold off

figure(2)
plot(T,R) ;hold on
plot([T0 T_end],[r1(1) r1(2);r1(1) r1(2)],':b')
plot([T0 T_end],[r2(1) r2(2);r2(1) r2(2)],':r','color',[0 .5 0])
% plot(p_time1*[1 1],y_range_sp,'k')
% plot(p_time2*[1 1],y_range_sp,'k')
plot([T0 T_end],[0 0],':k')
legend('R_{spring1}','R_{spring2}')
xlabel('Time_[s]')
ylabel('Reaction_force_[N]')

```

```

hold off

figure(3)
subplot(1,2,1)
plot(U_1_2,R(1,:)) ;hold on
plot([min(U_1_2) max(U_1_2)],[0 0], 'k')
legend('R_{spring1}_vs_(u_1-u_2)')
xlabel('Displacement_[m]')
ylabel('Reaction_force_[N]')
hold off

subplot(1,2,2)
plot(U(2,:),R(2,:)) ;hold on
plot([min(U(2,:)) max(U(2,:))],[0 0], 'k')
legend('R_{spring2}_vs_u_2')
xlabel('Displacement_[m]')
ylabel('Reaction_force_[N]')
hold off

```

Appendix D The optimization factors

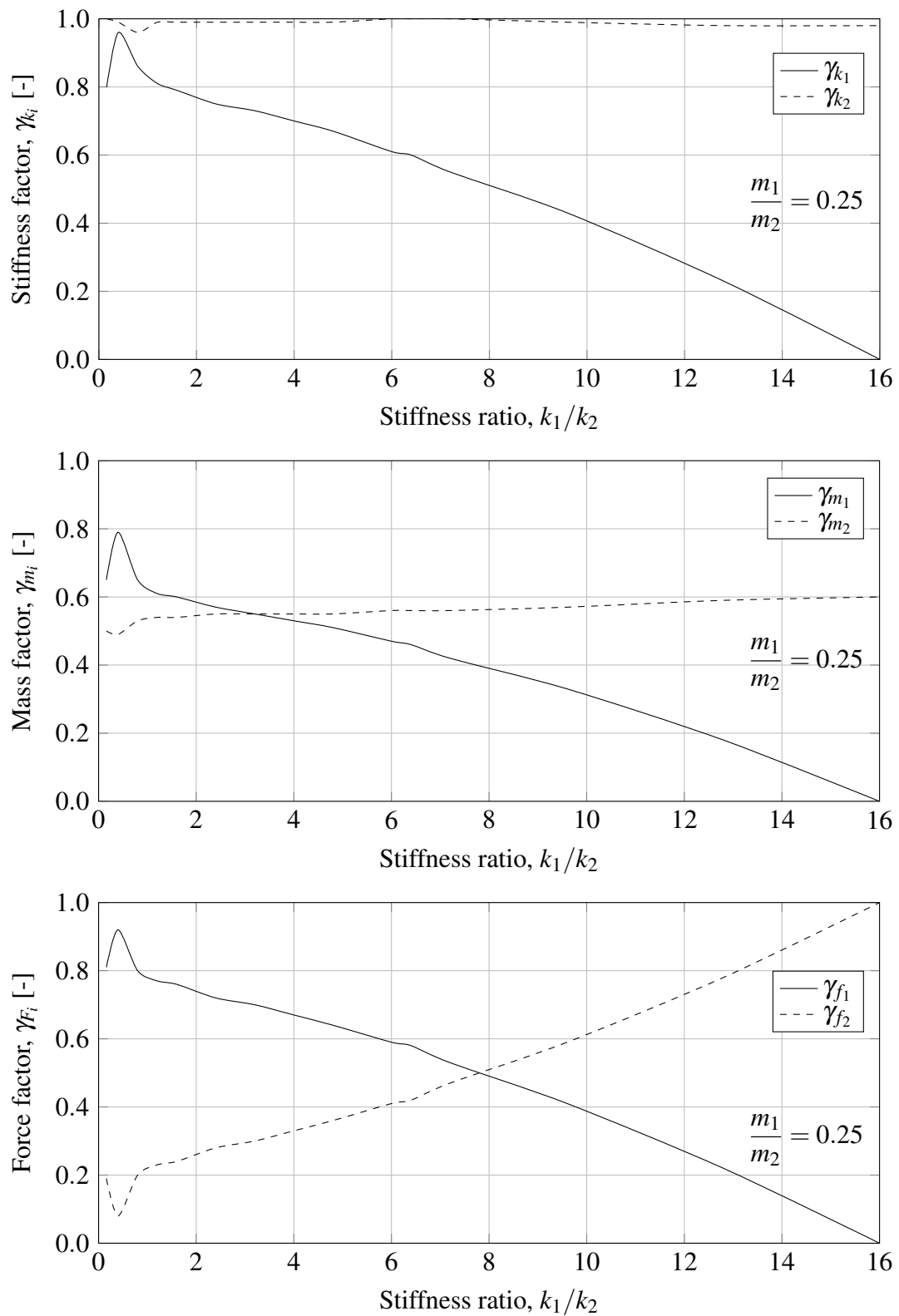


Figure D.1: Optimisation factors as a function of stiffness ratio k_1/k_2 . Valid for mass ratio of $m_1/m_2 = 0.25$

Table D.1: *Optimization factors for a mass ratio of $m_1/m_2 = 0.25$.*

k_1/k_2	γ_{k_1}	γ_{k_2}	γ_{m_1}	γ_{m_2}	γ_{F_1}	γ_{F_2}
0.50	0.9350	0.9825	0.7550	0.5000	0.8900	0.1100
1.00	0.8350	0.9750	0.6300	0.5350	0.7850	0.2150
1.50	0.7950	0.9900	0.6025	0.5400	0.7625	0.2375
2.00	0.7700	0.9900	0.5850	0.5450	0.7400	0.2600
2.50	0.7475	0.9900	0.5675	0.5500	0.7175	0.2825
3.00	0.7350	0.9900	0.5550	0.5500	0.7050	0.2950
3.50	0.7188	0.9900	0.5425	0.5500	0.6888	0.3113
4.00	0.7000	0.9900	0.5300	0.5500	0.6700	0.3300
4.50	0.6813	0.9900	0.5175	0.5500	0.6513	0.3488
5.00	0.6600	0.9917	0.5033	0.5517	0.6317	0.3683
5.50	0.6350	0.9958	0.4867	0.5558	0.6108	0.3892
6.00	0.6100	1.0000	0.4700	0.5600	0.5900	0.4100
6.50	0.5938	1.0000	0.4550	0.5600	0.5738	0.4263
7.00	0.5625	1.0000	0.4300	0.5600	0.5425	0.4575
7.50	0.5350	0.9988	0.4088	0.5613	0.5150	0.4850
8.00	0.5100	0.9967	0.3900	0.5633	0.4900	0.5100
8.50	0.4850	0.9946	0.3713	0.5654	0.4650	0.5350
9.00	0.4600	0.9925	0.3525	0.5675	0.4400	0.5600
9.50	0.4350	0.9904	0.3338	0.5696	0.4150	0.5850
10.00	0.4050	0.9888	0.3113	0.5725	0.3863	0.6138
10.50	0.3738	0.9872	0.2878	0.5756	0.3566	0.6434
11.00	0.3425	0.9856	0.2644	0.5788	0.3269	0.6731
11.50	0.3113	0.9841	0.2409	0.5819	0.2972	0.7028
12.00	0.2800	0.9825	0.2175	0.5850	0.2675	0.7325
12.50	0.2488	0.9809	0.1941	0.5881	0.2378	0.7622
13.00	0.2156	0.9800	0.1688	0.5906	0.2063	0.7938
13.50	0.1797	0.9800	0.1406	0.5922	0.1719	0.8281
14.00	0.1438	0.9800	0.1125	0.5938	0.1375	0.8625
14.50	0.1078	0.9800	0.0844	0.5953	0.1031	0.8969
15.00	0.0719	0.9800	0.0563	0.5969	0.0688	0.9313
15.50	0.0359	0.9800	0.0281	0.5984	0.0344	0.9656
16.00	0.0000	0.9800	0.0000	0.6000	0.0000	1.0000

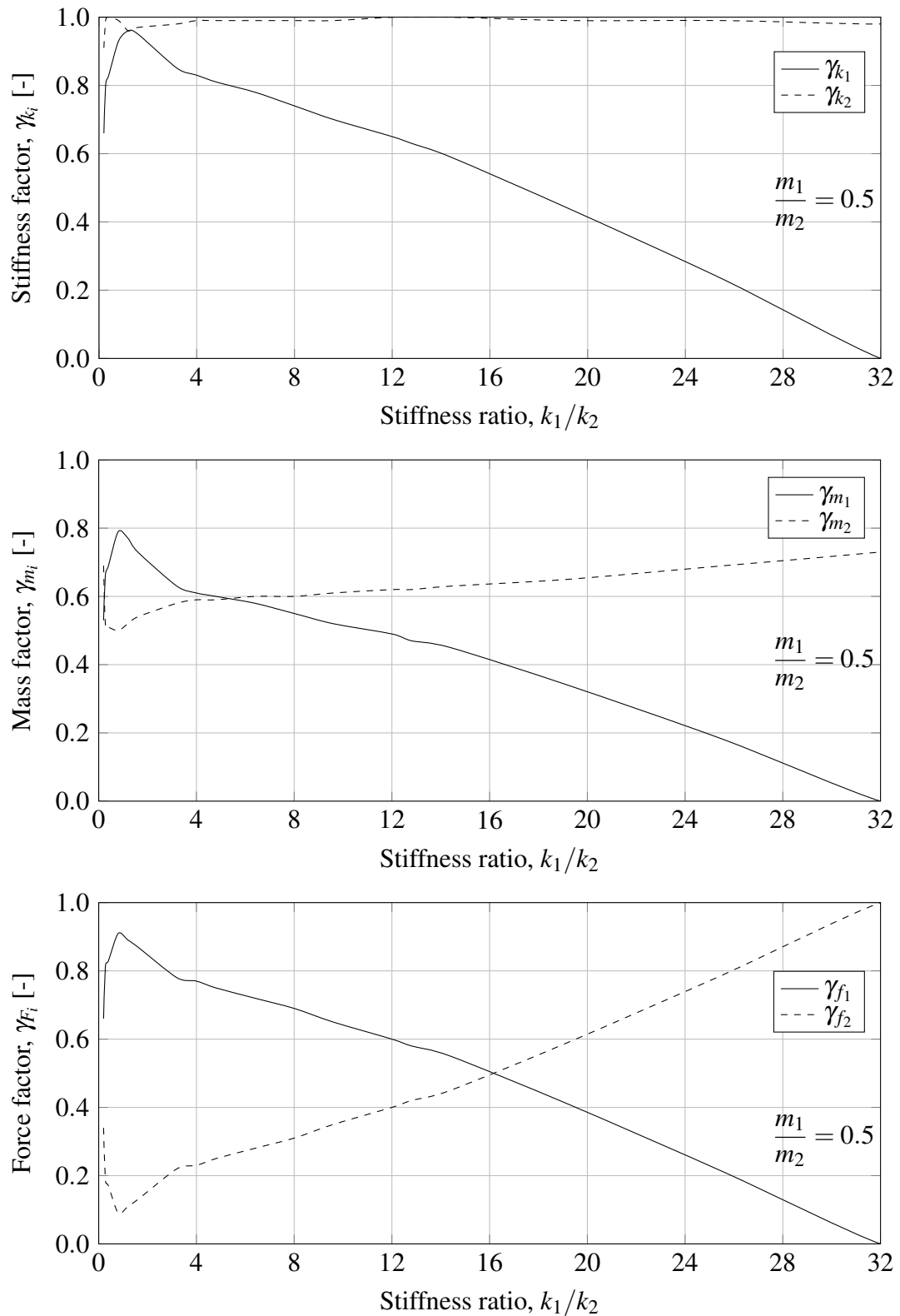


Figure D.2: Optimisation factors as a function of stiffness ratio k_1/k_2 . Valid for mass ratio of $m_1/m_2 = 0.5$

Table D.2: Optimization factors for a mass ratio of $m_1/m_2 = 0.5$.

k_1/k_2	γ_{k_1}	γ_{k_2}	γ_{m_1}	γ_{m_2}	γ_{F_1}	γ_{F_2}
0.50	0.8550	0.9975	0.7150	0.5075	0.8500	0.1500
1.00	0.9450	0.9750	0.7800	0.5100	0.9000	0.1000
1.50	0.9525	0.9675	0.7400	0.5350	0.8750	0.1250
2.00	0.9250	0.9725	0.7050	0.5500	0.8475	0.1525
2.50	0.8938	0.9756	0.6738	0.5625	0.8194	0.1806
3.00	0.8625	0.9788	0.6425	0.5750	0.7913	0.2088
3.50	0.8425	0.9838	0.6225	0.5838	0.7763	0.2238
4.00	0.8300	0.9900	0.6100	0.5900	0.7700	0.2300
4.50	0.8175	0.9900	0.6038	0.5900	0.7575	0.2425
5.00	0.8062	0.9900	0.5975	0.5913	0.7462	0.2538
5.50	0.7968	0.9900	0.5912	0.5944	0.7368	0.2632
6.00	0.7874	0.9900	0.5849	0.5975	0.7274	0.2726
6.50	0.7773	0.9900	0.5780	0.6000	0.7180	0.2820
7.00	0.7648	0.9900	0.5686	0.6000	0.7086	0.2914
7.50	0.7524	0.9900	0.5593	0.6000	0.6993	0.3007
8.00	0.7400	0.9900	0.5500	0.6000	0.6900	0.3100
8.50	0.7275	0.9900	0.5406	0.6031	0.6775	0.3225
9.00	0.7150	0.9900	0.5313	0.6063	0.6650	0.3350
9.50	0.7025	0.9900	0.5219	0.6094	0.6525	0.3475
10.00	0.6917	0.9917	0.5150	0.6117	0.6417	0.3583
10.50	0.6813	0.9938	0.5088	0.6138	0.6313	0.3688
11.00	0.6708	0.9958	0.5025	0.6158	0.6208	0.3792
11.50	0.6604	0.9979	0.4963	0.6179	0.6104	0.3896
12.00	0.6500	1.0000	0.4900	0.6200	0.6000	0.4000
12.50	0.6375	1.0000	0.4775	0.6200	0.5875	0.4125
13.00	0.6250	1.0000	0.4675	0.6213	0.5763	0.4238
13.50	0.6125	1.0000	0.4613	0.6244	0.5669	0.4331
14.00	0.6000	1.0000	0.4550	0.6275	0.5575	0.4425
14.50	0.5869	0.9998	0.4477	0.6304	0.5471	0.4529
15.00	0.5713	0.9988	0.4363	0.6325	0.5325	0.4675
15.50	0.5556	0.9977	0.4248	0.6346	0.5179	0.4821
16.00	0.5400	0.9967	0.4133	0.6367	0.5033	0.4967
16.50	0.5244	0.9956	0.4019	0.6388	0.4888	0.5113
17.00	0.5088	0.9946	0.3904	0.6408	0.4742	0.5258
17.50	0.4931	0.9935	0.3790	0.6429	0.4596	0.5404
18.00	0.4775	0.9925	0.3675	0.6450	0.4450	0.5550
18.50	0.4619	0.9915	0.3560	0.6471	0.4304	0.5696
19.00	0.4463	0.9904	0.3446	0.6492	0.4158	0.5842
19.50	0.4302	0.9900	0.3325	0.6519	0.4006	0.5994
20.00	0.4138	0.9900	0.3200	0.6550	0.3850	0.6150
20.50	0.3973	0.9900	0.3075	0.6581	0.3694	0.6306
21.00	0.3809	0.9900	0.2950	0.6613	0.3538	0.6463
21.50	0.3645	0.9900	0.2825	0.6644	0.3381	0.6619
22.00	0.3481	0.9900	0.2700	0.6675	0.3225	0.6775
22.50	0.3317	0.9900	0.2575	0.6706	0.3069	0.6931
23.00	0.3153	0.9900	0.2450	0.6738	0.2913	0.7088
23.50	0.2989	0.9900	0.2325	0.6769	0.2756	0.7244
24.00	0.2825	0.9900	0.2200	0.6800	0.2600	0.7400
24.50	0.2661	0.9900	0.2075	0.6831	0.2444	0.7556
25.00	0.2497	0.9900	0.1950	0.6863	0.2288	0.7713
25.50	0.2333	0.9900	0.1825	0.6894	0.2131	0.7869
26.00	0.2156	0.9894	0.1688	0.6925	0.1969	0.8031
26.50	0.1977	0.9886	0.1547	0.6956	0.1805	0.8195
27.00	0.1797	0.9878	0.1406	0.6988	0.1641	0.8359
27.50	0.1617	0.9870	0.1266	0.7019	0.1477	0.8523

Table D.2: Optimization factors for a mass ratio of $m_1/m_2 = 0.5$.

k_1/k_2	γ_{k_1}	γ_{k_2}	γ_{m_1}	γ_{m_2}	γ_{F_1}	γ_{F_2}
28.00	0.1438	0.9863	0.1125	0.7050	0.1313	0.8688
28.50	0.1258	0.9855	0.0984	0.7081	0.1148	0.8852
29.00	0.1078	0.9847	0.0844	0.7113	0.0984	0.9016
29.50	0.0898	0.9839	0.0703	0.7144	0.0820	0.9180
30.00	0.0719	0.9831	0.0563	0.7175	0.0656	0.9344
30.50	0.0539	0.9823	0.0422	0.7206	0.0492	0.9508
31.00	0.0359	0.9816	0.0281	0.7238	0.0328	0.9672
31.50	0.0180	0.9808	0.0141	0.7269	0.0164	0.9836
32.00	0.0000	0.9800	0.0000	0.7300	0.0000	1.0000

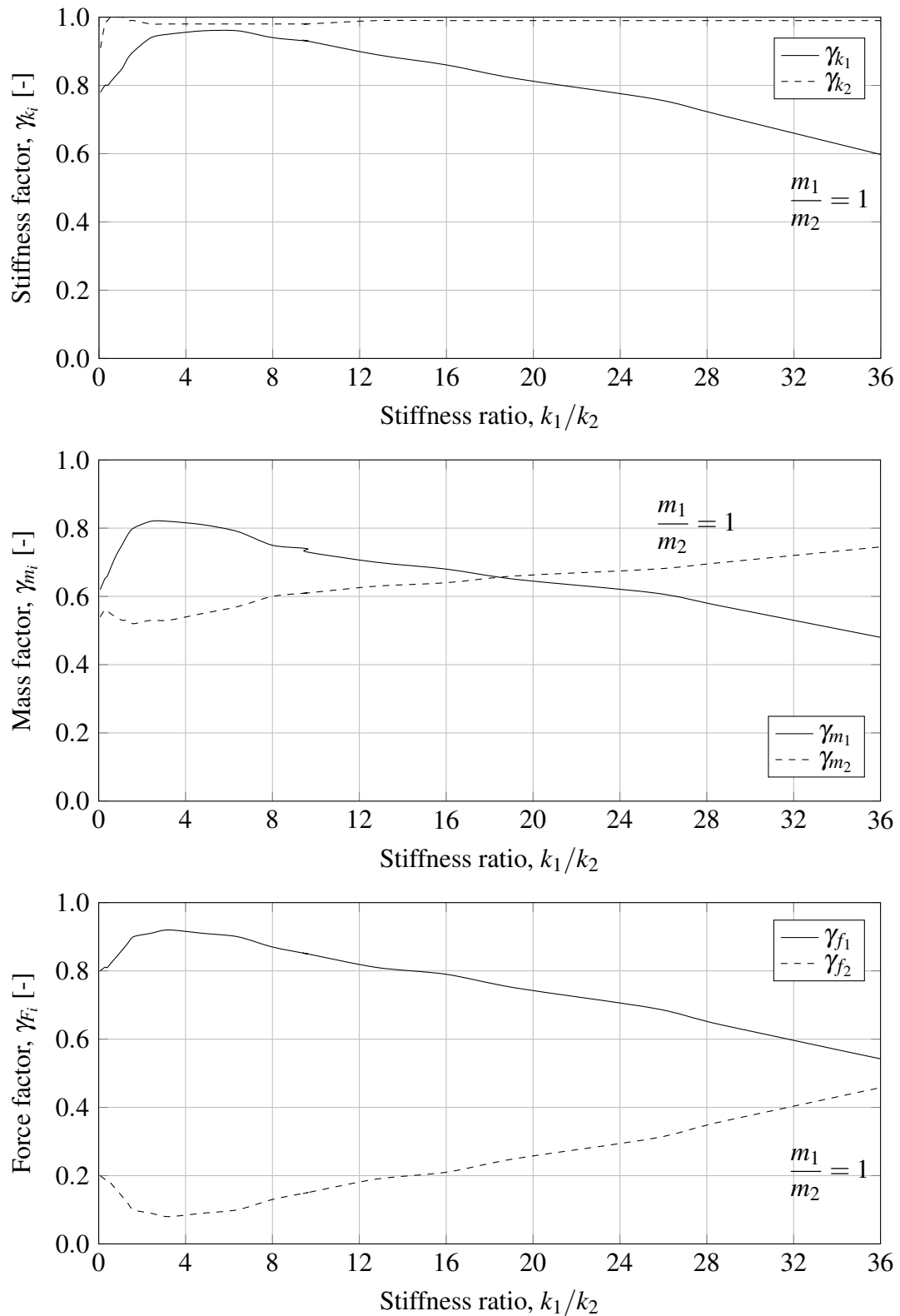


Figure D.3: Optimisation factors as a function of stiffness ratio k_1/k_2 . Valid for mass ratio of $m_1/m_2 = 1$

Table D.3: Optimization factors for a mass ratio of $m_1/m_2 = 1$.

k_1/k_2	γ_{k_1}	γ_{k_2}	γ_{m_1}	γ_{m_2}	γ_{F_1}	γ_{F_2}
0.50	0.8077	0.9977	0.6754	0.5523	0.8177	0.1823
1.00	0.8448	1.0000	0.7422	0.5326	0.8548	0.1452
1.50	0.8926	0.9900	0.7926	0.5237	0.8926	0.1074
2.00	0.9200	0.9850	0.8100	0.5250	0.9050	0.0950
2.50	0.9413	0.9800	0.8200	0.5300	0.9113	0.0888
3.00	0.9475	0.9800	0.8200	0.5300	0.9175	0.0825
3.50	0.9519	0.9800	0.8181	0.5338	0.9181	0.0819
4.00	0.9550	0.9800	0.8150	0.5400	0.9150	0.0850
4.50	0.9581	0.9800	0.8119	0.5463	0.9119	0.0881
5.00	0.9600	0.9800	0.8075	0.5525	0.9088	0.0913
5.50	0.9600	0.9800	0.8013	0.5588	0.9056	0.0944
6.00	0.9600	0.9800	0.7950	0.5650	0.9025	0.0975
6.50	0.9587	0.9800	0.7875	0.5719	0.8981	0.1019
7.00	0.9525	0.9800	0.7749	0.5813	0.8887	0.1113
7.50	0.9462	0.9800	0.7623	0.5908	0.8792	0.1208
8.00	0.9399	0.9800	0.7499	0.6001	0.8699	0.1301
8.50	0.9368	0.9800	0.7468	0.6032	0.8636	0.1364
9.00	0.9337	0.9800	0.7437	0.6063	0.8574	0.1426
9.50	0.9306	0.9800	0.7406	0.6094	0.8511	0.1489
10.00	0.9250	0.9813	0.7262	0.6125	0.8450	0.1550
10.50	0.9187	0.9828	0.7215	0.6156	0.8387	0.1613
11.00	0.9124	0.9844	0.7168	0.6188	0.8324	0.1676
11.50	0.9062	0.9860	0.7121	0.6219	0.8262	0.1738
12.00	0.8999	0.9875	0.7074	0.6250	0.8199	0.1801
12.50	0.8936	0.9891	0.7027	0.6282	0.8136	0.1864
13.00	0.8880	0.9900	0.6987	0.6307	0.8087	0.1913
13.50	0.8834	0.9900	0.6956	0.6322	0.8056	0.1944
14.00	0.8787	0.9900	0.6925	0.6338	0.8025	0.1975
14.50	0.8740	0.9900	0.6893	0.6353	0.7993	0.2007
15.00	0.8693	0.9900	0.6862	0.6369	0.7962	0.2038
15.50	0.8647	0.9900	0.6831	0.6384	0.7931	0.2069
16.00	0.8600	0.9900	0.6800	0.6400	0.7900	0.2100
16.50	0.8538	0.9900	0.6753	0.6431	0.7838	0.2163
17.00	0.8475	0.9900	0.6706	0.6463	0.7775	0.2225
17.50	0.8413	0.9900	0.6659	0.6494	0.7713	0.2288
18.00	0.8350	0.9900	0.6613	0.6525	0.7650	0.2350
18.50	0.8288	0.9900	0.6566	0.6556	0.7588	0.2413
19.00	0.8225	0.9900	0.6519	0.6588	0.7525	0.2475
19.50	0.8172	0.9900	0.6481	0.6609	0.7472	0.2528
20.00	0.8125	0.9900	0.6450	0.6625	0.7425	0.2575
20.50	0.8078	0.9900	0.6419	0.6641	0.7378	0.2622
21.00	0.8031	0.9900	0.6388	0.6656	0.7331	0.2669
21.50	0.7984	0.9900	0.6356	0.6672	0.7284	0.2716
22.00	0.7938	0.9900	0.6325	0.6688	0.7238	0.2763
22.50	0.7891	0.9900	0.6294	0.6703	0.7191	0.2809
23.00	0.7844	0.9900	0.6263	0.6719	0.7144	0.2856
23.50	0.7797	0.9900	0.6231	0.6734	0.7097	0.2903
24.00	0.7750	0.9900	0.6200	0.6750	0.7050	0.2950
24.50	0.7703	0.9900	0.6169	0.6766	0.7003	0.2997
25.00	0.7656	0.9900	0.6138	0.6781	0.6956	0.3044
25.50	0.7609	0.9900	0.6106	0.6797	0.6909	0.3091
26.00	0.7538	0.9900	0.6050	0.6825	0.6838	0.3163
26.50	0.7459	0.9900	0.5988	0.6856	0.6759	0.3241
27.00	0.7381	0.9900	0.5925	0.6888	0.6681	0.3319
27.50	0.7303	0.9900	0.5863	0.6919	0.6603	0.3397

Table D.3: *Optimization factors for a mass ratio of $m_1/m_2 = 1$.*

k_1/k_2	γ_{k_1}	γ_{k_2}	γ_{m_1}	γ_{m_2}	γ_{F_1}	γ_{F_2}
28.00	0.7225	0.9900	0.5800	0.6950	0.6525	0.3475
28.50	0.7147	0.9900	0.5738	0.6981	0.6447	0.3553
29.00	0.7069	0.9900	0.5675	0.7013	0.6373	0.3627
29.50	0.6991	0.9900	0.5613	0.7044	0.6305	0.3695
30.00	0.6913	0.9900	0.5550	0.7075	0.6238	0.3763
30.50	0.6834	0.9900	0.5488	0.7106	0.6170	0.3830
31.00	0.6756	0.9900	0.5425	0.7138	0.6102	0.3898
31.50	0.6678	0.9900	0.5363	0.7169	0.6034	0.3966
32.00	0.6600	0.9900	0.5300	0.7200	0.5967	0.4033
32.50	0.6522	0.9900	0.5238	0.7231	0.5899	0.4101
33.00	0.6444	0.9900	0.5175	0.7263	0.5831	0.4169
33.50	0.6366	0.9900	0.5113	0.7294	0.5764	0.4236
34.00	0.6288	0.9900	0.5050	0.7325	0.5696	0.4304
34.50	0.6209	0.9900	0.4988	0.7356	0.5628	0.4372
35.00	0.6131	0.9900	0.4925	0.7388	0.5560	0.4440
35.50	0.6053	0.9900	0.4863	0.7419	0.5493	0.4507
36.00	0.5975	0.9900	0.4800	0.7450	0.5425	0.4575

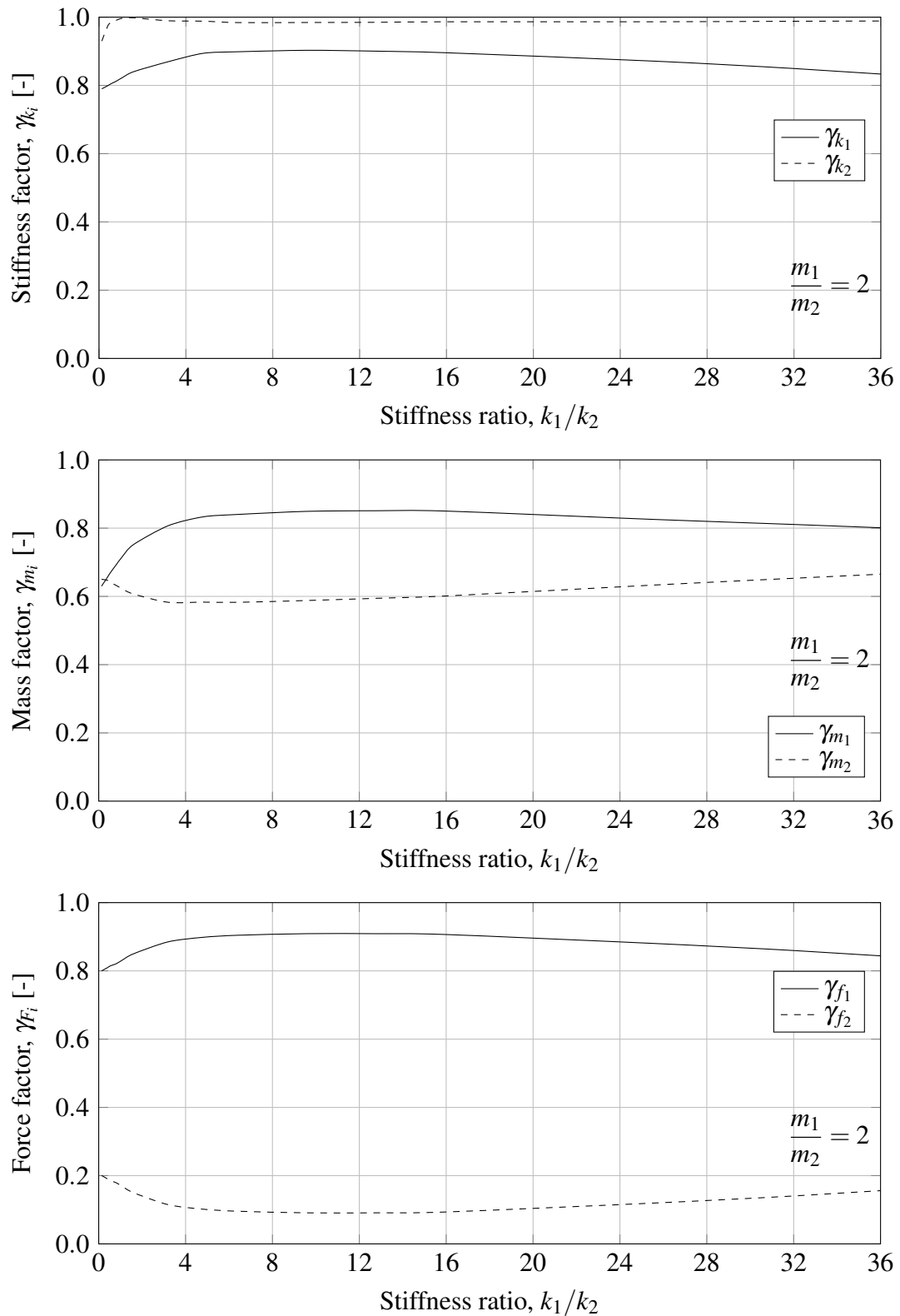


Figure D.4: Optimisation factors as a function of stiffness ratio k_1/k_2 . Valid for mass ratio of $m_1/m_2 = 2$

Table D.4: *Optimization factors for a mass ratio of $m_1/m_2 = 2$.*

k_1/k_2	γ_{k_1}	γ_{k_2}	γ_{m_1}	γ_{m_2}	γ_{F_1}	γ_{F_2}
0.50	0.8029	0.9810	0.6659	0.6427	0.8133	0.1867
1.00	0.8201	0.9953	0.7091	0.6252	0.8282	0.1718
1.50	0.8370	0.9978	0.7449	0.6099	0.8464	0.1536
2.00	0.8477	0.9958	0.7656	0.6009	0.8587	0.1413
2.50	0.8569	0.9932	0.7829	0.5933	0.8697	0.1303
3.00	0.8660	0.9905	0.8002	0.5857	0.8807	0.1193
3.50	0.8743	0.9892	0.8120	0.5828	0.8876	0.1124
4.00	0.8819	0.9888	0.8201	0.5830	0.8917	0.1083
4.50	0.8895	0.9884	0.8281	0.5831	0.8958	0.1042
5.00	0.8947	0.9877	0.8339	0.5831	0.8991	0.1009
5.50	0.8961	0.9864	0.8361	0.5829	0.9009	0.0991
6.00	0.8975	0.9851	0.8383	0.5827	0.9028	0.0972
6.50	0.8987	0.9841	0.8404	0.5828	0.9045	0.0955
7.00	0.8994	0.9842	0.8418	0.5836	0.9052	0.0948
7.50	0.9001	0.9842	0.8432	0.5845	0.9059	0.0941
8.00	0.9008	0.9843	0.8447	0.5853	0.9067	0.0933
8.50	0.9014	0.9843	0.8461	0.5861	0.9074	0.0926
9.00	0.9021	0.9843	0.8475	0.5870	0.9081	0.0919
9.50	0.9028	0.9844	0.8489	0.5878	0.9089	0.0911
10.00	0.9026	0.9845	0.8494	0.5888	0.9090	0.0910
10.50	0.9022	0.9845	0.8497	0.5898	0.9090	0.0910
11.00	0.9018	0.9846	0.8500	0.5908	0.9090	0.0910
11.50	0.9014	0.9847	0.8503	0.5918	0.9089	0.0911
12.00	0.9010	0.9848	0.8506	0.5928	0.9089	0.0911
12.50	0.9005	0.9849	0.8508	0.5938	0.9089	0.0911
13.00	0.9000	0.9850	0.8509	0.5948	0.9087	0.0913
13.50	0.8993	0.9853	0.8508	0.5959	0.9084	0.0916
14.00	0.8986	0.9855	0.8506	0.5970	0.9080	0.0920
14.50	0.8978	0.9858	0.8505	0.5980	0.9076	0.0924
15.00	0.8971	0.9860	0.8503	0.5991	0.9072	0.0928
15.50	0.8964	0.9863	0.8502	0.6002	0.9069	0.0931
16.00	0.8957	0.9865	0.8500	0.6013	0.9065	0.0935
16.50	0.8944	0.9865	0.8487	0.6029	0.9051	0.0949
17.00	0.8931	0.9865	0.8474	0.6046	0.9037	0.0963
17.50	0.8918	0.9865	0.8461	0.6063	0.9024	0.0976
18.00	0.8905	0.9865	0.8448	0.6079	0.9010	0.0990
18.50	0.8892	0.9865	0.8436	0.6096	0.8996	0.1004
19.00	0.8880	0.9865	0.8423	0.6113	0.8983	0.1017
19.50	0.8867	0.9865	0.8410	0.6130	0.8969	0.1031
20.00	0.8854	0.9865	0.8397	0.6146	0.8955	0.1045
20.50	0.8841	0.9865	0.8385	0.6163	0.8942	0.1058
21.00	0.8828	0.9865	0.8372	0.6180	0.8928	0.1072
21.50	0.8816	0.9865	0.8359	0.6197	0.8914	0.1086
22.00	0.8803	0.9865	0.8346	0.6213	0.8901	0.1099
22.50	0.8790	0.9865	0.8334	0.6230	0.8887	0.1113
23.00	0.8777	0.9865	0.8321	0.6247	0.8873	0.1127
23.50	0.8764	0.9865	0.8308	0.6264	0.8860	0.1140
24.00	0.8751	0.9865	0.8295	0.6280	0.8846	0.1154
24.50	0.8739	0.9865	0.8282	0.6297	0.8832	0.1168
25.00	0.8726	0.9865	0.8270	0.6314	0.8819	0.1181
25.50	0.8713	0.9865	0.8257	0.6331	0.8805	0.1195
26.00	0.8697	0.9866	0.8245	0.6346	0.8789	0.1211
26.50	0.8680	0.9867	0.8234	0.6362	0.8773	0.1227
27.00	0.8663	0.9868	0.8222	0.6377	0.8757	0.1243
27.50	0.8646	0.9869	0.8211	0.6392	0.8741	0.1259

Table D.4: *Optimization factors for a mass ratio of $m_1/m_2 = 2$.*

k_1/k_2	γ_{k_1}	γ_{k_2}	γ_{m_1}	γ_{m_2}	γ_{F_1}	γ_{F_2}
28.00	0.8629	0.9871	0.8200	0.6408	0.8725	0.1275
28.50	0.8613	0.9872	0.8188	0.6423	0.8709	0.1291
29.00	0.8596	0.9873	0.8177	0.6439	0.8693	0.1307
29.50	0.8579	0.9874	0.8165	0.6454	0.8677	0.1323
30.00	0.8562	0.9875	0.8154	0.6469	0.8660	0.1340
30.50	0.8545	0.9876	0.8142	0.6485	0.8644	0.1356
31.00	0.8529	0.9878	0.8131	0.6500	0.8628	0.1372
31.50	0.8512	0.9879	0.8119	0.6516	0.8612	0.1388
32.00	0.8495	0.9880	0.8108	0.6531	0.8596	0.1404
32.50	0.8474	0.9881	0.8096	0.6546	0.8576	0.1424
33.00	0.8454	0.9882	0.8084	0.6561	0.8556	0.1444
33.50	0.8433	0.9883	0.8071	0.6576	0.8536	0.1464
34.00	0.8412	0.9884	0.8059	0.6591	0.8516	0.1484
34.50	0.8391	0.9885	0.8047	0.6606	0.8496	0.1504
35.00	0.8371	0.9886	0.8035	0.6621	0.8476	0.1524
35.50	0.8350	0.9887	0.8023	0.6635	0.8457	0.1543
36.00	0.8329	0.9888	0.8011	0.6650	0.8437	0.1563

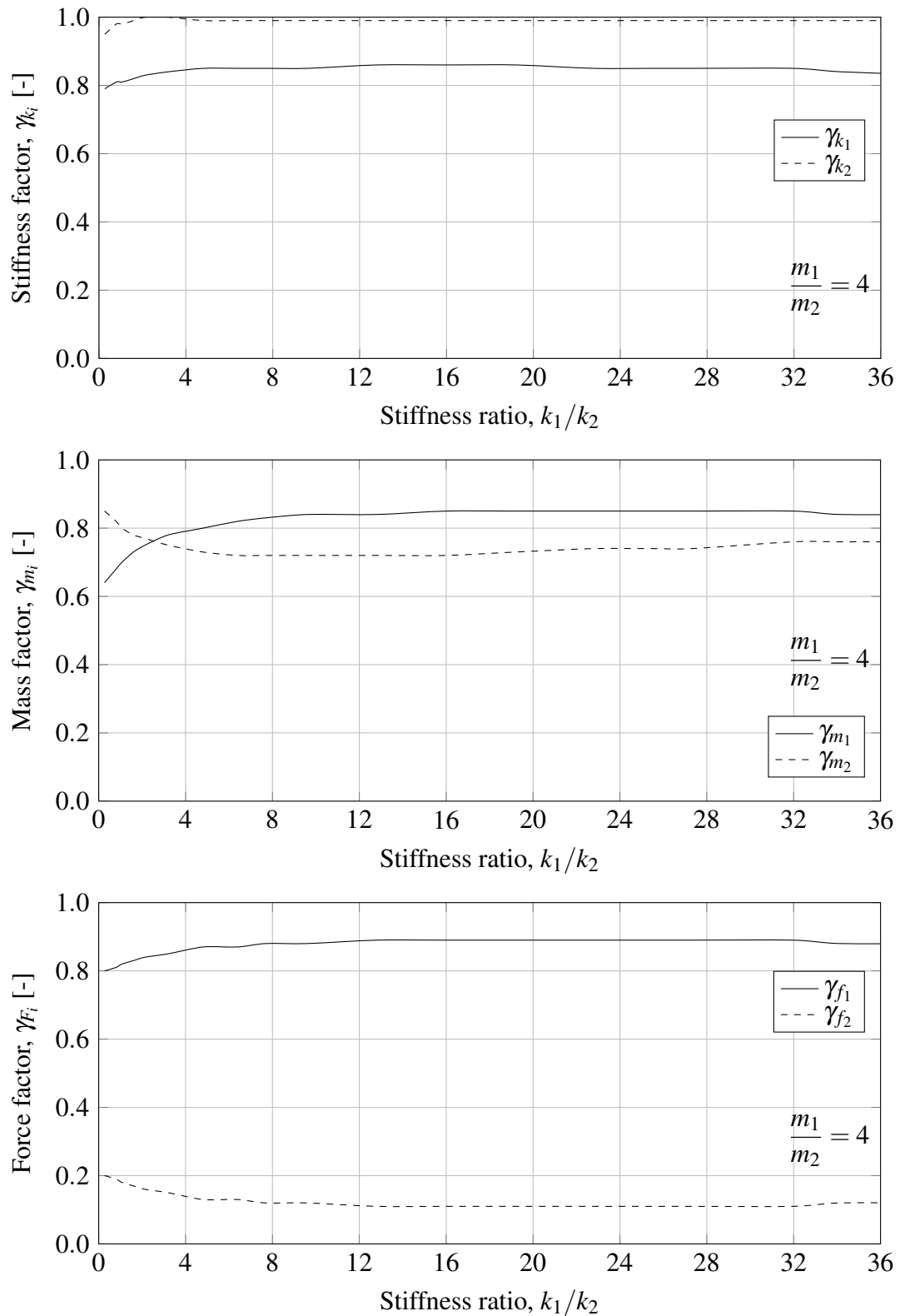


Figure D.5: Optimisation factors as a function of stiffness ratio k_1/k_2 . Valid for mass ratio of $m_1/m_2 = 4$

Table D.5: Optimization factors for a mass ratio of $m_1/m_2 = 4$.

k_1/k_2	γ_{k_1}	γ_{k_2}	γ_{m_1}	γ_{m_2}	γ_{F_1}	γ_{F_2}
0.50	0.7987	0.9630	0.6574	0.8370	0.8043	0.1957
1.00	0.8100	0.9800	0.6948	0.8052	0.8174	0.1826
1.50	0.8181	0.9881	0.7243	0.7838	0.8281	0.1719
2.00	0.8275	0.9975	0.7451	0.7725	0.8375	0.1625
2.50	0.8335	1.0000	0.7604	0.7631	0.8435	0.1565
3.00	0.8381	1.0000	0.7744	0.7537	0.8481	0.1519
3.50	0.8419	0.9981	0.7838	0.7463	0.8538	0.1463
4.00	0.8450	0.9950	0.7900	0.7400	0.8600	0.1400
4.50	0.8481	0.9919	0.7963	0.7338	0.8663	0.1338
5.00	0.8500	0.9900	0.8025	0.7288	0.8700	0.1300
5.50	0.8500	0.9900	0.8088	0.7256	0.8700	0.1300
6.00	0.8500	0.9900	0.8150	0.7225	0.8700	0.1300
6.50	0.8500	0.9900	0.8208	0.7200	0.8708	0.1292
7.00	0.8500	0.9900	0.8247	0.7200	0.8747	0.1253
7.50	0.8500	0.9900	0.8286	0.7200	0.8786	0.1214
8.00	0.8500	0.9900	0.8317	0.7200	0.8800	0.1200
8.50	0.8500	0.9900	0.8343	0.7200	0.8800	0.1200
9.00	0.8500	0.9900	0.8369	0.7200	0.8800	0.1200
9.50	0.8500	0.9900	0.8395	0.7200	0.8800	0.1200
10.00	0.8513	0.9900	0.8400	0.7200	0.8813	0.1187
10.50	0.8528	0.9900	0.8400	0.7200	0.8828	0.1172
11.00	0.8544	0.9900	0.8400	0.7200	0.8844	0.1156
11.50	0.8560	0.9900	0.8400	0.7200	0.8860	0.1140
12.00	0.8575	0.9900	0.8400	0.7200	0.8875	0.1125
12.50	0.8591	0.9900	0.8400	0.7200	0.8891	0.1109
13.00	0.8600	0.9900	0.8407	0.7200	0.8900	0.1100
13.50	0.8600	0.9900	0.8422	0.7200	0.8900	0.1100
14.00	0.8600	0.9900	0.8438	0.7200	0.8900	0.1100
14.50	0.8600	0.9900	0.8453	0.7200	0.8900	0.1100
15.00	0.8600	0.9900	0.8469	0.7200	0.8900	0.1100
15.50	0.8600	0.9900	0.8484	0.7200	0.8900	0.1100
16.00	0.8600	0.9900	0.8500	0.7200	0.8900	0.1100
16.50	0.8600	0.9900	0.8500	0.7216	0.8900	0.1100
17.00	0.8600	0.9900	0.8500	0.7231	0.8900	0.1100
17.50	0.8600	0.9900	0.8500	0.7247	0.8900	0.1100
18.00	0.8600	0.9900	0.8500	0.7263	0.8900	0.1100
18.50	0.8600	0.9900	0.8500	0.7278	0.8900	0.1100
19.00	0.8600	0.9900	0.8500	0.7294	0.8900	0.1100
19.50	0.8592	0.9900	0.8500	0.7308	0.8900	0.1100
20.00	0.8578	0.9900	0.8500	0.7322	0.8900	0.1100
20.50	0.8563	0.9900	0.8500	0.7337	0.8900	0.1100
21.00	0.8549	0.9900	0.8500	0.7351	0.8900	0.1100
21.50	0.8535	0.9900	0.8500	0.7365	0.8900	0.1100
22.00	0.8521	0.9900	0.8500	0.7379	0.8900	0.1100
22.50	0.8507	0.9900	0.8500	0.7393	0.8900	0.1100
23.00	0.8500	0.9900	0.8500	0.7400	0.8900	0.1100
23.50	0.8500	0.9900	0.8500	0.7400	0.8900	0.1100
24.00	0.8500	0.9900	0.8500	0.7400	0.8900	0.1100
24.50	0.8500	0.9900	0.8500	0.7400	0.8900	0.1100
25.00	0.8500	0.9900	0.8500	0.7400	0.8900	0.1100
25.50	0.8500	0.9900	0.8500	0.7400	0.8900	0.1100
26.00	0.8500	0.9900	0.8500	0.7400	0.8900	0.1100
26.50	0.8500	0.9900	0.8500	0.7400	0.8900	0.1100
27.00	0.8500	0.9900	0.8500	0.7400	0.8900	0.1100
27.50	0.8500	0.9900	0.8500	0.7408	0.8900	0.1100

Table D.5: *Optimization factors for a mass ratio of $m_1/m_2 = 4$.*

k_1/k_2	γ_{k_1}	γ_{k_2}	γ_{m_1}	γ_{m_2}	γ_{F_1}	γ_{F_2}
28.00	0.8500	0.9900	0.8500	0.7430	0.8900	0.1100
28.50	0.8500	0.9900	0.8500	0.7451	0.8900	0.1100
29.00	0.8500	0.9900	0.8500	0.7473	0.8900	0.1100
29.50	0.8500	0.9900	0.8500	0.7494	0.8900	0.1100
30.00	0.8500	0.9900	0.8500	0.7515	0.8900	0.1100
30.50	0.8500	0.9900	0.8500	0.7537	0.8900	0.1100
31.00	0.8500	0.9900	0.8500	0.7558	0.8900	0.1100
31.50	0.8500	0.9900	0.8500	0.7580	0.8900	0.1100
32.00	0.8499	0.9900	0.8499	0.7600	0.8899	0.1101
32.50	0.8475	0.9900	0.8475	0.7600	0.8875	0.1125
33.00	0.8452	0.9900	0.8452	0.7600	0.8852	0.1148
33.50	0.8429	0.9900	0.8429	0.7600	0.8829	0.1171
34.00	0.8406	0.9900	0.8406	0.7600	0.8806	0.1194
34.50	0.8391	0.9900	0.8400	0.7600	0.8800	0.1200
35.00	0.8380	0.9900	0.8400	0.7600	0.8800	0.1200
35.50	0.8368	0.9900	0.8400	0.7600	0.8800	0.1200
36.00	0.8356	0.9900	0.8400	0.7600	0.8800	0.1200

Appendix E Results - response of a structural system

E.1 Spectrum of analysis

Out of the parametric beams described in Section 4.2.1, a total of 97 structures were constructed and analysed in ADINA. Within this range, a variety of stiffness and mass ratios was obtained. The spectrum of the analysed structures can be seen in Figure E.1. Some representative cases are also marked with circles in the figure, for further analysis and showing the results.

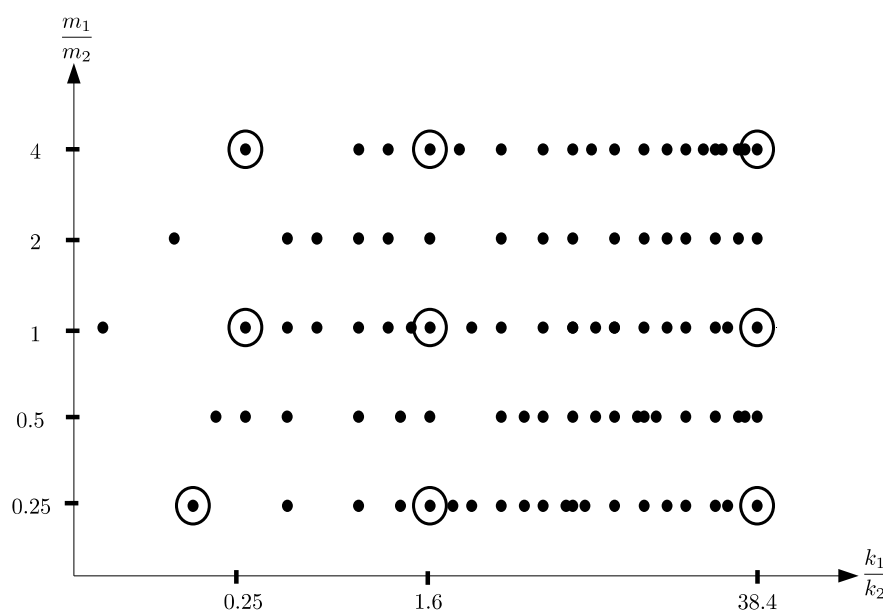


Figure E.1: *Spectrum of the analysis. Circles indicate representative cases.*

E.2 Eigenmodes

For the selected cases, the first two eigenmodes are shown in Figure E.2 and Figure E.3. The first frequency calibration of the 2DOF model was made so that the eigenfrequencies of the model correspond to those eigenmodes. Although as stated in Section 4.4.2, the general shape of all the modes is similar, there exist some discrepancies between them, visible at closer look.

For the first eigenmode, the higher the stiffness ratio, the more resemblance between the lower beam deformation and a half sine wave is present. At the same time, the upper beam remains more straight with increasing stiffness ratio. For the low stiffness ratio, a reverse case can be observed. The lower beams remain almost straight, and the upper beams' deflection shape resembles a half sine wave.

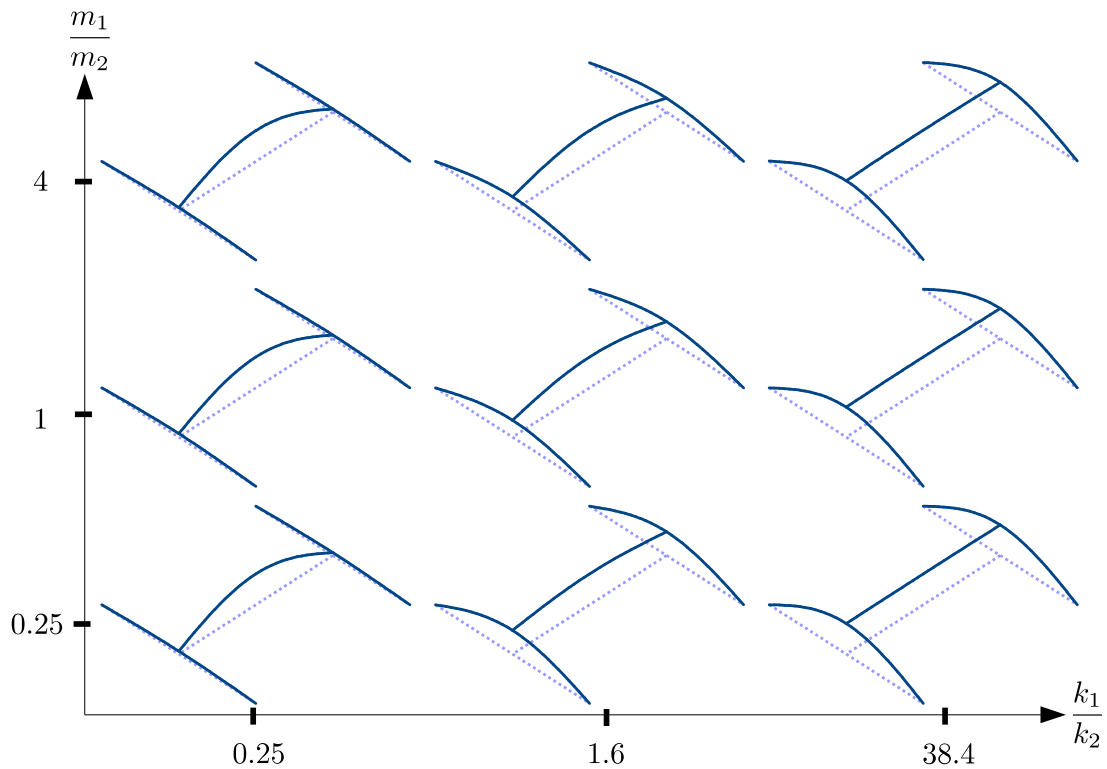


Figure E.2: *Eigenmode 1 for several structures throughout the analysed spectrum.*

For the second eigenmode, the behaviour is more complex. Although all the eigenmode shapes are similar at the first look, some inconsistencies can also be found. For low stiffness ratios, the deflection shape of both parts of the structure resembles a half sine wave. However, the higher the mass ratio, the steeper and straight close to supports the deflection shape of the upper beam is. For intermediate stiffness ratios, the deformation shape for both parts of the structure resembles a half sine wave. For high stiffness ratio some differences are present. Even though the deflection shape of the upper beam can still be described with a half sine wave, the lower beams show a different behaviour. It cannot be described with a half sine wave any more, but rather with a superposition of a half sine wave and one-and-a-half sine wave. One-and-a-half sine wave represents a higher eigenmode of a simply supported beam. This tendency becomes clearer with decreasing mass ratio. A structure with a high stiffness ratio and a low mass ratio has a high angular frequency ratio, which was already shown and discussed in Section 6.2. An equivalent 2DOF model might not give good results when analysing structures with such parameters.

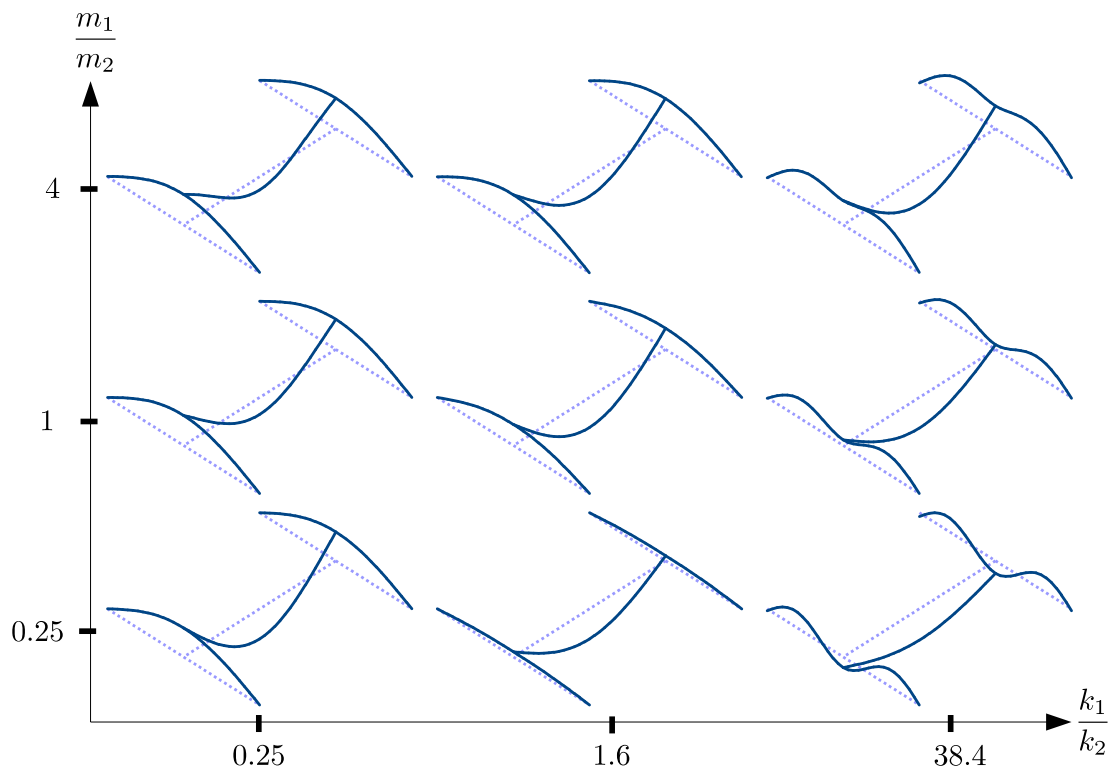


Figure E.3: *Eigenmode 2 for several structures throughout the analysed spectrum.*

E.3 Response of the upper and lower beam

To better understand the behaviour of the beam-on-beams structural system with various stiffness and mass ratios, several results of the analyses made in ADINA are shown in Figure E.4 - Figure E.12. The representative cases correspond to those for which the eigenmodes were shown in Figure E.2 and Figure E.3. For clarity, only the response obtained from ADINA is shown. The equivalent 2DOF model response was not shown here, since the model was calibrated to those results and will agree with them well.

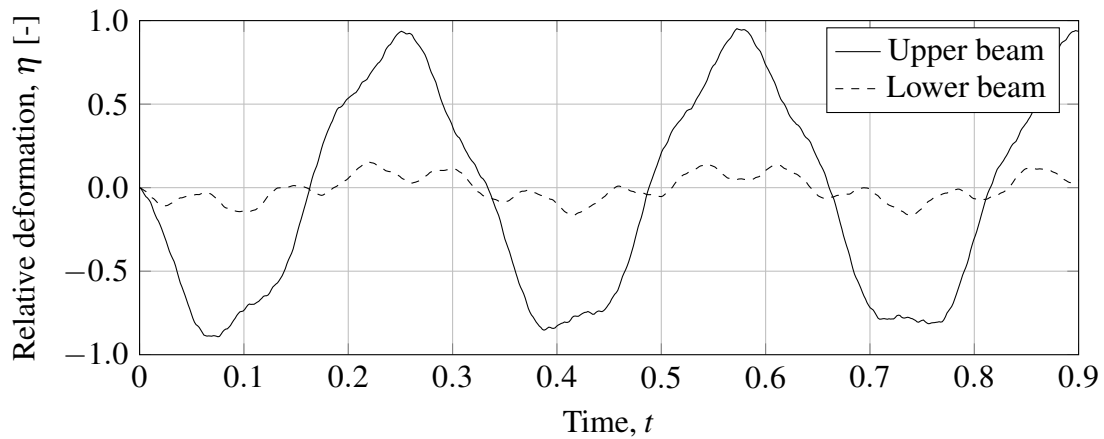


Figure E.4: Response of the structural system consisting of beam no. 5 supported on beams no. 2. Stiffness ratio, $k_1/k_2 = 0.27$, mass ratio, $m_1/m_2 = 4$.

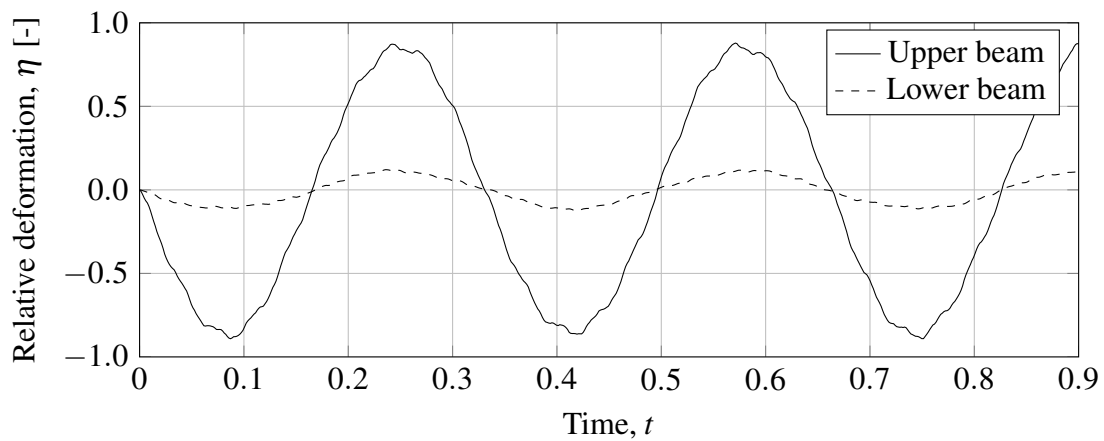


Figure E.5: Response of the structural system consisting of beam no. 5 supported on beams no. 1. Stiffness ratio, $k_1/k_2 = 0.27$, mass ratio, $m_1/m_2 = 1$.

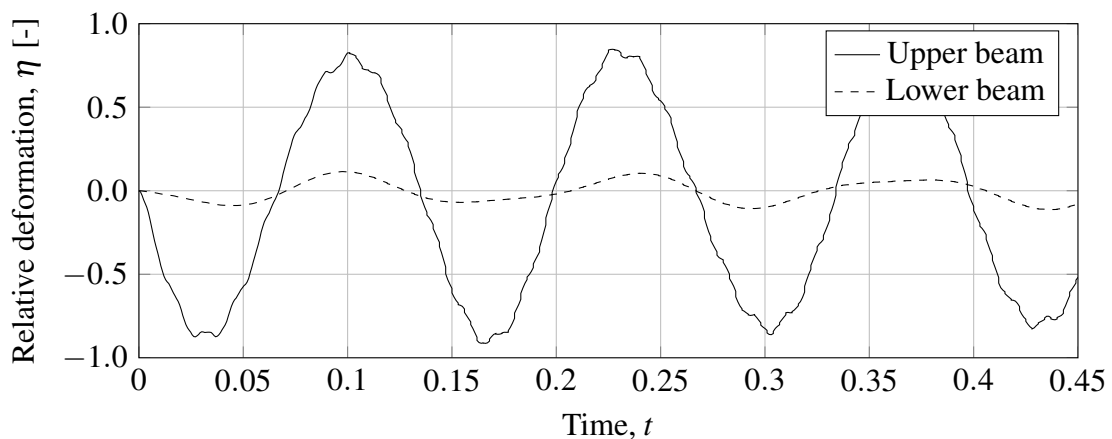


Figure E.6: Response of the structural system consisting of beam no. 1 supported on beams no. 6. Stiffness ratio, $k_1/k_2 = 0.16$, mass ratio, $m_1/m_2 = 0.25$.

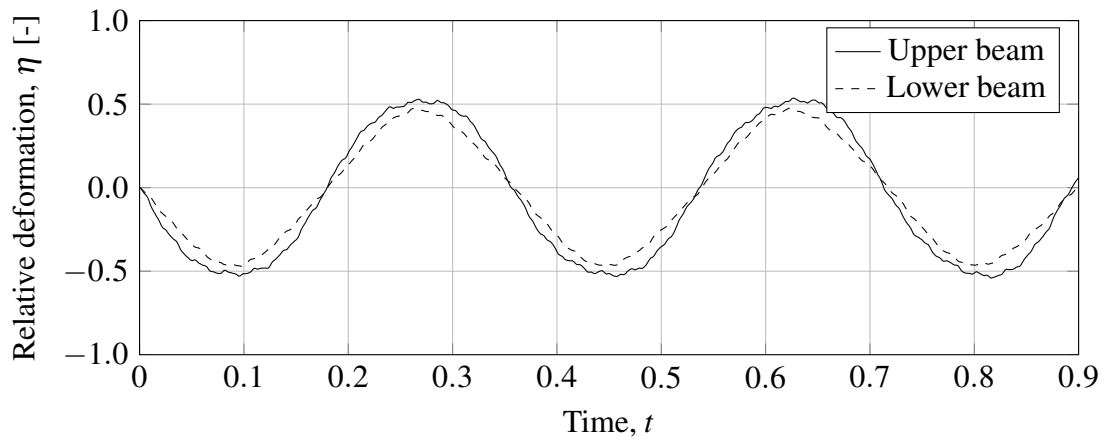


Figure E.7: Response of the structural system consisting of beam no. 3 supported on beams no. 1. Stiffness ratio, $k_1/k_2 = 1.6$, mass ratio, $m_1/m_2 = 4$.

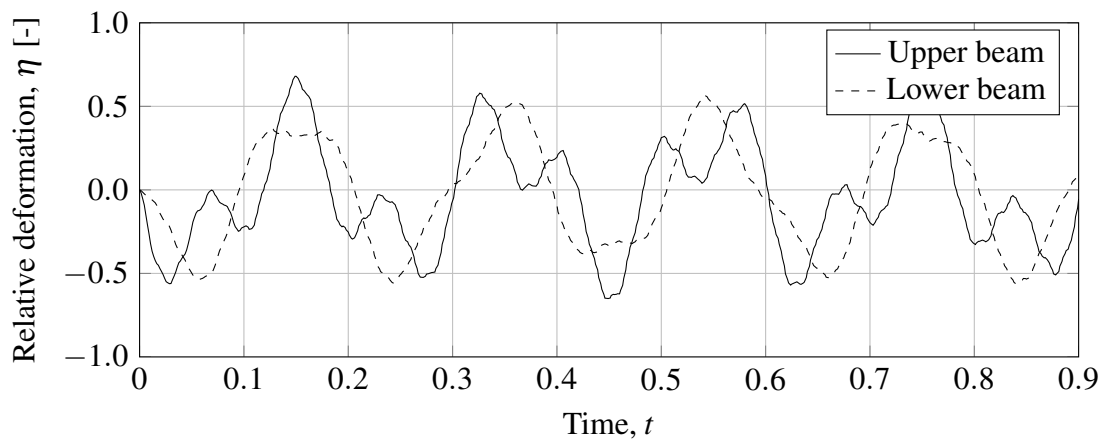


Figure E.8: Response of the structural system consisting of beam no. 1 supported on beams no. 1. Stiffness ratio, $k_1/k_2 = 1.6$, mass ratio, $m_1/m_2 = 1$.

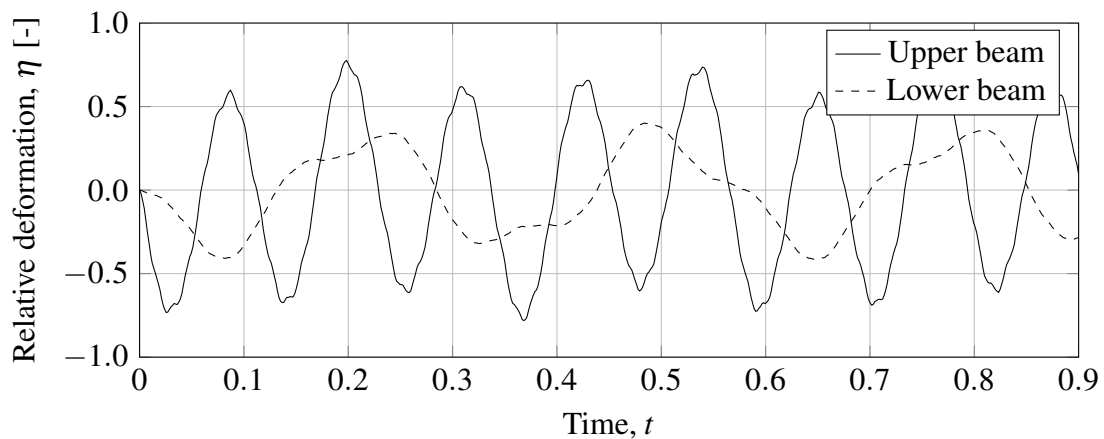


Figure E.9: Response of the structural system consisting of beam no. 1 supported on beams no. 3. Stiffness ratio, $k_1/k_2 = 1.6$, mass ratio, $m_1/m_2 = 0.25$.

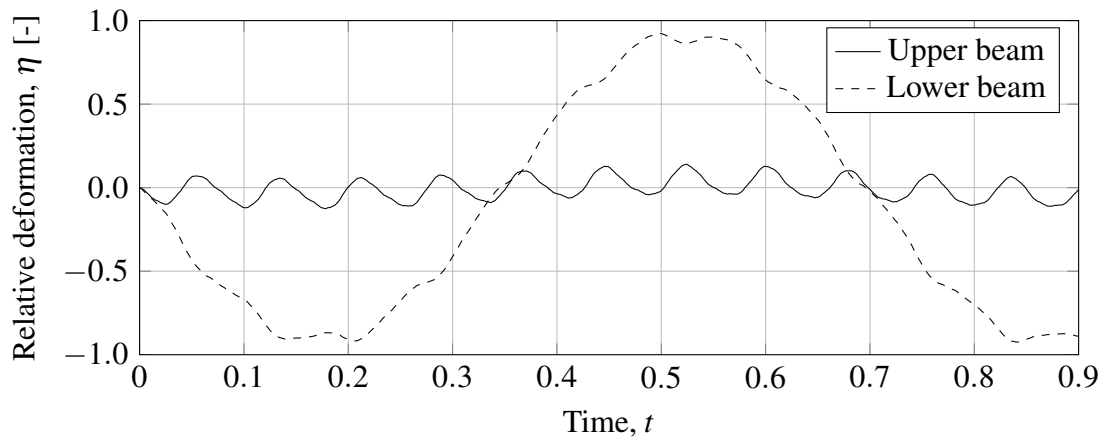


Figure E.10: *Response of the structural system consisting of beam no. 1 supported on beams no. 5. Stiffness ratio, $k_1/k_2 = 38.4$, mass ratio, $m_1/m_2 = 4$.*

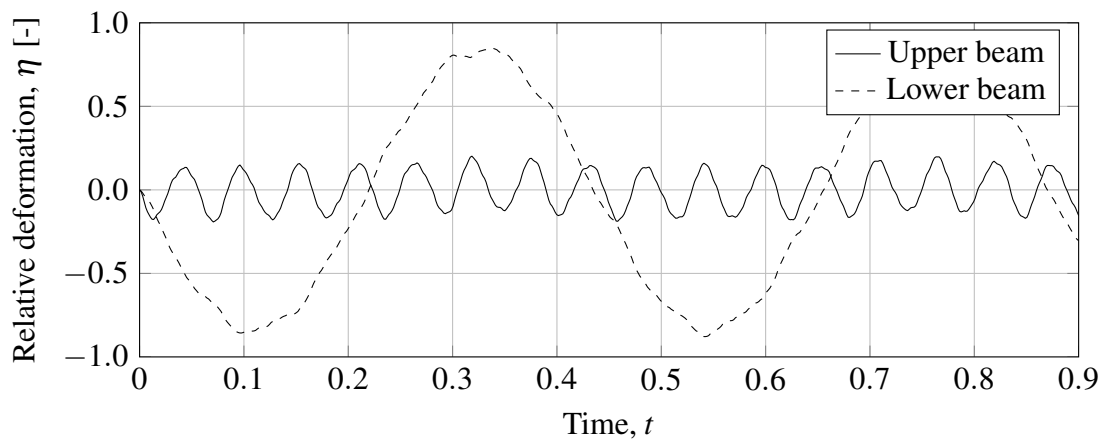


Figure E.11: *Response of the structural system consisting of beam no. 2 supported on beams no. 5. Stiffness ratio, $k_1/k_2 = 38.4$, mass ratio, $m_1/m_2 = 1$.*

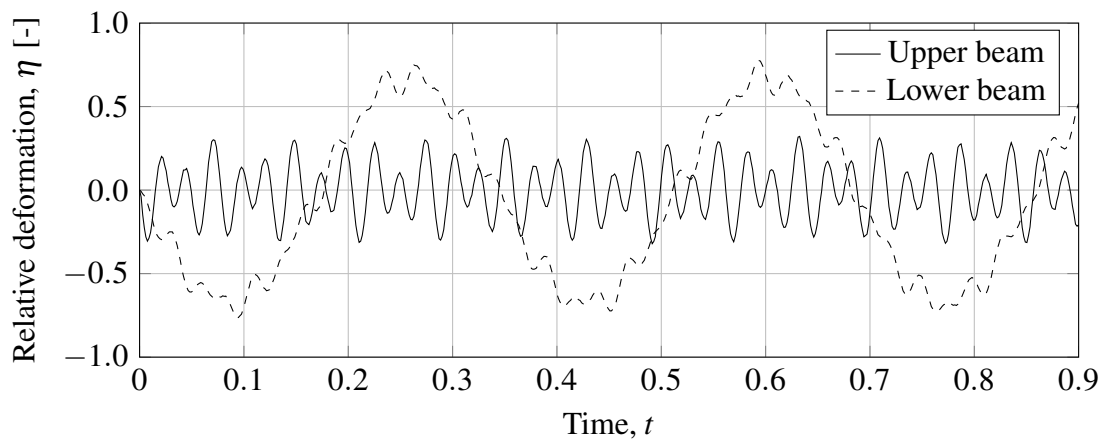


Figure E.12: *Response of the structural system consisting of beam no. 13 supported on beams no. 5. Stiffness ratio, $k_1/k_2 = 38.4$, mass ratio, $m_1/m_2 = 0.25$.*

Appendix F Optimisation of the upper beam's model

F.1 Optimisation of the upper beam's model

F.1.1 General notes

The two SDOF systems presented in Section 5.3 and Section 5.3.2 are able to approximately describe the behaviour of the upper beam within a limited range - up until the stiffness ratio $k_1/k_2 = 1$, which may symbolise the domination of the upper beam in the total motion of the structural system. After that, the structure enters the range of intermediate stiffness, and the properties of both members have notable influence on the behaviour of the structure. Nevertheless, it is desired to further develop a model for the upper beam, which can describe its response in a wider range, i.e. $k_1/k_2 > 1$. Therefore an optimisation process of the beam-on-springs was carried out in this section in order to create a model which can describe the behaviour of the upper beam in structures with the stiffness ratio up to 2.5 - 3.

F.1.2 Adjusted mass and stiffness

Although the response of a SDOF model equivalent to the beam on springs includes the movements of the spring supports (hence the beam deformation must be computed subsequently), the optimised model considers the SDOF system to pertain to the beam only. Therefore it is adjusted in such a way, that the maximum deformation of the mass-spring system corresponds directly to the beam's deformation. This is done to simplify and expedite hand calculations.

The numerical data from the case studies carried out in ADINA in Chapter 4 contains the maximum upper beam's deformation, $u_{U,max,ADINA}$, and the eigenfrequencies of the structural system, $\omega_{i,ADINA}$. An additional facilitation of an optimised system would be to give a correct lowest eigenfrequency of the system, since they usually differ from the eigenfrequencies of separate elements.

In order to obtain those results analytically, the adjusted mass, m_a , and the adjusted stiffness, k_a are defined. The known displacement and eigenfrequency can be expressed as:

$$u_{U,max,ADINA} = \frac{I_k}{m_a \omega_{1,ADINA}} \quad (F.1)$$

$$\omega_{1,ADINA} = \sqrt{\frac{k_a}{m_a}} \quad (F.2)$$

From Equation (F.1), the adjusted mass can be calculated.

$$m_a = \frac{I_k}{u_{U,max,ADINA} \omega_{1,ADINA}} \quad (F.3)$$

And after that, the adjusted stiffness can be computed from Equation (F.2).

$$k_a = m_a \omega_{1,ADINA}^2 \quad (F.4)$$

Parameters defining the properties of the system are defined as:

$$k_e = \frac{2k_1k_2}{2k_2 + k_1} \quad (\text{F.5})$$

$$m_e = m_1 + 2m_2 \quad (\text{F.6})$$

Finally, the properties can be linked with the adjusted mass and stiffness with optimisation factors γ .

$$\gamma_m = \frac{m_a}{m_e} \quad (\text{F.7})$$

$$\gamma_k = \frac{k_a}{k_e} \quad (\text{F.8})$$

Those factors were computed for all different mass ratios and the stiffness ratios up to 2.5. The results can be seen in Figure F.1 and Figure F.2.

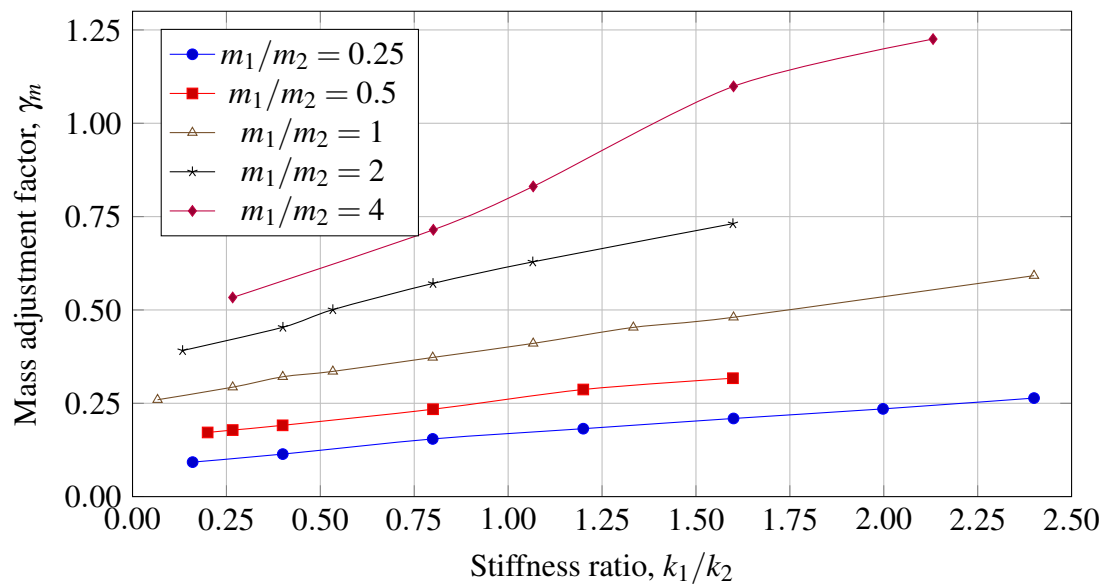


Figure F.1: Mass adjustment factor, γ_m as a function of the stiffness ratio, k_1/k_2 for various mass ratios.

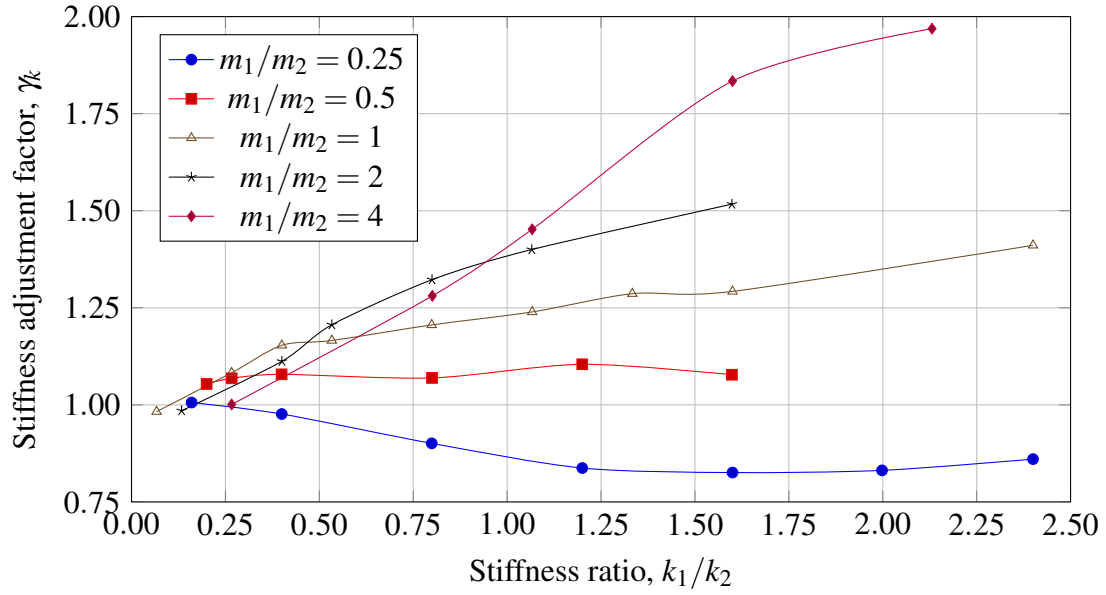


Figure F.2: Stiffness adjustment factor, γ_k as a function of the stiffness ratio, k_1/k_2 for various mass ratios.

F.1.3 Empirical model fitting

By looking at the graphs in Figure F.1 and Figure F.2, it can be seen that the curves resemble straight lines, and an empirical model describing all of them could be developed. If the results were extrapolated, it could be found that the line representing γ_m intersect with the x axis in the vicinity of the point $(-1,0)$. On the other hand, extrapolation of the lines representing γ_k shows that they intersect with the y axis at approximately $(1,0)$. Those points were assumed to be the origins of the lines, and the unknown slope of the line is believed to be dependent on the mass ratio, i.e $\alpha_i(m_1/m_2)$. Hence the tentative equations can be expressed in the slope-intercept form:

$$\gamma_m \left(\frac{k_1}{k_2}, \frac{m_1}{m_2} \right) = \alpha_1 \left(\frac{m_1}{m_2} \right) \cdot \left(\frac{k_1}{k_2} + \beta_1 \right) \quad (\text{F.9})$$

$$\gamma_k \left(\frac{k_1}{k_2}, \frac{m_1}{m_2} \right) = \alpha_2 \left(\frac{m_1}{m_2} \right) \cdot \frac{k_1}{k_2} + \beta_2 \quad (\text{F.10})$$

The slopes, α_i , were computed using the least squares fitting method. After that, various trend lines were tested, and the results can be seen in Figure F.3. For the slopes describing curves related to γ_k , a logarithmic relation was deemed to reflect the results in the best way. Similarly, for the slopes describing the curves belonging to γ_m , a polynomial trend line was chosen.

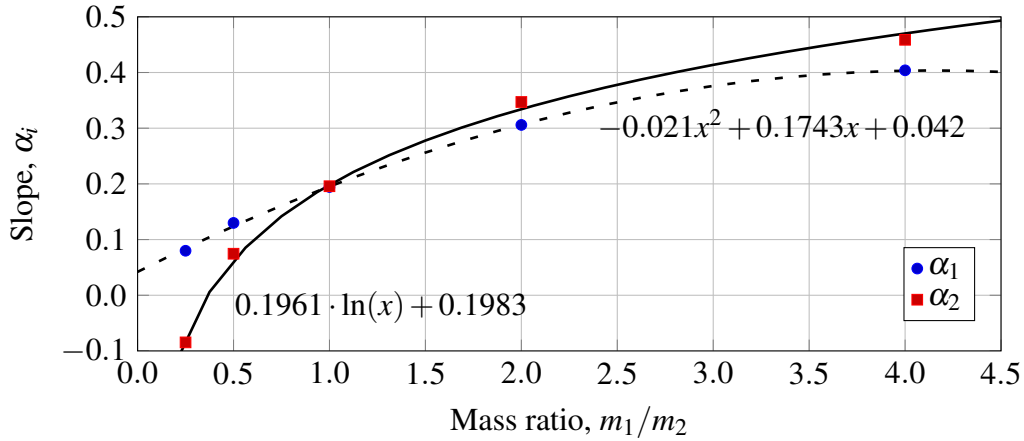


Figure F.3: Slopes of the curves, α_i as a function of the mass ratio, m_1/m_2 .

The credibility of the actual expressions for the trend lines is not very high, as there are just a few points present. Nevertheless, the logarithmic and polynomial form of the expression can be used in further optimisation of the model. Hence, the expressions for the adjustment factors, γ_m and γ_k can be expressed with the unknown parameters b_1 to b_4 and a_1 to a_4 as:

$$\gamma_m = \left(b_1 + b_2 \cdot \frac{m_1}{m_2} + b_3 \cdot \left(\frac{m_1}{m_2} \right)^2 \right) \left(\frac{k_1}{k_2} + b_4 \right) \quad (\text{F.11})$$

$$\gamma_k = \left(a_1 + a_2 \cdot \ln \left(\frac{m_1}{m_2} \right) \right) \cdot \frac{k_1}{k_2} + a_3 \quad (\text{F.12})$$

The resultant angular frequency and maximum deformation of the beam can be solved with the following equations:

$$\omega_{SDOF} = \sqrt{\frac{\gamma_k k_e}{\gamma_m m_e}} \quad (\text{F.13})$$

$$u_{U,max,SDOF} = \frac{I_k}{\gamma_m m_e \omega_{SDOF}} \quad (\text{F.14})$$

For optimisation, the Nelder-Mead simplex algorithm was used. For more information about the method, the reader is referred to Lagarias et al. (1998). The procedure is the same as was presented in Section 4.5.1 and Section 4.5.2. The obtained trend line coefficients were used as guess values. The most important factors in the objective function was the maximum displacement. Moreover, results on the unsafe side are not desired, so again corrective measures were implemented. Furthermore, the objective function takes the resultant frequency into account as well, but it is not as important as the maximum displacement. The function can be expressed as:

$$L = \sum 4 \left(\frac{u_{U,max,SDOF}}{u_{U,max,ADINA}} - 1 \right)^2 + 8 \left\langle \frac{u_{U,max,ADINA}}{u_{U,max,SDOF}} - 1 \right\rangle^2 + \left(\frac{\omega_{SDOF}}{\omega_{1,ADINA}} \right) \quad (\text{F.15})$$

where the angle brackets signify the Macaulay bracket function. The response of the modified SDOF system, i.e. the maximum deformation and angular frequency of the structure are calculated with Equation (F.13) and Equation (F.14).

After optimisation, the following empirical expressions were obtained:

$$\gamma_m = \left(0.0288 + 0.1697 \left(\frac{m_1}{m_2} \right) - 0.0233 \left(\frac{m_1}{m_2} \right)^2 \right) \cdot \left(\frac{k_1}{k_2} + 1.3023 \right) \quad (\text{F.16})$$

$$\gamma_k = 0.9961 + \left(0.1767 + 0.1853 \ln \left(\frac{m_1}{m_2} \right) \right) \cdot \frac{k_1}{k_2} \quad (\text{F.17})$$

The differential equation of motion for the system takes the form:

$$\gamma_m m_e \ddot{u}_U + \gamma_k k_e u_U = F(t) \quad (\text{F.18})$$

Appendix G Stiffness transformation factor

G.1 General notes

Throughout the work, it has been attempted to find a quick hand calculation procedure for the 2DOF system. The actual structure vibrates mainly with two eigenfrequencies simultaneously, which are directly linked to the structure's eigenmodes. Several attempts have been made in order to ascertain if SDOF systems can efficiently describe the respective modes. If such simplified systems could be found, it would be possible to obtain the deformation of both bodies in a quick and simple way, therefore eliminating the need of creating other calibrated SDOF systems (as it was done in Chapter 5). However, such attempts were not successful.

In all previous models, the transformation factors are calculated from the deformation shape under static loading. Even though it is a correct approach for separate elements, such as beams or slabs, it was of interest if the same assumption are valid for a structural system. As already shown in Figure E.2 and Figure E.3, the resultant eigenmodes can sometimes differ greatly from the assumed deformation shape under static loading.

As already stated in Section 2.5.4, according to Biggs (1964), the stiffness transformation factor is equal to the force transformation factor, i.e.

$$\kappa_k = \kappa_F \quad (\text{G.1})$$

Now, it was decided to check if this correlation is true also for a structural system. Instead of deformation shaped under static loading, the deformation shapes according to the prevailing eigenmodes are used in calculation of the transformation factors κ , i.e.

$$\kappa_m = \int_0^L \frac{m'(x) \cdot \phi(x)^2}{m \cdot u_s^2} dx \quad (\text{G.2})$$

$$\kappa_F = \int_0^L \frac{q(x) \cdot \phi(x)}{F \cdot u_s} dx \quad (\text{G.3})$$

$$\kappa_k = \int_0^L \frac{M(x) \cdot \phi''(x)}{F \cdot u_s} dx \quad (\text{G.4})$$

where $\phi(x)$ is the respective eigenmode shape.

G.2 First eigenmode

In order to calculate the transformation factors, a function describing the eigenmode is needed first. Such function should be twice differentiable and continuous. Since the shape of the first eigenmode resembles half sine functions for the upper beam (see Figure E.2), a relevant function can be found. For the lower beam, a function consisting of a half sine wave as well as one-and-a-half sine wave was used as the assumed mode. It should be noted, that the results are known after the modal analyses in ADINA, and

the fitting is done in order to validate the theory. Had the eigenmodes been unknown (as they usually are in the initial phase of design), it would have not been possible.

$$\phi_U(x) = s_2 \sin\left(\frac{\pi x}{L}\right) \quad (\text{G.5})$$

$$\phi_L(x) = s_1 \sin\left(\frac{\pi x}{L}\right) + (1 - s_1) \sin\left(\frac{3\pi x}{L}\right) \quad (\text{G.6})$$

The parameters s_1 and s_2 are obtained with the least square fit method, so that the functions simulate the eigenmode in the best possible way. In most cases, the deviation between the adapted function and the actual eigenmode were very small. Having the tentative deformation functions, it was possible to calculate the transformation factors.

For a case where the mass per length for both beams is constant, the length of both beams is the same and the uniformly distributed load per length is constant. Following relations were obtained:

$$\kappa_F = \frac{1}{L} \int_0^L \frac{\phi_U(x)}{u_s} dx = \dots = \frac{\pi + 2s_2}{\pi(s_2 + 1)} \quad (\text{G.7})$$

The stiffness of the structure can be expressed as

$$k_e = \frac{F}{u_s} \quad (\text{G.8})$$

where the stiffness k_s is the equivalent stiffness, i.e. $k_e = \frac{2k_1 k_2}{2k_2 + k_1}$. Therefore the stiffness transformation factor takes the form:

$$\begin{aligned} \kappa_k &= \int_0^L \frac{M(x) \cdot \phi''(x)}{k_e \cdot u_s^2} dx = \frac{1}{k_e u_s^2} \int_0^L EI_1 \phi_U''(x)^2 + 2EI_2 \phi_L''(x)^2 dx = \dots = \\ &= \frac{\pi^4 \left(82EI_2 s_1^2 - 162EI_2 s_1 + \frac{EI_1 s_2^2}{2} + 81EI_2 \right)}{L^3 k_e (s_2 + 1)^2} \end{aligned} \quad (\text{G.9})$$

Finally the mass transformation factor can be calculated as:

$$\begin{aligned} \kappa_m &= \int_0^L 2 \frac{\frac{m_2}{L} \phi_L(x)^2}{(m_1 + 2m_2) u_s^2} + \frac{\frac{m_1}{L} \phi_U(x)^2}{(m_1 + 2m_2) u_s^2} dx = \dots = \\ &= \frac{4\pi m_2 s_1^2 - 4\pi m_2 s_1 + \pi m_1 s_2^2 + 8m_1 s_2 + 2\pi m_1 + 2\pi m_2}{2\pi (m_1 + 2m_2) (s_2 + 1)^2} \end{aligned} \quad (\text{G.10})$$

With this approach, the resultant stiffness and force transformation factor were no longer equal. The eigenfrequency of this system can now be computed as:

$$\omega = \sqrt{\frac{\kappa_k k_e}{\kappa_m m_e}} \quad (\text{G.11})$$

where m_e is the total mass of the structure, i.e. $m_e = m_1 + 2m_2$. And the amplitude of the eigenmode can be calculated with the expression for the maximum deformation of a SDOF system, i.e.:

$$u_{max,SDOF} = \frac{\kappa_F I_k}{\kappa_m m \omega} \quad (G.12)$$

If the reasoning was correct, the obtained deformation would be equal to the amplitude obtained from the FFT for the first eigenfrequency. However, the FFT analysis is not accurate enough, because of the sampling time. Therefore to facilitate things, another curve fitting procedure was made. Namely, a superposition of two sine functions was used to reflect the actual deformation of the first system point, u_{1A} , present in ADINA. It means that two sine functions were found, which were assumed to describe the respective eigenmodes. Another option would be to rerun the analyses and use mode superposition method to solve the displacement instead of an implicit integration method. Finally, the quotient between the calculated deformation, $u_{max,SDOF}$ and the amplitude of the sine function reflecting the first eigenmode was computed for each case. The results can be seen in Figure G.1.

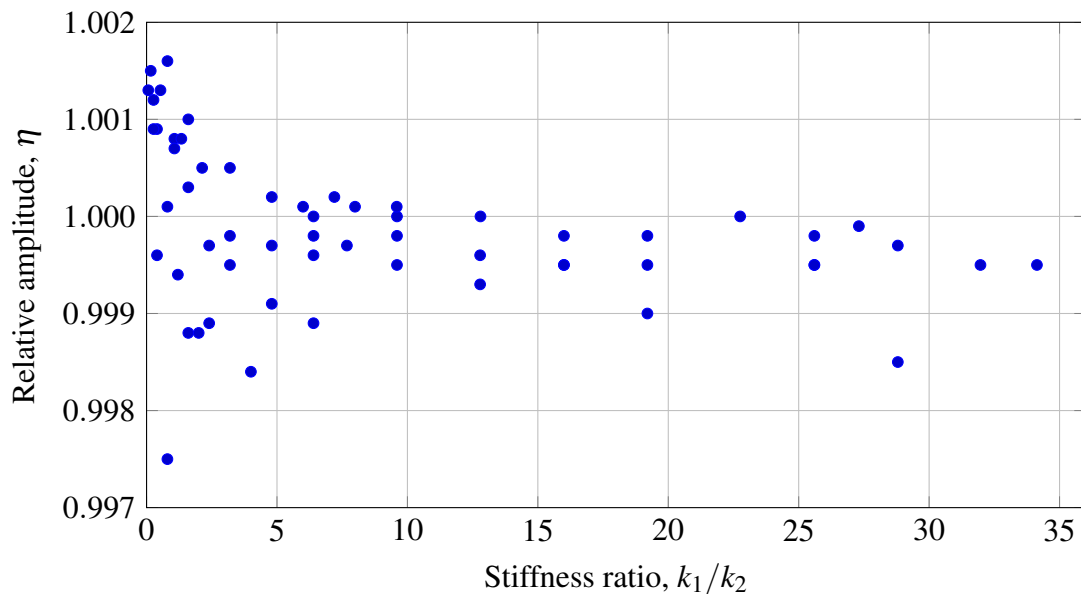


Figure G.1: *Relative amplitude of the system point in reference to the first eigenmode.*

It can be seen that there is good correspondence within the whole spectrum, which means that the first eigenmode can be successfully described with a SDOF system, but the transformation factors must be redefined.

G.3 Second eigenmode

In order to describe the second eigenmode, virtually the same approach was used. However, the shapes are now more complex, as can be seen in Figure E.3, where nine representative eigenmodes were shown. The same functions were adopted for the assumed modes, and all the formulas for the transformation factors remain unchanged. The only thing that changed were the parameters s_1 and s_2 since they had to be adapted to another shape now.

With calculated transformation factors, the maximum deformation of the SDOF system, $u_{max,SDOF}$ can be computed for each studied case. These results were compared with the amplitude of the second sine function obtained earlier in the curve fitting procedure. The conformity of the result can be seen in Figure G.2.

The structures for which the second eigenmode deformation was lower than 5 % of the first eigenmode deformation were discarded. This was done to assure more credibility to the results, since very low numbers are sensitive to numerical errors and can therefore result in considerable quotients which cannot be deemed representative and feasible.

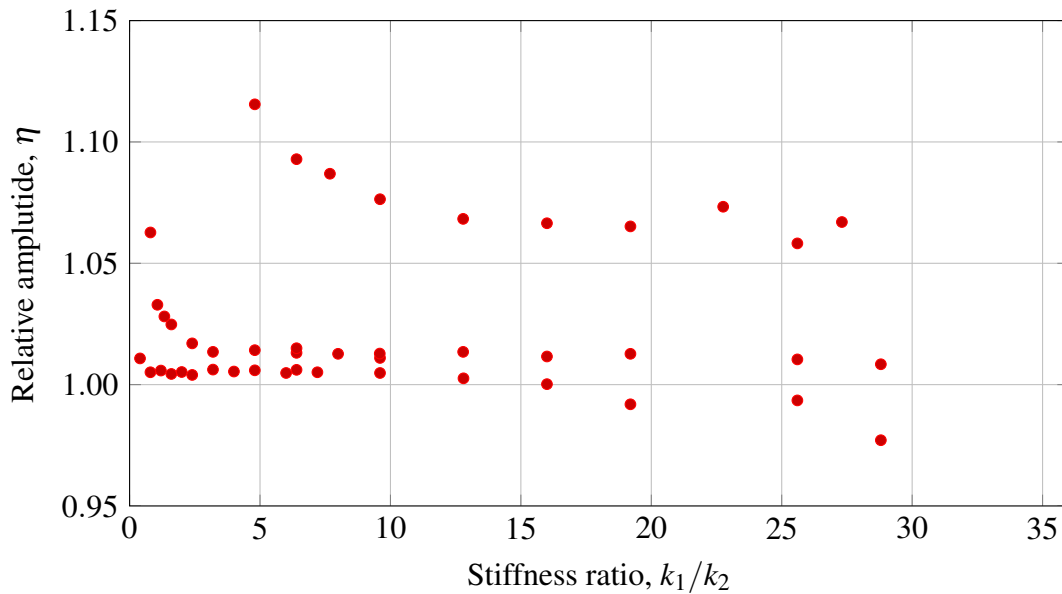


Figure G.2: Relative amplitude of the system point in reference to the second eigenmode.

The model shows good correspondence within the whole spectrum. It is believed that the outcome could be improved if a better assumed mode shape was chosen, since there is a big difference in how the second eigenmode will actually look like, depending on the structural properties of the structural system.

It is worth to add, that the obtained deformation is the deformation of the first system point - namely u_1 . This means that having the functions describing the eigenmodes, the deformation of an arbitrary point can easily be computed. To obtain the deformation of the upper beam, the displacement of the second system point is needed first, and then a simple subtraction will give the desired result.

G.4 Final remarks

To conclude, it was shown that it is possible to describe both eigenmodes with separate SDOF systems with reasonably high precision. This approach was tried when developing modified SDOF systems in Chapter 5, but the results were unsuccessful. The idea was to somehow create two SDOF systems, each one for respective eigenmode, and then simply add the maximum deformations in order to obtain the total structural response. The results were not promising, and even when they were reasonable, the accordance was not achieved within the whole spectrum of studied structures.

This is believed to be caused by the ansatz, that the stiffness and force transformation factors are the same, i.e. $\kappa_k = \kappa_F$. They are the same (or at least very close to each other) for simple structures such as beams, where only one eigenmode dominates the behaviour. In a beam structure, there are higher modes as well present during its vibration, but their influence is negligible. For a structural system, the response depends on the structural properties of its constitutive elements, meaning that it may vibrate with more distinct eigenfrequencies. For such structures, the stiffness transformation factor, κ_k , cannot be assumed to be equal to the force transformation factor, κ_F , anymore.

Even though the study included in this chapter showed that it is possible to simplify respective eigenmodes with equivalent SDOF systems (without any calibration or optimisation), the shape of the eigenmodes was needed to compute the transformation factors. Since this information is not known in the initial phase of the design, a new problem arises. What makes the matter worse is the fact, that the shape of the second eigenmode varies for different structural properties of the elements. Perhaps some general correspondence between the structural properties of a structural system and the shape of its eigenmodes could be found, which would enable a quick and easy way to estimate the response of the structural system with simple SDOF systems throughout the whole spectrum of the structures. This is proposed as a matter of further research.